

COMPONENT CO₂ EMISSIONS OF PLANTED PINE FORESTS

**CHARACTERIZING AND QUANTIFYING
ECOSYSTEM COMPONENT CO₂ EMISSIONS
FROM DIFFERENT-AGED, PLANTED,
PINE FORESTS**

By

MYROSLAVA KHOMIK

A Thesis

Submitted to the School of Graduate Studies
in Partial Fulfillment of the Requirements

For the Degree:
Doctor of Philosophy

McMaster University

© Copyright by Myroslava Khomik, April 2009

**CHARACTERIZING AND QUANTIFYING
ECOSYSTEM COMPONENT CO₂ EMISSIONS
FROM DIFFERENT-AGED, PLANTED,
PINE FORESTS**

By

MYROSLAVA KHOMIK

A Thesis
Submitted to the School of Graduate Studies
in Partial Fulfillment of the Requirements

For the Degree:
Doctor of Philosophy

McMaster University

© Copyright by Myroslava Khomik, April 2009

DOCTOR OF PHILOSOPHY (2009)
(Biogeosciences)

McMaster University
School of Geography and Earth
Sciences, Hamilton, ON

TITLE: Characterizing and quantifying ecosystem component CO₂
emissions from different-aged, planted, pine forests.

AUTHOR: Myroslava Khomik

SUPERVISOR: Professor M. Altaf Arain

NUMBER OF PAGES: xxii, 241

ABSTRACT

The rapid increase of anthropogenically-derived CO₂ in the atmosphere, during the past century, has been linked to unprecedented global climate change. Forests and various forest management techniques have been proposed as a potential way to help sequester some of the atmospheric CO₂. In order to evaluate the CO₂ sink potential of forests, a good understanding of their carbon dynamics is required over various stages of their development and growth.

This dissertation reports results of a field study that focused on characterizing and quantifying CO₂ emissions from various components of planted white pine (*Pinus Strobus* L.) forest ecosystems, growing in southern Ontario, Canada. The study site, called the Turkey Point Flux Station (TPFS), consisted of four stands, aged: 70-, 35-, 20- and 7 years-old, as of year 2009. Three major components of ecosystem respiration, Re, were studied using the chamber-method: soil respiration, Rs (both, autotrophic and heterotrophic), foliar respiration, Rf, and live woody-tissue respiration, Rw.

Chamber-based estimates of annual Re across the four different stands were: 1527 ± 137 , 1313 ± 137 , 2079 ± 293 , and 769 ± 46 g C m⁻² yr⁻¹ for the 70-, 35-, 20-, and 7-year-old stands, respectively, and were generally higher compared to literature reported values. Annually Rf accounted for 48, 40, 58, and 31 % of Re at the 70-, 35-, 20-, and 7-year-old stands, respectively, and dominated Re during the growing season at the three oldest stands. In contrast, Rs was the dominant Re component at the youngest stand and during the winter months at all four sites. Annually Rs accounted for 44, 40, 29, and 69 % of Re across the respective TPFS sites. Rw was the smallest component of annual Re, accounting for only 9, 15, 13 and 0.1% of Re, respectively. Differences in leaf area indices among the stands were responsible for most of the intersite variability in Re, as well as for differences between Re values obtained in this study and those reported in the literature. Results from this study highlight the importance of considering site age and knowledge of past land-use history when assessing carbon budgets of afforested or planted ecosystems. They also suggest that Rf may be the more dominant and determinant component of Re in young to mature afforested stands, which is in contrast to the widely reported Rs dominance of Re in forest ecosystems.

Soil respiration was studied in detail across TPFS, as part of this dissertation, to determine the driving factors of its temporal variability, considering seasonal, interannual (3 years of measurements) and decadal (over the TPFS age-sequence) timescales. The range of Rs values across TPFS over the course of three study years was 539 ± 31 to 732 ± 31 g C m⁻² yr⁻¹. In general, annual soil emissions from the oldest stand were higher compared to those from the youngest two stands. However, emissions from the 35-year-old stand were comparable to those from the 20- and 7-year-old stands. Intersite differences in soil emissions were driven mostly by stand physiology, while interannual differences reflected interannual variability in climatic factors, as well as

differences in stand physiology that modified the site's microclimates. In particular, results from this study suggest that soil moisture may have a larger effect on the heterotrophic rather than on the rhizospheric component of soil respiration in these forest ecosystems, supporting evidence from other literature-reported studies.

Finally, the chamber-based R_e values derived in this study were compared with R_e values derived from congruent eddy covariance measurements at TPFS. Based on annual totals, R_e calculated from chamber measurements overestimated R_e calculated from eddy covariance measurements on average by: 18, 75, 24 and 39% at the 70-, 35-, 20-, and 7-year-old stands, respectively. These results highlight the continued need to resolve the discrepancy between the two methodologies used to estimate R_e , before measurements from both methods can be used together to make conclusions about the composition of forest carbon budgets.

As part of this dissertation, a statistical method of data analysis was used to implement temporal flexibility in the conventional Q_{10} model, widely used to simulate various R_e components of forested ecosystems. The outcome of that analysis highlighted two things: a) for the case of soil respiration, the exponential relationship between R_s and T_s may be limited to the so called “ecologically optimum T_s range” for fine root growth; b) the functional form of the Q_{10} model is inadequate for simulating the R_s - T_s relationship across a wide range of T_s values, even after the implementation of temporal flexibility into the model, which allowed both of its model parameters to vary. The consequence of the latter result led to the development of a new empirical model – the Gamma model - for use in simulating respiration with temperature. The statistical method and the new empirical model were used to simulate CO_2 emissions in this study and to identify additional environmental and physiological factors that explained some of the variability in the individual R_e components across TPFS. Thus, temperature was found to be the dominant controlling factor of respiration at all four sites. However, occurrence of precipitation events, vapour pressure deficit, photosynthetically active radiation, the thickness of the LFH soil horizon (i.e. litter layer), and soil nutrients, were also shown to explain some of the variability of the various respiratory components.

This dissertation fills some of the gaps in literature on studies of R_e component fluxes of planted young to mature forests, especially of those growing in the temperate climate of eastern North America, where afforestation and plantations are most likely to occur. The study should be of interest to carbon cycle modellers, field ecologists, the eddy covariance community. It should also be of interest to those involved in forest carbon accounting, management, and policy development, by adding knowledge to our understanding of global carbon cycling and the potential for using afforested sites in global warming mitigation attempts.

ACKNOWLEDGEMENTS

I would like to thank my supervisor, Dr. Altaf Arain, for providing me the opportunity to pursue my PhD within his research group at McMaster University, for his patience, guidance, encouragement and constructive criticism throughout this work. I am also very grateful to Dr. Harry McCaughey from Queen's University, who, together with Dr. Arain, secured funding for my PhD work, facilitated data collection at the Turkey Point (TPFS) and Groundhog River (GRFS) Flux Stations, and assisted with field work.

I am thankful to all the members of my various PhD Committees throughout the years: Drs. Pierre Bernier, Paulin Coulibaly, Kao-Lee Liaw, Harry McCaughey, Jim Smith, and Mike Waddington for their time, encouragement, and guidance.

A special thank you is extended to Dr. Kao-Lee Liaw for introducing me to some very interesting and practical statistical methods of data analysis, which allowed me to finally solve the nagging problem of how to best simulate my respiration data!

I would also like to thank the Canadian Carbon Program (former Fluxnet-Canada) members for their financial support for my graduate studies; for all the great educational opportunities they provided at the Carbon courses and the annual meetings; and for opportunities to attend conferences and courses at other institutions. Thank you also for all the intellectual support/discussions outside of the scheduled lectures and talks, whether it was getting tips on methodology or key readings to help me in my research – in that regard I extend special thanks to Drs. Pierre Bernier, Andy Black, Jing Chen, Larry Flanagan, Mike Lavigne and their research groups.

Thank you to everyone from our Hydrometeorology and Climatology Research Group at McMaster University (Bin, Emily, Fengming, Jagadeesh, Jason, Josh, Mahmoud, Matthias, Natalia, Samantha, Suo, Rao, Rose, Yi and Zav), and to everyone from the Queen's University Climatology Group and Ontario Ministry of Natural Resources (OMNR) involved with GRFS (Alan, Bob, Dan, Don, Joe, Laura, Lauren, Leanne, Shiela, Stan, Troy and Valerie) for your help with field activities, for maintaining the research sites, for providing auxiliary data for my work, for numerous constructive discussions regarding research and for an overall camaraderie in work. I also extend my gratitude to the following additional field volunteers for help with TPFS data collection: Dali, Eugenia, Fauzia, Lara, Olesia, Sven, and Talar. A special thanks to the hosts at Scotch Lake Camps, Air Ivanhoe, White Pine Lodge, and Mooseland for being great hosts and for helping out in times of need during my field adventures into the "remote and wild" Ontario, where bears roam freely, grouse stubbornly adhere to their right of way, and mosquitoes devour the delicacy called "the southern Ontario city-dweller"!

A special thank you is extended to the research groups of Drs. Jim Smith, Mike Waddington and Leslie Warren, here at the School of Geography and Earth Sciences (SGES), for allowing me to borrow and use some equipment/resources from their labs during my research.

We thank Frank Bahula and Bruce Whitside, and their families, for providing access to the forests on their properties. We thank Steve Williams, from OMNR, for his assistance in the selection and maintenance of the oldest TPFS site.

Thanks to everyone at LI-COR, Inc., especially Tanvir and Shannon, for your technical support and advice regarding the LI-6400.

To all staff, faculty and students, here, in SGES – thanks for the friendly and encouraging work atmosphere!

I appreciated the financial support provided for my PhD through McMaster University by the Ontario Graduate Student (OGS) scholarship in Science and Technology: The David and Grace Prosser Scholarship and an OGS Fellowship.

To my parents I am most thankful, since without their help and encouragement, this work would have been impossible. Дякую моїм рідним за їхню постійну підтримку, натхнення і турботу! Нарешті догризла граніт науки ☺.

Thank You

TABLE OF CONTENTS

TITLE PAGE	i
DESCRIPTIVE NOTE	ii
ABSTRACT	iii
ACKNOWLEDGEMENTS	v
TABLE OF CONTENTS	vii
LIST OF FIGURES	xi
LIST OF TABLES	xvii
PREFACE	xx

CHAPTER 1: INTRODUCTION

1.1 Broader significance of this study	1
1.2 Novel aspects	
1.2.1 Filling gaps in literature on studies of Re and its component fluxes across different-aged coniferous forests in eastern North America	3
1.2.2 Improving models used to simulate and assess respiration	4
1.2.3 Unique methodology	7
1.3 Study sites – Turkey Point Flux Station, TPFS	7
1.4 Overview of methodology	8
1.5 Study objectives	10
1.6 References	10

CHAPTER 2: CHARACTERIZING TEMPORAL VARIABILITY OF SOIL RESPIRATION AND ITS TEMPERATURE SENSITIVITY IN DIFFERENT-AGE FORESTS

2.1 Abstract	20
2.2 Introduction	22
2.3 Methods	
2.3.1 Study sites	25
2.3.2 Flux and meteorological measurements	26
2.3.3 Model development	
2.3.3.1 Identifying temporal variability in measured climatic variables and Rs	27
2.3.3.2 Adding temporal flexibility into the Q ₁₀ model	31
2.3.3.3 Adding soil moisture variability into the Q ₁₀ model	34
2.3.3.4 Assessing the relative importance of the explanatory factors in the model	35

2.4 Results	
2.4.1 The temporally flexible Q_{10} model	36
2.4.2 Temporal variability in R_{10} and Q_{10} at TPFS	38
2.4.3 Comparison between the temporally flexible and conventional versions of the Q_{10} models	41
2.4.4 Relative importance of the temporal factors in the Best model	42
2.5 Discussion	44
2.6 Conclusions	51
2.7 Acknowledgements	53
2.8 References	53

CHAPTER 3: THE DEBUT OF A FLEXIBLE MODEL FOR SIMULATING SOIL RESPIRATION-SOIL TEMPERATURE RELATIONSHIP: THE GAMMA MODEL

3.1 Abstract	68
3.2 Introduction	69
3.3 Methodology	
3.3.1 Study sites	72
3.3.2 The Gamma model and usefulness of model linearization	72
3.3.3 Model parameterization and comparison of model fits	76
3.3.4 Comparison of annual and seasonal estimated R_s computed using two different estimation methods	77
3.4 Results and Discussion	
3.4.1 Comparison of model fits	81
3.4.2 Comparison of annual and seasonal estimated R_s computed using two different estimation methods	82
3.4.3 Expanding the Gamma model – Oak site case study	83
3.5 Conclusions	88
3.6 Acknowledgements	90
3.7 References	91

CHAPTER 4: CONTROL OF CLIMATE, EDAPHIC CONDITIONS AND STAND PHYSIOLOGY ON INTERSITE AND INTERANNUAL VARIABILITY OF SOIL RESPIRATION ACROSS FOUR, DIFFERENT-AGE, PLANTED FORESTS

4.1 Abstract	110
4.2 Introduction	111
4.3 Methods	

4.3.1 Study site	113
4.3.2 Soil respiration measurements	115
4.3.3 Meteorological and edaphic measurements	116
4.3.4 Data analysis and simulations of daily Rs	117
4.4 Results	
4.4.1 Variability in environmental factors	119
4.4.2 Impact of climate, edaphic and physiological factors on simulated Rs-Ts relationship	121
4.4.3 Comparison of simulated Rs values.....	124
4.4.4 Relative contribution of seasonal Rs to total annual Rs	127
4.5 Discussion	
4.5.1 Comparison of soil C emissions among different-age stands	128
4.5.2 Environmental and physiological controls on Rs ...	130
4.6 Conclusions	134
4.7 Acknowledgements	136
4.8 References	136
APPENDIX 4A	
4.A.1 Model development and evaluation	148
4.A.2 Rs-Ts model with climate, edaphic and physiological factors	150

**CHAPTER 5: RELATIVE CONTRIBUTIONS OF SOIL, FOLIAR
AND WOODY TISSUE RESPIRATION TO TOTAL ECOSYSTEM
RESPIRATION IN FOUR, DIFFERENT-AGE, FORESTS**

5.1 Abstract	152
5.2 Introduction	154
5.3 Methods	
5.3.1 Study sites	156
5.3.2 Eddy covariance measurements and weather stations	157
5.3.3 Chamber-based measurements	159
5.3.3.1 Soil respiration, Rs	159
5.3.3.2 Heterotrophic soil respiration, Rh	160
5.3.3.3 Foliar respiration, Rf	162
5.3.3.4 Woody tissue respiration, Rw	163
5.3.4 Data Analysis	164
5.3.5 Upscaling to ecosystem level	166
5.3.5.1 Upscaling Rf to stand level	166
5.3.5.2 Upscaling Rw to stand level	168
5.4 Observations and Results	
5.4.1 Meteorology during study period	169
5.4.2 Annual and seasonal trends of component fluxes	

5.4.2.1 Soil respiration, R_s	169
5.4.2.2 Heterotrophic respiration, R_{sh}	171
5.4.2.3 Foliar respiration, R_f	172
5.4.2.4 Woody tissue respiration, R_w	174
5.4.3 Contribution of R_s , R_f , and R_w to R_e	175
5.4.4 Comparison of R_e derived by chamber vs EC methods	178
5.5 Discussion	
5.5.1 Annual and seasonal variability in component fluxes	
5.5.1.1 Soil respiration, R_s	178
5.5.1.2 Foliar respiration, R_f	182
5.5.1.3 Woody tissue respiration, R_w	183
5.5.2 Comparison of R_{10} and Q_{10} from TPFS with literature studies	184
5.5.3 Contribution of R_s , R_f , and R_w to R_e across TPFS	185
5.5.4 Comparison of R_e derived by chamber vs EC methods	189
5.6 Conclusions	191
5.7 Acknowledgements	193
5.8 References	194
5.9 APPENDICES	
APPENDIX 5A: Empirical models used to simulate respiration	226
APPENDIX 5B: Environmental and biological controls on TPFS's respiration	227
 CHAPTER 6: CONCLUDING REMARKS	
6.1 Scientific contribution of the study	231
6.2 Summary of results	232
6.3 Suggestions for future work	234
6.4 References	238

LIST OF FIGURES

CHAPTER 1

- Figure 1.1:** 17
 At the time of this study, Turkey Point Flux Station was an associate site of former Fluxnet-Canada (now the Canadian Carbon Program). It is located on the northern edge of Lake Erie in southern Ontario, Canada.
- Figure 1.2:** 19
- a) The LI-COR 6400 instrument with the 6400-009 soil chamber attachment, used to measure soil respiration during this study. In the photo the chamber, on the right, is actually placed above one of the collars used for R_s measurements. Next to the chamber is the soil temperature probe (6400-013), inserted into soil. The “box” is the console, a computer that controls the instrument. The IRGA analyzer is connected directly to the soil chamber (the rectangular block with plumbing, right on top of the chamber).
- b) A sample trenched plot at TP02, lined with industrial landscape cloth, before being back-filled with soil. These were dug to help estimate heterotrophic component of R_s at the sites. The soil collars for R_h measurements were installed inside each collar, as described in Chapter 5.
- c) View of foliar 2x3 LI-6400 chamber, fitted with the artificial light source, for R_f measurements. Needles were placed inside the chamber for measurement, lined-up in a single layer, along the chamber’s length.
- d) Sample collar attached to the tree bole at TP39, used for R_w measurements (see Chapter 5 for more details) with the LI-6400 and its soil chamber attachment. The soil chamber was attached horizontally against the tree trunk, to the collar, during measurements.

CHAPTER 2

- Figure 2.1:** 63
- a) Daily mean soil respiration, R_s , measured at each of the four age-sequence TPFS stands (TP39, TP74, TP89 and TP02, as defined in text), b) the corresponding daily mean soil temperature, T_s , measurements, and c) daily mean soil moisture, θ_s , from site-specific weather stations. Measurements are means of all observations collected on the given day, at a particular site (mean along all sampling points along the transect, including both morning and afternoon measurements, except for θ_s). Error bars represent ± 1 standard deviation. TP39, TP74, TP89 and TP02 correspond to site names, as defined in text. Also shown are mean annual air temperature (T_a) and total annual precipitation (Ppt) for each

study year. The 30-year-norm for the area was 7.9°C for Ta 1010 mm for Ppt. The horizontal dotted lines outline the data in the “optimum” Ts range, during which Rs was most responsive to changes in Ts.

Figure 2.2: 65
 Observed Rs values plotted against those predicted by the standard Q₁₀ model (i.e. no temporal variability), plotted for each site individually, for clarity: (a) 67-, (b) 32-, (c) 17- and (d) 4 year-old TPFS forest sites. However, note that all data points were used to parameterize the model and the curve in each panel is the same: $R_s = (1.3) * 2.5^{(T_s - 10)/10}$, $R^2 = 0.63$. The vertical dotted lines outline the data in the “optimum” Ts range, during which Rs was most responsive to changes in Ts.

Figure 2.3: 67
 Observed Rs values plotted against those predicted by Best Q₁₀ model (Equation 2.6), plotted for each site individually, for clarity: (a) 69-, (b) 34-, (c) 19- and (d) 6-year old TPFS forest sites. However, note that all data points were used to parameterize the temporal model.

CHAPTER 3

Figure 3.1: 101
 a) Natural log (Ln) transformed observed soil respiration, LnRs, measurements versus soil temperature, Ts, for the TP39 site (symbols). Also included are the Ln-transformed predicted Rs values (line curve). Taking the Ln of observed values helped to avoid the heteroscedacity problem. b) Standard deviations of observed Rs measurements binned by Ts values, for Ln-transformed Rs (filled symbols) versus non-transformed data (open symbols). c) comparison of predicted Rs curves derived from Ln-transformed and untransformed Rs, using the Gamma model. Grey symbols are observed Rs.

Figure 3.2: 103
 Comparison of models fitted, individually, to soil respiration (Rs) and soil temperature (Ts) data from the five sites a) TP39, b) TP02, c) GRFS d) SOBS, and e) Oak. Note that as Ts range increases, Rs tends to decrease at high Ts values (above ~ 20 °C) and the Gamma model has the flexibility to reflect that decrease in Rs, which is especially well illustrated by data for TP02 and Oak sites. The Gamma model was also flexible enough to take on the shape of an exponential Q₁₀ model (GRFS) and logistic model (TP39), as dictated by observed data.

Figure 3.3: 105
 Comparison of predicted soil respiration for the young temperate pine forest (TP02). Rs was predicted with models parameterized using two different

parameter estimation methods: ordinary least squares, OLS, (solid line) and the weighted absolute deviation, WAD, (dashed line). The comparison is made for all four empirical models tested in this study: a) Q_{10} , b) Lloyd-Taylor, c) Log, and d) Gamma. These results highlight the importance of choosing the proper functional form for the Rs-Ts relationship. Open symbols represent observed Rs measurements.

Figure 3.4: 107
Comparison of predicted soil respiration (Rs) for the young temperate pine forest (TP02). Rs was predicted with the Gamma model, parameterized using three different parameter estimation methods: ordinary least squares, OLS, (solid line); the weighted absolute deviation, WAD, (dashed line); and OLS method applied to \log_e transformed data (dotted line). Open symbols represent observed Rs measurements. These results show that the once the functional form of the Rs-Ts relationship is chosen well, the differences between the estimation methods used for model parameterization are no longer as important.

Figure 3.5: 109
Comparison of predicted soil respiration, Rs, values, obtained from the expanded (moisture & soil C - sensitive) Gamma model (curves) to that of observed Rs values (symbols). For clarity, Rs measurements belonging to the low (grey lines and circle symbols) and high (black lines and star symbols) soil moisture, θ_s , categories are distinguished in the plot. Also the low (open symbols and broken lines) and high soil C data is distinguished. The model (Equation 3.5 in text) was fitted with all 1095 data points, in a single regression step.

CHAPTER 4

Figure 4.1: 145
Plot of monthly mean and total values of climatic and edaphic environmental conditions across all four stands, as well as that of calculated monthly Rs: a) Mean monthly air temperature, T_{air} (line) and total monthly precipitation, PPT (bars) with number of precipitation events per month listed above each corresponding bar; b) comparison of mean monthly soil temperature (Ts) across TPFS; c) comparison of mean monthly volumetric water content (θ_s) across TPFS; d) comparison of total monthly emissions across all four stands. In the right upper corner of each panel, mean or total annual values of each of the above variables are also listed, for each year and site, including mean annual down-welling photosynthetically active radiation (PARa) in (a).

Figure 4.2: 147
Time series of observed mean daily Rs values (symbols) and the associated daily predicted Rs (lines), calculated using the *best* model ($R^2 = 0.8199$), and plotted individually for each site: a) the 69-year-old stand, TP39, b) the 34-year-old stand,

TP74, c) the 19-year-old stand, TP89, and d) the 6-year-old stand, TP02. Error bars represent ± 1 standard deviation about the mean and reflect spatial variability in R_s , which was not covered in this paper. In the upper right hand corner of each panel, for year year, the mean, mimimum and maximum simulated R_s values are also listed.

CHAPTER 5

Figure 5.1: 203
 Comparison of climatic and edaphic conditions across TPFS during the 2006 study year: a) daily mean air temperature (T_{air}); b) daily total precipitation (PPT); c) daily mean soil temperature (mean of all sensors in top 20 cm of mineral soil) (T_s); and d) daily mean soil moisture content (mean of all sensors in top 20 cm of mineral soil) (θ_s). Also listed in top right corner of each plot are the annual mean or total values, as well as the annual minimum and maximum values.

Figure 5.2: 205
 Comparison of simulated daily mean soil respiration, R_s , in $g\ C\ m^{-2}$, across TPFS during the 2006 study year (a), and relationships between observed R_s (in $\mu mol\ CO_2\ m^{-2}\ s^{-1}$) versus soil temperature (T_s) across TPFS (b-e). Symbols respresent measured values, while lines the T_s -only Gamma model. In the upper right corner of plot (a) annal mean, minimum, and maximum simulated R_s values are listed as are total annual emissions with their estimated errors, all in units of $g\ C\ m^{-2}$.

Figure 5.3: 207
 Comparison of the relative percent contribution of various components of soil respiration (R_s) across TPFS sites, on monthly basis throughout 2006: a) TP39, b) TP74, c) TP89, and d) TP02. The considered components included: the autotrophic soil respiration component (R_{sa}), the heterotrophic soil respiration from the mineral soil (R_{sh_m}), and, where applicable, heterotrophic respiration from the LFH layer (R_{sh_L}) – as stacked bars. In the upper left corner of the plot, annual totals for each component are listed in $g\ C\ m^{-2}\ yr^{-1}$.

Figure 5.4: 209
 Comparison simulated daily mean folier respiration, R_f , in $g\ C\ m^{-2}$, across TPFS during the 2006 study year (a), and relationships between observed R_f (in $\mu mol\ CO_2$ per (half-needle surface area in m^{-2}) s^{-1}) versus air temperature (T_a) across TPFS (b-e). Symbols respresent measured values, while lines the T_s -only Gamma model. In the upper right corner of plot (a) annal mean, minimum, and maximum simulated R_f values are listed, as are total annual emissions with their estimated errors, all in units of $g\ C\ m^{-2}$.

Figure 5.5: 211

Comparison simulated daily mean woody tissue respiration, R_s , in g C m^{-2} , across TPFS during the 2006 study year, which included both branch and stem respiration (a), and the relationships between observed R_w (in $\mu\text{mol CO}_2$ per (sapwood volume of stem in m^{-3}) s^{-1}) versus tree bole temperature (T_b) across TPFS (b-d). Symbols represent measured values, while lines the Ts-only Gamma model. In the upper right corner of plot (a) annual mean, minimum, and maximum simulated R_w values are listed, as are total annual emissions with their estimated errors, all in units of g C m^{-2} .

- Figure 5.6:** 213
Intersite comparison of annual totals of the three major ecosystem respiration components: total soil (R_s), woody tissue (R_w) and foliar (R_f) respiration, in $\text{g C m}^{-2} \text{ yr}^{-1}$. Also included are estimated errors on each total, shown as \pm error bars and numerically.
- Figure 5.7:** 215
Stacked area plots comparing total daily ecosystem respiration (R_e) and its three major components: soil (R_s), woody tissue (R_w) and foliar (R_f) at a) TP39, b) TP74, c) TP89, and d) TP02. The area below each line curve represents mean daily contribution of each component to R_e , with the total sum of all areas comprising R_e . In the upper right corner of each plot, annual mean, minimum, maximum, as well as annual total R_e with its estimated error are also listed. All in units of g C m^{-2} .
- Figure 5.8:** 217
Intersite comparison of total monthly carbon emissions from the three major R_e components: a) soil (R_s), b) woody tissue (R_w), and c) foliage (R_f). In d) total monthly ecosystem respiration (R_e) is compared. Error bars represent \pm estimated errors.
- Figure 5.9:** 219
Pie graphs comparing breakdown of annual total ecosystem respiration (R_e) into soil (R_s), woody tissue (R_w) and foliage (R_f) respiration, as relative percentage of annual total R_e at a) TP39, b) TP74, c) TP89, and d) TP02.
- Figure 5.10:** 221
Comparison of percentage relative contribution of monthly soil (R_s), woody tissue (R_w), and foliage (R_f) to total monthly ecosystem respiration at a) TP39, b) TP74, c) TP89, and d) TP02.
- Figure 5.11:** 223
Pie graphs comparing breakdown of annual total ecosystem respiration (R_e) into total ecosystem autotrophic (R_a) and total ecosystem heterotrophic (R_h)

components, presented as relative percentage of annual total Re at a) TP39, b) TP74, c) TP89, and d) TP02.

Figure 5.12: 225
 Comparison of mean daily ecosystem respiration estimated by the chamber-based method (Re_ch) and by the eddy covariance-based method (Re_ec), represented by lines. Also shown, as symbols, are daily mean night time net ecosystem observations from available tower measurements across TPFS: a) TP39, b) TP74, c) TP89, and d) TP02. In the upper right corner of each plot, annual totals estimated from each method in $\text{g C m}^{-2} \text{ yr}^{-1}$ and their ratios are also given.

LIST OF TABLES

CHAPTER 2

Table 2.1:	59
Site characteristics of Turkey Point Flux Station's (TPFS) forests.	
Table 2.2:	60
Explanation of the temporal variability in R_s at TPFS based on the maximizing and fixed coefficient methods, by comparison of coefficients of determination (R^2) between Best model and various reduced model fits, as discussed in text. Also shown are estimates of coefficients for each variable and their associated t-values, for each model run, from the maximizing method, as described in text.	
Table 2.3:	61
(a) R_{10} values, calculated from the estimated coefficients of the Best model (Table 2.2, column 1) ; (b) Q_{10} values, calculated from the estimated coefficients of the Best model (Table 2.2, column 1).	
Table 2.4:	61
The effect of soil temperature on the relationship between soil respiration (natural-log transformed, \ln) and soil moisture.	

CHAPTER 3

Table 3.1:	95
Description of forest sites and their associated R_s measurements used in this paper for the model comparison.	
Table 3.2:	96
Soil respiration models used in Chapter 3	
Table 3.3:	97
(a) Comparison of the goodness-of-fit of the R_s - T_s models shown in Figure 3.2, using coefficients of determination (R^2) values. Also shown are the sample size (n) and ranges of the observed R_s and T_s values used to parameterize each model, at each forest site. (b) Comparison of the goodness-of-fit of the R_s - T_s models, using residual sum of squares (RSS) and Akaike's Information Criterion (AIC) values.	
Table 3.4:	98
Comparison of annual and seasonal R_s totals calculated from each model for the young temperate stand (TP02), for year 2005, using the weighted absolute deviation (WAD) and the ordinary least squares (OLS) parameter estimation	

methods, as well as OLS on Ln-transformed data for Gamma model only. Errors shown are ± 2 standard deviations of the sum.

Table 3.5: 99
 Resulting estimates of the parameters (i.e. the “unknown coefficients”) for the Ts-only and the moisture-&-soil-carbon-sensitive Gamma models, fitted to the Oak site data. (n=1095, in both cases).

CHAPTER 4

Table 4.1: 141
 Description of Turkey Point Flux Station (TPFS) stand characteristics.

Table 4.2: 142
 Estimates of coefficients for each variable and their associated t-values, for each of the full (Best) and reduced Gamma models, computed using the maximizing method, as described in text. Also included are coefficients of determination (R^2) for the full Gamma model and various reduced versions of the model, derived with the maximizing and fixed-coefficient methods. The difference in R^2 between the reduced model and the Best model gives the marginal contribution in R^2 (MCR) of the deleted factor from the associated reduced model.

Table 4.3: 143
 Relative percent contribution of total soil CO₂ emissions from each season to the respective total annual soil CO₂ emissions, across TPFS, given for each year and site.

CHAPTER 5

Table 5.1: 200
 Some relevant TPFS site characteristics.

Table 5.2: 201
 Calculated R_{10} and Q_{10} values of each component at TPFS from the two Q_{10} -models fitted to measured TPFS data. R_{10} for R_s is given in units of $\mu\text{mol of CO}_2 \text{ m}^{-2} \text{ s}^{-1}$, while that for R_f is given in $\mu\text{mol of CO}_2$ (half-surface area of needles, m^{-2}) s^{-1} and R_w is given in $\mu\text{mol of CO}_2$ (sapwood volume, m^{-3}) s^{-1} .

Table 5A.1: 229
 List of models used to simulate daily fluxes of component ecosystem respiration across TPFS: Q_{10} models (a) and (b), and Gamma models (c) and (d).

Table 5A.2: 230

Comparison of model statistics for all the models used in simulating component respiration across TPFS in this study. Annual totals estimated by each model for each respiration component is also given by site.

PREFACE

This dissertation consists of four manuscripts (ms) that are in the process of being submitted for publication to scientific journals. Results presented in this dissertation stem mostly from research done at the Turkey Point Flux Station (TPFS). There is some overlap in the information and results presented in each of the chapters. However, all four of the main chapters present distinct ideas and components of my PhD work.

The overall goal of the study was to characterize and quantify components of ecosystem respiration (R_e) across TPFS. Thus, Chapters 2 and 3 (first and second ms) develop statistical methods of data analysis and identify suitable empirical models to be used in simulating R_e component fluxes. Chapter 4 (third ms) investigates variability of soil respiration (R_s) and its driving factors. R_s is often reported as the dominant R_e component in forests and therefore is considered in detail in a separate ms. Chapter 5 (fourth ms) focuses on characterizing and quantifying all three R_e component fluxes across TPFS, concluding with the overall goal of this study. Further details of each ms enclosed in this work, and how they all relate, are given below.

Manuscript 1 (Chapter 2): The Q_{10} model is one of the most widely used empirical models in carbon research for simulating carbon emissions driven by temperature variability. However, the conventional form of the model does not allow model parameters to vary temporally and has been criticized for this lack of temporal variability. Thus, this chapter focused on modifying the Q_{10} model to make it temporally flexible (i.e. to allow its model parameters, R_{10} and Q_{10} , to vary seasonally, interannually, and decadal). Furthermore, the relative importance of including seasonal, interannual, intersite and soil moisture variability in the Q_{10} model was also assessed, as was the possibility of constant Q_{10} values over limited temperature ranges across TPFS. An important outcome of the analysis in Chapter 2 was that the overall mathematical form of the Q_{10} model was inadequate in representing R_s - T_s variability across TPFS, even after modifications that allowed for temporal flexibility. This outcome led us on a bit of a detour from our final goal. However, the consequence was the discovery and development of an empirical model that was better than the Q_{10} model in simulating R_e components.

Manuscript 2 (Chapter 3): Chapter 3 focused on developing an alternative empirical model to the Q_{10} model. The new model was called the Gamma model, after the name of the function from which it was derived. In Chapter 3, the suitability of the Gamma model for simulating respiration was tested across a range of ecosystems: two boreal forests (data for one of which, Groundhog River Flux Station, was also collected as part of my PhD work), a Mediterranean forest, and two temperate forests (i.e. from TPFS sites). The Gamma model was tested against three of the widely-used in literature respiration-temperature models: the

Q_{10} model, the Lloyd-Taylor model, and the logistic model. The results in Chapter 3 showed that indeed the Gamma model better reflected seasonal variability of observed respiration data. Across all sites tested, the new model was statistically comparable or better in its fit compared to the other three models tested. Thus, we used the Gamma model in our subsequent analysis to simulate respiration fluxes across TPFS sites.

Manuscript 3 (Chapter 4): In Chapter 4, three years of soil respiration measurements across the four, different-aged, TPFS sites were analyzed to identify key climatic, soil and physiological driving factors of R_s variability. Since the measurements were conducted using a portable instrument, on a biweekly to monthly basis, an empirical model, the Gamma model, was used to simulate daily emissions. The simulated emissions were summed to monthly and annual totals, which were compared between sites and years of measurement.

Manuscript 4 (Chapter 5): The methods of analysis, developed in Chapters 2-4, were applied in Chapter 5, to develop empirical models for simulating daily, monthly, and annual CO_2 emissions from chamber measurements of three major forest ecosystem respiration components: foliar, woody tissue, and soil respiration (including soil autotrophic and heterotrophic respiration). Chamber-based estimates were upscaled to ecosystem level, using site-specific biometric indices, and compared across TPFS sites to assess intersite variability in R_e among the stands. Note that the Q_{10} model is also used in Chapter 5 to simulate each of the component fluxes, but this is done for comparison purposes only (i.e. to relate our results to literature reported studies, where the use of Q_{10} and R_{10} prevails).

.....

Naturally, as in many research publications stemming from large projects such as TPFS, there will be a number of contributors to the publications. Here is an outline of the contributions from each of the authors of the four papers presented as part of this dissertation:

(Chapter 2): Khomik M, Arain MA, Liaw K-L (2009) Characterizing temporal variability of soil respiration and its temperature sensitivity in different-age forests. (in Review: A modified version of this chapter has been submitted for publication to *Agricultural and Forest Meteorology* in April 2009)

M. Khomik (the PhD candidate) collected soil respiration data used in the manuscript, completed data analysis and wrote the manuscript. M.A. Arain secured funding for the project and provided editorial critique of the ms. K-L Liaw taught M.Khomik the statistical method used in the ms, provided editorial criticism of the mathematical details in the ms and technical support in data analysis.

(Chapter 3): Khomik M, Arain MA, Liaw K-L, McCaughey JH (2008) The debut of a flexible model for simulating soil respiration-soil temperature relationship: the Gamma model. (accepted, *in press: Journal of Geophysical Research – Biogeosciences*)

M. Khomik (the PhD candidate) collected soil respiration data for three of the sites used in the ms (TP39, TP02 and GRFS), completed data analysis and wrote the manuscript. M.A. Arain secured funding for the project, helped to acquire SOBS and Oak sites' data sets, and provided editorial critique of the ms. K-L Liaw introduced M.Khomik to the Gamma function, provided mathematical guidance in Gamma model development and data analysis and editorial criticism of the ms. J.H. McCaughey secured funding for research at GRFS, provided supporting meteorological data collected at GRFS and editorial critiques on ms stemming from GRFS work.

(Chapter 4): Khomik M, Arain MA (2009) Control of climate, edaphic conditions and stand physiology on intersite and interannual variability of soil respiration across four, different-age, planted forests.

M. Khomik (the PhD candidate) collected soil respiration data used in the ms, completed data analysis and wrote the ms. M.A. Arain secured funding for the project and provided editorial criticism of the ms.

(Chapter 5): Khomik M, Arain MA, Brodeur J, Peichl M, Restrepo-Coupé N, McLaren JD (2009) Relative contributions of soil, foliar and woody tissue respiration to total ecosystem respiration in four, different-age, forests.

M. Khomik (the PhD candidate) collected chamber respiration data used in the ms, completed data analysis and wrote the manuscript. M.A. Arain secured funding for the project and provided editorial critique of the ms. J. Brodeur provided cleaned meteorological data, from TPFS weather stations, used in model simulations in the ms. J. Brodeur also computed ecosystem respiration from eddy covariance measurements at TPFS and provided cleaned observed night time NEE data used in the ms. N. Restrepo-Coupé and M.Peichl provided biometric data used for up-scaling chamber measurements. M.Peichl was also involved in collecting weather station and eddy covariance data used in the analysis. JD McLaren collected weather station data at the oldest TPFS stand in 2006. All of the above authors helped the first author in the field, at one point or another throughout the project.

CHAPTER 1

INTRODUCTION

1.1 Broader significance of study

A major constituent of the global carbon cycle is carbon dioxide (CO₂) gas, which has been identified as an important contributor to the global greenhouse effect (Bates et al., 2008). Variability of atmospheric CO₂ has been reported, with seasonal fluctuations attributed to seasonal CO₂ cycling in terrestrial ecosystems, particularly of those in the northern hemisphere (Keeling et al., 1996). Consequently, over the past few decades, great interest has emerged in understanding the role of terrestrial ecosystems in the global carbon cycle (Dixon et al., 1994; Gough et al., 2008; Lindner and Karjalainen, 2007; Liu et al., 2002; Nabuurs et al., 1997).

Forests constitute about 30% of Earth's total land cover. Two thirds of these are found in only 10 of the world's countries, the top three being: Russia, Brazil and Canada (FAO, 2006). Traditionally, forests have been valued mostly for their wood and pulp products. This is not surprising, since, for example, in Canada the forest product industry generates about \$78 billion in annual revenues and accounts for 5% of all the jobs in the country (FPAC, 2008). However, more recently, planting and managing of forests have been proposed as a potential means to sequester atmospheric CO₂, to offset human greenhouse gas emissions (IPCC, 2000; Watson and Noble, 2005). This is because forests dominate the carbon exchange between the terrestrial biosphere and the atmosphere (Puhe and

Ulrich, 2001). Therefore, forests are quickly becoming a valuable new commodity (i.e. in the sense that they have the potential to absorb and store carbon) in the emerging global carbon economy (Barford et al., 2001; Gough et al., 2008; Jarvis et al., 2005). As such, they drive the need for research on understanding and predicting forest carbon budgets and dynamics.

Forest's net carbon balance consists of two major fluxes: CO₂ sequestration through photosynthesis and CO₂ emission through respiration processes. While photosynthesis, in the form of gross primary or ecosystem productivity (GPP or GEP, respectively, where GEP is GPP less autotrophic respiration), has been extensively studied and is mechanistically modelled (c.f. Farquhar et al., 1980) the same cannot be said for ecosystem respiration (Re). Yet, of the two fluxes it is Re that has been shown to determine the annual net carbon sink/source strength of forest ecosystems (Valentini et al., 2000).

Ecosystem respiration consists of a number of components, such as soil, foliar, and woody tissue respiration¹. Of all the major components, soil respiration (Rs) often dominates Re, accounting for up to 90% of ecosystem CO₂ emissions (Hanson et al., 2000). Therefore, understanding the dynamics and driving causes of Rs is worth particular attention in studies of forest ecosystem respiration. Individually, all three components have been shown to vary

¹ Note that only live woody-tissue respiration has been considered in this dissertation, due in part to limited resources and time for the experiments. However, past studies have indicated that the contribution from decomposition of dead wood tissue has a smaller contribution to Re, compared to the three major fluxes we considered. For example, in the study by Tang et al (2008) quoted in Chapter 5, respiration from coarse woody debris was only 4-3% compared to soil (67-72%), foliage (8-11%), and live woody-tissue (8-11%). Furthermore, at our youngest stand there was yet no dead wood accumulation.

temporally and spatially, with variability accredited to a number of environmental and biological factors (ex.: Lavigne, 1996; Maier, 2001; Matteucci et al., 2000; Monsoon et al., 2006; Vose and Ryan, 2002). However, the interactions of individual component fluxes with each other, their environment and stand physiology are still poorly understood, especially in young to mature afforested sites.

1.2 Novel aspects of this study

1.2.1 Filling gaps in literature on studies of Re and its component fluxes across different-aged coniferous forests in eastern North America

If forests are to be used for carbon management purposes, it is crucial to know how their annual and seasonal carbon budgets and dynamics vary with stand age. Re is an important component of a forest's carbon cycle. Variability in Re will reflect variability of its component fluxes. Several studies are available in the literature, which assess Re composition of forests using scaled-up chamber measurements (Boldstad et al., 2004; Griffis et al., 2004; Gaumont-Guay et al., 2006; Harmon et al., 2004; Lavigne et al., 1997; Law et al., 1999; Tang et al., 2008; Zha et al., 2007). However, most of these studies focused on naturally-regenerated or post-harvest stands, some of which are over old-growth forests, over 100-years-old. However, recently afforested or planted sites can behave differently from naturally regenerated and old-growth stands, especially if influenced by their past land-use history and resulting stand characteristics.

This dissertation focuses on characterizing R_e and its components in young to mature (6-70 years-old) forests, planted on marginal lands and abandoned agricultural lands in the temperate climate of eastern North America, where plantation forests make-up a significant portion of the land cover and afforestation has a great potential for atmospheric carbon sequestration. Therefore, results from this dissertation will fill some knowledge gaps in an emerging research field.

1.2.2 Improving models used to simulate and assess respiration

In terrestrial carbon research, models are widely used to fill data gaps or to simulate daily, seasonal, and annual C emissions from a smaller sample of observations. Respiration (R_i) is very often modeled as a function of temperature (T_i), using the modified van't Hoff's equation (van't Hoff, 1884), also known as the Q_{10} -model (Qi et al., 2002; Davidson et al., 2005; Lloyd and Taylor, 1994). One general form of this function is:

$$R_i = R_{10} * Q_{10}^{\frac{(T_i-10)}{10}} \quad 1.1$$

where R_i is CO_2 efflux of component i , T_i is temperature of the respiring component i , and R_{10} and Q_{10} are parameters to be estimated. R_{10} represents R_i at $10^\circ C$ and Q_{10} describes the sensitivity of R_i for every $10^\circ C$ increase in T_i . The limitation of the above model is that both R_{10} and Q_{10} model parameters are assumed constant. However, a large body of literature already exists which shows

that Q_{10} values do vary spatially and temporally (Qi et al., 2004; Davidson et al., 2005), often confounded by other abiotic and biotic drivers, including: moisture (Davidson et al., 1998; Jassal et al., 2008), photosynthesis (Högberg et al., 2001), root activity (Boone et al., 1998; Lavigne et al., 2003), and foliar production (Curiel-Yuste et al., 2004). Similarly, temporal variability in R_{10} is also known (Curiel-Yuste et al., 2004), although it receives less attention in literature compared to Q_{10} variability.

Some researchers do compute seasonal R_{10} and Q_{10} values in their studies (Curiel-Yuste et al., 2004; Rey et al., 2002). They accomplish this by separating their data into categories and fitting the model *separately* to each category. Yet often the different driving factors of temporal variability in R_i , such as temperature and moisture, confound each other, potentially masking each other's explanatory power of R_i variability, depending on the time of year or environmental conditions. For example, in some sites prone to summer drought conditions, soil moisture tends to decrease with increasing temperatures, causing respiration to also decrease due to drought stress, despite warmer temperatures that normally would enhance respiration if sufficient moisture was available. Therefore, there seemed a need for two things in our field of research: 1) a statistical method that would modify the Q_{10} model, such that both of its model parameters, R_{10} and Q_{10} , can vary seasonally, interannually, and decadal; and 2) a method that would allow one to assess the relative importance of the individual

driving factors in the context of the other factors. Both of these issues are addressed in this dissertation (see Chapter 2 and Chapter 3).

At this point, we would like to acknowledge that in the final months of preparing this dissertation, a study was published, which also proposed a method of data analysis that allowed for Q_{10} and R_{10} to vary with time (i.e. Gu et al., 2008). This study was unknown to us prior to our method development. Gu et al. (2008) proposed a general method of analysis, applicable to any mathematical function describing soil respiration and soil temperature, which included the Q_{10} model. Their method is called the “localized” ratio fitting.

However, there are a number of differences between the method we propose and the method proposed by Gu et al. (2008), which still makes this study, and results, valuable to our research colleagues. For one, our approach is suitable for use with, both, large, high-frequency, data sets used by Gu et al. (2008), as well as smaller, low-frequency, data sets, such as those collected using manual chamber methods. In contrast, the Gu et al. (2008) approach works best with high frequency data, such as that from automated soil chamber measurements. Secondly, with our approach, the model can be expanded to include a number of additional driving factors, both qualitative (or categorical) and quantitative. In contrast, Gu et al. (2008) discuss the implementation of temporal variability only. Thirdly, our analytical method allows one to assess the relative importance of each explanatory factor to the model’s explanatory power. Such useful analysis was not part of Gu et al. (2008) work. Thus, there is merit to both approaches and

it is up to the individual researcher to decide which approach will work best for their particular application.

1.2.3 Unique methodology

In past studies, several different chamber systems have been used to measure the various Re components. However, to use a single system to measure all the major components of Re would seem most appropriate, since this way any variability in measurements, due to instrumentation differences, can be avoided. So far there have not been any published study in which all three major Re components (i.e. soil, foliar, and woody tissue) have been measured by a single chamber system, or exclusively by using the LI-6400 system. LI-6400 has several advantages over some other chamber systems, in that it is commercially available, compact and completely portable, and well calibrated for accuracy in measured fluxes. Furthermore, little auxiliary equipment is needed to set it up in the field to measure the various components of ecosystem respiration.

1.3 Study site –Turkey Point Flux Station, TPFS

The majority of respiration and supporting measurements used in this dissertation have been collected at the Turkey Point Flux Station (TPFS). The site was established in 2002 by the McMaster Climate Change Research Group. TPFS consists of four, afforested, white pine (*Pinus Strobus* L.) forest stands, aged: 70-, 35-, 20- and 7- years-old, as of 2009. They are located within 20 km of each

other, on the north-western shore of Lake Erie, in southern Ontario, Canada (42° 42' 55'' N and 80° 22' 20'' W) (Figure 1.1). The two oldest stands (70- and 35-year-old) were planted to stabilize local sandy soils, while the younger two stands (20- and 7-year-old) were planted on abandoned agricultural lands (last cultivated about 10 years prior to tree planting). Throughout this text, we refer to the four sites by their shortened code names: TP39, TP74, TP89, and TP02, respectively. The acronyms correspond to “Turkey Point”, followed by the short-form of stand’s establishment year, i.e. 1939, 1974, 1989, and 2002, respectively. TPFS is part of a global network of sites that measure carbon exchange of various ecosystems, called Fluxnet. In global Fluxnet synthesis data archives, TPFS sites are referred to as CA-TP4, CA-TP3, CA-TP2 and CA-TP1 (70-, 35-, 20- and 7-year-old, respectively).

1.4 Overview of methodology

One way to assess ecosystem respiration (R_e) is by the eddy covariance (EC) tower method (Baldocchi, 2003). Another, independent, way is through scaled-up chamber measurements (Lavigne et al., 1997; Law et al., 1999; Tang et al., 2008). Each method has some level of uncertainty associated with it and systematic differences between the methods exist, often requiring adjustment factors before data sets are compared (Lavigne et al., 1997; Law et al., 1999; Norman et al., 1997; Tang et al., 2008). However, chamber methods have one major advantage over the EC method: they allow researchers to appropriate

CO₂ emissions to various ecosystem components, such as soil, foliage, and woody tissue.

Several chamber systems, portable and automated, are available that can be used to estimate R_e in forest ecosystems (Leverenz and Hallgren, 1991; Sprugel and Benecke, 1991; Norman et al., 1997, Gaumont-Guay et al., 2006). Both types of systems have their advantages and disadvantages. For example, automated systems are better at capturing finer details of the temporal trends in respiration by providing continuous measurements of emissions. In contrast, continuous measurements with a portable system are not possible due to manual labour constraints. However, portable chambers are better at capturing the spatial variability of respiration. Also portable systems tend to be less costly to install and maintain, compared to the automated systems.

In this study, a portable chamber system was used: the LI-6400 photosynthesis system with various chamber attachments, developed by LI-COR Inc., Nebraska, USA (Figure 1.2). The LI-6400 is an infrared gas analyzer (IRGA)-based instrument, set to detect carbon dioxide gas (CO₂) and water vapour (H₂O) changes in sampled air (CO₂ detection limits of about $\pm 0.2 \mu\text{mol CO}_2$ per m² of measured tissue per second). Component fluxes, measured with the LI-6400, were upscaled to stand level (on per ground area basis) using biometric indices (i.e. sapwood volume for R_w and site specific leaf area indices² for R_f).

² Leaf area index (LAI) is defined as one half the total green leaf area per unit ground surface area (Chen and Black, 1992).

1.5 Study Objectives

The objectives of this dissertation were:

(1) To measure and characterize intersite and temporal variability of R_e and its component fluxes across four forests of different ages. The studied component fluxes included: soil respiration (autotrophic and heterotrophic), foliar, and live woody tissue respiration.

(2) To develop empirical models for simulating carbon emissions of the various respiratory components, which were measured periodically using a portable chamber system.

(3) To quantify and compare the contribution of soil, foliage, and live woody-tissue respiration to total ecosystem respiration across the forests of different ages on daily, seasonal, and annual time scales; and

(4) To compare total ecosystem respiration derived from scaled-up chamber measurements with that derived from eddy covariance tower measurements across the forests of different ages.

Results presented in this dissertation should be of interest to carbon cycle modellers, field ecologists, the eddy covariance research community, and those involved in forest carbon accounting, management, and policy development.

1.4 REFERENCES

Baldocchi (2003) Assessing the eddy covariance technique for evaluating carbon dioxide exchange rates of ecosystems: past, present and future. Review. *Global Change Biology*. 9: 479-492.

- Barford CC, Wofsy SC, Goulden ML, Munger JW, Pyle EH, Urbanski SP, Hutyra L, Saleska SR, Fitzjarrald D, Moore K (2001) Factors controlling long- and short-term sequestration of atmospheric CO₂ in a mid-latitude forest. *Science*, 294: 1688-1691.
- Bates, B.C., Z.W. Kundzewicz, S. Wu and J.P. Palutikof, *Eds.* (2008) Climate Change and Water. Technical Paper of the Intergovernmental Panel on Climate Change, IPCC Secretariat, Geneva, 210 pp.
- Bolstad PV, Davis KJ, Martin J, Cook BD, Wang W (2004) Component and whole-system respiration fluxes in northern deciduous forests. *Tree Physiology*, 24 (5): 493-504.
- Chen JM and Black TA (1992) Defining leaf area index for non-flat leaves. *Plant, Cell and Environment*, 15: 421-429.
- Curiel-Yuste J, Janssens IA, Carrara A, Ceulemans R (2004) Annual Q₁₀ of soil respiration reflects plant phenological patterns as well as temperature sensitivity. *Global Change Biology*, 10: 161-169.
- Davidson EA, Belk E, Boone RD (1998) Soil water content and temperature as independent or confounded factors controlling soil respiration in a temperate hardwood forest. *Global Change Biology*, 4: 217-227.
- Davidson EA, Janssens IA, Luo Y-Q (2006) On the variability of respiration in terrestrial ecosystems: moving beyond Q₁₀. *Global Change Biology*, 11: 1-11.
- Dixon RK, Brown S, Houghton RA et al (1994) Carbon Pools and flux of global forest ecosystems. *Science*, 263, (5144): 185-190.
- Farquhar GD, von Caemmerer S, Berry JA (1980) A Biochemical Model of Photosynthetic CO₂ Assimilation in Leaves of C₃ Species. *Planta*, 149: 78-90.
- Food and Agriculture Organization of the United Nations (FAO) (2006) Global Forest Resources Assessment 2005. Rome, Italy, 2006. available online at www.fao.org/forestry/site/fra2005/en [January 22, 2008].
- Forest Product Association of Canada (FPAC) (2008) Canada's forest products industry: Economic Outlook. December 16_press_kit_en.
- Gaumont-Guay D, Black TA, Griffis T, Barr AG, Morgenstern K, Rachhpal SJ, Nescic Z (2006) Influence of temperature and drought on seasonal and

- interannual variations of soil, bole, and ecosystem respiration in a boreal aspen stand. *Agricultural and Forest Meteorology*, 140: 203-219.
- Gu L, Hanson PJ, Post WM, Liu Q (2008) A novel approach for identifying the true temperature sensitivity from soil respiration measurements. *Global Biogeochemical Cycles*, 22: GB4009.
- Hanson PJ, Edwards NT, Garten CT, Andrews JA (2000) Separating root and soil microbial contributions to soil respiration: A review of methods and observations. *Biogeochemistry*, 48: 115-146.
- Högberg P, Nordgren A, Buchmann N et al (2001) Large-scale forest girdling shows that current photosynthesis drives soil respiration. *Nature*, 411: 789-792.
- IPCC (Intergovernmental Panel on Climate Change) Special Report (2000): Land Use, Land-Use change, and Forestry: Summary for policy makers. Watson RT et al. (Eds). Cambridge University Press, Cambridge.
- Janssens IA, Dore S, Epron D, Lankreijer H, Buchman N, Longdoz B, Brossaud J, Montagnani L (2003) Climatic Influences on Seasonal and Spatial Differences in Soil CO₂ Efflux. In Vantini R (Ed), *Fluxes of Carbon, Water and Energy of European Forests*. Ecological Studies 163. Springer-Verlag Berlin Heidelberg. Pp.: 233-253.
- Janssens IA, Lankreijer, Matteucci G, Kowalski AS, Buchmann N, Epron D, Pilegaard K, Kutsch W, Longdoz B, Grunwald T, Montagnani L, Dore S, Rebmanns C, Moors j, Grelle A, Rannik U, Morgenstern K, Oltchev S, Clement R, Gudmundsson J, Minerbi S, Berbigier P, Ibrom A, Moncrieff J, Aubinet M, Bernhofer C, Jensen NO, Vesala T, Granier A, Schulze E-D, Valentini R (2001) Productivity overshadows temperature in determining soil and ecosystem respiration across European forests. *Global Change Biology*. 7: 269-278.
- Jarvis PG, Ibrom A, Linder S (2005) ‘Carbon forestry’: managing forests to conserve carbon. In The Carbon Balance of Forest Biomes by Griffiths H and Jarvis PG (Eds). Taylor and Francis Group, NY, USA. Pp.331-349.
- Jassal RS, Black A, Novak MD, Gaumont-Guay D, and Nestic Z (2008) Effect of soil water stress on soil respiration and its temperature sensitivity in an 18-year-old temperate Douglas-fir stand. *Global Change Biology*, 14: 1-14.

- Keeling, CD, Chin JFS, Whorf TP (1996) Increased activity of northern vegetation inferred from atmospheric CO₂ measurements. *Nature* 382 (6587): 146-49.
- Lavigne (1996) Comparing stem respiration and growth of jack pine provenances from northern and southern locations. *Tree Physiology*. 16: 847-852.
- Lavigne MB, Boutin R, Foster RJ, Goodine G, Bernier PY, Robitaille G (2003) Soil respiration responses to temperature are controlled more by roots than by decomposition in balsam fir ecosystems. *Canadian Journal of Forest Research*, 33: 1744-1753.
- Lavigne MB, Ryan MG, Anderson DE, Baldocchi DD, Crill PM, Fitzharrald DR, Goulden ML, Gower ST, Massheder JM, McCaughey JH, Rayment M, Striegl RG (1997) Comparing nocturnal eddy covariance measurements to estimates of ecosystem respiration made by scaling chamber measurements at six coniferous boreal sites. *Journal of Geophysical Research*, 102: D24, 28,977-28,985.
- Law BE, Ryan MG, Anthoni PM (1999) Seasonal and annual respiration of a ponderosa pine ecosystem. *Global Change Biology*, 5: 169-182.
- Leverenz JW and Hallgren J-E (1991) Measuring Photosynthesis and Respiration of Foliage. In: Techniques and approaches in forest tree ecophysiology (Lassoie JP and Hinckely TM, eds). CRC Press Inc.: Boca Raton, Florida, pp.295-324.
- Lindner M and Karjalainen T (2007) Carbon inventory methods and carbon mitigation potentials of forests in Europe: a short review of recent progress. *European Journal of Forest Research*, 126: 149-156.
- Lindroth A, Lagergren F, Aurela M, Bjarnadottir B, Christensen T, Dellwik E, Grelle A, Ibrom A, Johansson T, Lankreijer H, Launiainen S, Laurila T, Vesala T (2008) Leaf area index is the principal scaling parameter for both gross photosynthesis and ecosystem respiration of Northern deciduous and coniferous forests. *Tellus B*, 60(2): 129-142.
- Liu J, Peng C, Apps M, Dang Q, Banfield E, Kurz W (2002) Historic carbon budgets of Ontario's forest ecosystems. *Forest Ecology and Management*, 169: 103-114.
- Lloyd, J and Taylor, JA (1994) On the temperature dependence of soil respiration. *Functional Ecology*, 8: 415-424.

- Maier CA (2001) Stem growth and respiration in loblolly pine plantations differing in soil resource availability. *Tree Physiology*, 21: 1183-1193.
- Matteucci G, Stivanello D, Stivaleno D (2000) Soil respiration in a Beech and Spruce forests in Europe: trends, controlling factors, annual budgets and implications for the ecosystem carbon balance. In Schulze ED: Carbon and nitrogen cycling in European forest ecosystems. Ecological Studies 142. Springer, Berlin: 217-236.
- Monson RK, Lipson DL, Burns SP, Turnipseed AA, Delany AC, Williams MW, Schmidt SK (2006) Winter forest soil respiration controlled by climate and microbial community composition. *Nature*, 439: 711-714.
- Nabuurs GJ, Päivinen R, Sikkema R, Mohren GMJ (1997) The role of European forests in the global carbon cycle – a review. *Biomass and Bioenergy*, 13: 345-358.
- Noormets A, Chen J, Crow T (2007) Age-dependent changes in ecosystem carbon fluxes in managed forests in northern Wisconsin, USA. *Ecosystems*, 10: 187-203.
- Norman, J.M., Kucharik, C.J., Gower, S.T., Baldocchi, D.D., Crill, P.M., Rayment, M., Savage, K., Striegl, R.G. December 26, 1997. A comparison of six methods for measuring soil-surface carbon dioxide fluxes. *Journal of Geophysical Research*, 102, D24: 28,771-28-777.
- Pregitzer KS and Euskirchen ES (2004) Carbon cycling and storage in world forests: biome patterns to forest age. *Global Change Biology*, 10: 2052-2077.
- Puhe J and Ulrich B (2001) Global climate change and human impacts on forest ecosystems: Postglacial development, present situation, and future trends in central Europe. Ecological Studies 143. Springer, Berlin. Pp. 91.
- Pumpanen J, Ilvesniemi H, Peramaki M, Hari P (2004) Seasonal patterns of soil CO₂ efflux and soil air CO₂ concentration in a Scots pine forest: comparison of two chamber techniques. *Global Change Biology*, 9: 371-382.
- Qi Y, Xu M, Wu J (2002) Temperature sensitivity of soil respiration and its effects on ecosystem carbon budget: nonlinearity begets surprises. *Ecological Modelling*. 154: 141-142.

- Rey A, Pegoraro E, Tedeschi V, De Parri I, Jarvis PG, Valentini R (2002) Annual variation in soil respiration and its components in a coppice oak forest in Central Italy. *Global Change Biology*, 8: 851-866.
- Ryan and Law (2005) Interpreting, measuring, and modeling soil respiration. *Biogeochemistry*, 73: 3-27.
- Scott-Denning A, Fung IY, Randall D (1995) Latitudinal gradient of atmospheric CO₂ due to seasonal exchange with land biota. *Nature*, 376: 240-243.
- Sprugel DG and Benecke U (1991) Measuring Woody-Tissue Respiration and Photosynthesis. *In: Techniques and approaches in forest tree ecophysiology* (Lassoie JP and Hinckley TM, eds). CRC Press Inc.: Boca Raton, Florida, pp.330-355.
- Tang J, Bolstad PV, Desai AR, Martin JG, Cook BD, Davis KJ, Carey EV (2008) Ecosystem respiration and its components in an old-growth forest in the Great Lakes region of the United States. *Agricultural and Forest Meteorology*, 148: 171-185.
- Valentini R, Matteucci G, Dolman AJ, Schulze E-D, Rebmann C, Moors EJ, Granier A, Gross P, Jensen NO, Pilegaard K, Lindroth A, Grelle A, Bernhofer C, Grunwald T, Aubinet M, Ceulemans R, Kowalski AS, Vesala T, Rannik U, Berbigier P, Loustau D, Gudmundsson J, Thorgeirsson H, Ibrom A, Morgenstern K, Clement R, Moncrieff J, Montagnani L, Minerbi S, Jarvis PG (2000) Respiration as the main determinant of carbon balance in European forests. *Nature*, 404: 861-865.
- Van't Hoff JH (1884) *Etudes de dynamique chimique*. Frederrk Muller & Co., Amsterdam.
- Vose and Ryan (2002) Seasonal respiration of foliage, fine roots, and woody tissues in relation to growth, tissue N, and photosynthesis. *Global Change Biology* 8: 182-193.
- Watson RT and Noble IR (2005) The global imperative and policy for carbon sequestration. *In The Carbon Balance of Forest Biomes* by Griffiths H and Jarvis PG (Eds). Taylor and Francis Group, NY, USA. Pp.1-17.
- Zha TS, Xing ZS, Wang KY, Kellomaki S, Barr AG (2007) Total and component fluxes of a Scots pine ecosystem from chamber measurements and eddy covariance. *Annals of Botany*, 99: 345-353.

Figure 1.1 : At the time of this study, Turkey Point Flux Station was an associate site of former Fluxnet-Canada (now the Canadian Carbon Program). It is located on the northern edge of Lake Erie in southern Ontario, Canada.

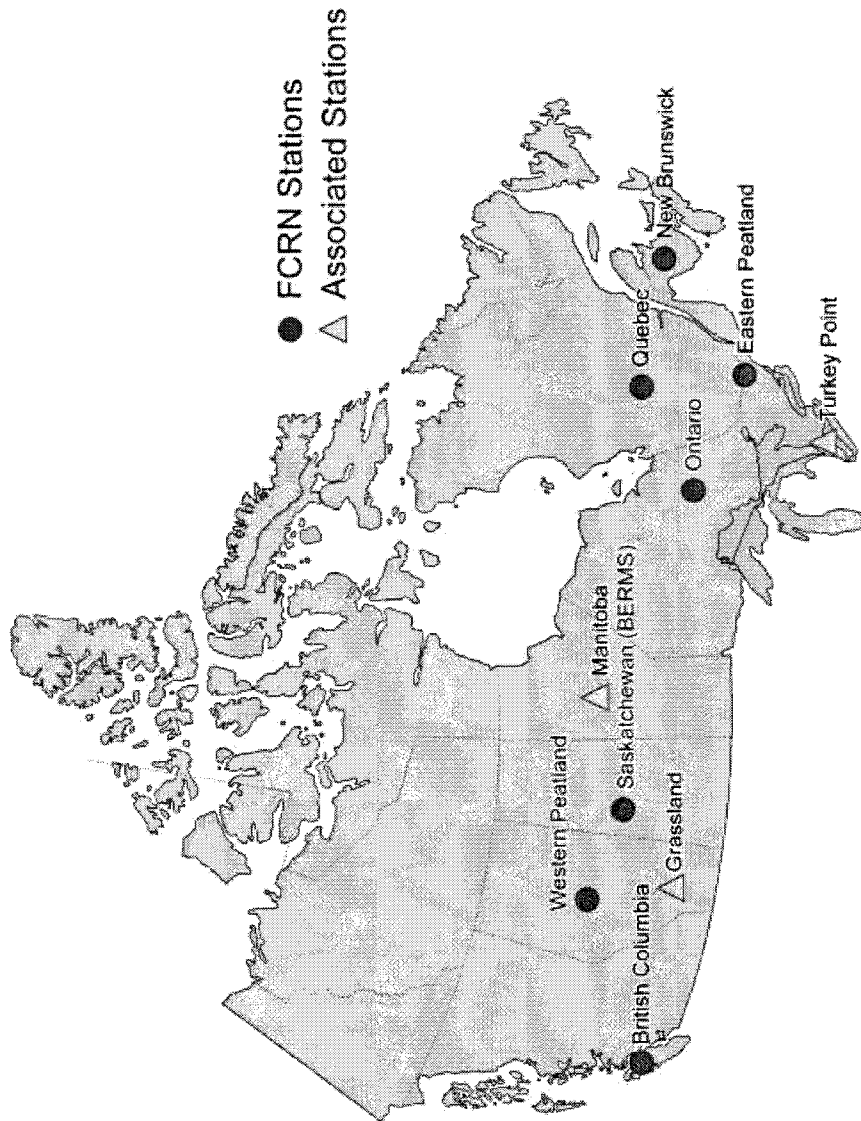
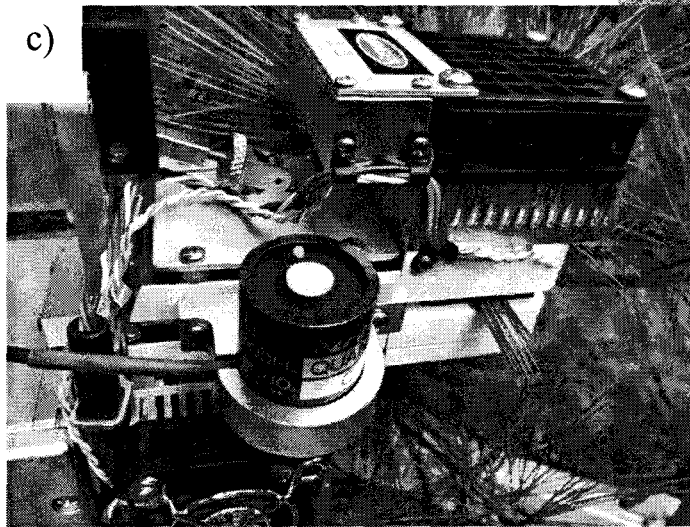
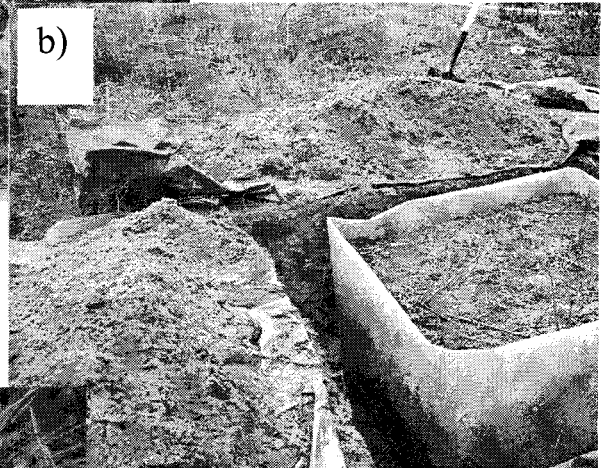
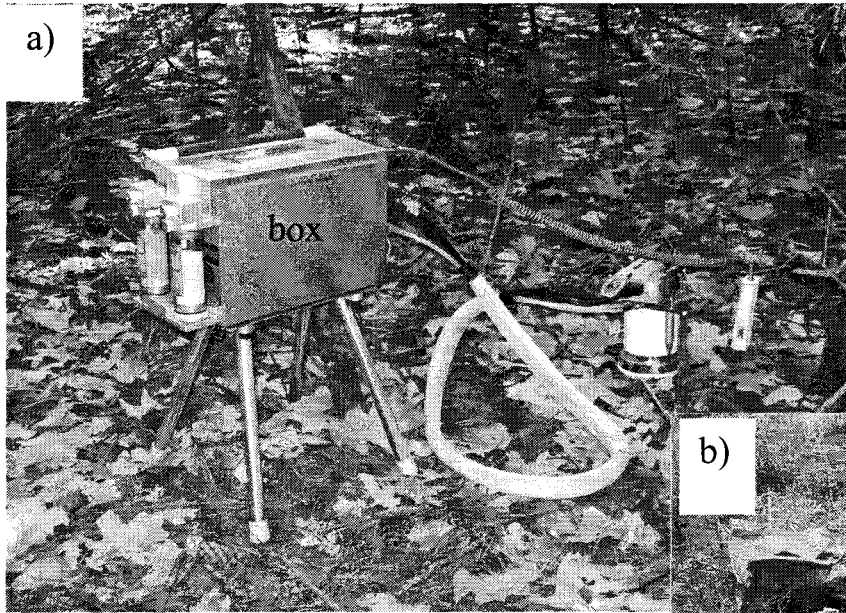


Figure 1.2: a) the LI-COR 6400 instrument with the 6400-009 soil chamber attachment, used to measure soil respiration during this study. In the photo the chamber, on the right, is actually placed above one of the collars used for R_s measurements. Next to the chamber is the soil temperature probe (6400-013), inserted into soil. The “box” is the console, a computer that controls the instrument. The IRGA analyzer is connected directly to the soil chamber (the rectangular block with plumbing, right on top of the chamber).

b) A sample trenched plot at TP02, lined with industrial landscape cloth, before being back-filled with soil. These were dug to help estimate heterotrophic component of R_s at the sites. The soil collars for R_h measurements were installed inside each square, as described in Chapter 5.

c) View of foliar 2x3 LI-6400 chamber, fitted with the artificial light source, for R_f measurements. Needles were placed inside the chamber for measurement, lined-up in a single layer, along the chamber’s length (see Chapter 5 for more details).

d) Sample collar attached to the tree bole at TP39, used for R_w measurements (see Chapter 5 for more details) with the LI-6400 and its soil chamber attachment. The soil chamber was attached horizontally against the tree trunk, to the collar, during measurements.



CHAPTER 2

CHARACTERIZING TEMPORAL VARIABILITY OF SOIL RESPIRATION AND ITS TEMPERATURE SENSITIVITY IN DIFFERENT-AGE FORESTS³

2.1 ABSTRACT

We characterized the temporal variability of temperature-sensitivity of soil respiration (R_s) across four pine forests of different age (67-, 32-, 17- and 4- year-old), growing in the temperate climate of eastern North America. The Q_{10} model was used in the analysis, since it is one of the most widely-used empirical models in carbon research for simulating carbon emissions driven by temperature variability. We developed a novel way of implementing temporal variability into the conventional Q_{10} model, using a combination of statistical approaches. We also considered the influence of soil moisture on the relationship. The resulting temporally-flexible and moisture-sensitive Q_{10} model better reflected the temporal changes of our observed data sets by allowing both, R_{10} – respiration at 10 °C and Q_{10} - the temperature sensitivity of respiration for every 10 °C increase, to vary seasonally, interannually, and between four forests of different age. R_{10} values were lowest (0.64 to 1.83 $\mu\text{mol CO}_2 \text{ m}^{-2} \text{ s}^{-1}$) for the youngest stand with an open canopy and highest (0.85 to 2.46 $\mu\text{mol CO}_2 \text{ m}^{-2} \text{ s}^{-1}$) for the 67- and 17-year-old stands with closed canopies. R_{10} values increased from winter to summer months. They were lowest (0.64 to 0.85 $\mu\text{mol CO}_2 \text{ m}^{-2} \text{ s}^{-1}$) when soil temperature (T_s) was below 4 °C and highest (1.83 to 2.46 $\mu\text{mol CO}_2 \text{ m}^{-2} \text{ s}^{-1}$) when T_s was above 14 °C. R_{10} values were higher for years with higher mean annual air temperatures.

Q_{10} values were also lowest (1.03 to 3.93) at the youngest stand and highest (1.24 to 4.76) at the 67- and 17-year-old stands. However, the highest Q_{10} values (3.46 to 4.76) were observed when T_s was between 4 to 14 °C, mostly during spring and autumn months. This T_s range was most likely the “ecologically optimum” T_s range for fine root growth at our forest sites. Seasonally, the lowest Q_{10} values (1.03 to 1.42) were observed when T_s was above 14 °C, mostly during summer months. Interannually, the highest Q_{10} values were obtained for the year with the highest total annual precipitation.

We show that accounting for seasonality in the conventional Q_{10} model improved the model fit to observed R_s by 12%, accounting for intersite variability improved the model fit by 4.2 %, accounting for interannual variability improved the model fit by 0.6%, while accounting for soil moisture variability improved the model fit by only 0.3%. This study adds to our understanding of the dynamics of the R_s - T_s relationship at seasonal and inter-annual, time scales, as well as

³ A modified version of this chapter was submitted for publication to *Agricultural and forest meteorology* in April 2009: Khomik M, Arain MA, Liaw K-L (2009) Characterizing temporal variability of soil respiration and its temperature sensitivity in different-age forests (*in Review*).

between forests of different age. It will be of interest to carbon cycle modellers, field ecologists, and the eddy covariance community.

2.2 INTRODUCTION

In forest ecosystems soil respiration (Rs) can account for up to two thirds of annual ecosystem respiration (Hanson et al., 2000; Valentini et al., 2000). Therefore, errors in its estimation can introduce major uncertainty in the annual carbon (C) budget of a forest. Forest Rs consists mostly of rhizospheric respiration (Ra) and heterotrophic respiration (Rh). Ra refers to carbon dioxide gas (CO₂) emissions from the soil due to the metabolic activity of roots and their associated microorganisms, while Rh refers to CO₂ emissions due to the metabolic activity of soil organisms involved in soil organic matter decomposition. The contribution of each component to total Rs varies temporally and spatially (Hanson et al., 2000; Lavigne et al., 2003 and 2004).

Temporal variability of Rs is often exponentially related to temporal variability in soil temperature (Ts). The Rs-Ts relationship is often modeled by the modified van't Hoff's equation (van't Hoff, 1884), also known as the Q₁₀-relationship (Qi et al., 2002; Davidson et al., 2005; Lloyd and Taylor, 1994). One general form of this formulation is:

$$R_{S_i} = R_{10,i} Q_{10,i}^{\frac{(T_{s,i}-10)}{10}} \quad 2.1$$

where for an *i*th observation: R_{S_i} is soil CO₂ efflux, T_{s_i} is soil temperature, and $R_{10,i}$ and $Q_{10,i}$ are the model parameters to be estimated. R_{10} represents Rs at 10 °C and Q_{10} describes the sensitivity of Rs for every 10 °C increase in T_s .

Q_{10} values have been shown to vary spatially and temporally (Curiel-Yuste et al., 2004, Qi et al., 2004) and are often confounded by abiotic and biotic factors, including: soil moisture (Davidson et al., 1998; Jassal et al., 2008), photosynthesis (Högberg et al., 2001), root activity (Boone et al., 1998; Lavigne et al., 2003), canopy cover (Curiel-Yuste et al., 2004) and substrate availability (Liu et al., 2006). Further problems may arise from the variable T_s -sensitivity of the different R_s sources, mainly R_a and R_h (Lavigne et al., 2003, Gaumont-Guay et al., 2008). Their variable percent contribution to total R_s throughout the year may reduce, enhance, or overshadow the individual responses and thus may lead to erroneous Q_{10} estimates. For example, R_a contribution to R_s may be more pronounced during the growing season, compared to R_h . Therefore, R_a sensitivity to T_s may dominate during the growing season, as opposed to the non-growing season when Q_{10} may be more reflective of R_h 's temperature sensitivity.

Variability of R_{10} has not received much attention in literature compared to Q_{10} , despite the fact that base respiration which depend on the soils' carbon content and quality, as well as the seasonal dynamics of microbial populations is also expected to vary temporally. For example, Scott-Denton et al. (2006) have shown that in winter large amounts of sucrose can be released by frost-damaged trees, providing increased substrate availability for microbial decomposition and thus increased R_s . Similarly, different microbial populations have been shown to thrive under different soil temperature regimes, increasing in population during certain times of year (Monson et al., 2006). Temporal variability in

photosynthesis and translocation of photosynthates to the rhizosphere may also cause temporal variability in R_a (Carbone et al., 2007).

The conventional form of the Q_{10} model, as shown in Equation 2.1 does not allow R_{10} and Q_{10} to vary temporally. Some researchers (Curiel-Yuste et al., 2004; Lavigne et al., 2004) have reported seasonal R_{10} and Q_{10} values by separating their measured data into seasons and then fitting the model to each subset of data separately. However, often in observational data, different driving factors have overlapping explanatory powers and evaluating sub-sets of the observed data separately may not account for such overlap (Otomo and Liaw 2003). Therefore, there is a need for a method, which may allow both R_{10} and Q_{10} model parameters to vary temporally to enable carbon cycle researchers to assess the explanatory power of the different driving factors used in empirical respiration models.

The objective of this study was to characterize temporal variability of R_{10} and Q_{10} across an age-sequence (67, 32, 17, and 4 year-old) of temperate pine forests, using three years (2004-2006) of measured soil respiration data. The temporal scales we considered were: seasonal, interannual, and between the four stands of varying age, to which we will refer to as “decadal”⁴. For this analysis, we used a modified version of the Q_{10} model, which allowed for temporal flexibility in R_{10} and Q_{10} parameters and also included soil moisture variability.

⁴ Note that for investigating true decadal variability, it would have been statistically most proper to have several replicates of the four different-aged stands we studied. This however was not feasible practically due to limited resources and logistics.

We derived this modified Q_{10} model, using dummy variables and multivariate linear regression analysis.

2.3 METHODS

2.3.1 Study sites

Study sites are located on the north-western shore of Lake Erie in southern Ontario, Canada (42°N, 80°W) and they are known as at the Turkey Point Flux Station (TPFS). TPFS consists of four, afforested, white pine (*Pinus Strobus* L.) stands (67-, 32-, 17- and 4-year-old, at the time the study ended in 2006), located within 20 km of each other. Hereafter, we refer to the four stands by their shortened code names: TP39, TP74, TP89, and TP02, respectively. The acronyms correspond to “Turkey Point”, followed by the short-form of year the stand was established, i.e. 1939, 1974, 1989, and 2002, respectively.

All four stands grow on sandy soil (Brunisolic Gray Brown Luvisols, following the Canadian Soil Classification Scheme (Presant and Acton, 1984)). TP39 and TP74 were planted on marginal nutrient poor soils, while TP89 and TP02 were planted on former agricultural lands (last cultivated about 10 years prior to afforestation). At the time of this study, TP39, TP74 and TP89 had relatively closed canopies and an accumulated organic forest soil layer (i.e. LFH horizon), while TP02 had an open canopy and no accumulated LFH layer (Table 1). The climate in the region is cool temperate, with annual mean air temperature

of 7.8 °C and annual mean precipitation of 1010 mm, distributed evenly throughout the year, of which 133 mm falls as snow (based on a 30-year-record from a World Meteorological Organization (WMO)-accredited, Environment Canada, weather station, located 10 km north of TPFS, at Delhi, Ontario). Some additional site characteristics are given in Table 2.1. Further site details are given in Arain and Restrepo-Coupé (2005) and Peichl and Arain (2006).

2.3.2 Flux and meteorological measurements

At each stand, R_s was measured on a biweekly to monthly basis from January 1, 2004 to December 31, 2006, along 50-m-long transects, using a LI-COR 6400 portable photosynthesis system that had a LI-COR 6400-09 soil chamber attachment and a LI-COR 6400-013 soil temperature probe attachment (LI-COR, inc., Lincoln, Nebraska, USA). Along each transect, 12 permanent sampling locations were established. At each sampling point, three replicate R_s measurements were recorded. At the same time, soil temperature ($T_{s_LI_COR}$) was also measured, within 20-30 cm of each collar, at 15 cm depth, using the 15-cm-long temperature probe (LI-COR 6400-013) inserted vertically to its full length. Half-hourly meteorological variables, such as radiation, air temperature, humidity and soil temperature (2, 5, 10, 20, 50, 100 cm depths) and soil moisture (5, 10, 20, 50, 100 cm depths) were measured year-round at all four sites using automated weather stations (Campbell Scientific Inc. (CSI), Logan, Utah, USA). These weather stations were part of the eddy covariance flux measurements carried-out

across TPFS (Arain and Restrepo-Coupé, 2005). Precipitation was measured at TP39 using a heated tipping bucket rain gauge (model 52202; R.M. Young Company, Michigan, USA), mounted above the canopy on the flux tower. Above canopy air temperatures across all four sites were comparable (for a 1:1 linear relationship, $R^2=1.00$ and slope = 1.0, plot not shown). Therefore, the annual climatic variables presented below are those from the main TPFS site, TP39.

2.3.3 Model development and data analysis

2.3.3.1 Identifying temporal variability in measured climatic variables and Rs

Interannual variability in climatic variables between the three study years indicated that mean annual air temperature in 2004 was only 1.3% higher than the 30-year normal for the area and was only about 5% (55 mm) drier than the normal (Figure 2.1b). In contrast, both 2005 and 2006 were warmer by 17 % (1.3°C) and 26 % (2.0°C) respectively, compared to the normal. Year 2005 was drier than the normal by 15% (148 mm), while year 2006 was wetter by 18% (177 mm). R_s also appeared to vary interannually, being higher in the warmest (2005) and wettest (2006) years, compared to the near-normal year (2004). Seasonal variability in R_s closely followed that of seasonal variability in T_s : rising in the spring, peaking during summer months and falling again in the autumn in each year (Figure 2.1a and b). Soil temperature between the sites, and also between different months of the year, was statistically different, within ± 1 standard deviation (Figure 2.1b). A similar trend was observed for R_s (Figure 2.1a), but was less pronounced due to

the larger spatial variability superimposed on the temporal trend. In general, soil moisture (θ_s) was high when T_s was low, and vice versa (Figure 2.1b and c). Overall, temporal variability in θ_s was lower compared to T_s , and the two variables were negatively correlated ($R^2 = 0.39$, plot not shown). These observations suggested that, if we were to use the Q_{10} model to simulate annual R_s values and R_s - T_s trends at our sites then we needed to account for the apparent temporal differences in these relationships on seasonal scales, between sites of different ages, and potentially between years.

Careful examination of measured R_s and T_s trends showed that the positive effect of increasing soil temperature on R_s was limited to the T_s range of about 4 to 14 °C across all four sites (grey areas in Figure 2.1). When T_s was below 4 °C, there also appeared a positive relationship between R_s and T_s , however, it was less pronounced compared to the 4 to 14 °C range. In contrast, at T_s above 14 °C variability in soil temperature seemed to have little influence on variability in R_s . Therefore, in our analysis we defined seasons using the following T_s categories instead of calendar months: (i) $T_s < 4$ °C, (ii) $4 \leq T_s \leq 14$ °C and (iii) $T_s > 14$ °C. The range with T_s below 4 °C corresponded mostly to winter months; that with T_s between 4 and 14 °C corresponded mostly to spring and autumn; while the range with T_s above 14 °C corresponded to summer months (Figure 2.1).

These soil temperature categories better reflected the physiological changes across the sites with increasing stand age. For example, careful

evaluation of observed Rs-Ts time series across all four sites (Figure 2.1a and b), showed that soil at the youngest stand, TP02, usually warmed-up about one month earlier compared to the three older stands (e.g. months of March). This was due to its open canopy (less shading of ground) and lack of litter layer which might insulate the ground (Table 2.1). Consequently, Rs at TP02 tended to increase about one month earlier of the older three stands. This signal would have been lost, had we analyzed our data based on seasons defined by calendar months, since the month of March is considered part of winter season in the region.

Another reason for evaluating our data using Ts ranges is related to the concept of “ecologically optimum” soil temperatures for fine root growth and activity. For example, Teskey and Hickley (1981) observed that most the root elongation in a white oak forest in Missouri, USA occurred between soil temperatures of 2 to 17 °C. They referred to this temperature range as the “ecological optimum” for root growth at their particular forest site. They also reported that seasonally most root growth occurred at bud break in spring and during leaf senescence in autumn. Increased root growth/activity may impart a strong influence on the Ts sensitivity of Rs. A careful analysis of some studies in literature that used the Q_{10} model to characterize the Rs-Ts relationship in forest ecosystems suggest that the temperature sensitivity of Rs may be restricted to the ecologically optimum Ts range for fine root growth. This Ts range may be specific to the regional climate or species, or a combination of both. For example, Curiel-Yuste et al. (2004) reported the highest Q_{10} values in the Ts range of 4 to

14 °C at their temperate maritime pine forest in Belgium. In an associated study at their pine site, Konôpka et al. (2006) showed an increase in root biomass from March to June (i.e. over spring months) and then again from August to September (late summer and autumn months). The results presented by Gaumont-Guay et al., (2006) suggested an optimal T_s range somewhere between 0 to 8 °C for a mature boreal aspen forest in Canada. In three balsam fir forests growing in different climates in eastern Canada, the T_s range with the highest Q_{10} values appeared to be between 5 to 15 °C (Lavigne et al., 2003).

The ecologically optimum T_s range for fine root growth may be constrained by environmental factors that influence fine root growth, such as moisture availability. For example, Tedeschi et al. (2006) reported that the Q_{10} model fit their observed R_s - T_s data best between T_s was between of 6 to 16 °C at their Mediterranean oak forest. Beyond 16 °C, variability in R_s was not sensitive to T_s , but was instead related to soil moisture variability (Tedeschi et al., 2006). The 6-16 °C may be the optimal T_s range for fine root growth at their site, where temperature-sensitivity of R_s was most pronounced. Therefore, our measurements and those of others seem to suggest that it may be more accurate to express seasonality in the Q_{10} model, based on soil temperature ranges, as opposed to calendar months. Furthermore, it may be important to also consider the effects of moisture variability on R_s in the model. Both of these considerations were incorporated into our temporally-flexible model, as described below.

2.3.3.2 Adding temporal flexibility into the Q_{10} model

In order to add temporal flexibility into Equation 2.1, we first linearized the statistical-form of the equation, by applying a natural log-transformation to it. This resulted in a standard linear regression model, with one explanatory variable:

$$y_i = B_0 + B_1 X_i + \varepsilon_i \quad 2.2$$

where for an i th observation, y_i is $\ln[R_s]$, where R_s is soil respiration in $\mu\text{mol CO}_2 \text{ m}^{-2} \text{ s}^{-1}$; X_i is $(T_s - 10)/10$, where T_s is soil temperature in $^{\circ}\text{C}$ (mean of top 20 cm of the mineral soil in this study); B_0 is $\ln[R_{10}]$ where R_{10} is R_s at 10°C ; B_1 is $\ln[Q_{10}]$ where Q_{10} is the temperature sensitivity of R_s for every 10°C increase in T_s ; and ε_i is the error term to account for the effects of random error (and uncontrolled factors). Following the convention in statistics, we call B_0 and B_1 “unknown regression coefficients” (also known as model parameters in our area of research).

Secondly, to allow the unknown coefficients, B_0 and B_1 in Equation 2.2, to change with seasons, years, and stand age, we introduced categorical variables (i.e. represented by dummy or indicator variables (McClave and Sincich, 2003, p.630) into Equation 2.2. We began with the knowledge that for each explanatory factor (i.e. year of measurement, season, and stand age) with k categories, $k-1$ dummy variables were needed to fully distinguish the k categories. For example, to represent decadal variability we used stand age, which was represented by three dummy variables, because it had four categories (i.e. 67-, 32-, 17-, 4-year old stands, corresponding to TP39, TP74, TP89, and TP02, respectively). We let A_{2i} be a dummy variable such that it assumed the value of 1, if the i th observation

belonged to TP74, and zero otherwise. Similarly, we let $A3_i$ be a dummy variable such that it assumed the value of 1, if the i th observation belonged to TP89; and $A4_i$ be a dummy variable such that it assumed the value of 1, if the i th observation belonged to TP02, and zero otherwise. Therefore, if $A2_i = 0$, $A3_i = 0$, and $A4_i = 0$, then the i th observation belonged to TP39; if $A2_i = 1$, $A3_i = 0$, and $A4_i = 0$ then the i th observation belonged to TP74; if $A2_i = 0$, $A3_i = 1$, and $A4_i = 0$ then the i th observation belonged to TP89; and if $A2_i = 0$, $A3_i = 0$, and $A4_i = 1$, then the i th observation belonged to TP02. TP39 was called the *reference category*, because all three dummy or indicator variables for that case were zero. The researcher has the complete freedom to choose any category as the reference category. However, the reference category should be one with a sufficiently large number of observations (i.e. at least more than the number of model variables). Otherwise, the estimated coefficients of the dummy variables are likely to be untrustworthy. To represent interannual variability, we used year of observation. We chose 2004 as the reference category and let $Y5_i$ and $Y6_i$ be the dummy variables representing 2005 and 2006, respectively. For seasonality, we chose the range of ($4 \leq T_s \leq 14$ °C) as the reference category and let $S2_i$ and $S3_i$ be the dummy variables representing ($T_s < 4$ °C) and ($T_s > 14$ °C), respectively.

Based on these dummy variables, the intercept in Equation 2.2 above (i.e. B_0) now becomes completely flexible:

$$B_0 = B_{01} + B_{02}A_{2i} + B_{03}A_{3i} + B_{04}A_{4i} + C_{02}S_{2i} + C_{03}S_{3i} + D_{05}Y_{5i} + D_{06}Y_{6i}$$

2.3a

where B_{01} , B_{02} , B_{03} , B_{04} , C_{02} , C_{03} , D_{05} , D_{06} are unknown coefficients to be estimated. The slope, B_1 , also becomes completely flexible:

$$B_1X_i = B_{11}X_i + B_{12}A_{2i}X_i + B_{13}A_{3i}X_i + B_{14}A_{4i}X_i + C_{12}S_{2i}X_i + C_{13}S_{3i}X_i + D_{15}Y_{5i}X_i + D_{16}Y_{6i}X_i$$

2.3b

where B_{11} , B_{12} , B_{13} , B_{14} , C_{12} , C_{13} , D_{15} and D_{16} are the unknown coefficients to be estimated. In Equation 3b, the terms involving the product of a dummy variable and X_i are called “interaction terms”. By considering the product of a dummy variable and X_i as a new explanatory variable, transforms Equation 2.2 into a multivariate linear regression model. In this model all of the unknown coefficients can be simultaneously estimated by using a linear regression procedure in any widely available statistical software, such as SAS (SAS Institute Inc., NC, USA) or SPSS (SPSS Inc., IL, USA).

To obtain a better understanding of the meanings of the coefficients in the expanded model (i.e. the temporally flexible Q_{10} model), consider first the model for the reference case (i.e. the case where the i th observation belonged to TP39, was taken in 2004, and had T_s values in the 4 to 14 °C range). For this reference case, the model becomes:

$$y_i = B_{01} + B_{11}X_i + \varepsilon_i \quad 2.4a$$

where B_{01} and B_{11} are, respectively, the intercept ($\ln[R_{10}]$) and slope ($\ln[Q_{10}]$) of the regression line for all observations in the reference category. Next, consider a non-reference case (i.e. the j th observation that belonged to TP02, taken in 2006 that had T_s values above 14°C). For this non-reference case, the model becomes:

$$y_j = (B_{01} + B_{04} + C_{03} + D_{06}) + (B_{11} + B_{14} + C_{13} + D_{16}) X_j + \varepsilon_j \quad 2.4b$$

where B_{04} represents the expected difference in $\ln[R_{10}]$ between TP02 and TP39. Similarly, B_{14} represents the expected difference in $\ln[Q_{10}]$ between TP02 and TP39. C_{03} represents the expected difference in $\ln[R_{10}]$ between the ($T_s > 14^\circ\text{C}$) and ($4 \leq T_s \leq 14^\circ\text{C}$) seasonal categories, whereas C_{13} represents the corresponding difference in $\ln[Q_{10}]$ between the seasonal categories. Similarly, D_{06} represents the expected difference in $\ln[R_{10}]$ between 2006 and 2004, whereas D_{16} represents the expected difference in $\ln[Q_{10}]$ between 2006 and 2004. Therefore, for the observations in this particular non-reference category, the intercept and slope of the regression line are $(B_{01} + B_{04} + C_{03} + D_{06})$ and $(B_{11} + B_{14} + C_{13} + D_{16})$, respectively.

2.3.3.3 Adding soil moisture variability into the Q_{10} model

Soil moisture was added into Equation 2.2 as an additional explanatory variable. Unlike the categorical dummy variables representing the temporal

factors, soil moisture was represented by a single continuous variable, θ_s . The moisture-sensitive version of temporally-flexible Q_{10} model becomes:

$$y_i = B_0 + B_1 X_i + M\theta_s + \varepsilon_i \quad 2.5$$

where for an i th observation, M is the estimated coefficient of the soil moisture variable, with θ_s being the mean daily soil volumetric water content in $\text{cm}^3 \text{cm}^{-3}$ (mean of 5, 10 and 20 cm deep sensors). The other variables and estimated coefficients are as described above, with B_0 and B_1 given by Equations 2.4a and 2.4b respectively.

2.3.3.4 Assessing the relative importance of the explanatory factors in the model

To estimate the unknown coefficients in the moisture-sensitive temporally-flexible Q_{10} model, we used a linear regression procedure, PROC REG, of the SAS statistical software package (SAS systems Inc., NC, USA). In the procedure, the software uses the *least squares method* to estimate the unknown coefficients, and R^2 (i.e. coefficient of determination) to measure the model's explanatory power.

The relative importance of the three temporal factors (seasonality, year of measurement and stand age) and soil moisture (θ_s) in improving the model's explanatory power, was assessed as follows: the soil moisture variable and subsets of dummy variables representing each of the three factors were excluded, in turn, from the best specification of our modified Q_{10} model (i.e. Best model). This resulted in the so called “reduced” models. The decrease in R^2 of the “reduced”

model compared to the full Best model indicated the relative importance of the deleted factor. The greater was the decrease, the more important was the deleted factor. We called this decrease in R^2 the deleted factor's *marginal contribution in R^2* .

By convention, the standard linear regression procedure (i.e. PROC REG in SAS) allows the values of the remaining explanatory variables of the reduced model to change, so that the new R^2 is maximized. This method is called the *maximizing method* (Liaw and Frey, 2007). However, when the explanatory power of a deleted factor overlaps substantially with that of the remaining factors, this assessment method can seriously understate the importance of the deleted factor. Since overlaps in explanatory powers occur frequently in observational research, we also used the so-called *fixed-coefficient method* (Liaw and Frey, 2007), as an alternative way to assess the relative importance of the three factors. As suggested by its name, this method does not allow the estimated coefficients of the remaining variables in the reduced model to change when the *marginal contribution in R^2* is computed.

2.4. RESULTS

2.4.1 The temporally flexible Q_{10} model

From our analysis, the best specification of the temporally-flexible and moisture-sensitive Q_{10} model (i.e. Best model), for the TPFS data set, turned-out to be of the following form:

$$y_i = (\underline{B}_{01} + \underline{B}_{02}A2_i + \underline{B}_{04}A4_i + \underline{C}_{02}S2_i + \underline{C}_{03}S3_i + \underline{D}_{05}Y5_i + \underline{D}_{06}Y6_i) + (\underline{B}_{11} + \underline{B}_{12}A2_i + \underline{B}_{14}A4_i + \underline{C}_{12}S2_i + \underline{C}_{13}S3_i + \underline{D}_{16}Y6_i)X_i + \underline{M}\theta s_i + \varepsilon_i$$

2.6

where for an i th observation, y_i is the predicted value of Y_i (as defined in Equation 2.2); $A2$, $A4$, $S2$, $S3$, $Y5$ and $Y6$ are the dummy variables, as defined above; and all the underlined coefficients are the “unknown coefficients” generated by the least squares method. Note that while all $(k-1)$ dummy variables were tested initially in the model (Equation 2.5), in our Best model (Equation 2.6) we retained only those variables whose estimated coefficients were statistically significant (i.e. their associated p -values were less than 0.05).

The estimated coefficients of our Best Q_{10} model (Equation 2.6) are shown in Table 2.2 (column-1). Following the general examples presented above (Equations 2.4a and b), here we describe an example of how one would compute the R_{10} and Q_{10} values from the model output given in Table 2.2 (column-1). Using the estimated coefficients from column 1 in Table 2.2 for the reference case (i.e. R_s at TP39, in 2004, when T_s was between 4 to 14 °C, Equation 2.4a) the model becomes:

$$y_i = 0.25 + (1.43)Ts_i + (2.21)\theta s + \varepsilon_i \quad 2.7a$$

The R_{10} in that case is simply the exponentially transformed estimated coefficient of the intercept, B_{01} : $R_{10} = \exp(0.25) = 1.28$. Similarly, the exponentially

transformed estimated coefficient of the slope (i.e. $\exp(1.43)$) is the estimated Q_{10} of the reference case (i.e. $Q_{10} = 4.18$).

For the non-reference case (i.e. Equation 2.4b, representing Rs collected at TP02, in 2006, when Ts was above 14 °C), the model becomes:

$$y_j = (0.25 - 0.29 + 0.09 + 0.55) + (1.43 - 0.19 - 1.21)Ts_j + (2.21)\theta s_j + \varepsilon_j \quad 2.7b$$

The R_{10} for this case is again the exponentially transformed intercept = 1.81 (i.e. the sum in the brackets on the left = $\exp(0.60) = 1.81$). Similarly, the Q_{10} is the exponentially transformed slope = 1.03 (i.e. sum in the brackets on the right in Equation 2.7b = $\exp(0.03) = 1.03$).

The resulting R_{10} and Q_{10} values from our Best model, for each temporal case are listed in Table 2.3. Note that the estimated coefficient of the dummy variable representing TP89 was not significantly different from the reference case ($p > 0.05$) and hence does not appear in Table 2.2. Therefore, the estimated intercepts and slope for TP89 are the same as for TP39, within the 95% confidence interval (i.e. R_{10} and Q_{10} were statistically indistinguishable between TP39 and TP89, Table 2.3). Similarly, there was no statistical difference in the Q_{10} values between year 2004 and 2005 (Table 2.3b).

2.4.2 Temporal variability in R_{10} and Q_{10} at TPFS

Our results show that R_{10} and Q_{10} values did vary temporally across all four different aged forest sites, as reflected by the variable magnitudes of the

estimated model coefficients (Table 2.2, column-1) and the resulting computed R_{10} and Q_{10} values (Table 2.3). Between the four different-age stands, the youngest stand, TP02, had the lowest R_{10} and Q_{10} values (0.64 ± 0.08 to $1.83 \pm 0.04 \mu\text{mol CO}_2 \text{ m}^{-2} \text{ s}^{-1}$ and 1.03 ± 0.05 to 3.93 ± 0.03 , respectively). R_{10} and Q_{10} values were lower for the 32-year-old stand, TP74 (0.73 ± 0.06 to $2.10 \pm 0.08 \mu\text{mol CO}_2 \text{ m}^{-2} \text{ s}^{-1}$ and 1.20 ± 0.05 to 4.57 ± 0.16 , respectively) compared to the 67-year-old stand, TP39 (0.85 ± 0.07 to $2.46 \pm 0.09 \mu\text{mol CO}_2 \text{ m}^{-2} \text{ s}^{-1}$ and 1.24 ± 0.05 to 4.76 ± 0.14 , respectively). However, there was no statistical difference in R_{10} and Q_{10} between TP39 and the 17-year-old stand, TP89. Therefore a single R_{10} and Q_{10} value for each year and season is reported for both sites in Table 2.3.

Seasonally, both R_{10} and Q_{10} values varied across all four stands (Table 2.3). R_{10} values increased with increasing T_s (Table 2.3a). The lowest R_{10} values (0.64 ± 0.08 to $0.85 \pm 0.07 \mu\text{mol CO}_2 \text{ m}^{-2} \text{ s}^{-1}$) were observed at T_s below 4°C , corresponding mostly to winter months, and the highest R_{10} values (1.83 ± 0.04 to $2.46 \pm 0.09 \mu\text{mol CO}_2 \text{ m}^{-2} \text{ s}^{-1}$) were observed when T_s was above 14°C , corresponding mostly to summer months. In contrast, the lowest Q_{10} values (1.03 ± 0.05 to 1.42 ± 0.06) were observed when T_s was above 14°C , mostly during the summer months, while the highest Q_{10} values (3.46 ± 0.03 to 4.76 ± 0.14) were observed during the so called ecologically optimum T_s range for fine root growth (4 to 14°C), corresponding mostly to spring and autumn months. These results suggested that at the Turkey Point different age forest sites, the R_s - T_s exponential

relationship derived from fitting *annual* data with the Q_{10} model, was mostly driven by the temperature response in the 4 to 14 °C range.

Both years, 2005 and 2006, were statistically different from year 2004 in their R_{10} values (Table 2.3). R_{10} values in 2005 and 2006 were higher (0.70 ± 0.08 to $2.46 \pm 0.09 \mu\text{mol CO}_2 \text{ m}^{-2} \text{ s}^{-1}$) compared to R_{10} values in 2004 (0.64 ± 0.08 to $2.23 \pm 0.08 \mu\text{mol CO}_2 \text{ m}^{-2} \text{ s}^{-1}$). These trends may be reflective of mean annual air temperature (T_a) differences between the years. T_a values were similar between 2005 and 2006 and higher compared to T_a in year 2004 (Figure 2.1b). Higher temperatures may have stimulated growth and microorganism activity, as reflected in interannual differences in R_{10} values. In contrast, Q_{10} values were found to be statistically different only between year 2004 and 2006, but not between 2004 and 2005. Q_{10} values were higher in 2006 (1.17 ± 0.05 to 4.76 ± 0.14) compared to 2004 and 2005 (1.03 ± 0.05 to 4.18 ± 0.11). Once again the trend may be related to climatic differences between the years, but this time in terms of precipitation (Ppt). Total annual Ppt was 18% higher in 2006 compared to 2004 (Figure 2.1b), while in 2005 it was about 10% lower compared to 2004. We acknowledge that three years of data may be insufficient for interannual analysis of respiration. More often data records of 10 years or longer are used for interannual analysis. Nonetheless, the above results suggest interesting patterns, which warrant further investigation at other sites, especially where several years of high frequency R_s data are available.

2.4.3 Comparison between the temporally-flexible and the conventional Q_{10} models

To compare our temporally-flexible model (i.e. Equation 2.6) with the conventional Q_{10} model, we also fitted the linearized form of the conventional Q_{10} model (i.e. Equation 2.6) to the same data set (Figure 2.6). We used the coefficients of determination (R^2) to represent the model's goodness of fit. When the model has many coefficients and the number of observations is relatively small, R^2 may be misleading. In such cases, the use of adjusted R^2 values for model comparison is more appropriate. However, in our case the sample size was much bigger compared to the number of coefficients to be estimated (i.e. 7445 observations versus 13 coefficients in the Best model (i.e. Equation 2.6)), so that the difference between adjusted R^2 and R^2 was trivial (0.0001 to 0.0003). Therefore, we report only the R^2 values in Table 2.2. We found that our Best model was much better than the conventional Q_{10} model in fitting the observed data: the values of R^2 were 0.812 versus 0.630, respectively (Table 2.2, columns 1 and 6; and also Figures 2.2 and 2.3).

The most improvement in the model was seen at high T_s range, where the new model was flexible enough to level-off, following observations (Figure 2.3), instead of continuing to increase exponentially with increasing T_s (Figure 2.2). There still remained a large scatter about the predicted lines, which our Best model failed to explain (Figure 2.3). Some of the scatter was due to spatial

variability, which was not considered in this paper, because it focused on temporal variability only.

2.4.4 Relative importance of the temporal factors in the Best model

The subsequent deletions of the three temporal factors (i.e. seasons, years and stand-age) and soil moisture from the Best model, which resulted in the reduced models (Table 2.2, columns 2 to 5), helped us to assess the relative importance of each deleted factor to the model's explanatory power. Of the three temporal factors considered, seasonality had, by far, the strongest explanatory power based on its marginal contribution in R^2 (MCR) generated by the fixed-coefficient method. It accounted for 12% of the model's explanatory power (i.e. $MCR=0.120$, Table 2.2). Stand age accounted for 4.2% of the model's explanatory power, while interannual variability contributed only 0.6%. This suggested that at sites where several years of non-continuous data are available, those records could be pooled together to study seasonal and inter-site variability.

A consequence of the large difference in explanatory power between seasonality and interannual variability was that the deletion of seasonality from the Best model resulted in the reversal of the signs of the coefficients of the dummy variables representing interannual variability (i.e. years 2005 and 2006) (Table 2.2, columns 1 and 4). A very important methodological point demonstrated by this finding is that when two explanatory factors are correlated and have very different explanatory powers, the failure to include the stronger

explanatory factor in the model could result in substantively misleading estimated coefficients for the weaker explanatory factor (Otomo and Liaw, 2003). Such useful information can not be extracted from the output of analysis of covariance, highlighting the usefulness of our method of analysis.

Compared to the time factors (i.e. stand age, interannual and seasonal), variability in soil moisture had the least explanatory power in our model, improving the model fit by only 0.3% (Table 2.2, column 5), yet it was still statistically significant. The low influence of soil moisture variability on R_s variability across Turkey Point stands may be attributed to well-drained sandy soils and the drought-tolerance of white pines, as discussed previously by McLaren et al. (2008). Furthermore, at these sites θ_s was found to be strongly correlated with T_s as mentioned previously ($R^2 = 0.39$, plot not shown). At its own, θ_s was able to explain about 26% of R_s variability, on annual basis, when it was linearly regressed against naturally-log transformed R_s (Table 2.4). However, once T_s was also included in the model, both, the estimated coefficient for θ_s and its associated t-value were reduced by a magnitude of 10 (Table 2.4), suggesting that most of the explanatory power in θ_s was actually attributed to T_s .

Furthremore, note that if temporal variability is not accounted for in the model (i.e. as in our Best model), the estimated coefficient for θ_s is negative (Table 2.4), which does not make physical sense for these drought-prone sites, where in general the relationship between R_s and θ_s should be positive. These results highlight the need for researchers to be aware of the strength of the various

explanatory factors and their interactions in a given system that they study.

Failure to account for the stronger explanatory factors in the model (in our case this was temporal variability) could lead to incorrect inferences about the relationships among the dependent and independent variables in the models (i.e. R_s and θ_s in our case).

2.5 DISCUSSION

The Q_{10} and R_{10} values obtained at the Turkey Point age-sequence sites were within the range of literature-reported values. The conventional Q_{10} model produced Q_{10} of 2.5, which was similar to the well accepted global median value of 2.4 (Raich et al., 1992), but failed to follow the seasonality of the observed R_s - T_s data. Our Best model produced Q_{10} values in the range of 1.03 ± 0.05 to 4.76 ± 0.14 among the sites (Table 2.3b) and these were also within literature-reported values. For example, Raich et al. (1992) reported a global range of Q_{10} values from 1.3 to 3.3, while Metteucci et al. (2000) reported values of 2.5 to 4.1 for different forests across Europe.

Our Q_{10} values for R_s observations at T_s above $14\text{ }^\circ\text{C}$ were in the range of 1.03 ± 0.05 to 1.42 ± 0.06 , while the Q_{10} values for R_s observations at T_s below $14\text{ }^\circ\text{C}$ (i.e. corresponding to winter, spring and autumn months), ranged from 2.45 ± 0.07 to 4.76 ± 0.14). These results agreed with Curiel-Yuste et al. (2004), who also reported seasonality in the Q_{10} parameters of a temperate maritime pine forest they studied in Europe. Their Q_{10} values were 0.7 ± 0.26 to 1.1 ± 0.28 during

summer months, and higher, up to 4.2 ± 0.49 , for winter, spring and autumn months.

Our R_{10} values ranged from 0.64 ± 0.08 to 2.46 ± 0.09 $\mu\text{mol CO}_2 \text{ m}^{-2} \text{ s}^{-1}$ (Table 2.3a) and were also within those reported in the literature. For example, Lindroth et al. (2008) reported R_{10} values of 2.5 ± 0.3 to 5.8 ± 0.2 $\mu\text{mol of CO}_2 \text{ m}^{-2} \text{ s}^{-1}$ in a number of northern forests of various ages in Denmark, Finland and Sweden, which were somewhat higher compared to our values. However, in their analysis, they used the Lloyd-Taylor equation to calculate R_{10} values (Lloyd and Taylor 1994; Lindroth et al., 2008), which is known to overestimate R_s at low T_s values (Janssens et al., 2003). In contrast, Curiel-Yuste et al. (2004) reported R_{10} values from 0.9 ± 0.2 to 2.2 ± 0.6 $\mu\text{mol of CO}_2 \text{ m}^{-2} \text{ s}^{-1}$ for their temperate maritime pine forest, with the largest R_{10} values observed in July-August months and lowest in January-February. The seasonal trends we observed in our data were also similar to the seasonal trends reported by Curiel-Yuste et al. (2004).

Between the sites, the lowest mean annual R_{10} and Q_{10} values were obtained for the youngest TP02 stand throughout the year (Table 2.3). This was expected, given that this site has sparse litter cover and canopy, and young seedling trees with relatively small root systems, compared to the older mature stands. Overall, root density and litter input at TP02 were smallest, compared to the older three stands (Peichl and Arain, 2006). An increase in those sources of carbon with stand age should contribute to an overall increase in emitted CO_2 . Likewise, changes in annual T_s regime, associated with age-related changes in

stand canopy cover and litter thickness (Table 2.1), can also influence the composition of the soil community over time. Different microorganisms, in turn, can have differing Ts-sensitivities and therefore cause Q_{10} to vary as well.

R_{10} and Q_{10} values were lower for the 32-year-old stand, TP74, compared to the 17-year-old stand, TP89. One of the reasons for the discrepancy may be due to differences in past land-use between the two sites. Unlike TP74, TP89 was used for crop-farming until about 10 years prior to afforestation. As a result, soil at TP89 is higher in nutrients compared to TP74, which was not farmed at all (Khomik 2004). This higher nutrient content should be more favourable for plant growth and associated activity of microorganisms responsible for soil respiration. Interestingly, when the two groups of stands were considered separately (i.e. non-farmed: TP39 and TP74; and farmed: TP89 and TP02), the expected age trend was maintained within the two groups: R_{10} and Q_{10} values did decrease from TP39 to TP74, as they did from TP89 to TP02. It may also be possible that at the time of this study, TP89 was in an inherently more active stage of growth. Lancaster and Leak (1978) reported that growth and production in white pine species tends to peak around the age of 15. Increased productivity has been linked to increased respiratory fluxes in a forest ecosystem (Litton et al., 2007), since as productivity increases in terms of biomass growth and production, so will metabolic activity of the stand and subsequently its respiration rate.

The interannual patterns in R_{10} and Q_{10} , which we observed, were also in agreement with previous findings reported in the literature. For example,

Gaumont-Guay et al. (2006b) reported higher R_{10} and Q_{10} values for years with higher mean annual air temperature in their boreal aspen forest, based on a three-year study. Curiel-Yuste et al. (2003) studied the effect of seasonal precipitation on Q_{10} at their temperate maritime forest and reported that in general both R_{10} and Q_{10} values increased after a sufficiently large precipitation event. We also observed a positive relationship between Q_{10} and precipitation, with Q_{10} values being higher during the wettest year at our sites.

The categorization of Rs-Ts responses into Ts-ranges, as dictated by our observed data, could be specific to the dynamics of vegetation grown in the temperate climate zones. In a study of tree line limits at high altitudes across the globe, Alvarez-Uria and Körner (2007) found that trees stop growing at Ts of about 6 °C, with a range of 3.2 to 7 °C (Körner and Paulsen, 2004). They suggest this may be related to a minimum Ts threshold for tree root growth (i.e. below that Ts threshold root growth stops). Our value of 4 °C⁵ may be the trigger for the start of fine root growth/activity at Turkey Point sites in spring and its end in autumn, which would also be supported by our findings of increasing R_{10} values when Ts went above 4 °C. Lyr and Hoffmann (1967) listed a cardinal Ts for the start of fine root growth for *Pinus Strobus* L. as 5-6 °C, but they also mentioned that ecological optimum values tend to be lower and dependent on other growth factors, such as moisture and carbohydrate supply (i.e. long-term field conditions), unlike the physiological optimum values that they reported, which tend to reflect

⁵ Based on observed Ts values, measured at 15 cm soil depth across TPFS.

short-term experimentation, often carried out under controlled conditions in laboratory environments. Therefore, our lower threshold T_s (i.e. 4 °C) may be reflective of some ecological optimum T_s at our sites.

Increased fine root activity at T_s between 4 and 14 °C may have imparted a strong seasonal autotrophic respiration (R_a) signature to the R_s - T_s relationship at Turkey Point sites. Gaumont-Guay et al. (2008) have shown that R_a was more sensitive to T_s , compared to R_h . Indeed, their Q_{10} values for root respiration reflected our values in the 4 to 14 °C T_s range, where we suspect most fine root activity to occur at our sites. Their Q_{10} was 4.0 ± 0.5 for R_a , and 3.0 ± 0.2 for R_h , compared to our Q_{10} value of 3.46 ± 0.03 to 4.76 ± 14 for the 4 to 14 °C T_s range. Boone et al. (1998) also reported that R_a dominates R_s - T_s sensitivity in their mature mixed-wood forest in Massachusetts, USA. They also observed higher Q_{10} values for soils that contained roots (3.5 ± 0.4), compared to those that did not (2.5 ± 0.4). Similarly, Lavigne et al. (2003), in their study of three balsam fir forests from eastern Canada, reported that R_a dominated R_s and was more sensitive to T_s compared to R_h . Our results agree with the literature and suggest R_a - T_s dominance of the overall R_s - T_s relationship at Turkey Point age-sequence forests. However, we will go further to suggest that at a particular forest site, soil respiration is most sensitive to T_s in the so called ecologically optimum temperature range for fine root growth, which may be species and/or climate region specific. Therefore, it may be possible for modellers to use a constant Q_{10}

value in their models (e.g. Arain et al., 2002), but restricted to this ecologically optimum T_s range.

In the T_s range above 14 °C, corresponding mostly to peak growing season and summer months, photosynthesis may be more important in controlling temporal variability in R_s versus T_s . Cisneros-Dozal et al. (2006) have shown that roots respired carbon from different sources in different times of year. In dormant seasons, such as winters, roots respired old stored carbon, while in summer they tended to respire newly photosynthesized carbon (Cisneros-Dozal et al., 2006). The low T_s sensitivity of R_s (i.e. $Q_{10} \sim 1.0$) during the growing season may be reflective of the increased sensitivity of R_s to variability in photosynthesis instead of T_s , especially since soil temperatures tend to be less variable during the growing season, as compared to the transition seasons (i.e. spring and autumn) (Figure 2.1b, shaded versus non-shaded areas). This idea is supported by the findings of Liu et al. (2006), who reported temperature-independent variability in soil respiration in a temperate forest located in Oak Ridge, TN, USA. Using continuous CO_2 efflux measurements from autochambers, they showed that R_s closely followed the congruent variability in absorbed photosynthetically active radiation (i.e. a surrogate for gross ecosystem productivity) during the growing season, but not during the dormant season. Therefore, ecosystem productivity may impose temporal variability on R_s in the summer, resulting in the observed lack of T_s sensitivity of R_s at that time. We were not able to conduct an analysis similar to Liu et al. (2006) with our data set, since our record was periodic

(biweekly to monthly). Others have shown that newly photosynthesized carbon can be relocated to roots and respired back out into the atmosphere in as little as 4 days (Carbone et al., 2007; Moyano et al., 2008).

Finally, we would like to make a comment on the idea of continuing to use the Q_{10} model for R_s - T_s simulations within our research field. Despite statistical approaches that can help to improve the temporal flexibility of the model (Gu et al., 2008 and the method presented here), the mathematical form of the model still remains inadequate for simulating the complex seasonal pattern of the R_s - T_s relationship across varied ecosystems. This is especially true for sites, like our youngest TP02 stand, which experienced reductions in R_s at high T_s values. While the temporally-flexible model presented here, does level off at high T_s values, better reflecting our observed data (Figure 2.3d), the nature of the mathematical function (i.e. exponential) results in kinks in the simulated model (Figure 2.3). Alternative functions can be implemented into the Q_{10} model to allow for smoother transitions (Richardson et al., 2006; Gu et al., 2008; Chen et al., 2009), however, that tends to complicate the model unnecessarily. In our view, the results of this study highlight the need for researchers to consider alternative mathematical functions for representing the R_s - T_s relationship. These alternative models should be able to at least rise and fall naturally (such as quadratic functions), in order to better simulate the annual course of R_s - T_s in forested ecosystems, especially given that seasonality was shown to be the most important temporal factor in explaining R_s - T_s variability of annual data sets. We

also would like to note that the method of data analysis we presented above (ie. using dummy variables and multivariate regression analysis), which allows model parameters to vary, can be applied to other functions and is not limited to the Q_{10} model as presented above.

2.6 CONCLUSIONS

We characterized the temporal variability of the relationship between soil temperature and soil respiration, across an age-sequence of planted forest stands (67-, 32-, 17-, and 4-year-old), growing in the temperate climate of eastern North America. We used a novel temporally-flexible and moisture-sensitive Q_{10} model, considering the following temporal factors: seasonality, interannual variability (i.e. between three years of measurements) timescales, and across the age-sequence. In the temporally-flexible model, both model parameters, R_{10} and Q_{10} , were allowed to vary with time. Soil moisture was also included in the model. Our results showed that accounting for seasonality in the Q_{10} model was most important, as it explained 12% of the variability in the Rs-Ts relationship, this was followed by intersite variability (4.2%) and interannual variability (0.6%). In the drought-tolerant white pine forest that we studied, soil moisture variability had the least influence on Rs variability, explaining only 0.3% of the model's fit.

Both R_{10} and Q_{10} values were the lowest at the youngest forest stand with an open canopy, while the highest R_{10} and Q_{10} values were observed for the 67- and 17-year old stands with the thickest canopy cover. Interannually, years with

warmer mean annual temperatures had higher R_{10} values, while the year with higher total annual precipitation had the highest Q_{10} values. Seasonally, R_{10} increased with increasing T_s , being lowest during winter months when T_s was below 4 °C and highest during the summer months, when T_s was above 14 °C. In contrast, the highest Q_{10} values were observed in the 4 to 14 °C T_s range, across all four age-sequence sites. This temperature range may represent the so called “ecologically optimum” soil temperature range for fine root growth, which may be site and/or species specific. Above this ecologically optimum T_s range, R_s was least sensitive to T_s variability (i.e. $Q_{10} \sim 1.0$).

This study adds to our understanding of the variability of the Q_{10} model at various timescales from seasons to decades. The results and analytical methodology presented herein should be of interest to carbon cycle modellers and field ecologists.

2.7 ACKNOWLEDGEMENTS

Funding for this study was provided by the Natural Sciences and Engineering Research Council (NSERC) of Canada Discovery and Strategic Project Grants and NSERC, the Canadian Foundation for Climate and Atmospheric Sciences (CFCAS), and BIOCAP Canada Foundation funded Fluxnet-Canada Research Network (FCRN), while CFCAS funded the Canadian Carbon Program (CCP). Support from the Canadian Foundation of Innovation (CFI), the Ontario Innovation Trust (OIT), and McMaster University, is also acknowledged. In-kind support from the Ontario Ministry of Natural Resources (OMNR), the Long Point Recreation and Conservation Authority (LPRCA), the Canadian Forest Service (CFS) and Ontario Power Generation (OPG) is appreciated. We thank Steve Williams, from OMNR, for his assistance in site selection and maintenance of the oldest stands. We thank Frank Bahula and Bruce Whitside for providing access to the forests on their properties (TP89 and TP02). We are grateful to Eugenia Aoucheva, Rose Blair, Jason Brodeur, Fauzia Arain, Josh McLaren, Matthias Peichl, Mahmoud Pejam, Olesia Peshko, Natalia Restrepo-Coupé, Shuhua Yi, Sven D'Souza, Fengming Yuan, Dali and Jagadeesh Yeluripati, and to the rest of our volunteers, for their help in the field.

2.8 REFERENCES

Alvarez-Uria P and Körner C (2007) Low temperature limits of root growth in deciduous and evergreen temperate tree species. *Function Ecology*, 21: 211-218.

- Arain MA, Black TA, Barr AG, Jarvis PG, Massheder JM, Verseghy DL, Nesic Z (2002) Effects of seasonal and interannual climate variability on net ecosystem productivity of boreal deciduous and conifer forests. *Canadian Journal of Forest Research*, 32: 878-891.
- Arain, MA and Restrepo-Coupe, N (2005) Net ecosystem production in a temperate pine plantation in southeastern Canada. *Agricultural and Forest Meteorology*, 128: 223-241.
- Boone RD, Nadelhoffer KJ, Canary JD, Kaye JP (1998) Roots exert a strong influence on the temperature sensitivity of soil respiration. *Nature*, 496: 570-572. (AND OTHERS)
- Carbone MS, Czimczik CI, McDuffee KE, Trumbore SE (2007) Allocation and residence time of photosynthetic products in a boreal forest using low-level ¹⁴C pulse-chase labeling technique. *Global Change Biology*, 14: 466-477.
- Chen JM, Govind A, Sonnentag O, Zhang Y, Barr A, Amiro B (2006) Leaf area index measurements at Fluxnet-Canada forest sites. *Agricultural and Forest Meteorology*, 140: 257-268.
- Chen JM, Huang SE, Ju W, Gaumont-Guay D, Black TA (2009) Daily heterotrophic respiration model considering the diurnal temperature variability in the soil. *Journal of Geophysical Research: Biogeoscience*, 114: G01022.
- Cisneros-Dozal LM, Trumbore S, Hanson PJ (2006) Partitioning sources of soil-respired CO₂ and their seasonal variation using a unique radiocarbon tracer. *Global Change Biology*, 12: 194-204.
- Curiel-Yuste J, Janssens IA, Carrara A, Ceulemans R (2004) Annual Q₁₀ of soil respiration reflects plant phenological patterns as well as temperature sensitivity. *Global Change Biology*, 10: 161-169.
- Curiel-Yuste J, Janssens IA, Carrara A, Meiresonne L, Ceulemans R (2003) Interactive effects of temperature and precipitation on soil respiration in a temperate maritime pine forest. *Tree Physiology*, 23: 1263-1270.
- Davidson EA, Belk E, Boone RD (1998) Soil water content and temperature as independent or confounded factors controlling soil respiration in a temperate hardwood forest. *Global Change Biology*, 4: 217-227.

- Davidson EA, Janssens IA, Luo Y-Q (2005) On the variability of respiration in terrestrial ecosystems: moving beyond Q_{10} . *Global Change Biology*, 11: 1-11.
- Environment Canada - Canadian Climate Normals from
http://www.climate.weatheroffice.ec.gc.ca/climate_normals/index_e.html
[July 10, 2007]
- Gaumont-Guay D, Black TA, Barr AG, Rachhpal SJ, Nestic Z (2008) Biophysical controls on rhizospheric and heterotrophic components of soil respiration in a boreal black spruce stand. *Tree Physiology*, 28: 161-171.
- Gaumont-Guay D, Black TA, Griffis T, Barr AG, Morgenstern K, Rachhpal SJ, Nestic Z (2006) Influence of temperature and drought on seasonal and interannual variations of soil, bole, and ecosystem respiration in a boreal aspen stand. *Agricultural and Forest Meteorology*, 140: 203-219.
- Gu L, Hanson PJ, Post WM, Liu Q (2008) A novel approach for identifying the true temperature sensitivity from soil respiration measurements. *Global Biogeochemical Cycles*, 22: GB4009.
- Hanson PJ, Edwards NT, Garten CT, Andrews JA (2000) Separating root and soil microbial contributions to soil respiration: A review of methods and observations. *Biogeochemistry*, 48: 115-146.
- Högberg P, Nordgren A, Buchmann N et al (2001) Large-scale forest girdling shows that current photosynthesis drives soil respiration. *Nature*, 411: 789-792.
- Janssens IA, Dore S, Epron D, Lankreijer H, Buchman N, Longdoz B, Brossaud J, Montagnani L (2003) Climatic Influences on Seasonal and Spatial Differences in Soil CO₂ Efflux. In Vantini R (Ed), Fluxes of Carbon, Water and Energy of European Forests. Ecological Studies 163. Springer-Verlag Berlin Heidelberg. Pp.: 233-253.
- Jassal RS, Black A, Novak MD, Gaumont-Guay D, and Nestic Z (2008) Effect of soil water stress on soil respiration and its temperature sensitivity in an 18-year-old temperate Douglas-fir stand. *Global Change Biology*, 14: 1-14.
- Khomik M (2004) Soil CO₂ efflux from temperate and boreal forests in Ontario, Canada. MSc Thesis, McMaster University, Hamilton, Ontario, Canada.

- Konôpka B, Curiel-Yuste J, Janssens IA, Ceulemans R (2006) Comparison of fine root dynamics in Scots pine and pedunculate oak in sandy soil. *Plant and Soil*, 276: 33-45.
- Körner C and Paulsen J (2004) A world-wide study of high altitude treeline temperatures. *Journal of Biogeography*, 31: 713-732.
- Lancaster KF and LeakWB (1978) A silvicultural guide for white pine in the northeast. Forest Service General Technical Report NE-41. Forest Service, US Department of Agriculture.
- Lavigne MB, Boutin R, Foster RJ, Goodine G, Bernier PY, Robitaille G (2003) Soil respiration responses to temperature are controlled more by roots than by decomposition in balsam fir ecosystems. *Canadian Journal of Forest Research*, 33: 1744-1753.
- Lavigne MB, Foster RJ, Goodine G (2004) Seasonal and annual changes in soil respiration in relation to soil temperature, water potential and trenching. *Tree Physiology*, 24: 415-424.
- Liaw, K. L. and Frey, W. H. (2007). "Multivariate Explanation of the 1985-1990 and 1995-2000 Destination Choices of Newly Arrived Immigrants in the United States: The Beginning of a New Trend?" *Population, Space and Place*, Vol. 13, pp.377-399. (www.interscience.wiley.com)(DOI: 10.1002/psp.459)
- Litton CM, Raich, JW, Ryan MG (2007) Review: Carbon allocation in forest ecosystems. *Global Change Biology*, 13: 2089-2109.
- Liu HS, Li HL, Han XG, Huang JH, Sun JX, Wang HY (2006) Respiratory substrate availability plays a crucial role in the response of soil respiration to environmental factors. *Applied Soil Ecology*, 32: 284-292.
- Liu Q, Edwards NT, Post WM, Gu L, Ledford J, Lenhart S (2006) Temperature-independent diel variation in soil respiration observed from a temperate deciduous forest. *Global Change Biology*, 12: 1-10.
- Lloyd J and Taylor JA (1994) On the temperature dependence of soil respiration. *Functional Ecology*. 8: 415-424.
- Lyr H and Hoffmann G (1967) Growth rates and growth periodicity of tree roots. *In International Review of Forestry Research*, vol. 2: 181-236.

- Matteucci G, Stivanello D, Stivaleno D (2000) Soil respiration in a Beech and Spruce forests in Europe: trends, controlling factors, annual budgets and implications for the ecosystem carbon balance. *In* Schulze ED: Carbon and nitrogen cycling in European forest ecosystems. Ecological Studies 142. Springer, Berlin: 217-236.
- McClave JT and Sincich T (2003) Statistics. 9th Ed. Prentice Hall, Upper Saddle River, NJ, USA.
- McLaren JD, Arain MA, Khomik M, Peichl M and Brodeur J (2008) Water flux components and soil water-atmospheric controls in a temperate pine forest growing in a well-drained sandy soil. *Journal of Geophysical Research: Biogeoscience*, 113: G04031.
- Monson RK, Lipson DL, Burns SP, Turnipseed AA, Delany AC, Williams MW, Schmidt SK (2006) Winter forest soil respiration controlled by climate and microbial community composition. *Nature*, 439: 711-714.
- Moyano FE, Kutsch WL, Rebmann C (2008) Soil respiration fluxes in relation to photosynthetic activity in broad-leaf and needle-leaf forest stands. *Agricultural and Forest Meteorology*, 148: 135-143.
- Otomo A and Liaw K-L (2003) “An Invitation to Multivariate Analysis: An Example About the Effect of Educational Attainment on Migration Propensities in Japan,” *SEDAP Research Paper*, No. 113, SEDAP Research Program, McMaster University, Hamilton, Ontario, L8S 4M4, Canada.
- Peichl M, Arain MA (2006). Above- and belowground ecosystem biomass and carbon pools in an age-sequence of temperate pine plantation forests. *Agricultural and Forest Meteorology*, 140, 51-63.
- Presant EW and Acton CJ (1984) The soils of the regional municipality of Haldimand-Norfolk, Vol.2. Report No.57 of the Institute of Pedology: Research Branch, Agriculture Canada, Ministry of Agriculture and Food.
- Qi Y, Xu M, Wu J (2002) Temperature sensitivity of soil respiration and its effects on ecosystem carbon budget: nonlinearity begets surprises. *Ecological Modelling*. 154: 141-142.
- Raich JW and Schlesinger WH (1992) The global carbon dioxide flux in soil respiration and its relationship to vegetation and climate. *Tellus*. 44B: 81-99.

- Richardson AD, Braswell BH, Hollinger DY, Burman P, Davidson EA, Evans RS, Flanagan LB, Munger JW, Savage K, Urbanski SP, Wofsy SC (2006) Comparing simple respiration models for eddy flux and dynamic chamber data. *Agricultural and Forest Meteorology*, 141: 219-234.
- Scott-Denton LE, Rosenstiel TN, Monson RK (2006) Differential controls by climate and substrate over the heterotrophic and rhizospheric components of soil respiration. *Global Change Biology*, 12: 205-216.
- Tedeschi V, Rey A, Manca G, Valentini R, Jarvis P, Borghetti M (2006) Soil respiration in a Mediterranean oak forest at different developmental stages after coppicing. *Global Change Biology*, 12: 110-121.
- Teskey RO and Hinckley TM (1981) Influence of temperature and water potential on root growth of white oak. *Physiologia Plantarum*, 52: 363-369.
- Valentini R, Matteucci G, Dolman AJ, Schulze E-D, Rebmann C, Moors EJ, Granier A, Gross P, Jensen NO, Pilegaard K, Lindroth A, Grelle A, Bernhofer C, Grunwald T, Aubinet M, Ceulemans R, Kowalski AS, Vesala T, Rannik U, Berbigier P, Loustau D, Gudmundsson J, Thorgeirsson H, Ibrom A, Morgenstern K, Clement R, Moncrieff J, Montagnani L, Minerbi S, Jarvis PG (2000) Respiration as the main determinant of carbon balance in European forests. *Nature*, 404: 861-865.
- Van't Hoff JH (1884) *Etudes de dynamique chimique*. Frederrk Muller & Co., Amsterdam.

Table 2.1: Site characteristics of Turkey Point Flux Station's (TPFS) forests.

	TP39	TP74	TP89	TP02
Stand Age (years)	67	32	17	4
LAI	8.0	5.9	12.8	N/A
Litter accumulation –LFH (cm)	3.5 ± 0.5	3.0 ± 0.4	4.0 ± 0.2	0.8 ± 0.3
Litter C:N	17.4 ± 4.8	24.5 ± 5.6	16.1 ± 7.1	N/A
Mineral soil %OM (top 20 cm)	1.3 ± 0.3	1.1 ± 0.3	2.0 ± 0.3	0.8 ± 0.2

LAI (leaf area index) taken from Chen et al (2006)

LFH – forest organic soil horizon (i.e. litter layer) thickness taken from Peichl (2006)

OM – organic matter; C:N – carbon (C) to nitrogen (N) ratio reported above as mean of measurements taken along the transects at each site in 2004.

TP – Turkey Point, followed by year forest was planted (ex. TP39 – TPFS stand planted in 1939)

Table 2.2: Explanation of the temporal variability in Rs at TPFS based on maximizing and fixed coefficient methods, by comparison of coefficients of determinations (R^2) between Best model and various reduced model fits, as discussed in text. Also shown are estimates of coefficients for each variable and their associated t-values, for each model run, from the maximizing method, as described in text.

Explanatory Variables	(1)		(2)		(3)		(4)		(5)		(6)	
	Best Model		No site age		No interannual variability		No seasonality		No moisture		Conventional Q_{10} model**	
	Coefficient	t-value	Coefficient	t-value	Coefficient	t-value	Coefficient	t-value	Coefficient	t-value	Coefficient	t-value
Intercept [Bo = lnR ₁₀]	0.527	51.0	0.447	55.1	0.538	53.3	0.380	40.5	0.535	51.4	0.292	48.6
TP74 [A2]	-0.134	-11.5	---	---	-0.133	-11.4	-0.129	-10.1	-0.138	-11.7	---	---
TP89 [A3]	0.028	2.5	---	---	0.033	2.9	0.081	6.5	0.023	2.0	---	---
TP02 [A4]	-0.290	-22.0	---	---	-0.296	-22.3	-0.304	-21.1	-0.287	-21.6	---	---
2005 [Y5]	0.056	5.4	0.053	4.8	---	---	0.101	9.2	0.043	4.1	---	---
Ts < 4°C [S2]	-0.370	-5.4	-0.449	-6.1	-0.402	-6.2	---	---	-0.233	-3.4	---	---
Ts > 14°C [S3]	0.423	21.3	0.678	35.8	0.402	20.6	---	---	0.509	27.2	---	---
Slope = Ts*	1.332	52.3	1.229	45.9	1.401	56.8	1.229	92.9	1.306	51.0	0.901	113.2
Ts*_TP74 [Ts* * A2]	-0.048	-3.2	---	---	-0.050	-3.3	-0.094	-5.8	-0.043	-2.9	---	---
Ts*_TP02 [Ts* * A4]	-0.197	-12.6	---	---	-0.202	-12.8	-0.466	-30.7	-0.163	-10.5	---	---
Ts*_2005 [Ts* * Y5]	0.123	6.6	0.153	7.7	---	---	0.100	5.2	-0.001	-0.1	---	---
Ts*_2006 [Ts* * Y6]	0.136	9.3	0.183	11.7	---	---	0.045	2.9	0.152	10.3	---	---
Ts*_{Ts < 4°C} [Ts* * S2]	-0.278	-3.4	-0.337	-3.9	-0.297	-3.9	---	---	-0.076	-0.9	---	---
Ts*_{Ts > 14°C} [Ts* * S3]	-0.996	-29.8	-1.371	-42.4	-0.962	-29.0	---	---	-1.107	-34.2	---	---
Ts*_0s05 [Ts* * 0s05]	-0.247	-12.1	-0.130	-6.0	-0.179	-12.1	-0.594	-30.3	---	---	---	---
Maximizing method												
R ²	0.815		0.785		0.811		0.774		0.811		0.633	
marginal contribution in R ²	---		0.030		0.004		0.041		0.004		0.182	
Fixed coefficient method												
R ²	0.815		0.771		0.807		0.693		0.803			
marginal contribution in R ²	---		0.044		0.008		0.122		0.012			

Notes: Ts* = (Ts-10)/10; All variables in the Best were statistically significant ($p < 0.05$). The symbols in square brackets are the symbols used to represent the respective dummy variables in text.

** conventional Q_{10} model (i.e. Equations 2.1 and 2.2).

Table 2.3:

(a) R_{10} values, calculated from the estimated coefficients of the Best model (Table 2.2, column 1)

Year	Season	TP39 and TP89	TP74	TP02
2004	Ts < 4	0.85 ± 0.07	0.73 ± 0.06	0.64 ± 0.08
	4 ≤ Ts ≤ 14	1.28 ± 0.04	1.10 ± 0.04	0.96 ± 0.03
	Ts > 14	2.23 ± 0.08	1.91 ± 0.07	1.66 ± 0.04
2005	Ts < 4	0.94 ± 0.07	0.80 ± 0.06	0.70 ± 0.08
	4 ≤ Ts ≤ 14	1.41 ± 0.05	1.21 ± 0.04	1.05 ± 0.04
	Ts > 14	2.46 ± 0.09	2.10 ± 0.08	1.83 ± 0.04
2006	Ts < 4	0.93 ± 0.07	0.80 ± 0.06	0.69 ± 0.08
	4 ≤ Ts ≤ 14	1.40 ± 0.05	1.20 ± 0.04	1.04 ± 0.04
	Ts > 14	2.43 ± 0.09	2.08 ± 0.08	1.81 ± 0.04

(b) Q_{10} values, calculated from the estimated coefficients of the Best model (Table 2.2, column 1)

Year	Season	TP39 and TP89	TP74	TP02
2004 and 2005	Ts < 4	2.96 ± 0.26	2.84 ± 0.26	2.45 ± 0.07
	4 ≤ Ts ≤ 14	4.18 ± 0.11	4.02 ± 0.13	3.46 ± 0.03
	Ts > 14	1.24 ± 0.05	1.20 ± 0.05	1.03 ± 0.05
2006	Ts < 4	3.36 ± 0.30	3.23 ± 0.29	2.78 ± 0.09
	4 ≤ Ts ≤ 14	4.76 ± 0.14	4.57 ± 0.16	3.93 ± 0.03
	Ts > 14	1.42 ± 0.06	1.36 ± 0.06	1.17 ± 0.05

Notes:

TP – Turkey Point, followed by year forest was planted (ex. TP39 – TPFS stand planted in 1939).

Table 2.4: The effect of soil temperature on the relationship between soil respiration (natural-log transformed, Ln) and soil moisture.

Model	θ_s parameter estimate	t-value	p-value	R^2
LnRs vs θ_s	-16.5389	-50.84	<.0001	0.258
LnRs vs (θ_s and Ts)	-1.67028	-5.87	<.0001	0.634
Best Q_{10} model	2.21087	9.21	<.0001	0.815

Figure 2.1: (a) Daily mean soil respiration, R_s , measured at each of the four age-sequence TPFS stands (TP39, TP74, TP89 and TP02, as defined in text), (b) the corresponding daily mean soil temperature, T_s , measurements (15 cm depth), and (c) daily mean soil moisture, θ_s , from site-specific weather stations (means of 2 cm, 5 cm, 10 cm and 20 cm deep sensors). Measurements are means of all observations collected on the given day, at a particular site (mean along all sampling points along the transect, including both morning and afternoon measurements, except for θ_s). Error bars represent ± 1 standard deviation. TP39, TP74, TP89 and TP02 correspond to site names, as defined in text. Also shown are mean annual air temperature (T_a) and total annual precipitation (Ppt) for each study year. The grey-highlighted areas outline the data in the “ecologically optimum” T_s range, during which R_s was most responsive to changes in T_s .

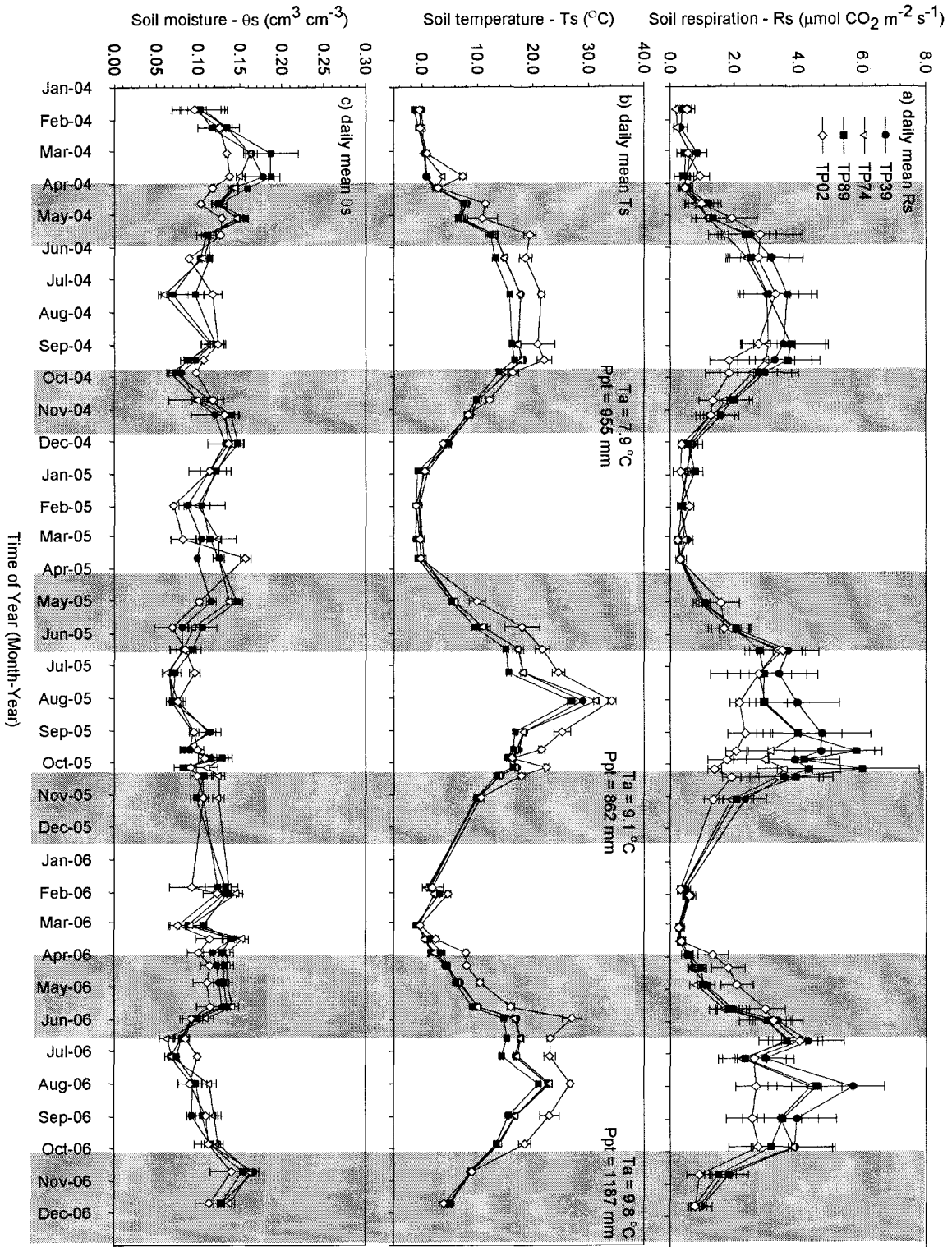


Figure 2.2: Observed R_s values plotted against those predicted by the conventional Q_{10} model (i.e. no temporal or soil moisture variability), for clarity plotted individually for each site: (a) 67-, (b) 32-, (c) 17- and (d) 4-year old TPFS forest sites. However, note that all data points were used to parameterize the model and the curve in each panel is the same: $R_s = (1.3)2.5^{(T_s-10)/10}$, $R^2 = 0.63$. The vertical dotted lines outline the data in the “optimum” T_s range, during which R_s was most responsive to changes in T_s .

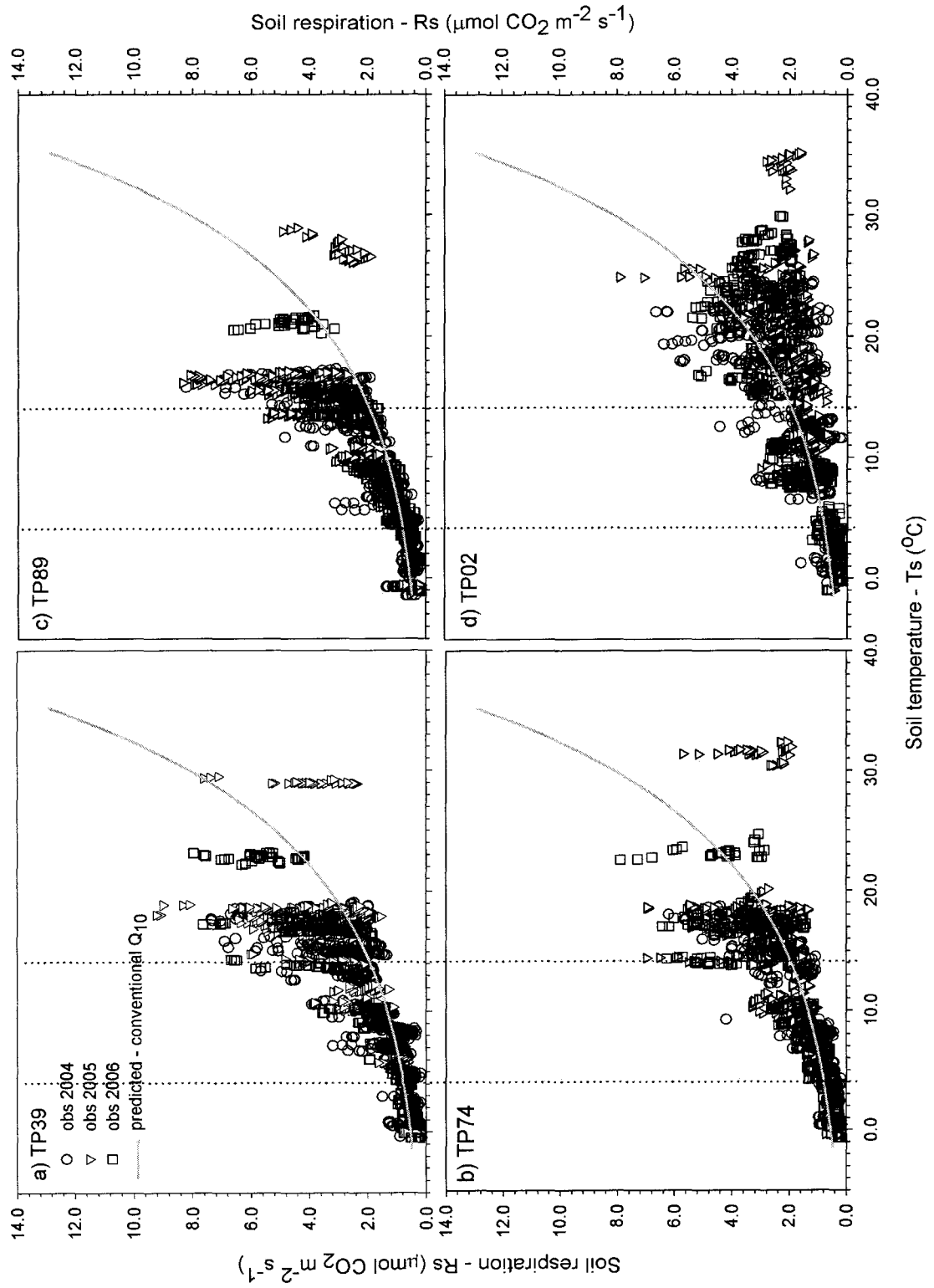
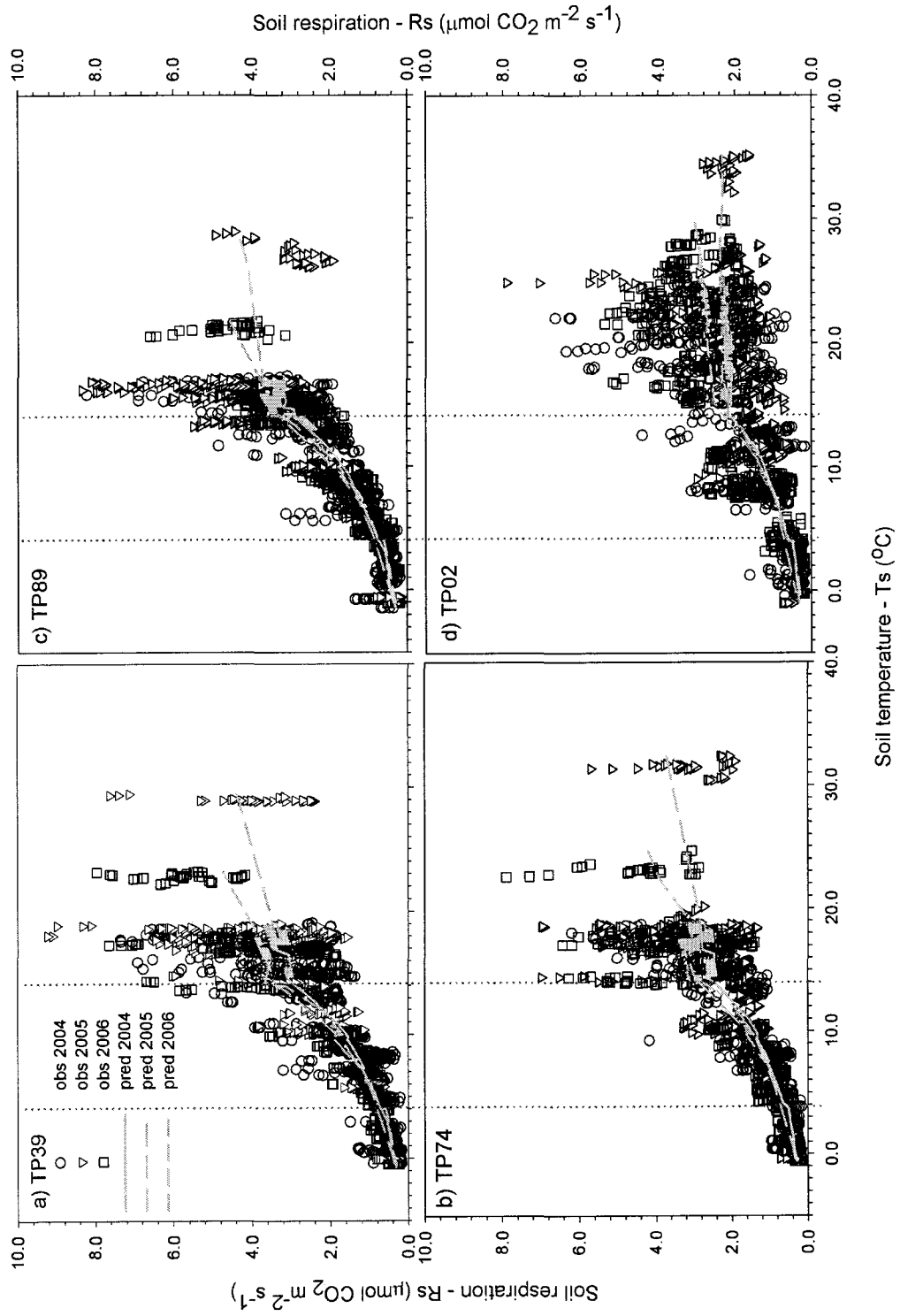


Figure 2.3: Observed R_s values plotted against those predicted by Best Q_{10} model (Equation 2.6), for clarity plotted individually for each site: (a) 67-, (b) 32-, (c) 17- and (d) 4-year old TPFS forest sites. However, note that all data points were used to parameterize the temporal model.



CHAPTER 3

THE DEBUT OF A FLEXIBLE MODEL FOR SIMULATING SOIL RESPIRATION-SOIL TEMPERATURE RELATIONSHIP: THE GAMMA MODEL ⁶

3.1 ABSTRACT

A number of empirical models are used in the literature to simulate the response of soil respiration (Rs) to soil temperature (Ts). The most widely used ones are: the exponential Q_{10} model and the sigmoid-shaped Lloyd-Taylor and logistic models. None of these models are applicable across a wide range of ecosystems or climates, and none allow Rs to decrease at high Ts values. Here we present a new, more flexible, empirical model, the so called Gamma model, which can take on the shapes of the three models mentioned above and is mathematically flexible enough to allow for Rs to decrease at high Ts values, as dictated by data. We compared the Gamma model fits to the Q_{10} , Lloyd-Taylor, and logistic models, using coefficient of determination (R^2), residual sum of squares, and Akaike's Information Criterion (AIC). The models were tested across a wide Ts range (-18 to 35°C), in five forest ecosystems, spanning three different climate zones: boreal, temperate, and Mediterranean. Compared to the other three models, the Gamma model performed just as well, or better, in simulating the Rs-Ts relationship at all sites. Annual emissions simulated with all four models were within the range of literature reported values. Simulations were carried out using models parameterized by the ordinary least squares and weighted absolute deviation estimation methods. Our results showed that once a model with proper functional form was chosen, Rs derived from the two estimation methods was comparable. We also showed how the Gamma model can be expanded to help researchers analyze the Rs-Ts relationship in the context of other environmental factors, such as soil moisture and nutrients, using relatively simple mathematics.

⁶ A modified version of this chapter has been accepted for publication by the *Journal of Geophysical Research - Biogeosciences*: Khomik M, Arain MA, Liaw K-L, McCaughey JH (2009). The debut of a flexible model for simulating soil respiration-soil temperature relationship: the Gamma model. (*in press*).

3.2. INTRODUCTION

Soil respiration (R_s) is an important component of the global carbon (C) cycle, accounting for about 62% of the overall total carbon dioxide (CO_2) emitted into the atmosphere (Schlesinger and Andrews, 2000). Proper assessment of R_s is crucial, especially in estimates of net ecosystem fluxes, where R_s may constitute up to 90% of ecosystem CO_2 emissions (Hanson et al., 2000). To-date, we still know relatively little about the complex processes and interactions that drive R_s variability in various terrestrial ecosystems over time. This makes simulating R_s a difficult task.

To simulate R_s , C-cycle researchers often resort to empirical models. These models are simpler compared to process-based models and require fewer site variables, which may not always be readily available for model input. In many terrestrial ecosystems, most of the variability in R_s is often driven by variability in soil temperature (T_s). Therefore, the bases of the most widely used empirical models are mathematical functions that try to capture this R_s - T_s response. In current literature, three R_s - T_s models prevail: a) the modified van't Hoff's model, also known as the Q_{10} model (van't Hoff, 1884; Davidson et al., 2006); b) the Lloyd-Taylor model (equation 11 in Lloyd and Taylor (1994)); and c) a log-growth or logistic model (Richards, 1959). Different groups use different models, for example, Lloyd-Taylor model in Falge et al. (2002), Kolari et al. (2004), Mäkiranta et al. (2008) versus Q_{10} in Curiel-Yuste et al. (2003), Gaumont-

Guay et al. (2006), Jansens and Pilegard (2004), versus logistic in Rodeghiero and Cescatti (2005), which makes intersite comparison of modelled R_s a challenge.

None of the above models have the functional form that will allow R_s to decrease at high T_s values. Instead, the expected value of R_s either increases exponentially (i.e. Q_{10} model) or levels-off at a maximum value (i.e. Lloyd – Taylor and logistic). However, biological organisms, which tend to dominate CO_2 production in soils, as opposed to chemical and physical processes, do have an upper optimum temperature limit (Atkin and Tjoelker, 2003; Davidson et al., 2006). At high enough temperatures, specific to each organism, R_s may decline with increased T_s because of limited enzyme capacity caused by heat stress (Atkin et al., 2000; Atkin and Tjoelker, 2003; Davidson et al., 2006). Thus, there remains a need for a more flexible, simple, empirical model to simulate R_s - T_s – one that would capture better the rise and fall of R_s with increasing T_s .

In addition to T_s , other factors can contribute to temporal and spatial variability in R_s , interacting with T_s , and distorting or masking the expected R_s - T_s relationship (Davidson et al., 1998; Jassal et al. 2008; Högberg et al., 2001; Boone et al., 1998; Lavigne et al., 2003; Curiel-Yuste et al., 2003 and 2004). For example, in some drought-stressed ecosystems, such as those in the Mediterranean climate, normally high T_s values are often accompanied by low soil moisture content. These conditions can limit decomposition and the supply of available carbon for metabolic activity, thereby decreasing R_s (Atkin and Tjoelker, 2003; Davidson et al., 2006). Therefore, any new alternatives to current

empirical models should also have the capacity to incorporate easily additional explanatory variables, other than T_s . This capability could help researchers investigate the interactions among various factors that drive R_s variability in their ecosystems.

The objective of this paper is to introduce a new, more flexible, empirical model for simulating the response of soil respiration to soil temperature. We call this model the Gamma model, because its functional form is similar to the

integrand of the Gamma function (i.e. $\Gamma(z) = \int_0^{\infty} x^{z-1} e^{-x} dx$; Press et al., 2007,

p.256). We tested the performance of the Gamma model across a wide range of forest ecosystems: two temperate coniferous forests of varying age, a mature boreal mixedwood forest, a mature boreal coniferous forest, and a mixed-age coppiced Mediterranean oak forest. We show that the newly proposed model is able to take on the shapes of the Q_{10} , Lloyd-Taylor, and logistic models, as dictated by observed R_s data. We compare how well the Gamma model is able to simulate seasonal and total annual soil C emissions versus the other three models, using data from one of the temperate coniferous sites. Simulated R_s was calculated with models parameterized using both the ordinary least squares estimation method and the weighted absolute deviation estimation method proposed by Richardson and Hollinger (2005). We also show how additional environmental factors that drive R_s variability can be easily incorporated into the Gamma model to investigate their effect on the R_s - T_s relationship. This is

illustrated by including soil moisture and soil carbon in Gamma model simulations of R_s from the drought-stressed Mediterranean Oak site and comparing our findings to those reported previously for that site (Rey et al., 2002 and Tedeschi et al., 2006).

3.3. METHODOLOGY

3.3.1 Study sites

Soil respiration observations used in this study came from ecosystems of various management type: natural regeneration of spruce and mixedwood (Southern Old Black Spruce site, SOBS, and Groundhog River Forest site, GRFS, respectively); pine plantations (Turkey Point mature site, TP39, and Turkey Point young site, TP02); and coppiced oak sites (Lazio Oak forest site, OAK) (Table 3.1). The data spanned three different climate zones: temperate, boreal and Mediterranean. The soil temperature range, over which the models were tested, ranged from $-18\text{ }^{\circ}\text{C}$ to $+35\text{ }^{\circ}\text{C}$ and measured R_s ranged from 0.1 to $13.0\text{ }\mu\text{mol of CO}_2\text{ m}^{-2}\text{ s}^{-1}$ (Table 3a). The observed R_s measurements varied from those collected half-hourly by automated soil chambers to those collected periodically (weekly to monthly) using manual soil chamber techniques (Table 3.1). In general, each site's data set spanned at least one full year of measurements.

3.3.2 The Gamma model and usefulness of model linearization

The models considered in this study are listed in Table 3.2, with further references on the widely used ones listed therein. Below we present more details on the Gamma model. The statistical form of the Gamma model (Table 3.2) to be applied to real-world data is written as follows:

$$Y_i = X_i^\alpha e^{\beta_0 + \beta_1 X_i + \varepsilon_i} \quad 3.1$$

where for an i th observation, Y_i is R_s (soil respiration in $\mu\text{mol of CO}_2 \text{ m}^{-2} \text{ s}^{-1}$); X_i is $(T_s + 40 \text{ }^\circ\text{C})$, where T_s is soil temperature in $^\circ\text{C}$; α , β_0 and β_1 are unknown coefficients to be estimated; and ε_i is the error term to account for the effects of random error (and uncontrolled factors) on the i th observed value of R_s .

Useful features of the Gamma model include special cases of the model: exponential and power. When α is equal to zero, the model becomes an exponential function, and when β_1 is equal to zero, the model becomes a power function. Furthermore, unlike quadratic functions, which would also allow R_s to decrease at high T_s values, the Gamma model does not have to be symmetric about its maximum value. The T_s value at which R_s peaks (i.e. T_{\max} in $^\circ\text{C}$) can be easily determined from the Gamma model, as:

$$T_{\max} = \left(\frac{\alpha}{-\beta_1} - 40 \right) \quad 3.2$$

where α and β_1 are described in Table 2 and Equation 3.1.

To parameterize the Gamma model, we first linearized it. The linear-in-parameters version of the model becomes a multiple linear regression model with two explanatory variables:

$$y_i = \alpha \text{Ln}(X_i) + \beta_0 + \beta_1 X_i + \varepsilon_i \quad 3.3$$

where y_i is the natural logarithm of the i th observation (i.e. $\text{Ln}[R_s]$), $\text{Ln}(X_i)$ is the natural logarithm of X_i , and the other terms are as described in Equation 3.1. Note that, while in reality $\text{Ln}(X_i)$ and X_i both represent the same driving factor, T_s , the usefulness of the linear regression procedure is greatly enhanced when $\text{Ln}(X_i)$ and X_i are treated as two distinct explanatory variables. For the ordinary least squares method to yield a unique set of estimated parameters, it is only necessary that the explanatory variables are not linearly dependent. Since in our empirical data $\text{Ln}(X)$ and X are not linearly dependent of each other, their joint usage is appropriate (Theil, 1971, pp. 109-111).

In the Gamma model, the temperature term, X_i , is modified, such that all of its values are positive. This is done, in part, because unless α is 0, negative T_s values in the non-linear form of the model (Equation 3.1) would result in negative or imaginary R_s values, which make no biological sense. In the linearized version of the model, zero and negative T_s values would also be problematic (i.e. $\text{Ln}(0)$ is negative infinity and the natural logarithm of a negative number is an imaginary number). Since R_s measurements are conducted year round and, in many boreal and temperate ecosystems, T_s measurements do go below 0°C , a new arbitrary zero for soil temperature had to be established. Soil temperature of -20°C is commonly reported in studies as the lowest soil temperature at which R_s is detected in the field. However, a recent study, where arctic soil was incubated in the laboratory, reported biological CO_2 emissions at temperatures down to -39°C

(Panikov et al., 2006). Therefore, we chose $-40\text{ }^{\circ}\text{C}$ to be our arbitrary zero and 40 was added to all input T_s values in the Gamma models evaluated herein, so that $X_i = (T_s + 40\text{ }^{\circ}\text{C})$. We note that the Kelvin scale was also tested. However, its scale was too broad, causing the models to fail to converge properly for the boreal sites, where the observed T_s range was relatively narrow (results not shown).

A benefit of applying natural logarithm (Ln) to R_s and using the Ln-transformed version of the Gamma model, was the alleviation of the *heteroscedasticity* problem (i.e. the violation of the assumption that the variance of the error term of the statistical form of the model remains constant at all values of the independent variable (Theil, 1971, p. 160)). The spread of Ln R_s values about the predicted curve was consistent with the assumption of constant variance (Figure 1a), whereas the spread of untransformed observed R_s values about the predicted curve was not (Figure 3.1d). Since we used ordinary least squares analysis (OLS) for model parameterization, avoiding heteroscedasticity in R_s data was important. Ln transforming the data reduced the variance of random error at high T_s values and amplified the variance at low T_s values (Figure 3.1b). Thus, the relatively small sample of R_s observation at high T_s , with large standard deviations, would contribute less in OLS estimates of model parameters, compared to R_s observations at lower T_s with lower standard deviations. The resulting effect was similar to using weighed absolute deviation (WAD) estimation method (Richardson and Hollinger, 2005), as discussed further below.

Another benefit of linearized models is that they can easily incorporate additional explanatory variables (both qualitative, i.e. dummy variables, and quantitative), as we show below. Multivariate linear regression analysis can be used to evaluate the Rs-Ts relationship in the context of these environmental variables, all within a single regression step. While additional explanatory variables can be also incorporated into non-linearized models, the mathematics of model parameterization often becomes too complex in those cases.

3.3.3 Model parameterization and comparison of model fits

The models (Table 3.2) were parameterized with observed Rs-Ts data, individually for each site, using a non-linear curve fitting procedure, PROC NLIN (Raphson-Newton's algorithm), in SAS 9.1 software (SAS Institute Inc, USA) for Q_{10} , LT and logistic models on untransformed data, but a linear curve-fitting procedure, PROC REG, for the Gamma model on Ln-transformed data (except when the WAD optimization method was used, in which case PROC NLN was used to evaluate the non-linear version of the Gamma model). The predicted values from the PROC REG procedure for the Gamma model were back-transformed and regressed against observed data to compute the coefficient of determination (R^2) and sum of residuals squared (RSS) that were comparable to those computed by PROC NLIN on untransformed data (Table 3.3). Akaike's Information Criterion (AIC) was calculated to compare the models based on an information-theoretical approach, following Anderson et al. (2000):

$$AIC = nLN\left(\frac{RSS}{n}\right) + 2K \quad 3.4$$

where n is the number of observations and K is the number of parameters. The AIC approach for model ranking differs from R^2 and RSS criteria, by being sensitive to the number of model parameters, favouring models with fewer parameters. Note that all models must have y_i in same units (i.e. either all Rs or all LnRs) for the comparison of computed AIC to be valid. In the analysis of the Oak Rs data set, when soil moisture and soil carbon were incorporated into the Gamma model (see Results and Discussion), the AIC values were computed using results from linear regression analysis on Ln transformed data (Table 3.5) and should not be compared directly with AIC values presented in Table 3.3, where all four Ts-only models are compared based on regressions to non-transformed data.

3.3.4 Comparison of annual and seasonal estimated Rs computed using two different estimation methods

We compared the Gamma model's ability to simulate annual and seasonal Rs emissions to that of the other three models, using data from the young temperate pine stand, TP02. Data from TP02 was chosen for this analysis due to the broad Ts range experienced by the site, which captured the decrease in observed Rs at high Ts values. This provided the wide range of data needed to demonstrate the full potential of the Gamma model in simulating Rs-Ts. Furthermore, unlike for the Oak site, we had replicate measurements of Rs for this

site, which allowed us to compute the random error variance required for the weighted absolute deviation (WAD) estimation method (Richardson and Hollinger, 2005), as discussed below.

We used the ordinary least squares (OLS) method to parameterize our models for comparing model fits using R^2 , RSS, and AIC criteria. However, a number of recent publications (Hollinger and Richardson, 2005; Richardson and Hollinger, 2005; Richardson et al., 2006b; Savage et al., 2008) suggested that the use of OLS was inappropriate for estimating model parameters of various respiration models, citing problems with non-Gaussian distribution of random error and heteroscedasticity of flux data. Instead, an alternative method was proposed and used in above studies: the weighted absolute deviation (WAD) estimation method (Richardson and Hollinger, 2005), which was sensitive to the variable random error in flux data. Furthermore, Richardson and Hollinger (2005) have shown that WAD and OLS can yield varying annual sums. Therefore, we also used the WAD method to parameterize our models and use these to compute R_s , which we compared to those computed from models parameterized by the OLS method.

However, we also realized that spatial variability in R_s , which also scales with R_s , being larger during the growing season and lower during the non-growing season, also made-up the observed variability in our data sets (Figure 3.2). This spatial variability can not be attributed to random error and thus cannot be compensated-for by the WAD method. Therefore, we also used natural

logarithm transformations (Ln) of R_s to stabilize the variance in our data set (McClave and Sincich, 2003, p.675) and help avoid the heteroscedasticity in the data, when parameterizing the models using the OLS method. We refer to this method as LN_OLS. We compared predicted R_s values obtained by the LN_OLS to that of the WAD and OLS methods for the Gamma model.

Here we would also like to mention that while the heteroscedasticity in our data was resolved by Ln-transformations, as was shown and discussed above (Figure 3.1), the problem of non-Gaussian distribution of the random error flux was not. In a separate analysis (results not shown) we found the random error distribution resembled the double exponential one, as was found by others for automated soil chamber data (Savage et al., 2008) and for ecosystem respiration data derived from eddy covariance measurements (Hollinger and Richardson, 2005) at other flux sites. However, unlike the situation in the above studies, the tails of our distribution were narrow, with most of the observations centered about a mean zero value. This suggested that OLS analysis on Ln-transformed data may still be valid in our case, despite the non-Gaussian distribution, and provided more reasons to try the LN_OLS approach.

For the WAD optimization method an estimate of the standard deviation of the random error (σ_r) was required in the weighing factor in the optimization method (for more details, see: Richardson and Hollinger, 2005; Richardson et al., 2006a). We estimated (σ_r) for TP02 using replicate R_s measurements, similar to the approach used by Richardson et al. (2006b) and Savage et al. (2008), scaled

by the R_s flux, which resulted in $\sigma_r = 0.041R_s + 0.018$. Briefly, for each collar, we had two to three replicate measurements of R_s . We took the mean of those replicate measurements and then the difference between the mean and each of the replicates. These differences were an estimate of random error for our measurements, which we plotted against the corresponding mean R_s values. The regression line fitted to this plot gave the σ_r .

Daily R_s emissions, calculated with models parameterized by all three methods, were calculated from continuous meteorological data available from TP02 weather station, which is operated as part of tower flux measurements at the site. Daily mean T_s values (mean over 2 to 20 cm soil depth) were used as input to the models to obtain daily R_s estimates. However, observed R_s - T_s data was used to parameterize the model. Calculated daily R_s emissions were converted to grams of C per meter squared per day and summed to annual and seasonal totals (Winter = December - March; Spring = April-May; Summer = June-September; Autumn = October-November). Errors on each sum were estimated as ± 2 standard deviations (i.e. $2\sqrt{n\sigma_s^2}$), where n is the sample size and σ_s^2 is the error mean square). Although 3 years of data were available at TP02, the relative trends in emissions between years were comparable, and we chose to present results only for year 2005. This was also the year with the largest T_s range (-3 to +31 °C) of the three study years.

3.4. RESULTS AND DISCUSSION

3.4.1 Comparison of model fits

For all sites, statistically the fit of the Gamma model was comparable or stronger compared to the fits of the other three models, as was suggested by the trends in R^2 , RSS and AIC (i.e. high R^2 (Table 3.3a) and low RSS and AIC values for the better-fitted model (Table 3b)). In their comparison of simple respiration models, Richardson et al. (2006a) also found the Q_{10} and two-parameter LT model to perform poorly compared to sigmoid shaped models for various field respiration data (i.e. soil and ecosystem respiration). Similarly, Tuomi et al. (2008) found that the Q_{10} model produced worse fits compared to the LT model, in their comparison of different empirical models for simulating soil respiration data obtained from various laboratory incubation experiments.

Our results showed that the Gamma model can take on the shapes of the other three models (Figure 3.2). For example, often in cool boreal climates, the range of soil temperatures over which R_s is measured is narrower compared to the warmer climate zones and the maximum T_s measured is often around 20°C (Figure 3.2, Table 3.3). At such sites, R_s - T_s relationship tends to follow an exponential-type curve, often simulated well by the Q_{10} model (e.g. Gaumont-Guay et al., 2006; Khomik et al., 2006). For both boreal stands, the Gamma model showed an exponential-type shape and was similar to the Q_{10} curve, except at high T_s values. At high T_s , the Gamma curve did not increase exponentially, better reflecting observations compared to Q_{10} (Figure 3.2 c and d). At TP39, R_s data took on a sigmoid-type shape and the Gamma model was able to simulate

well this shape, following the curve obtained from the logistic model (Figure 3.2a).

In the case of TP02 and the Oak stands, R_s decreased at high T_s (above $\sim 20^\circ\text{C}$). Of the four models tested here, only the Gamma model had a mathematical form capable of replicating that decrease (Figure 3.2 b and e). For these two sites, using the Gamma model to describe the R_s - T_s relationship produced the most improvement in model fit versus the other models (Table 3.3). The decrease in R_s at high T_s values at TP02 was likely due in part to disproportionate seasonal growth of various herbaceous species compared to TP39 (Peichl and Arain, 2006). We observed that this growth tended to peak in June and die-off over July, when some of the highest T_s values were observed for the site. Thus, a seasonal decrease in respiring biomass in mid to end of the growing season may have been responsible for the decrease in R_s above 25°C at TP02. This was in contrast to the decrease in R_s at high T_s experienced by the Mediterranean Oak site, where soil moisture played a greater role, as discussed below.

3.4.2 Comparison of annual and seasonal estimated R_s computed using two different estimation methods

All models produced annual emissions that were within the range of values reported in the literature. For example, Raich et al. (1992) reported R_s of 681 ± 95 g C per m^{-2} yr^{-1} for temperate coniferous forests. This was comparable to our estimates of 540 ± 17 to 678 ± 37 g C per m^{-2} yr^{-1} for the temperate pine stand, TP02 (Table 3.4).

In general, annual estimates from the Q₁₀ and LT models were statistically different from those generated by the Logistic and Gamma models, for both OLS and WAD methods (Table 3.4). The only exception was the LT model's annual sum obtained from OLS analysis, which was comparable, within error estimates, to the logistic and Gamma estimates (Table 3.4). The differences in annual emissions between models seemed to be driven by differences in winter estimates. In winter, both the Q₁₀ and LT models generally produced higher Rs sums compared to the logistic and Gamma models, irrespective of the optimization method (Table 3.4).

Our results, allowed us to assess whether the choice of estimation methods was indeed more important than the choice of model functional form (Richardson and Hollinger, 2005). We found that unlike the logistic and Gamma models, the Q₁₀ and LT models overestimated observed Rs at Ts values up to about 5°C and above 25°C, for both the OLS and WAD methods (cf. Figure 3.3 (a and b) versus (d and e)). This overestimation resulted in the differences in seasonal and annual sums reported above. These result suggested that the choice of the functional form of the model was more important than the choice between estimation methods. More specifically, we found that when the model was well chosen, the estimated values of OLS method and especially LN_OLS method turned out to be nearly identical to those of the WAD method (Figure 3.4).

3.4.3 Expanding the Gamma model – the Oak site case study

Previous publications characterized R_s at the Oak sites (Rey et al., 2002; Tedeschi et al., 2006) in detail and determined that variability in R_s was controlled by both T_s and soil moisture variabilities. The authors reported that when soil volumetric water content (θ_s) was above 20%, R_s variability was largely controlled by T_s variability (Rey et al., 2002; Tedeschi et al., 2006). However, below that threshold, θ_s took on a more dominant control, causing R_s to decline at high T_s values. The data set we obtained from the researchers (Venessa Tedeschi, *pers communications*) consisted of measurements conducted at three different stands of various age after coppicing (1 to 17 years). Tedeschi et al (2006) reported statistical differences in observed R_s between the recently coppiced Oak stand and the one coppiced 17 years prior to their study. They also reported differences in soil C content between the sites, which may help to explain some of the intersite variability. Thus, we choose the Oak data to demonstrate how additional explanatory variables can be added into the linearized Gamma model to simulate better the observed R_s at the site, and to study the various interactions of the controlling factors. A categorical variable (i.e. a dummy variable) was used to differentiate observations collected at θ_s above 20% (i.e. wet conditions) and those collected at θ_s below 20% (i.e. dry conditions). We let Ms_{20_i} be the dummy variable such that it assumed the value of 1, if the θ_s of the i th observation was above 20%, otherwise, it assumed the value of 0.

To allow the Gamma model to yield two predicted values for CO_2 emission at any given soil temperature (one under the dry condition, the other

under the wet condition), we modified Equation 3.3 to allow its parameters to vary, as follows:

$$\beta_0 = \beta_{01} + \beta_{02} Ms20_i \quad 3.4a$$

$$\alpha X_i = \alpha_{01} X_i + \alpha_{02} Ms20_i X_i \quad 3.4b$$

$$\beta_1 \ln(X_i) = \beta_{11} \ln(X_i) + \beta_{12} Ms20_i \ln(X_i) \quad 3.4c$$

where α_{01} , α_{02} , β_{01} , β_{02} , β_{11} , and β_{12} were the unknown coefficients to be estimated; and the other variables are as defined previously. In equations 3.4b and 3.4c, the terms involving the product of the dummy variable and X_i , as well as the dummy variable and $\ln(X_i)$, are both called “interaction terms”.

Interaction terms were treated as additional explanatory variables in the model.

The category with $\theta_s < 20\%$ was used as the reference category.

The site PIs also provided us measurements of the soil carbon (C) content with their Rs-Ts data set. A mean site C (mg/g) was used in the model. This variable ($X_{i,2}$) was added only into the exponential part of the model, because we found that its inclusion as a power function was unnecessary. Thus, the fully flexible statistical formulation of the expanded, moisture-and-C-sensitive Gamma model for the Oak site was as follows:

$$Y_i = X_i^{\alpha_{01}} X_i^{(\alpha_{02} Ms20_i)} e^{(\beta_{01} + \beta_{02} Ms20_i) + (\beta_{11} X_i) + (\beta_{12} Ms20_i X_i) + \beta_2 X_{i,2} + \varepsilon_i} \quad 3.5$$

where α_{01} , α_{02} , β_{01} , β_{02} , β_{11} , β_{12} , and β_2 were unknown coefficients to be estimated. In this model, all of the unknown coefficients can be estimated simultaneously, by using a regression procedure in any widely available statistical package (ie. SAS, SPSS, Matlab).

Equation 3.5 can be interpreted as follows. For dry soil condition case (i.e. $\theta_s < 20\%$ and $M_{s20i} = 0$), the model simply becomes:

$$Y_i = X_i^{\alpha_{01}} e^{\beta_{01} + \beta_{11}X_i + \beta_2 X_{i,2} + \varepsilon_i} \quad 3.6a$$

For the wet soil case (i.e. $\theta_s > 20\%$ and $M_{s20i} = 1$), the model becomes:

$$Y_i = X_i^{(\alpha_{01} + \alpha_{02})} e^{(\beta_{01} + \beta_{02}) + (\beta_{11} + \beta_{12})X_i + \beta_2 X_{i,2} + \varepsilon_i} \quad 3.6b$$

with all variables as defined above. Clearly, the inclusion of θ_s and C in the model improved the model fit compared to the T_s -only model (i.e. R^2 increased, while RSS and AIC decreased, Table 3.5).

In their analysis, Rey et al. (2002) applied two different models to simulate R_s at the site: the exponential Q_{10} model (i.e. driven by T_s only) whenever θ_s was above 20% and a linear one that related R_s to θ_s when θ_s was below 20%. At low θ_s , neither Ray et al. (2002), nor Tedeschi et al. (2006), were able to characterize the R_s - T_s relationship at their site. In contrast, here we applied a single model, the expanded Gamma model, which included both T_s and θ_s , simultaneously and could characterize R_s - T_s under both, wet and dry, conditions. For the high θ_s case, the Gamma model took-on the shape of a power function (i.e. $\beta_{11} + \beta_{12} \sim 0$), resembling the Q_{10} model used by Rey et al (2002) (Figure 3.5). When θ_s was included in the model, the magnitudes of the associated estimated coefficients for T_s variables decreased and their associated t -values almost halved (i.e. compare Table 3.5, column 1 vs 2), suggesting interactions between the two explanatory factors. We also estimated the T_s at

which maximum R_s can be observed at the site: 16.3°C (i.e. $T_{\max} = \left(\frac{31.54}{0.56} - 40 \right)$), following Equation 3.2 above and using the model output from Table 3.5, column (2)). This value was in agreement with Tedeschi et al. (2006), who reported that they could best fit the Q_{10} model across the Oak stands for T_s only up to 16°C . Above 16°C , the chance of observing dry conditions at the site increased, which masked the response of R_s to T_s , such that the Q_{10} model was no longer applicable (Tedeschi et al., 2006) (i.e. R_s began to decrease). At this point, we would also like to note that we did test the Gamma model, using θ_s as a continuous variable (i.e. measured at each sampling point along with R_s). However, soil moisture as a continuous variable was found to be statistically insignificant for this site ($p > 0.1$) in the final model (results not shown). Therefore, we did not include that variable in our analysis.

Our results were also in agreement with Tedeschi et al. (2006) finding that R_s was statistically higher at the older Oak stand (17 years after coppicing), compared to the younger stands (1 and 10 years post-coppicing). However, we were able to go a step further with our analysis, linking intersite variability in R_s to intersite differences in soil C content. In our initial investigations of the expanded Gamma model, we created and used dummy variables to represent observations from the different aged coppiced stands, using the youngest stand as the reference category. We found that the 1- and 10- year-old stands were statistically similar (i.e. the estimated coefficient for the dummy variable

representing the 10-year-old stand was statistically indistinguishable at $p < 0.001$ from that of the reference category – the 1-year-old site, results not shown). In contrast, the variable representing the 17-year-old stand was statistically different, and so it was retained in the initial model (results not shown). Next, we incorporated soil C into the model, as above, and found that the two variables were mutually exclusive (i.e. the estimated coefficients associated with the site dummy variable and the C variable were statistically insignificant (i.e. $p > 0.1$), when both variables were present in the model, requiring one of them to be dropped; results not shown). This finding suggested that intersite differences in R_s at the Oak site, were related to intersite difference in soil C, with R_s being higher for soils with high C. This trend was upheld for both dry and wet soil moisture conditions (Figure 3.5).

Finally, we would like to mention that all of the above analysis (i.e. adding θ_s and C into the model) could have also been done using the Q_{10} model, which also lends itself to linearization. However, the Q_{10} model would not be able to simulate the decrease in R_s at high T_s values, due to the limitations of its mathematical form, and thus would produce worse model fits.

3.5. CONCLUSIONS

We introduced a new empirical model for simulating R_s with T_s , called the Gamma model. This model had the ability to take-on the exponential or logistical shapes that often characterize R_s - T_s data from boreal and temperate

climates. More importantly, this new model was able to simulate the decrease in R_s at high T_s values, which was observed at the young temperate and Mediterranean sites we studied. In general, the Gamma model fit the data better compared to the Q_{10} and LT models, and was comparable in fit to the logistic model, based on R^2 , RSS and AIC values. The annual soil C emissions, simulated with the Gamma model, were within the range of values reported in the literature, lower compared to the sums generated by the LT and Q_{10} models, and comparable to those generated by the logistic model. Our results also suggested that once the proper functional form of the R_s - T_s relationship is chosen for a given data set, the differences between ordinary least squares (OLS) and weighted absolute deviation (WAD) estimation methods, used to parameterize the models, are no longer as important. Therefore, in cases where the use of the WAD method may be complicated (i.e. if random error can not be determined), the use of OLS method should still give reasonable predictions, provided the model is well chosen. We also showed that the Gamma model can easily incorporate additional explanatory factors, such as soil moisture and soil nutrients, to help researchers simulate better and interpret the R_s - T_s relationship at their sites in the context of these additional factors.

We hope this new model will lead to improved simulations of the R_s - T_s relationship across a range of terrestrial ecosystems and provide researchers an additional tool for studying the relationship between soil respiration and soil temperature within the context of its environment.

3.6 ACKNOWLEDGEMENTS

Funding for this study was provided by the Natural Sciences and Engineering Research Council (NSERC) of Canada Discovery and Strategic Project Grants and NSERC, the Canadian Foundation for Climate and Atmospheric Sciences (CFCAS), and the BIOCAP Canada Foundation funded Fluxnet-Canada Research Network (FCRN). FRCN is presently known as Canadian Carbon Program (CCP), which was funded by CFCAS. Support from the Canadian Foundation of Innovation (CFI), the Ontario Innovation Trust (OIT), McMaster University and Queen's University is also acknowledged. In-kind support from the Ontario Ministry of Natural Resources (OMNR), the Long Point Recreation and Conservation Authority (LPRCA), the Canadian Forest Service (CFS) and the Ontario Power Generation (OPG) is appreciated. We thank OMNR research groups from both the Simcoe area and Sault St. Marie offices for their assistance in field work and site maintenance. We thank Bruce Whitside for providing access to the forest on his property (TP02). We would like to acknowledge Andy Black and David Gaumont-Guay (SOBS) and Venessa Tedeschi (Oak site) for sharing their data sets with us. We thank Andrew Richardson for sharing with us his WAD schemes in SAS and also for advice on random error analysis. We are grateful to Natalia Restrepo-Coupé, Mahmoud Pejam, Jason Brodeur, Josh McLaren, Matthias Peichl and numerous field assistants for helping with data collection.

3.7 REFERENCES

- Anderson DR, Burnham KP, Thompson WL (2000) Null Hypothesis Testing: Problems, Prevalence, and an Alternative. *The Journal of Wildlife Management*, 64, 4: 912-923.
- Atkin OK and Tjoelker MG (2003) Thermal acclimation and the dynamic response of plant respiration to temperature. *TRENDS in Plant Science*, 8, 7: 343-351.
- Atkin OK, Edwards EJ, Loveys BR (2000) Research review: Response of root respiration to changes in temperature and its relevance to global warming. *New Phytologist*, 147: 141-154.
- Boone RD, Nadelhoffer KJ, Canary JD, Kaye JP (1998) Roots exert a strong influence on the temperature sensitivity of soil respiration. *Nature*, 496: 570-572.
- Curiel-Yuste J, Janssens IA, Carrara A, Ceulemans R (2004) Annual Q_{10} of soil respiration reflects plant phenological patterns as well as temperature sensitivity. *Global Change Biology*, 10: 161-169.
- Curiel-Yuste J, Janssens IA, Carrara A, Meiresonne L, Ceulemans R (2003) Interactive effects of temperature and precipitation on soil respiration in a temperate maritime pine forest. *Tree Physiology*, 23: 1263-1270.
- Davidson EA, Belk E, Boone RD (1998) Soil water content and temperature as independent or confounded factors controlling soil respiration in a temperate hardwood forest. *Global Change Biology*, 4: 217-227.
- Davidson EA, Janssens IA, Luo Y-Q (2006) On the variability of respiration in terrestrial ecosystems: moving beyond Q_{10} . *Global Change Biology*, 11: 1-11.
- Falge E, Baldocchi D, Tenhunen J, Aubinet M, Bakwin P, Berbigier P, Bernhofer C, Burba G, Clement R, Davis KJ, Elbers JA, Goldstein AH, Grelle A, Granier A, Guðmundsson J, Hollinger D, Kowalski AS, Katu G, Law BE, Malhi Y, Meyers T, Monson RK, Munger JW, Oechel W, Paw U KT, Pilegaard K, Rannik Ü, Rebmann C, Suyker A, Valentini R, Wilson K, Wofsy S (2002) Seasonality of ecosystem respiration and gross primary production as derived from FLUXNET measurements. *Agricultural and Forest Meteorology*, 113: 53-74.
- Gaumont-Guay D, Black TA, Griffis T, Barr AG, Morgenstern K, Rachhpal SJ, Nesic Z (2006) Influence of temperature and drought on seasonal and interannual variations of soil, bole, and ecosystem respiration in a boreal aspen stand. *Agricultural and Forest Meteorology*, 140: 203-219.

- Hanson PJ, Edwards NT, Garten CT, Andrews JA (2000) Separating root and soil microbial contributions to soil respiration: A review of methods and observations. *Biogeochemistry*, 48: 115-146.
- Högberg P, Nordgren A, Buchmann N et al (2001) Large-scale forest girdling shows that current photosynthesis drives soil respiration. *Nature*, 411: 789-792.
- Hollinger DY and Richardson AD (2005) Uncertainty in eddy covariance measurements and its application to physiological models. *Tree Physiology*, 25: 873-885.
- Janssens IA, Pilegaard K (2004) Large Seasonal changes in Q₁₀ of soil respiration in a beech forest. *Global Change Biology*, 9: 911-918.
- Jassal RS, Black A, Novak MD, Gaumont-Guay D, and Nesic Z (2008) Effect of soil water stress on soil respiration and its temperature sensitivity in an 18-year-old temperate Douglas-fir stand. *Global Change Biology*, 14: 1-14.
- Khomik M, Arain MA, McCaughey JH (2006) Temporal and spatial variability of soil respiration in a boreal mixedwood forest. *Agricultural and Forest Meteorology*, 140: 244-256.
- Kolari P, Pumpanen J, Rannik Ü, Ilvesniemi H, Hari P and Berninger F (2004) Carbon balance of different aged Scots pine forests in Southern Finland. *Global Change Biology*, 10: 1106-1119.
- Lavigne MB, Boutin R, Foster RJ, Goodine G, Bernier PY, Robitaille G (2003) Soil respiration responses to temperature are controlled more by roots than by decomposition in balsam fir ecosystems. *Canadian Journal of Forest Research*, 33: 1744-1753.
- Lloyd, J and Taylor, JA (1994) On the temperature dependence of soil respiration. *Functional Ecology*. 8: 415-424.
- Mäkiranta P, Minkkinen K, Hytönen J, Laine J (2008) Factors causing temporal and spatial variation in heterotrophic and rhizospheric components of soil respiration in afforested organic soil croplands in Finland. *Soil Biology and Biochemistry*, 40: 1592-1600.
- McClave JT and Sincich T (2003) *Statistics*. 9th Ed. Prentice Hall, Upper Saddle River, NJ, USA.
- Panikov NS, Flanagan PW, Oechel WC, Mastepanov MA, Christensen TR (2006) Microbial activity in soils frozen below -39°C. *Soil Biology and Biochemistry*, 38: 785-794.
- Peichl M, Arain MA (2006). Above- and belowground ecosystem biomass and carbon pools in an age-sequence of temperate pine plantation forests. *Agricultural and Forest Meteorology*, 140: 51-63.

- Press WH, Teukolsky SA, Vetterling WT, Flannery BP (2007) *Numerical Recipes: The Art of Scientific Computing*. 3rd Ed. Cambridge University Press, NY, USA.
- Raich, JW and Schlesinger, WH (1992) The global carbon dioxide flux in soil respiration and its relationship to vegetation and climate. *Tellus*, 44B: 81-99.
- Rey A, Pegoraro E, Tedeschi V, De Parri I, Jarvis PG, Valentini R (2002) Annual variation in soil respiration and its components in a coppice oak forest in Central Italy. *Global Change Biology*, 8: 851-866.
- Richards FJ (1959) A flexible growth function for empirical use. *Journal of Experimental Botany*, 10: 20-300.
- Richardson AD, Braswell BH, Hollinger DY, Burman P, Davidson EA, Evans RS, Flanagan LB, Munger JW, Savage K, Urbanski SP, Wofsy SC (2006a) Comparing simple respiration models for eddy flux and dynamic chamber data. *Agricultural and Forest Meteorology*, 141: 219-234.
- Richardson AD and Hollinger DY (2005) Statistical modeling of ecosystem respiration using eddy covariance data: Maximum likelihood parameter estimation, and Monte Carlo simulation of model and parameter uncertainty, applied to three simple models. *Agricultural and Forest Meteorology*, 131: 191-208.
- Richardson AD, Hollinger DY, Burba GG, Davis KJ, Flanagan LB, Katul GG, Munger JW, Ricciuto DM, Stoy PC, Suyker AE, Verma SB, Wofsy SC (2006b) A multi-site analysis of random error in tower-based measurements of carbon and energy fluxes. *Agricultural and Forest Meteorology*, 136: 1-18.
- Rodeghiero M and Cescatti A (2005) Main determinants of forest soil respiration along an elevation/temperature gradient in the Italian Alps. *Global Change Biology*, 11: 1024-1041.
- Savage K, Davidson EA, Richardson AD (2008) Belowground responses to climate change: A conceptual and practical approach to data quality and analysis procedures for high-frequency soil respiration measurements. *Functional Ecology*, 22: 1000-1007.
- Schlesinger WH and Andrews JA (2000) Soil respiration and the global carbon cycle. *Biogeochemistry*, 48: 7-20.
- Tedeschi V, Rey A, Manca G, Valentini R, Jarvis P, Borghetti M (2006) Soil respiration in a Mediterranean oak forest at different developmental stages after coppicing. *Global Change Biology*, 12: 110-121.
- Theil, H (1971) *Principles of Econometrics*. New York: John Wiley & Sons, Inc.

Tuomi M, Vanhala P, Karhu K, Fritze H, Liski J (2008) Heterotrophic soil respiration – Comparison of different models describing its temperature dependence. *Ecological Modelling*, 211: 182-190.

Van't Hoff JH (1884) *Etudes de dynamique chimique*. Frederrk Muller & Co., Amsterdam.

Table 3.1: Description of sites and their associated respiration measurements used in this paper for model comparison.

Site Code	Age	Ecosystem	Climate	Mean annual Ta (°C)	Total annual Ppt (mm)	Location	Rs Measurement frequency	Measurements
TP39	69	White pine (planted forest)	Temperate	7.8	1010	42.712°N 80.357°W, Turkey Point Flux Station, Southern Ontario, Canada	2004-2006, biweekly to monthly (year-round)	Soil respiration (Rs), manually using a portable dynamic chamber system: LI-6400, LI-COR Biosciences, NB, USA Rs, same as above
TP02	6	White pine (planted forest)	Temperate	7.8	1010	42.661°N 80.560°W, Turkey Point Flux Station, Southern Ontario, Canada	Same as above	Rs, same as above
GRFS	79	Mixedwood (coniferous and broadleaf species) forest (naturally regenerated)	Boreal	1.5	814	48.217°N 82.156°W, Groundhog River Flux Station, Central Ontario, Canada	2004-2006, monthly (March to November, annually)	Rs, same as above
SOBS	111	Black-spruce forest (naturally regenerated)	Boreal	0.4	467	53.98717°N, 105.11779°W, Southern Old Black Spruce Flux Station, Northern Saskatchewan, Canada	2003, half-half-hourly (year-round)	Rs, automated, using a dynamic chamber system (Gaumont-Guay et al 2006).
Oak	0-18	Coppiced mixed-oak forest	Mediterranean	14	755	42°24'N, 11°55'E, Roccarespampani forest, Viterbo, Central Italy.	2001-2002, monthly (year-round)	Rs, manually, using a portable dynamic chamber system: EMG-2, PP-Systems, UK (Ledeschi et al 2002).

Table 3.2: Respiration models used in this paper.

Model common names	Name used in paper	Mathematical Equation	Reference
Modified Van't Hoff or Q_{10}	Q_{10} model	$R = R_{10} Q_{10}^{\frac{(T-10)}{10}}$	Van't Hoff 1894, Davidson et al (2006)
Lloyd and Taylor	LT model	$R = R_{10} e^{E' \left(\frac{1}{(283.15-227.13)} - \frac{1}{(T-227.13)} \right)}$	Lloyd and Taylor (1994)
Log-growth or logistic	Logistic model	$R = \frac{R_{\max}}{1 + e^{-(a(T-1/2_{\max}) - \beta_1)}}$	Richards (1959)
(None)	Gamma model	$R = (T)^\alpha e^{\beta_0 + \beta_1(T)}$	This manuscript

Where R = respiration in $\mu\text{mol of CO}_2 \text{ m}^{-2} \text{ s}^{-1}$; T = temperature, which is in $^{\circ}\text{C}$ for all models, except in LT, where it is in degrees Kelvin; R_{10} , Q_{10} , E' , R_{\max} , $T_{1/2_{\max}}$, a , α , β_0 and β_1 are all model parameters to be estimated from measurements. R_{10} = respiration at 10°C ; Q_{10} = respiration temperature sensitivity for every 10°C increase in T ; R_{\max} = maximum R ; $T_{1/2_{\max}}$ = T at which half of maximum R is attained.

Table 3.3:

(a) Comparison of model performances based on R^2 values for the regressions of observed versus modelled R for each site. The models compared here were the ones driven only by soil temperature (Ts).

Site	n*	Observed Ts range (°C)	Observed R range ($\mu\text{mol CO}_2 \text{ m}^{-2} \text{ s}^{-1}$)	Observed versus Modeled (R^2)**			
				Q_{10}	LT	Logistic	Gamma
TP39	1944	-0.5 to 29.5	0.2 to 9.2	0.576	0.635	0.693	0.696
TP02	1743	-1.0 to 35.2	0.2 to 7.9	0.348	0.397	0.455	0.464
GRFS	3026	-0.3 to 19.0	0.1 to 11.5	0.535	0.557	0.594	0.598
SOBS	7644	-18.1 to 19.2	0.1 to 10.9	0.594	0.612	0.622	0.621
Oak	1095	2.6 to 30.1	0.5 to 13.0	0.067	0.090	0.182	0.256

(b) Comparison of model performances based on residual sum of squares (RSS) and Akaike's Information Criterion (AIC) values.

Site	n*	Q_{10}		LT		Logistic		Gamma	
		RSS	AIC	RSS	AIC	RSS	AIC	RSS	AIC
TP39	1944	2263	299	1924	-17	1594	-380	1577	-401
TP02	1743	1486	-274	1372	-414	1235	-595	1213	-625
GRFS	3026	6035	2093	5731	1937	5233	1664	5208	1649
SOBS	7644	10097	2131	9608	1752	9340	1538	9365	1558
Oak	1095	4051	1330	3979	1303	3609	1189	3347	1085

*n = number of data points used to fit each model.

**difference between R^2 and adj R^2 was <0.001 , therefore only R^2 values are reported above.

Number of parameters used to compute AIC was 2, 2, 3, and 3, for the Q_{10} , LT, Logistic and Gamma models, respectively.

Table 3.4: Comparison of annual and seasonal Rs totals calculated from each model for TP02 stands for year 2005, using ordinary least square estimation (OLS), OLS on LN-transformed data (Gamma model only), and weighted maximum likelihood estimation method. Estimated errors on sums are shown as ± 2 st.dev.

	Model	Modeled Rs range ($\mu\text{mol CO}_2 \text{ m}^{-2} \text{ s}^{-1}$)	Winter (g C m^{-2})	Spring (g C m^{-2})	Summer (g C m^{-2})	Autumn (g C m^{-2})	Annual (g C m^{-2})
WAD	Q ₁₀	0.6 to 4.0	86 \pm 16	89 \pm 12	358 \pm 17	79 \pm 12	612 \pm 29
	LT	0.3 to 3.7	64 \pm 16	92 \pm 11	357 \pm 16	78 \pm 11	592 \pm 28
	Logistic	0.1 to 2.5	38 \pm 16	103 \pm 11	303 \pm 16	94 \pm 11	534 \pm 27
	Gamma	0.2 to 2.6	39 \pm 16	100 \pm 11	318 \pm 16	82 \pm 11	540 \pm 27
OLS	Q ₁₀	0.1 to 2.6	132 \pm 21	107 \pm 15	342 \pm 21	98 \pm 15	678 \pm 37
	LT	0.6 to 3.3	100 \pm 20	107 \pm 14	348 \pm 20	94 \pm 14	649 \pm 35
	Logistic	0.2 to 2.8	46 \pm 19	109 \pm 14	340 \pm 19	90 \pm 14	586 \pm 33
	Gamma	0.2 to 2.7	45 \pm 19	109 \pm 14	339 \pm 19	90 \pm 14	583 \pm 33
LN_OLS	Q ₁₀	0.4 to 4.4	72 \pm 8	84 \pm 7	376 \pm 8	73 \pm 7	605 \pm 11
	Gamma	0.1 to 2.6	41 \pm 10	99 \pm 7	318 \pm 10	82 \pm 7	540 \pm 17

Note: seasons are defined as: Winter (Jan-Mar, Dec); Spring (Apr & May); Summer (Jun – Sep); Autumn (Oct & Nov).

Table 3.5: Resulting estimates of the “unknown coefficients” for the Ts-only and the moisture-&-soil-carbon sensitive Gamma models, fitted to the Oak site data. (n=1095, in both cases). The linearized form of the Gamma model was used.

Unknown coefficient	<u>(1)</u>		<u>(2)</u>	
	<u>Ts-only model</u>		<u>Moisture and soil C-sensitive model</u>	
	Estimate	t-value	Estimate	t-value
α_{01}	35.97	14.6	31.54	7.0
α_{02}	---	---	-25.77	-3.7
β_{01}	-107.39	-14.7	-94.50	-6.9
β_{02}	---	---	74.60	3.6
β_{11}	-0.64	-13.8	-0.56	-6.9
β_{12}	---	---	0.53	4.0
β_2	---	---	0.01	3.6
R^2		0.241		0.300
Adj R^2		0.240		0.296
RSS		186		171
AIC		-1937		-2017

Note: All values significant at $p < 0.001$.

Figure 3.1: a) Natural log (Ln) transformed observed soil respiration, LnRs, measurements versus soil temperature, Ts, for the TP39 site (symbols). Also included are the Ln-transformed predicted Rs values (line curve). Taking the Ln of observed values helped to avoid the heteroscedacity problem. b) Standard deviations of observed Rs measurements binned by Ts values, for Ln-transformed Rs (filled symbols) versus non-transformed data (open symbols). c) comparison of predicted Rs curves derived from Ln-transformed and untransformed Rs, using the Gamma model. Grey symbols are observed Rs.

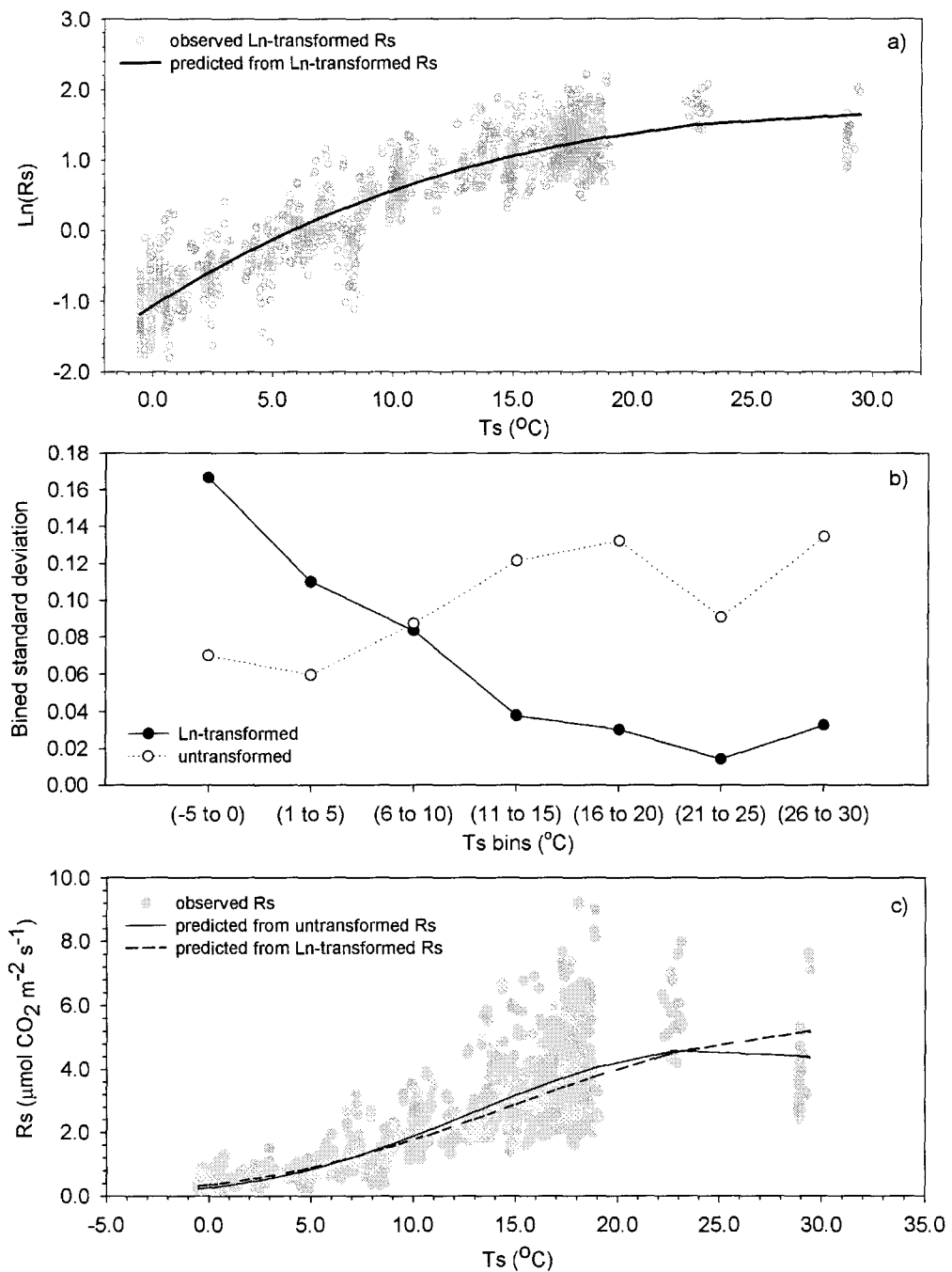


Figure 3.2: Comparison of models fitted, individually, to soil respiration (R_s) and soil temperature (T_s) data from the five sites a) TP39, b) TP02, c) GRFS d) SOBS, and e) Oak. Note that as T_s range increases, R_s tends to decrease at high T_s values (above ~ 20 °C) and the Gamma model has the flexibility to reflect that decrease in R_s , which is especially well illustrated by data for TP02 and Oak sites. The Gamma model was also flexible enough to take on the shape of an exponential Q_{10} model (GRFS) and logistic model (TP39), as dictated by observed data.

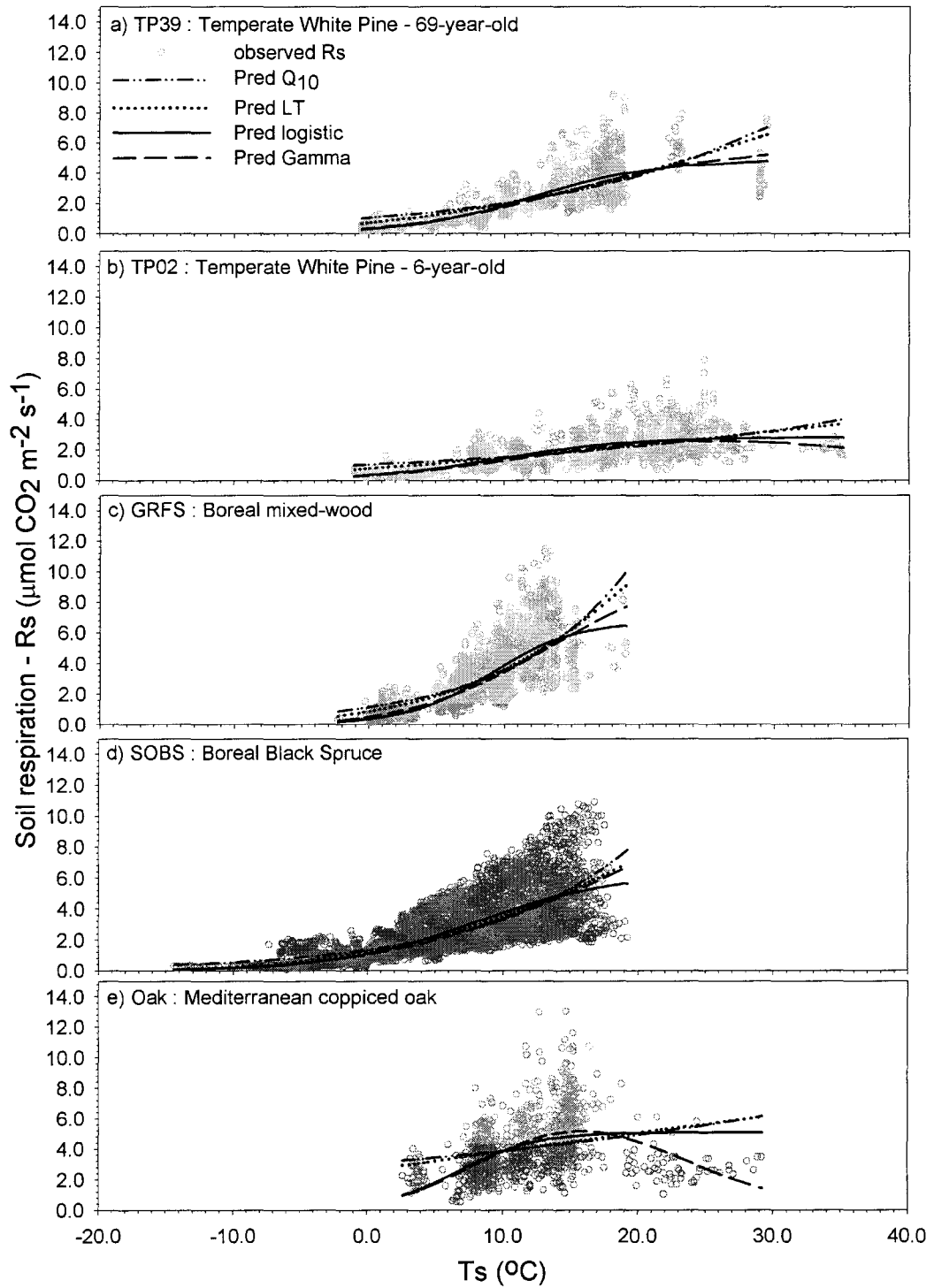


Figure 3.3: Comparison of predicted soil respiration for the young temperate pine forest (TP02). R_s was predicted with models parameterized using two different parameter estimation methods: ordinary least squares, OLS, (solid line) and the weighted absolute deviation, WAD, (dashed line). The comparison is made for all four empirical models tested in this study: a) Q_{10} , b) Lloyd-Taylor, c) Log, and d) Gamma. These results highlight the importance of choosing the proper functional form for the R_s - T_s relationship. Open symbols represent observed R_s measurements.

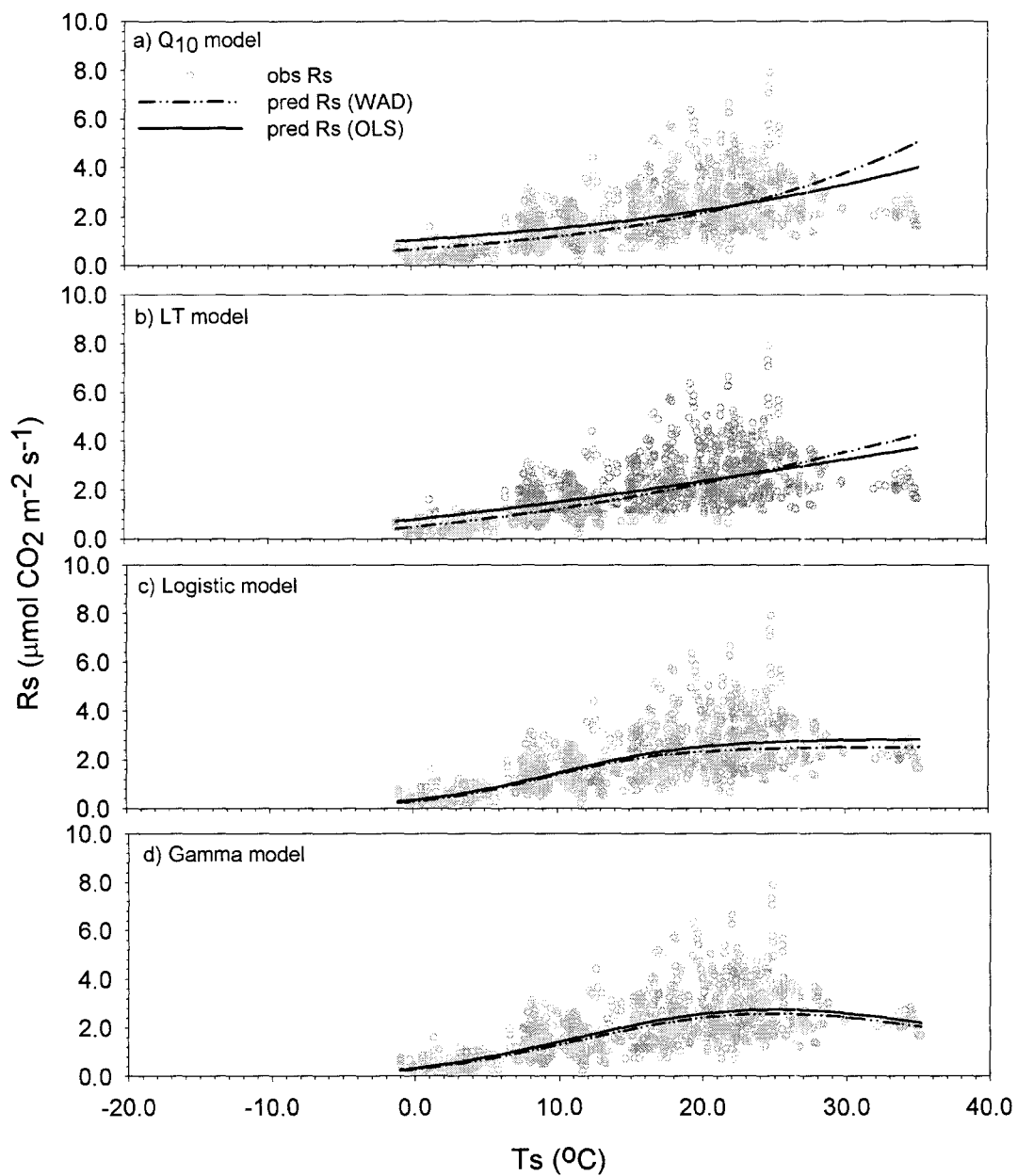


Figure 3.4: Comparison of predicted soil respiration (Rs) for the young temperate pine forest (TP02). Rs was predicted with the Gamma model, parameterized using three different parameter estimation methods: ordinary least squares, OLS, (solid line); the weighted absolute deviation, WAD, (dashed line); and OLS method applied to \log_e transformed data (dotted line). Open symbols represent observed Rs measurements. These results show that once the functional form of the Rs-Ts relationship is chosen well, the differences between the estimation methods used for model parameterization are no longer as important.

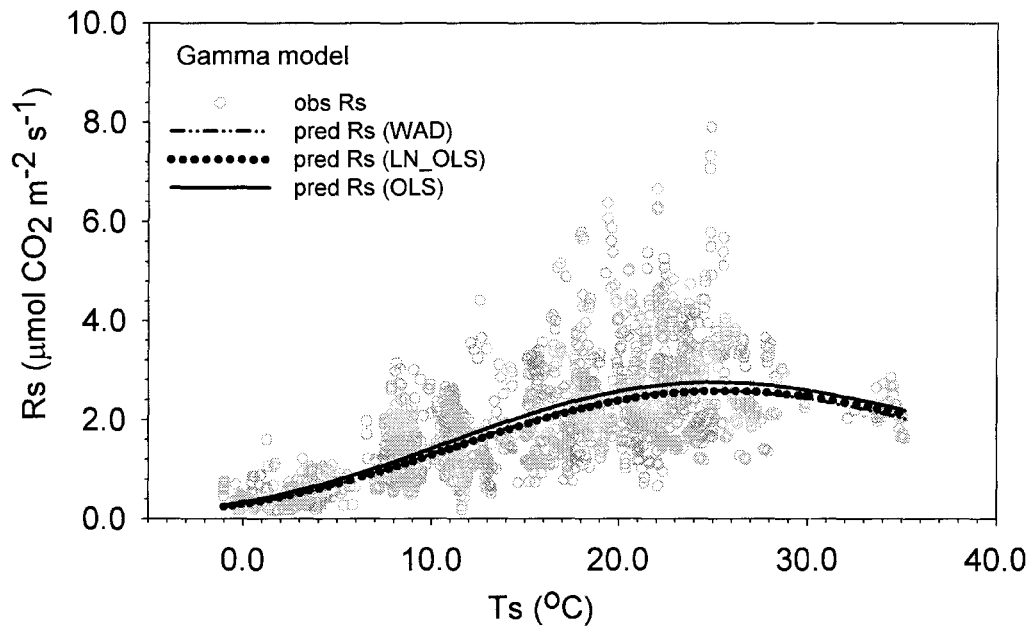
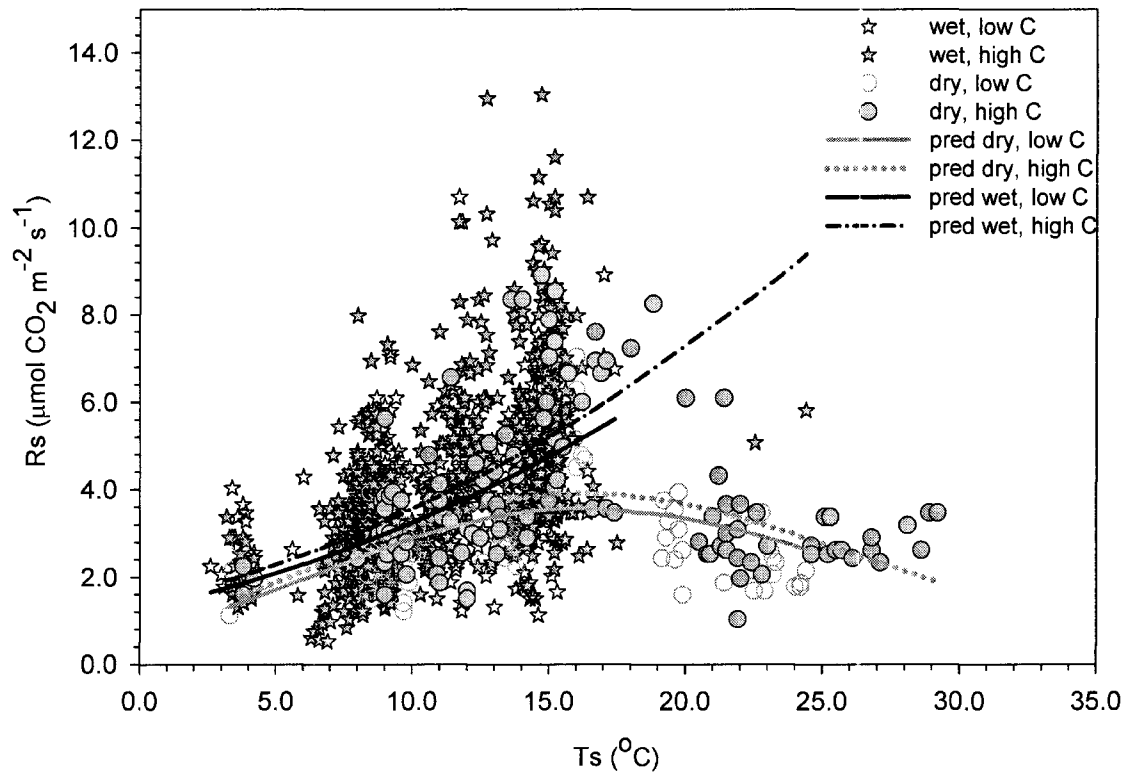


Figure 3.5: Comparison of predicted soil respiration, R_s , values, obtained from the expanded (moisture & soil C - sensitive) Gamma model (curves) to that of observed R_s values (symbols). For clarity, R_s measurements belonging to the low (grey lines and circle symbols) and high (black lines and star symbols) soil moisture, θ_s , categories are distinguished in the plot. Also the low (open symbols and broken lines) and high soil C data is distinguished. The model (Equation 5 in text) was fitted with all 1095 data points, in a single regression step.



CHAPTER 4

CONTROL OF CLIMATE, EDAPHIC CONDITIONS AND STAND PHYSIOLOGY ON INTERSITE AND INTERANNUAL VARIABILITY OF SOIL RESPIRATION ACROSS FOUR, DIFFERENT-AGE, PLANTED FORESTS ⁷

4.1 ABSTRACT

Soil respiration (Rs) was measured across four different-aged (6-, 19-, 34-, and 69-year old) planted white pine (*Pinus Strobus* L.) forests, located in southern Ontario, Canada, over the course of three years (2004 to 2006). These measurements were used to estimate daily, monthly and annual soil carbon emissions (Rs) across the sites and to investigate causes of temporal variability in Rs. Annual Rs ranged between 539 ± 31 to 600 ± 31 ; 558 ± 31 to 662 ± 31 ; 587 ± 31 to 665 ± 31 ; 645 ± 31 to 732 ± 31 $\text{g C m}^{-2} \text{yr}^{-1}$, for the 6-, 19-, 34-, and 69-year old stands, respectively. In general, annual emissions from the oldest stand were higher than emissions from the youngest two stands, during the study. However, emissions from the 34-year-old stand were comparable to those from the 19- and 6-year-old stands, within the margins of estimated error on the sums. Interannually, emissions during the two warmer study years were higher than those of the cooler year, but only for the three older stands. Intersite differences in emissions were driven mostly by stand physiology, while interannual differences reflected interannual variability in climatic factors, as well as differences in stand physiology that modified the site's microclimates. The highest daily Rs was observed during late July to early August. About half of the annual soil carbon was emitted during the summer across all four stands. During autumn months an additional 25-31% of carbon was emitted and in spring 12-22%. The lowest daily emissions were observed during winter, and accounted for only 5-8% of total annual Rs.

Soil temperature (Ts), mean annual and daily air temperatures, frequency of precipitation events, the thickness of the LFH soil horizon and its carbon to nitrogen ratio, and mean annual photosynthetically active radiation – all helped to explain variability in our observed Rs data. While Ts was the dominant controlling factor of Rs variability across our stands, the thickness of the litter layer explained about 6.8% of the temporal variability in the Rs-Ts relationship, followed by CN ratio (1.5%). The remaining factors contributed relatively less to the model's explanatory power (0.04 to 0.5%).

The study adds to our knowledge and understanding of temporal soil carbon dynamics in different-aged forests, growing in a temperate climate zone.

⁷ This paper will be submitted for publication to *Agricultural and Forest Meteorology*: Khomik M, Arain MA (2009) Control of climate, edaphic conditions and stand physiology on inter-site and inter-annual variability of soil respiration across four, different-age, planted stands.

4.2. INTRODUCTION

On annual time scales, photosynthesis and respiration processes tend to dominate the exchange of carbon dioxide (CO₂) in terrestrial ecosystems, determining the carbon sink or source strengths of a forest ecosystem. Many factors, biotic and abiotic, can affect carbon exchange of forests, pushing the balance of CO₂ emissions in either direction, from one year to the next (Baldochi, 2008). Unlike our understanding of photosynthesis (Farquahar et al., 1980), our understanding of forest respiration processes, especially what drives their temporal variability is still incomplete.

In forest ecosystems, soil respiration (Rs) can account for up to two thirds of total annual CO₂ emissions (Valentini, 2000; Law et al., 2001). Temporal variability in Rs is often associated with temporal variability in soil temperature (Ts). However, the temperature sensitivity of Rs is often confounded by other abiotic and biotic drivers. For example, soil moisture (θ_s) has been shown to decouple Rs from Ts, especially at high Ts values or in water stressed ecosystems (Davidson et al., 1998; Rey et al., 2002; Jassal et al., 2008). Precipitation (PPT) is another moisture-related factor that can affect Rs emissions (Raich and Schlessinger, 1992; Curiel-Yuste et al., 2003; Borken et al., 2003). For example, increase in soil moisture content after a precipitation event may help to increase substrate mobility and may activate dormant microbes. PPT can also enhance

emissions, either during or immediately following a rain event, due to percolating water that can displace gases from soil pores.

Soil respiration in forest ecosystems consists mainly from two sources: heterotrophic (Rh) and autotrophic (Ra) respiration. The former is respiration due to metabolic activities of decomposers, while the later is due to respiration by plant roots and the associated rhizospheric community. Ra has been shown to dominate Rs in forest ecosystems (Boone et al., 2002). Therefore, photosynthesis, which feeds Ra (Högberg et al., 2000) and factors which control it, such as air temperature, vapour pressure deficit and radiation, may also indirectly affect Rs (Irvine et al., 2008; Lui et al., 2006).

As forest stands mature they experience changes in stand physiology, such as increased canopy cover, and the accompanying development of the soil organic LFH layer (i.e. litter layer). These changes can, in turn, lead to changes in soil temperature (Ts) and soil moisture (θ_s) regimes and dynamics, which can affect the Rs-Ts relationship between stands of different ages. Previous studies have shown a positive relationship between the thickness of the organic layer at the site and Rs (Scott-Denton et al., 2003; Sulzman et al., 2005). Litter is a source of Rh that is strongly influenced by Ts and θ_s variability. Borken et al. (2003) have shown that Rh from litter layers can contribute significant bursts of CO₂ emissions during precipitation events. Thus, the presence of litter layer can also add variability on shorter timescales. Soil nutrients, especially in the top litter layer, have also been reported to contribute to differences in Rs between sites

(Janssens et al., 2003). Therefore, studies of soil respiration should incorporate analysis of the Rs-Ts relationship in the context of several environmental factors, to get a fuller understanding of their interacting effects on soil CO₂ emissions. Such analysis will lead to more accurate carbon budget estimations of forests at different stages of development.

We measured soil respiration across an age-sequence of four, afforested, white pine (*Pinus Strobus* L.) stands in southern Ontario, Canada. In this paper, we present our findings based on measurements conducted over the course of three years. The main objectives of this paper are: (a) to establish which of the environmental factors, other than soil temperature, accounted for variability in soil respiration in these forests of different ages (i.e. air temperature, precipitation, photosynthetically active radiation, soil moisture, litter layer thickness, and litter layer carbon to nitrogen ratio); (b) to quantify the relative contribution of each of these additional factors in explaining the temporal variability in the Rs-Ts relationship; and (c) to use a Rs-Ts model, which incorporated all of the additional explanatory variables, to calculate monthly and annual soil CO₂ emissions across the four stands, for intersite and interannual comparison.

4.3. METHODS

4.3.1 Study Site

This study was conducted at the Turkey Point Flux Station (TPFS), located on the north-western shore of Lake Erie, in southern Ontario, Canada

(42°N, 80°W) (Arain and Restrepo-Coupe, 2005; Peichl and Arain, 2006). TPFS consists of four planted white pine (*Pinus Strobus* L.) forest stands (6-, 34-, 19- and 69-year-old, as of 2008), located within 20 km of each other. The two oldest stands (69- and 34-year-old) were planted to stabilize local sandy soils, while the younger two stands (19- and 6-year-old) were planted on abandoned agricultural lands, last cultivated about 10 years prior to afforestation. Hereafter, we refer to the four sites by their shortened code names: TP39, TP74, TP89, and TP02. The acronyms correspond to “Turkey Point”, followed by stand establishment year, i.e. 1939, 1974, 1989, and 2002, respectively.

All four stands grow on sandy soils (Brunisolic Gray Brown Luvisols, following the Canadian Soil Classification Scheme (Presant and Acton, 1984)). TP39 had a well developed understory of white pine seedlings, black cherry (*Prunus serotina* Ehrh.), white oak (*Quercus alba* L.), poison ivy (*Rhus radicans* L. ssp.), bracken ferns (*Pteridium aquilinum* L.) and blackberry (*Rubus allegheniensis* Porter). TP74 had minimal understory vegetation, patches of moss cover consisting mostly of *Polytrichum* spp., and occasional fungi. TP89 had no understory growth, only a layer of pine needles and occasional fungi. The youngest stand (TP02) had no litter accumulation, but had seasonal herbaceous vegetation growth (grasses, weeds, etc.) from May to October. The climate in the region is cool temperate, with a mean annual air temperature of 7.8 °C and mean annual precipitation of 1010 mm, distributed evenly throughout the year, of which 133 mm falls as snow (based on a 30-year-record from a World Meteorological

Organization, WMO accredited Environment Canada station located 10 km north at Delhi). Other relevant site characteristics are given in Table 4.1.

4.3.2 Soil respiration measurements

At each stand, R_s was measured on a biweekly to monthly basis from January 1, 2004 to December 31, 2006, along 50-m- long transects, using a LI-COR 6400 portable photosynthesis system that had a LI-COR 6400-09 soil chamber attachment and a LI-COR 6400-013 soil temperature probe attachment (LI-COR, inc., Lincoln, Nebraska, USA). Along each transect, 12 PVC collars (10.16 cm in diameter, 7.5 cm long, inserted about 5 cm deep into the soil) were installed at 4 m intervals. Once installed, collars remained in the ground for the duration of the study. Vegetation inside collars was avoided during initial installation. Occasional herbacious species that grew-up inside any collar, during the three years of the study, were trimmed back to the soil surface.

In the first two years of the study, each site was measured twice a day, in the morning and afternoon, while in 2006 each site was measured only once a day. At each sampling point, three replicate R_s measurements were recorded. At the same time, soil temperature ($T_{s_LI_COR}$) was also measured, within 20-30 cm of each collar, using the 15 cm temperature probe (LI-COR 6400-013), inserted to its full length. The probe was not used during winter months, if the top of the soil was frozen. In model analysis below, missing $T_{s_LI_COR}$ measurements were supplemented with measurements from each site's weather station. The LI_COR

probe and the weather station soil temperature probes (within top 20 cm of soil surface) were comparable within 2% ($R^2=0.99-0.98$, in a 1:1 fit) (results not shown). In total, only 3% of Ts_{LI_COR} values were missing and had to be filled with weather station data.

4.3.3 Meteorological and edaphic measurements

Meteorological variables such as radiation (including downwelling, above-canopy, photosynthetically active portion, PAR, air temperature, T_{air} , etc.) were measured at all four sites, using an automatic weather station, as part of the eddy covariance flux tower system, following Fluxnet-Canada protocols. Soil temperature (using model 107B temperature probes; Campbell Scientific, Inc., Canada (CSI)) and soil moisture (using model CS615 water reflectometers; CSI) values were measured continuously at 2, 5, 10, 20, 50 and 100 cm and 5, 10, 20, 50 and 100 cm (up to 50 cm at TP02) depths, respectively, at two locations near the flux towers and within 20 m of the transects at each forest site. Additionally, at TP39, precipitation (PPT) was measured using a heated tipping bucket rain gauge (model 52202; R.M. Young Company, Michigan, USA), mounted above canopy, on the flux tower. Meteorological and soil data were recorded at half-hour intervals. The four sites experienced similar climate in terms of mean above canopy T_{air} and PPT. Above canopy air temperature measurements across all four sites were similar (a simple linear regression, resulted in a slope = 1.0 and $R^2=1.00$, plot not shown). Therefore, in our analysis below we used T_{air} , PPT,

and PAR from the main TPFS site, TP39, since it had the longest and most continuous record of these variables, of all the sites.

At the end of the 2004 growing season, litter layer thickness was measured and litter-layer samples (i.e. LFH) were collected within 20-30 cm of every other Rs collar along the transects, at three of the oldest TPFS stands. At the youngest site, no litter layer was collected, because none was present. All collected samples were analyzed in an accredited soil testing lab for carbon to nitrogen (CN) ratios (A & L Canada Laboratories Inc., London, ON).

4.3.4 Data analysis and simulations of daily Rs

Soil temperature, T_s , (a mean of measurements from 2-20 cm of the mineral soil layer) was the dominant controlling factor of temporal variability in R_s across all four sites (Figure 4.2). We used the Gamma model (Chapter 3) to represent this R_s - T_s relationship (i.e. the T_s -only Gamma model, Chapter 3) and as the basis of our soil respiration model. In this study, apart from soil temperature, we explored the impact of the following additional controlling factors on soil CO_2 emissions, by including them in the T_s -only Gamma model (see Appendix 4A for more details):

- (i) Air temperature (daily and annual);
- (ii) Precipitation occurrence (> 0 mm).
- (iii) Soil moisture in top 20 cm of the mineral soil layer.

- (iv) Organic LFH soil layer (i.e. litter layer) thickness, which we assumed to remain constant during the three study years. We used a mean litter thickness value from several measurements taken along the transects at each of the sites, as described above.
- (v) Litter layer carbon to nitrogen ratio (CN), which was also assumed constant during the three study years. This was also a mean of samples taken along the transects at each site. Litter thickness and associated CN ratios were set to zero at TP02 site, because there was no accumulated litter layer at this site during the study period. Below we denote this variable as “Litter”.
- (vi) Down-welling photosynthetically active radiation (daily and annual).

The p- and t-values of all the estimated coefficients of the variables, which represented the above listed explanatory factors, were evaluated to establish if the added variable was statistically significant (i.e. $p < 0.05$) to improving the model’s explanatory power (see Appendix 4A for more details). All statistical analysis and model parameterization was conducted using the SAS 9.1 software (SAS Institute Inc, USA). The model’s unknown coefficients (i.e. model parameters) were estimated using linear regression analysis (i.e. PROC REG in SAS). Observed respiration data and associated auxiliary measurements were used to parameterize the models. The relative importance of each additional factor to improving the model’s explanatory power was determined, by calculating the

factor's marginal contribution to the model's coefficient of determination (i.e. R^2 value), using the *fixed coefficient method* (Liaw and Frey (2007) and Chapter 2).

The resulting Best model (Appendix 4A.2, Equation 4A.3) was used to calculate daily R_s across TPFS, using T_{air} , T_s (i.e. 2-20 cm sensors), PAR and PPT from the sites weather stations. Daily R_s emissions for all sites were calculated in $\mu\text{mol of CO}_2 \text{ m}^{-2} \text{ s}^{-1}$ by the model. These emissions were then converted to grams of C per meter squared per day and summed to monthly and annual totals, used in comparisons below. Errors on each sum were estimated as ± 2 standard deviations about the predicted value (i.e. $2\sqrt{n\sigma_s^2}$), where n is the sample size (i.e. number of days in a month or year) and σ_s^2 is the error mean square from the model output). We also calculated the relative contribution (%) of soil CO_2 emissions from each season to total annual soil emissions for each year and site. For this analysis, we defined seasons based on calendar months, with winter represented by the months of December to February; spring by March to May; summer by June to August; and autumn by September to November.

4.4. RESULTS

4.4.1 Variability in environmental factors

Mean climate variables in year 2004 were comparable to the 30-year-mean for the area (i.e. $T_{air} = 7.9 \text{ }^\circ\text{C}$ and $\text{PPT} = 1010 \text{ mm}$, Environment Canada data from Delhi, ON station, 10 km north of TPFS sites) (Figure 4.1a). In contrast, both 2005 and 2006 were warmer than normal. Furthermore, overall 2005 was the

driest of the three (i.e. PPT = 862 mm), while year 2006 the wettest (i.e. PPT = 1486 mm). The distribution of PPT throughout the year also varied between the years: 2004 experienced low PPT at the end of the growing season (Aug-Sep 2004); 2005 experienced low PPT at the start of the growing season (May 2005); and 2006 experienced enhanced PPT at the end of the growing season (Sep-Oct 2006) (Figure 4.1 a).

Variability in climatic conditions was reflected in edaphic conditions across the sites. Soil temperature (T_s) variability followed that of T_{air} (Figures 4.1 a and b). In contrast, soil moisture (θ_s) variability was influenced by a combination of increasing T_s and variable PPT during the growing season. In general, as T_s increased, θ_s decreased (Figures 4.1 b and c). Increased PPT in 2006 was reflected in a slight increase in θ_s during the year compared to the other two years (Figures 4.1 a and c). However, mean annual θ_s values were comparable between the years, despite the more pronounced variability in PPT (Figures 4.1 a and c). This was reflective of the relatively well drained nature of the soils at TPFS.

Intersite differences in edaphic conditions were more pronounced than interannual differences, reflecting intersite differences in stand physiology. For example, soil temperature at TP02 was the warmest of all four sites during the growing season (Figure 4.1b). It was also most responsive to T_{air} variability. In contrast, T_s at TP89 was the coolest and least responsive to T_{air} (Figure 4.1b). TP02 had minimal canopy cover and no accumulated litter layer during this study

(Table 4.1), leaving its sandy soils exposed to sun and directly coupled to T_{air} . In contrast, TP89 had the thickest canopy cover and a relatively thick litter layer (Table 4.1), which moderated its response to changing atmospheric conditions.

4.4.2 Impact of climate, edaphic and physiological factors on simulated R_s - T_s relationship

Of all the additional explanatory factors considered in our model, the following were found to be statistically significant in their contribution to improving the model fit and so were retained in our final (i.e. Best, see Appendix 4A.2, Equation 4A.3) model: mean daily (T_{air}) and annual (T_{aira}) air temperatures; the thickness of the soil LFH horizon (Litter) and its CN ratio (CN); occurrence of precipitation events, on the day of R_s measurements (PPT_f) and one day prior to R_s measurements (PPT_{f-1}); and mean annual photosynthetically active radiation (PARa) (Table 4.2 and Appendix 4A). In contrast, mean soil moisture of the top 20 cm of the mineral soil (θ_s)⁸, and mean daily photosynthetically active radiation (PAR) were found to be insignificant (i.e. the p-values of the estimated coefficients of the model variables representing these two factors were less than 0.05) and so they were excluded from our Best model (Appendix 4A).

Soil temperature alone explained most of the temporal variability across all four forests of different ages ($R^2=0.7704$, plot not shown). Subsequent,

⁸ Note that we did not have measurements of soil moisture available for the LFH layers at TPFS, due to the difficulty measuring θ_s in relatively thin, 3-5 cm, layer and also limited resources. However, in future studies, now that we have evidence from this study suggesting the importance of θ_s in the LFH layer, it may be advisable for such measurements to be established or carried-out at the sites.

expansion of the model to include additional controlling factors, as described in the Appendix, improved the explanatory power of the model by about 5% ($R^2 = 0.8199$, Table 4.2, column 1). However, the individual factor's contribution to the model's R^2 value was more variable (ie. 0.04 to 6.8%, Table 4.2, columns 2-8), with several of the factors overlapping in their explanatory power, as determined from their marginal contribution (MRC) to R^2 (Table 4.2). Litter layer thickness accounted for about 6.8% of the explanatory power of the model (i.e. $MRC = 0.0677$ (Table 4.2, column 2, using the fixed-coefficient method, which accounts for overlapping power of variables, unlike the maximizing method). Inclusion of litter CN ratio contributed an additional 1.5% ($MRC = 0.0151$, Table 4.2, column 3). In contrast, the contributions from Tair (0.5%), Taira (0.3%), PARa (0.04%), PPT_f (0.4%) and PPT_{f_1} (0.4%) were found to be relatively lower, but still statistically significant (Table 4.2 columns 4-8, respectively). Our analysis showed that Taira and PARa helped to account for interannual variability in our data set, while Litter, and CN helped to account for intersite variability, as discussed below. Adding PPT_f into the model, caused soil moisture (θ_s) to become insignificant (Appendix 4A), thus PPT_f was better in explaining R_s variability across TPFS compared to θ_s .

All of the variables in the model were positively correlated with R_s , except for CN ratio, as shown by the negative value of its estimated coefficient (Table 4.2 column (1). This suggested that as the litter layer CN ratio increased, R_s decreased. In contrast, increases in mean and annual air temperature, site

litter-layer thickness, mean annual photosynthetically active radiation, and occurrence of precipitation on the day of R_s measurement and one day prior to R_s measurement caused an increase in R_s . These trends were consistent across all four TPFS stands.

The thickness of the litter layer (i.e. LFH) across TPFS was an important explanatory factor of R_s variability and was strongly correlated with other factors, including litter layer CN ratio, mean daily air temperature and occurrence of precipitation events, as reflected by the changes in the magnitudes of the estimated coefficients of the variables representing those factors, and their associated t-values, when Litter is removed from the model (i.e. compare Table 4.2 columns 1 and 2). An important methodological point is illustrated here: failing to account for the stronger explanatory factor in the model can generate misleading estimated coefficients for the weaker variables (Otomo and Liaw, 2003). In our case, when Litter is removed, the estimated coefficient for the CN variable becomes positive (c.f. Table 4.2, columns 1 and 2), which is in contrast to the findings of past studies on the relationship between R_s and CN of the litter layer. Past studies have shown that increases in litter CN ratio should be negatively related to R_s measured from the litter layer, because microbes responsible for litter decomposition tend to prefer litter with low CN ratio (i.e. high N content, Cotrufo et al., 2000). Thus, including Litter in our model was crucial if CN was to be included as well. Such useful information could not be

extracted from analysis of covariance, highlighting the usefulness of our statistical approach.

The intersite differences in R_s explained by Litter layer thickness could also be explained by intersite differences in the site's canopy cover (i.e. leaf area index, LAI, results not shown). The relationship has been shown previously for a number of northern temperate forests (Hibbard et al., 2005). However, the two factors excluded each other from the model such that only one was needed to account for intersite variability in the model. We chose to keep litter layer thickness in the model instead of LAI, since litter layer thickness was a factor more directly linked to R_s compared to LAI. First of all, the litter layer was part of the respiring soil (i.e. the LFH soil horizon). Secondly, the Litter variable was found to be strongly correlated with CN and excluding Litter from the model generated misleading estimated coefficients for the CN variable, as discussed above.

4.4.3 Comparison of simulated R_s values

Overall, our Best R_s model (Appendix 4A, Equation 4A.3) was able to explain about 82% of variability in our observed R_s data set (Table 4.2, column 1). The regressions of observed mean daily R_s versus predicted mean daily R_s values, showed that the model was better at predicting R_s of the older sites: $R^2 = 0.95$, slope = 0.84; $R^2 = 0.92$, slope = 0.91; $R^2 = 0.89$, slope = 0.86; and $R^2 = 0.81$, slope = 0.89, for TP39, TP74, TP89, and TP02, respectively (plots not shown). In

general, our simulated R_s tended to underestimate observed R_s values in mid-growing season, from about June to September (Figure 4.2), when R_s tended to peak.

Seasonal variability in simulated R_s emissions followed that of soil temperature variability: R_s values were low in winter months, increased progressively in spring with the increase in soil temperatures and finally decreased in autumn with the decrease soil temperatures (Figures 4.1b and 4.2). Simulated mean annual R_s values were comparable across the four TPFS stands of different age: 1.8 ± 0.2 to 2.0 ± 0.2 ; 1.6 ± 0.2 to 1.8 ± 0.2 ; 1.5 ± 0.2 to 1.8 ± 0.2 ; and 1.5 ± 0.2 to 1.6 ± 0.2 $\text{g C m}^{-2} \text{ day}^{-1}$ for TP39, TP74, TP89, and TP02, respectively (Figure 4.2).

During the three years of this study, soils at TPFS emitted between 539 ± 31 to 732 ± 31 $\text{g C m}^{-2} \text{ yr}^{-1}$, depending on the year and site (Figure 4.1d). In general, total annual soil CO_2 emissions from the oldest, 69-year-old TPFS stand (TP39) were higher, within the mean estimated error on the sums, than those from the two youngest TPFS stands (19- and 6-year-old, TP89 and TP02, respectively) during all three study years (Figure 4.1d, upper left corner). In contrast, emissions between TP39 and TP74 (the 34-year-old) stand were comparable, except during year 2006 (Figure 4.1d). Likewise, total annual emissions between TP74 and the youngest two stands, TP89 and TP02, were comparable within the margins of error, except during the warmest of the three years, 2005, when total annual emissions from TP02 were lower compared to TP74 and TP89 (Figure

4.1d). Interannual variability in total annual Rs was observed at the three oldest stands, with annual Rs being higher for years with higher mean annual air temperature (i.e. for 2005 and 2006 versus 2004). At the youngest stand (TP02), total annual emissions between all three years were comparable within the margins of error (Figure 4.1d).

Similar to annual totals, monthly Rs totals were also influenced by climatic variability between the years. For example, in May 2005, soil CO₂ emissions were the lowest of all three years; 51 ± 9 to 67 ± 9 g C m⁻² in 2005, versus 62 ± 9 to 73 ± 9 and 60 ± 9 to 74 ± 9 g C m⁻² in 2004 and 2006, respectively (Figure 4.1d). This was due to the relatively cooler air and soil temperatures experienced at all four sites in May 2005, compared to the same time of year during the other two years (c.f. Figure 4.1 a and b). Monthly mean air temperature was 13.4, 11.8 and 14.2 °C in 2004, 2005 and 2006, respectively, while Ts varied 10.2-16.1, 7.7-15.8, and 9.0-17.2 °C for the respective years, depending on the site.

Differences in monthly soil CO₂ emissions among the four different-aged stands reflected differences in stand physiology, similar to intersite differences in annual emissions. For example, despite being younger in age, monthly soil CO₂ emissions from TP02 sometimes matched or exceeded those of the oldest stands. In March, soils at TP02 were the first ones to warm-up across TPFS, due to the low canopy cover and absence of litter layer that helped to insulate soils at three older stands (Table 4.1). Consequently, TP02 soils started respiring earlier in the

spring and by April monthly R_s values at TP02 either exceeded or were comparable to those of the older three stands (Figure 4.1d).

The 34- and 19-year-old stands (TP74 and TP89, respectively) were comparable in their annual totals, but were more varied in their relative monthly soil CO_2 emissions. In the first half of the year, TP74 tended to emit more CO_2 compared to TP89, while, in the second half, TP89 would either be comparable to or exceed soil CO_2 emissions from TP74 (Figure 4.1d). A possible explanation for this may be that the canopy cover at TP89 was higher compared to that of TP74, as was litter-layer thickness (Table 4.1). These two factors helped to better decouple soils at TP89 from atmospheric controls, causing a slower rate of increase in R_s in the first half of the year and slower rate of decrease in the second half.

4.4.4 Relative contribution of seasonal R_s to total annual R_s

Across all TPFS stands, about half of the respired CO_2 was emitted during the summer season (45 to 51%, Table 4.3). During spring, the forests emitted 12 to 22% of their annual respired CO_2 and during autumn 25 to 31% (Table 4.3). Winter emissions made up only 5 to 8% of the annual totals across TPFS. The most discrepancy in the relative percent emissions occurred during the spring season and in particular between TP89 and TP02 – these were the sites with the two most extreme LAI and litter layer thickness values (Table 4.1). Thus, differences in seasonal contributions were reflective of intersite differences in

canopy closure and litter accumulation, as mentioned previously. Likewise, differences between years were reflective of the interannual variability in climatic factors. For example, the relative contribution of spring emissions to annual total was lower in 2005, compared to the other years (Table 4.3). Spring 2005 was the coolest of the three study years, as mentioned previously. These results were in agreement with previous studies that also found interannual variability in R_s driven by interannual variability in climate (Savage and Davidson, 2001).

4.5 DISCUSSION

4.5.1 Comparison of soil C emissions among different-age stands

The range and seasonal course of mean daily R_s across all four TPFS stands (i.e. 0.1-5.4 $\mu\text{mol CO}_2 \text{ m}^{-2} \text{ s}^{-1}$ observed R_s ; or 0.1-4.9 $\mu\text{mol CO}_2 \text{ m}^{-2} \text{ s}^{-1}$ simulated R_s) were comparable to literature reported values for forests growing in various climate zones and soil types. For example, Irvine and Law (2002) reported a R_s range of 0.4-4.0 $\mu\text{mol CO}_2 \text{ m}^{-2} \text{ s}^{-1}$ for an old-growth ponderosa pine forest growing in Oregon, USA. Litton et al. (2003) reported R_s of 0.6-3.6 $\mu\text{mol CO}_2 \text{ m}^{-2} \text{ s}^{-1}$ for a 13-year-old lodgepole pine forest in Yellowstone National Park, USA. Hibbard et al. (2005), in a synthesis study of northern temperate forests, reported that for evergreen temperate forests that do not experience late summer drought R_s tends to peak in July to September, with a mean maximum growing season R_s reported as $6.0 \pm 2.2 \mu\text{mol CO}_2 \text{ m}^{-2} \text{ s}^{-1}$. Our maximum R_s

values were in agreement with above, as was the peak in R_s , which occurs in late July to early August at TPFS (Figure 4.3).

The estimated annual soil CO_2 emissions at the Turkey Point sites (539 ± 31 to $732 \pm 31 \text{ g C m}^{-2} \text{ yr}^{-1}$) were also in good agreement with emissions reported in the literature. For example, McDowell et al. (2000) reported annual soil CO_2 emissions of $764 \text{ g of C m}^{-2} \text{ yr}^{-1}$ from a 70-year-old mixed-conifer forest located in northern Idaho. Campbell and Law (2005) studied R_s across a semi-arid ponderosa pine chronosequence in Oregon, USA, and reported R_s values in the range of 500 to $900 \text{ g C m}^{-2} \text{ yr}^{-1}$. In a study of several European forests, Janssens et al. (2001) reported a mean soil respiration of $760 \pm 340 \text{ g of C m}^{-2} \text{ yr}^{-1}$. Hibbard et al. (2005) reported a range of soil CO_2 emissions (428 to $1805 \text{ g C m}^{-2} \text{ yr}^{-1}$) from northern temperate forests in Europe and North America, with the age range of 9 to 300 years for the stands. In their synthesis, the highest R_s value was reported for a 17-year-old stand (Hibbard et al., 2005). Finally, Raich and Schlesinger (1992) used the results of a number of literature-reported studies to estimate mean soil CO_2 emissions for different terrestrial ecosystems around the world. Their estimate for temperate coniferous forests was $681 \pm 95 \text{ g of C m}^{-2} \text{ yr}^{-1}$.

Some literature studies have reported younger forest stands to have lower soil respiration compared to their older counterparts (Wiseman et al., 2004; Litton et al., 2003; Anthoni et al., 2002). One would expect older forests to have more litter and more extensive root system compared to younger stands. Consequently,

higher litter decomposition and higher densities of respiring roots would imply higher soil respiration. However, we observed that younger stands sometimes are comparable to or exceed emissions of their older counterparts (Figure 4.1d), both on annual and monthly time scales. Our results reflect the findings of Irvine and Law (2002), who reported that during their three-year study of soil respiration in different-aged ponderosa pine forests in Oregon, USA, only during one of those years did an older site (50 to 250-year-old) show higher respiration compared to the younger site (14-year-old). Results from our chronosequence study better reflected those presented by Saiz et al. (2006) for a Sitka spruce chronosequence (10-, 15-, 31- and 47- year-old) planted on former agricultural lands in Ireland. They reported annual R_s values of 991, 686, 556, and 564 $\text{g C m}^{-2} \text{yr}^{-1}$ for their stands, respectively, attributing the initial rise in R_s due to larger availability of organic matter (i.e. remnants of agricultural use) and increased root activity at the younger stands. Thus, the age-related trends in soil CO_2 emissions that we observed across TPFS reflected intersite differences in stand physiology or could be related to the inherently higher growth rate of the younger stands. Lancaster and Leak (1978) have reported that white pine species tend to peak in their growth and production around age of 15.

4.5.2 Environmental and physiological controls on R_s

Across all four TPFS forests, soil temperature was the dominant controlling factor in R_s variability. This was followed by the mean litter layer thickness. Litter thickness was positively related to R_s , which was in agreement

with past literature studies. For example, soil respiration was found to be lower above bare soil compared to litter-covered soils in a Ponderosa pine forest in Oregon, USA (Law et al., 2001). In another coniferous forest in Oregon, Sulzman et al. (2005) conducted an experiment where they excluded litter-fall from selected sites in their forest and added it onto nearby plots. They found that the plots with doubled litter accumulation had 34% higher soil CO₂ emissions compared to the control plots. In our study we also found that emissions from stands with lower litter layer thickness tended to be lower compared to the those that had a thicker accumulation, especially during warmer years (i.e. cf. Rs between TP39 and TP74 during 2006 or that of TP74/TP89 and TP02 during 2005, Figure 4.1d).

Mean CN ratio of the litter layer was found to be the third most important explanatory factor of Rs variability, following soil temperature and litter layer thickness. Rs and CN ratio were negatively correlated. This finding was in accordance with previously reported literature findings. For example, Janssens et al. (2003) reported a decrease in soil CO₂ emissions with an increase in its litter layer CN ratio, in several forests across Europe. Cotrufo et al. (2000) reviewed factors that affect litter decomposition in forest ecosystems, highlighting that decomposers prefer substrates low in CN ratios. Therefore, sites with a litter-layer that is high in CN should experience less decomposition and, consequently, reduced CO₂ emission compared to those with lower CN of their litter layer. The relatively higher mean CN ratio at TP74, compared to TP89 (Table 4.1), may

have explained why the total annual R_s values between the two stands were comparable during all three study years, despite their age differences (Figure 4.1d).

The positive relationship that we observed between precipitation occurrence and soil CO_2 emissions at TPFS was in agreement with previous studies. For example, our results support the idea proposed by Borken et al. (2003) that the frequency of occurrence of precipitation events throughout the year is more important in estimates of soil CO_2 emission than annual total precipitation amounts. We found that occurrences of precipitation during the day of R_s measurement and one day prior to R_s measurement were positively correlated with R_s . Borken et al. (2003) conducted a study of drying and wetting effects on CO_2 emissions from the organic soil horizon. They found that precipitation amounts, as little as 0.5 mm, resulted in increased R_s from the organic soil horizon within a few minutes of moistening. These small precipitation events may be enough to stimulate R_s in the organic layer, but they were not large enough to percolate deep into the mineral layer to be detected by soil moisture sensors. Therefore, in our study including both, litter thickness and frequency of precipitation occurrence in the model, instead of actual precipitation amount or soil moisture in the mineral layer (we do not have moisture sensors in the litter layer at our sites) helped to capture better these bursts of CO_2 emissions from the litter layer. These results highlight the importance of considering the effects of sources of moisture, other than volumetric water content of the mineral soil

(which is a common measure used in literature), when studying the temporal variability of R_s .

Liu et al. (2006) have reported temperature-independent variability in R_s in a temperate forest located in Oak Ridge, TN, USA. They showed that R_s closely followed the congruent variability in absorbed photosynthetically active radiation (PAR), a surrogate for photosynthetic carbon uptake. In our study we did not observe such a relationship, but this is due to the nature of our data. Carbone et al. (2007) have shown, that newly photosynthesized carbon can be relocated to roots and respired back out into the atmosphere in as little as four days. Since our observed data was collected on biweekly to monthly time scales, it is unlikely that we would be able to capture any such potential effects of PAR on R_s variability. Nonetheless, our data was still positively responsive to PAR, as was found by Liu et al. (2006), but only to the mean annual PAR value, suggesting that years with fewer cloud cover helped to enhance photosynthesis, which in turn could enhance R_s through the enhancement of the autotrophic component of soil respiration.

The lack of a significant relationship between soil moisture (from the top 20 cm of the mineral soil horizons) and R_s across all four TPFS stands may have reflected the drought tolerant nature of white pine tree species. White pines are known to thrive on nutrient-poor, dry, sandy soils, where other tree species tend to fail (Richardson and Rundel, 2000). A recent study showed evidence of the drought tolerance of white pine trees at TPFS and how the trees may be coping

with the overall relatively low soil moisture conditions experienced at TPFS during the growing season (McLarren et al., 2008). Furthermore, since most white pine roots at TPFS were within the top 55 cm of the mineral soil horizons (Peichl and Arain, 2006), and we found that soil moisture, in the form of precipitation, affected the very top organic soil horizon most, this suggests that at TPFS soil moisture availability may be more important for the heterotrophic fraction of R_s (i.e. decomposition activity in the litter layer) across TPFS, compared to the autotrophic fraction (i.e. root activity of white pines). Indeed, Scott-Denton et al. (2006) have shown that heterotrophic respiration may be more susceptible to drought than rhizospheric respiration. Thus, the results of this study highlight the need to consider variability of various components of the forest water budget when assessing its carbon budgets and dynamics.

4.6 CONCLUSIONS

Simulated total annual soil CO_2 emissions at four different-age TPFS stands were within literature reported values. Annual totals of R_s ranged from 539 ± 31 to 600 ± 31 ; 558 ± 31 to 662 ± 31 ; 587 ± 31 to 665 ± 31 ; and 645 ± 31 to 732 ± 31 $g\ C\ m^{-2}\ yr^{-1}$, for the 6-, 19-, 34-, and 69-year- old stands, respectively. Annual total soil CO_2 emissions were higher, within the margins of error, between the oldest TPFS stand and the two youngest ones, during all three study years. In contrast, emissions between the younger three stands were comparable, except during the warmest study year. Soil CO_2 emissions tended to

be higher for years with higher air temperatures. Intersite differences in emissions were driven mostly by stand physiology, while interannual and seasonal differences were driven by temporal variabilities in regional climate, as well as each site's microclimate. About half of annual soil CO₂ emissions across all four stands occurred during the summer (45 to 47%), and additional 12 to 22% during spring, 25 to 31% during autumn, and only 5 to 8% during winter.

We found that variability in mean daily and annual air temperatures; the occurrence of precipitation events; litter layer thickness and its CN ratio; and mean annual photosynthetically active radiation helped to explain some of the intersite and interannual variability in the observed Rs-Ts relationship across TPFS. Of these additional explanatory factors, the thickness of litter layer (i.e. the LFH soil horizon) was most important, accounting for about 6.8% of the variability in our Rs-Ts mode, and being highly correlated with the litter CN ratio. Litter layer CN ratio explained another 1.6%, while the explanatory power of the remaining factors was relatively smaller (0.04 to 0.5%).

This study adds to our understanding of how additional explanatory factors, other than soil temperature, may influence interannual and intersite variabilities in Rs. The study also enhances our knowledge and understanding of carbon dynamics across planted forests of different age, and, thus, should be of interest to forest carbon researchers and those considering afforestation as an effective means of atmospheric carbon sequestration.

4.7 ACKNOWLEDGEMENTS

Funding for this study was provided by the Natural Sciences and Engineering Research Council (NSERC) of Canada Discovery and Strategic Project Grants and NSERC, the Canadian Foundation for Climate and Atmospheric Sciences (CFCAS), and BIOCAP Canada Foundation funded Fluxnet-Canada Research Network (FCRN), Support from the Canadian Foundation of Innovation (CFI), the Ontario Innovation Trust (OIT), and McMaster University, is also acknowledged. In-kind support from the Ontario Ministry of Natural Resources (OMNR), the Long Point Recreation and Conservation Authority (LPRCA), the Canadian Forest Service (CFS) and Ontario Power Generation (OPG) is appreciated. We thank Steve Williams, from OMNR, for his assistance in site selection and maintenance of the oldest stands. We thank Frank Bahula and Bruce Whitside, and their families, for providing access to the forests on their properties (TP89 and TP02). We are grateful to Eugenia Aoucheva, Fauzia Arain, Rose Blair, Olesia Peshko, Shuhua Yi, Sven D'Souza, Fengming Yuan, Dali and Jagadeesh Yeluripati, and other dedicated field volunteers for their help with field measurements.

4.8 REFERENCES

- Anthoni PM, Unsworth MH, Law BE, Irvine J, Baldocchi DD, Van Tuyl S, Moore D (2002) Seasonal differences in carbon and water vapor exchange in young and old-growth ponderosa pine ecosystems. *Agricultural and Forest Meteorology*, 111, 203-222.
- Arain, MA and Restrepo-Coupe, N (2005) Net ecosystem production in a temperate pine plantation in southeastern Canada. *Agricultural and Forest Meteorology*, 128: 223-241.
- Baldocchi D (2008) Turner Review No 15: “Breathing” of the terrestrial biosphere: lessons learned from a global network of carbon dioxide flux measurement systems. *Australian Journal of Botany*, 56: 1-26.
- Boone RD, Nadelhoffer KJ, Canary JD, Kaye JP (1998) Roots exert a strong influence on the temperature sensitivity of soil respiration. *Nature*, 496: 570-572.
- Borken W, Davidson EA, Savage K, Gaudinski J, Trumbore SE (2003) Drying and wetting effects on carbon dioxide release from organic horizons. *Journal of Soil Science Society of America*, 67, 1888-1896.

- Borken W, Xu Y-J, Davidson EA, Beese F (2002) Site and temporal variation of soil respiration in European beech, Norway spruce, and Scots pine forests. *Global Change Biology*, 8, 1205-1216.
- Campbell JL and Law BE (2005) Forest soil respiration across three climatically distinct chronosequences in Oregon. *Biochemistry*, 73: 109-125.
- Carbone MS, Czimczik CI, McDuffee KE, Trumbore SE (2007) Allocation and residence time of photosynthetic products in a boreal forest using low-level ^{14}C pulse-chase labeling technique. *Global Change Biology*, 14: 466-477.
- Cotrufo MF, Miller M, Zeller B (2000) Litter Decomposition in Carbon and Nitrogen Cycling in European Forest Ecosystems. Schulze, ED (Ed). Ecological Studies 142. Springer, Berlin: 276-296.
- Curiel-Yuste J, Janssens IA, Carrara A, Ceulemans R (2004) Annual Q_{10} of soil respiration reflects plant phenological patterns as well as temperature sensitivity. *Global Change Biology*, 10, 161-169.
- Curiel-Yuste J, Janssens IA, Carrara A, Meiresonne L, Ceulemans R (2003) Interactive effects of temperature and precipitation on soil respiration in a temperate maritime pine forest. *Tree Physiology*, 23: 1263-1270.
- Davidson EA, Belk E, Boone RD (1998) Soil water content and temperature as independent or confounded factors controlling soil respiration in a temperate hardwood forest. *Global Change Biology*, 4, 217-227.
- Davidson EA, Richardson AD, Savage KE, Hollinger DY (2006) A distinct seasonal pattern of the ratio of soil respiration to total ecosystem respiration in a spruce-dominated forest. *Global Change Biology*, 12: 230-239.
- Environment Canada - Canadian Climate Normals from http://www.climate.weatheroffice.ec.gc.ca/climate_normals/index_e.html [July 10, 2008]
- Farquhar GD, von Caemmerer S, Berry JA (1980) A Biochemical Model of Photosynthetic CO_2 Assimilation in Leaves of C_3 Species. *Planta*, 149: 78-90.
- Hibbard KA, Law BE, Reichstein M, Sulzman J (2005) An analysis of soil respiration across northern hemisphere temperate ecosystems. *Biogeochemistry*, 73: 29-70.

- Högberg P, Nordgren A, Buchmann N et al (2001) Large-scale forest girdling shows that current photosynthesis drives soil respiration. *Nature*, 411: 789-792.
- Irvine J and Law BE (2002) Contrasting soil respiration in young and old-growth ponderosa pine forests. *Global Change Biology*, 8: 1183-1194.
- Irvine J, Law BE, Martin JG, Vickers D (2008) Interannual variation in soil CO₂ efflux and the response of root respiration to climate and canopy gas exchange in mature ponderosa pine. *Global Change Biology*, 14: 2848-2859.
- Janssens IA, Dore S, Epron D, Lankreijer H, Buchman N, Longdoz B, Brossaud J, Montagnani L (2003) Climatic Influences on Seasonal and Spatial Differences in Soil CO₂ Efflux. In Vantini R (Ed), *Fluxes of Carbon, Water and Energy of European Forests*. Ecological Studies 163. Springer-Verlag Berlin Heidelberg. Pp.: 233-253.
- Janssens IA, Kowalski AS, Ceulemans R (2001) Forest floor CO₂ fluxes estimated by eddy covariance and chamber-based model. *Agricultural and Forest Meteorology*, 106, 61-69.
- Jassal RS, Black A, Novak MD, Gaumont-Guay D, and Nesic Z (2008) Effect of soil water stress on soil respiration and its temperature sensitivity in an 18-year-old temperate Douglas-fir stand. *Global Change Biology*, 14: 1-14.
- Khomik M (2004) Soil CO₂ efflux from temperate and boreal forests in Ontario, Canada. MSc Thesis. McMaster University, Hamilton, Ontario, Canada.
- Lancaster KF and Leak WB (1978) A silvicultural guide for white pine in the northeast. Forest Service General Technical Report NE-41. Forest Service, US Department of Agriculture.
- Law BE, Thornton PE, Irvine J, Anthoni PM, Van Tuyl S (2001) Carbon storage and fluxes in ponderosa pine forests at different developmental stages. *Global Change Biology*, 7, 55-777.
- Liaw KL and Frey WH (2007). "Multivariate Explanation of the 1985-1990 and 1995-2000 Destination Choices of Newly Arrived Immigrants in the United States: The Beginning of a New Trend?". *Population, Space and Place*, Vol. 13, pp.377-399. (www.interscience.wiley.com)(DOI: 10.1002/psp.459)

- Litton, CM, Ryan MG, Knight DH, Stahl PD (2003) Soil-surface carbon dioxide efflux and microbial biomass in relation to tree density 13 years after a stand replacing fire in a lodgepole pine ecosystem. *Global Change Biology*, 9, 680-696.
- Liu Q, Edwards NT, Post WM, Gu L, Ledford J, Lenhart S (2006) Temperature-independent diel variation in soil respiration observed from a temperate deciduous forest. *Global Change Biology*, 12: 1-10.
- Lloyd, J., Taylor, J.A. 1994. On the temperature dependence of soil respiration. *Functional Ecology*. 8: 415-424.
- McDowell NG, Marshall JD, Hooker TD, Musselman R (2000) Estimating CO₂ flux from snowpacks at three sites in the Rocky Mountains. *Tree Physiology*, 20, 745-753.
- McLaren JD, Arain MA, Khomik M, Peichl M and Brodeur J (2008) Water flux components and soil water-atmospheric controls in a temperate pine forest growing in a well-drained sandy soil. *Journal of Geophysical Research*, 113:
- Otomo A and Liaw K-L (2003) “An Invitation to Multivariate Analysis: An Example About the Effect of Educational Attainment on Migration Propensities in Japan,” *SEDAP Research Paper*, No. 113, SEDAP Research Program, McMaster University, Hamilton, Ontario, L8S 4M4, Canada.
- Peichl M, and Arain MA (2006) . Above- and belowground ecosystem biomass and carbon pools in an age-sequence of temperate pine plantation forests. *Agricultural and Forest Meteorology*, 140, 51-63.
- Presant EW and Acton CJ (1984) The soils of the regional municipality of Haldimand-Norfolk, Vol.2. Report No.57 of the Institute of Pedology: Research Branch, Agriculture Canada, Ministry of Agriculture and Food.
- Raich JW and Schlesinger WH (1992) The global carbon dioxide flux in soil respiration and its relationship to vegetation and climate. *Tellus*. 44B: 81-99.
- Rey A, Pegoraro E, Tedeschi V, De Parri I, Jarvis PG, Valentini R (2002) Annual variation in soil respiration and its components in a coppice oak forest in Central Italy. *Global Change Biology*, 8:851-866.

- Richardson DM and Rundel P (2000) Ecology and biography of Pinus: an Introduction processes *In Ecology and Biography of Pinus*. Richardson DM (Ed). Cambridge University Press. Pp.3-40.
- Saiz G, Byrne KA, Butterbach-Bahl K, Kiese R, Blujdeas V, Farrell EP (2006) Stand age-related effects on soil respiration in a first rotation Sitka spruce chronosequence in central Ireland. *Global Change Biology*, 12: 1007-1020.
- Savage KE and Davidson EA (2001) Interannual variation of soil respiration in two New England forests. *Global Biogeochemical Cycles*, 15: 337-350.
- Scott-Denton LE, Rosenstiel TN, Monson RK (2006) Differential controls by climate and substrate over the heterotrophic and rhizospheric components of soil respiration. *Global Change Biology*, 12: 205-216.
- Scott-Denton LE, Sparks KL, Monson RK (2003) Spatial and temporal control of soil respiration rate in a high-elevation, subalpine forest. *Soil Biology and Biochemistry*, 35: 525-534.
- Sulzman EW, Brant JB, Bowden RD, Lajtha K (2005) Contribution of aboveground litter, belowground litter, and rhizosphere respiration to total soil CO₂ efflux in an old growth coniferous forest. *Biogeochemistry*, 27: 231-256.
- Valentini R, Matteucci G, Dolman AJ, Schulze E-D, Rebmann C, Moors EJ, Granier A, Gross P, Jensen NO, Pilegaard K, Lindroth A, Grelle A, Bernhofer C, Grunwald T, Aubinet M, Ceulemans R, Kowalski AS, Vesala T, Rannik U, Berbigier P, Loustau D, Gudmundsson J, Thorgeirsson H, Ibrom A, Morgenstern K, Clement R, Moncrieff J, Montagnani L, Minerbi S, Jarvis PG (2000) Respiration as the main determinant of carbon balance in European forests. *Nature*. 404: 861-865.
- Van't Hoff JH (1884) *Etudes de dynamique chimique*. Frederrk Muller & Co., Amsterdam.
- Wiseman PE and Seiler JR (2004) Soil CO₂ efflux across four age classes of plantation loblolly pine (*Pinus taeda* L.) on the Virginia Piedmont. *Forest Ecology and Management*, 192: 297-311.

Table 4.1: Description of Turkey Point different age site characteristics.

	TP39	TP74	TP89	TP02
Stand Age (years, as of 2008)	69	34	19	6
LAI	8.0	5.9	12.8	-
Stem density (stems/ha) ^{1*}	429 ± 166	1492 ± 322	1242 ± 263	1683 ± 147
Mean tree height (m) ^{1*}	20.2 ± 2.1	11.2	9.1	0.94 ± 0.17
Mean litter-layer accumulation (cm)	4.13 ± 1.09	3.63 ± 0.80	4.11 ± 1.27	0
Litter CN	17.4 ± 4.8	24.5 ± 5.6	16.1 ± 7.1	0
Mineral soil %OM (top 20 cm)	1.3 ± 0.3	1.1 ± 0.3	2.0 ± 0.3	0.8 ± 0.2

Abbreviations used: ha – hectare, 1ha = 10 000 m²; LAI (leaf area index); CN – carbon (C) to nitrogen (N) ratio; OM – organic matter; TP – Turkey Point, followed by year forest was planted (ex. TP39 – TPFS stand planted in 1939).

Notes: LAI from Chen et al. (2006), no measurements were available for TP02;

¹ From Peichl and Arain (2006);

* For trees with DBH ≥ 9 cm, except for TP02 were all trees were included.

Table 4.2: Estimates of coefficients for each variable and their associated t-values, for each of the full (Best) and reduced Gamma models, computed using the maximizing method, as described in text. Also included are coefficients of determination (R^2) for the full Gamma model and various reduced versions of the model, derived with the maximizing and fixed-coefficient methods. The difference in R^2 between the reduced model and the Best model gives the marginal contribution in R^2 (MCR) of the deleted factor from the associated reduced model.

Explanatory Variable	(1) Best Model		(2) No Litter		(3) No CN		(4) No Taira		(5) No Tair		(6) No PARa		(7) No PPT _t		(8) No PPT _{t-1}	
	Coefficient	t-value	Coefficient	t-value	Coefficient	t-value	Coefficient	t-value	Coefficient	t-value	Coefficient	t-value	Coefficient	t-value	Coefficient	t-value
Intercept	-76.624	-54.8	-74.989	-51.7	-76.559	-54.3	-72.644	-53.9	-83.033	-66.5	-75.812	-54.9	-70.238	-58.9	-77.509	-55.1
Ts	-0.390	-46.8	-0.394	-45.5	-0.390	-46.4	-0.372	-45.4	-0.411	-50.8	-0.386	-46.7	-0.355	-48.8	-0.393	-46.9
LN(Ts)	24.365	53.3	23.997	50.5	24.349	52.8	23.210	52.2	26.275	62.9	24.201	53.1	22.320	57.0	24.669	53.6
Litter	0.129	24.1	---	---	0.077	26.5	0.126	23.4	0.143	27.2	0.130	24.2	0.126	23.4	0.132	24.5
CN	-0.011	-11.6	0.009	15.8	---	---	-0.011	-11.5	-0.012	-11.7	-0.011	-11.5	-0.012	-11.7	-0.011	-11.4
Taira	0.055	9.9	0.049	8.3	0.056	9.8	---	---	0.069	12.7	0.058	10.4	0.039	7.1	0.054	9.5
Tair	0.015	10.0	0.023	15.9	0.015	10.1	0.018	12.7	---	---	0.015	10.0	0.017	12.0	0.013	8.6
PARa	0.001	3.7	0.001	4.3	0.001	3.5	0.002	4.9	0.001	3.9	---	---	0.001	3.8	0.001	3.1
PPT _t	26.139	9.8	21.803	7.9	26.566	9.9	22.277	8.4	31.600	12.0	26.298	9.8	---	---	31.841	12.0
Ts*PPT _t	0.166	9.3	0.137	7.4	0.169	9.4	0.144	8.1	0.200	11.4	0.168	9.4	---	---	0.206	11.7
LN(Ts)*PPT _t	-8.810	-9.7	-7.327	-7.7	-8.954	-9.7	-7.538	-8.3	-10.649	-11.8	-8.871	-9.7	---	---	-10.770	-11.9
PPT _{t-1}	0.103	11.0	0.114	11.8	0.103	10.9	0.101	10.7	0.091	9.8	0.101	10.8	0.128	14.0	---	---
<i>Maximizing method</i>																
R ²	0.8199		0.8051		0.8165		0.8174		0.8173		0.8195		0.8162		0.8168	
Marginal contribution in R ²			0.0148		0.0034		0.0025		0.0026		0.0004		0.0037		0.0031	
<i>Fixed coefficient method</i>																
R ²	0.8199		0.7522		0.8048		0.8168		0.8152		0.8195		0.8155		0.8164	
Marginal contribution in R ²			0.0677		0.0151		0.0031		0.0047		0.0004		0.0044		0.0035	

Notes:

- The Ts-only model had $R^2 = 0.7740$; $n = 7074$ in all cases;
- Ts = mean daily soil temperature in °C, adjusted by 40°C (mean of 2-20 cm probes; daily);
- Tair = mean daily air Temperature (daily);
- PPT_t = dummy variable which had a value of 1 whenever PPT > 0 mm the same day during which Rs was measured;
- Taira = mean annual air Temperature (varies by year);
- PARa = mean annual photosynthetically active radiation (PAR) for the area (varies by year);
- Litter = mean litter layer thickness, sampled along the transect where Rs was measured (sampled once, separate for each site);
- CN = mean C:N ratio of the litter layer, sampled along the transect where Rs was measured (sampled once per each site);
- PPT_{t-1} = dummy variable which had a value of 1 whenever PPT > 0mm one day prior to the day during which Rs was measured.

Table 4.3: Relative percent contribution of total soil CO₂ emissions from each season to the respective total annual soil CO₂ emissions, across all four stands, given for each year and site.

Season	TP39	TP74	TP89	TP02
Winter 2004	6%	6%	6%	5%
Winter 2005	6%	6%	6%	5%
Winter 2006	8%	8%	9%	6%
Spring 2004	19%	20%	18%	22%
Spring 2005	14%	15%	12%	20%
Spring 2006	18%	18%	16%	22%
Summer 2004	46%	46%	46%	45%
Summer 2005	50%	49%	51%	47%
Summer 2006	48%	48%	48%	46%
Autumn 2004	29%	29%	30%	28%
Autumn 2005	31%	30%	31%	29%
Autumn 2006	26%	26%	27%	25%

Figure 4.1: Plot of monthly mean and total values of climatic and edaphic environmental conditions across all four stands, as well as that of calculated monthly Rs: a) Mean monthly air temperature, T_{air} (line) and total monthly precipitation, PPT (bars) with number of precipitation events per month listed above each corresponding bar; b) comparison of mean monthly soil temperature (T_s) across TPFS; c) comparison of mean monthly volumetric water content (θ_s) across TPFS; d) comparison of total monthly emissions across all four stands. In the right upper corner of each panel, mean or total annual values of each of the above variables are also listed, for each year and site, including mean annual down-welling photosynthetically active radiation (PARa) in (a).

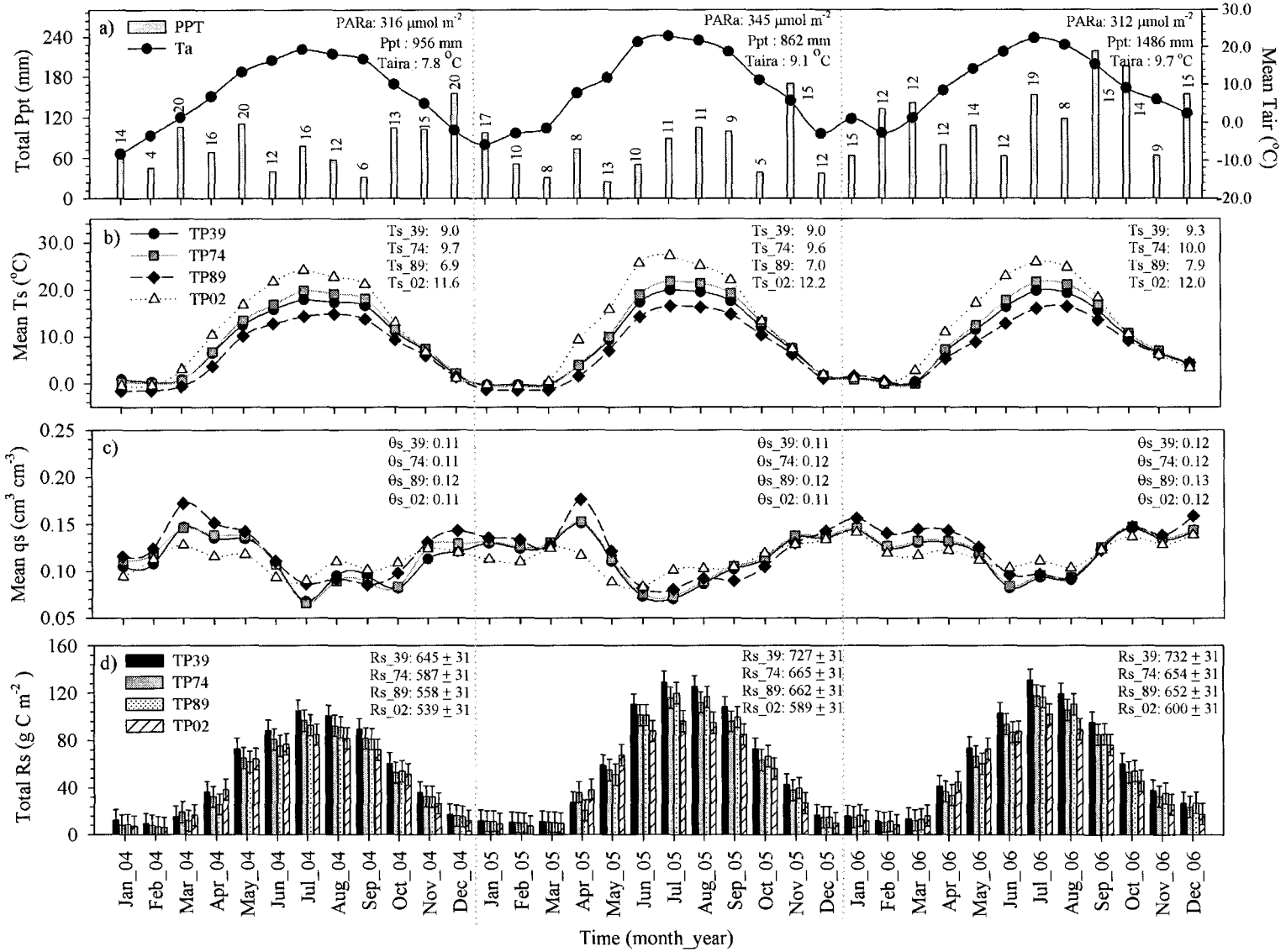
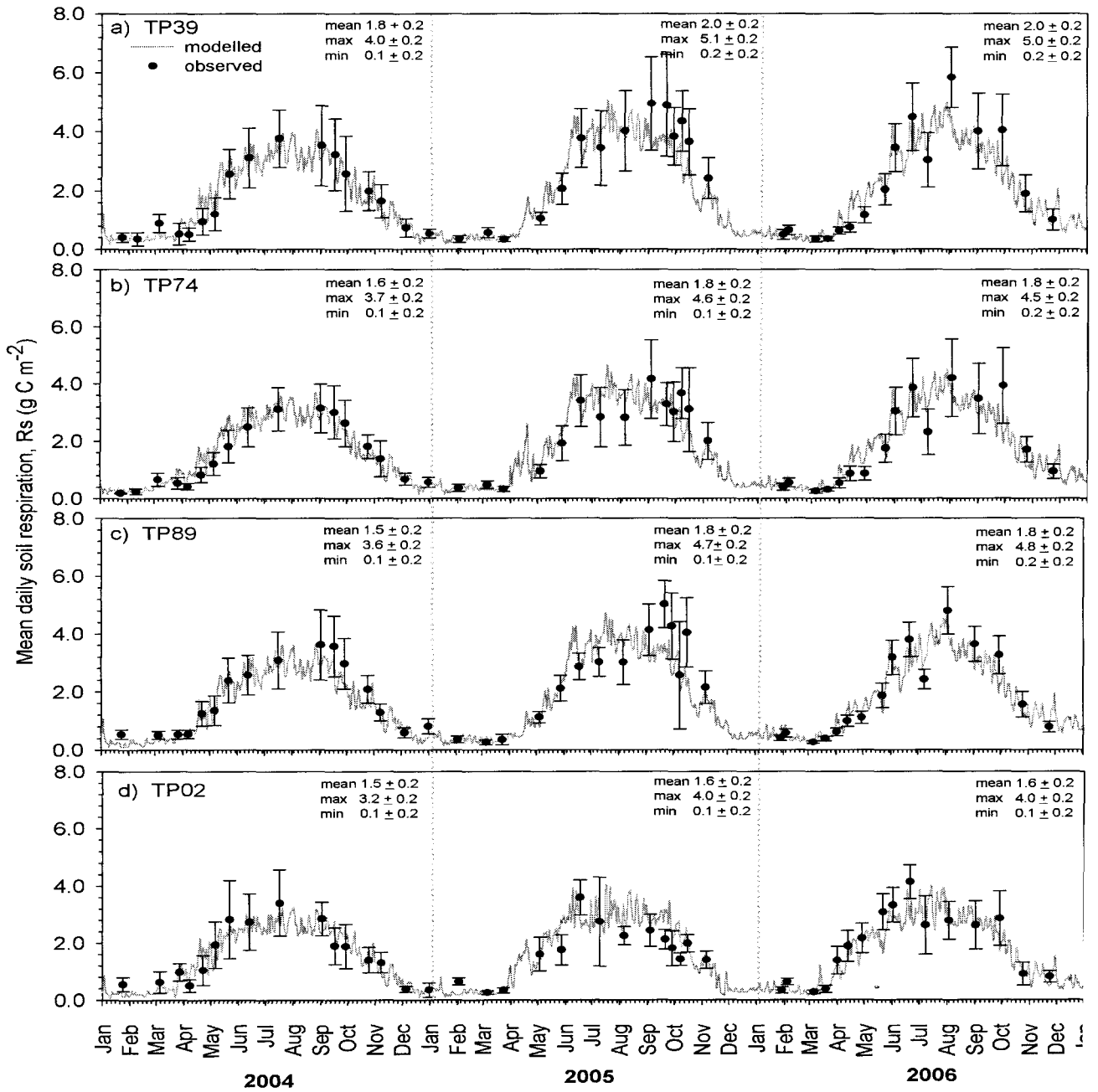


Figure 4.2: Time series of observed mean daily R_s values (symbols) and the associated daily predicted R_s (lines), calculated using the *best* model ($R^2 = 0.8199$), and plotted individually for each site: a) the 69-year-old stand, TP39, b) the 34-year-old stand, TP74, c) the 19-year-old stand, TP89, and d) the 6-year-old stand, TP02. Error bars represent ± 1 standard deviation about the mean and reflect spatial variability in R_s , which was not covered in this paper. In the upper right hand corner of each panel, for year year, the mean, minimum and maximum simulated R_s values are also listed.



APPENDIX 4A**4A.1 Model development and evaluation**

The Gamma model (see Chapter 3 for more details) was used to describe the overall Rs-Ts relationship at TPFs. The statistical form of the Gamma model is written as follows:

$$Y_i = X_i^\alpha e^{\beta_0 + \beta_1 X_i + \varepsilon_i} \quad 4A.1$$

where for an *i*th observation, Y_i is Rs (soil respiration in $\mu\text{mol of CO}_2 \text{ m}^{-2} \text{ s}^{-1}$); X_i is $(T_s + 40 \text{ }^\circ\text{C})$, where T_s is soil temperature in $^\circ\text{C}$; α , β_0 , and β_1 are unknown coefficients to be estimated; and ε_i is the error term to account for the effects of random error (and uncontrolled factors) on the *i*th observed value of Rs.

Taking the natural logarithm of Equation 4A.1, turns the Gamma model into a multiple linear regression model with two explanatory variables:

$$y_i = \alpha \text{Ln}(X_i) + \beta_0 + \beta_1 X_i + \varepsilon_i \quad 4A.2$$

where y_i is $\text{Ln}[Rs]$ of the *i*th observation and the other terms, as described in Equation 4A.1. Note that we treat $\text{Ln}(X_i)$ and X_i as two distinct explanatory variables (see Chapter 3 for more details).

To Equation 4A.2 we added, in sequence, a number of variables representing various environmental driving factors, which we thought may be responsible for some of the observed variability in our Rs data set. The environmental factors we considered (other than T_s) included:

- a) air temperature (daily mean, T_{air} , and annual mean, T_{aira})

- b) precipitation occurrence, which was represented by two dummy variables: one was called PPT_f , which took on a value of 1 whenever total daily precipitation for the day of R_s measurement was above 0 mm, and 0 otherwise. The second variable was called PPT_{f_1} and took on a value of 1 whenever precipitation one day prior to R_s measurement was above 0 mm. PPT_{f_1} was zero otherwise. For more details on using dummy variables in the Gamma model, see Chapter 3.
- c) mean daily soil moisture (θ_s , measured as volumetric water content in $\text{cm}^3 \text{cm}^{-3}$, in top 20 cm of the mineral soil);
- d) mean thickness of the soil LFH organic horizon at each site (i.e. litter layer, Litter), which we assumed remained constant during the three study years, measured in cm. This was a mean of samples taken along the transects at each of the sites, as described above;
- e) mean Litter carbon to nitrogen ratio (CN), which we assumed also remained constant during the three study years. This was also a mean of samples taken along the transects at each site. Note that at TP02 Litter and its CN ratio were set to zero, as there was no accumulated litter layer present at the site during this study;
- f) down-welling photosynthetically active radiation (mean daily, PAR, and mean annual, PARa).

After the addition of a new variable into the model, the resulting p- and t-values of their estimated coefficients were carefully analyzed to determine if they

were statistically significant (i.e. $p < 0.05$). Only variables, whose estimated coefficient's p-value was less than 0.05, were retained in the our final *best specification* of the model, to which we refer to as our Best model.

All statistical analysis and model parameterization, with observed Rs-Ts data, was completed using the SAS 9.1 software (SAS Institute Inc, USA). The unknown coefficients were estimated using a linear regression procedure, PROC REG, in the SAS software (SAS Institute Inc, USA). The relative importance of each of the additional environmental factors to improving the model's explanatory power (i.e. R^2), was determined from the factor's marginal contribution to model's R^2 , as calculated from fitted models using the *fixed coefficient method* (Liaw and Frey (2007)). The results of this analysis are presented in Table 4.2 and discussed in text. For more details on the statistical method of analysis, see Chapters 2 and 3.

4A.2 Rs-Ts model with climate, edaphic and physiological factors

The Best model for simulating TPFS soil respiration data turned out to be as follows:

$$y_i = \alpha_1 \ln(X_{i,1}) + \beta_{01} + \beta_{02} X_{i,3} + \beta_1 X_{i,1} + \beta_2 X_{i,2} + \beta_3 X_{i,3} + \beta_4 X_{i,4} + \beta_5 X_{i,5} + \beta_6 X_{i,6} + \beta_7 X_{i,7} + \beta_8 X_{i,8} + \varepsilon_i$$

4A.3

where α_1 , β_{01} , β_{03} , β_{02} , β_1 , β_2 , β_3 , β_4 , β_5 , β_6 , β_7 , and β_8 are unknown coefficients to be estimated; for every i th observation: y_i is $\ln(Rs)$; $X_{i,1}$ is soil temperature (Ts), as described in equation 4A.2 above (i.e. X_i); $X_{i,2}$ is daily mean air temperature

(T_{air}); $X_{i,3}$ is PPT_f , the dummy variable which took on the value of 1, whenever precipitation on the day of R_s measurement was above 0 mm. PPT_f was zero otherwise.; $X_{i,4}$ is PPT_{f_1} , the dummy variable which took on the value of 1 whenever precipitation one day prior to R_s measurement was above 0 mm. PPT_{f_1} was zero otherwise; $X_{i,5}$ is mean carbon to nitrogen ratio (CN); $X_{i,6}$ is mean thickness of the soil LFH layer for each site (Litter); $X_{i,7}$ is mean annual air temperature (T_{aira}); $X_{i,8}$ is mean annual photosynthetically active radiation (PARa); and ε_i is a variable that accounts for random error. Note that of all the variables we considered, only those which were statistically significant (ie. $p < 0.05$ for their estimated coefficients) were retained in the Best model. Thus, mean daily (T_{air}) and mean annual (T_{aira}) air temperatures; the thickness of the soil LFH horizon (Litter) and its CN ratio (CN); occurrence of precipitation events during (PPT_f), and one day prior to (PPT_{f_1}), R_s measurements; and mean annual photosynthetically active radiation (PARa) were all found to improve the explanatory power of the R_s - T_s relationship. In contrast, mean soil moisture of the top 20 cm of the mineral soil (θ_s) and mean daily photosynthetically active radiation (PAR) were found to be insignificant (i.e. $p > 0.05$) and so were excluded from the Best model.

CHAPTER 5

RELATIVE CONTRIBUTIONS OF SOIL, FOLIAR AND WOODY TISSUE RESPIRATION TO TOTAL ECOSYSTEM RESPIRATION IN FOUR, DIFFERENT-AGE, FORESTS ⁹

5.1. ABSTRACT

Forest ecosystem respiration (Re) consists of smaller components, such as soil (Rs), foliar (Rf), and woody tissue (Rw) respiration, which function at different temporal and spatial scales. Understanding the seasonal dynamics and intersite variability of component fluxes is necessary to adequately quantify variability in net ecosystem exchange of carbon in forest ecosystems.

We measured CO₂ emissions from soil (including autotrophic and heterotrophic components), foliage, and live woody tissue in four temperate white pine (*Pinus Strobus* L.) forests aged: 67-, 32-, 17- and 4-years-old at the time of the study, using a portable chamber system. These measurements were used to simulate daily, monthly and annual Re and its component fluxes. Annual Re values across the four stands were 1527 ± 137 , 1313 ± 137 , 2079 ± 293 , and 769 ± 46 g C m⁻² yr⁻¹ for the 67-, 32-, 17- and 4-year-old stands, respectively, and were generally higher, particularly at the 17-year-old stand, than Re values reported in literature for other temperate coniferous forests. Across all four stands, annual chamber-based estimates of Re were higher compared to tower-based eddy covariance estimates, on average by: 18, 75, 24 and 35% at the 67-, 32-, 17- and 4-year-old stands, respectively. However, this difference could vary from 6 to 93% across the different-age stands, if the uncertainty of our estimated chamber-based Re values is considered.

The lowest daily Re values were observed during the winter (December). Re peaked in August across all four stands, largely driven by Rf. The relative percent-contribution of each component to total annual Re varied among the stands. Rs dominated emissions at the youngest stand, while Rf dominated emissions at the 17-year-old stand. In contrast, at the two oldest stands, Rs and Rf were comparable. Rs was 44, 45, 29, and 69% of Re, across the 67-, 32-, 17- and 4-year-old stands, while Rf accounted for 48, 40, 58, and 31 % of Re, respectively. Rw was the smallest component of annual Re across the stands (9, 15, 13 and 0.1%, respectively). Thus, our results suggest that, in comparison to Rs, Rf could be comparable to or higher in its dominance of Re composition of young to mature afforested ecosystems growing in northern temperate climates, in contrast

⁹ A modified version of this chapter will be submitted for publication to *Agricultural and Forest Meteorology*: Khomik M, Arain MA, Brodeur J, Peichl M and Restrepo-Coupe N (2009) Relative contributions of soil, foliar and woody tissue respiration to total ecosystem respiration in four, forests of different ages.

to the more often reported dominance by R_s . Overall, autotrophic respiration, R_a (i.e. sum of R_f , R_w and autotrophic R_s) dominated R_e across all TPFS stands, comprising 64-85% of R_e . However, the relative composition of R_e varied considerably across the stands, when monthly totals were considered. Therefore, the trends in R_e composition, derived from annual numbers were not always upheld when monthly values were considered.

Intersite variability in emissions was attributed to differences in stand physiological characteristics, such as litter layer presence, amount of canopy cover, foliar and soil nutrient status. Unusually high LAI values at our sites were responsible for the discrepancy between our R_e values and those reported in the literature. The high LAI values were reflective of the past land-use history of the sites and their inherent active stage of growth, especially at the 17-year-old stand. This study highlights the importance of considering both stand physiology and records of past land-use history of the sites, in addition to climatic factors, when assessing carbon budgets of afforested or planted forest ecosystems.

5.2. INTRODUCTION

The net ecosystem carbon exchange (NEE) of terrestrial ecosystems consists of two major fluxes: uptake of atmospheric carbon dioxide gas (CO₂) through photosynthesis and emission of CO₂ through respiration processes. Ecosystem respiration (Re), consists of a number of components that have been shown to vary in their response to environmental and biological controlling factors. Re has been shown to determine the net carbon sink/source strength of forest ecosystems (Kolari et al., 2004; Valentini et al., 2000). Therefore, understanding the driving causes of Re variability and its temporal dynamics in forest ecosystems is of particular interest, since forests are viewed as potential sequesters of atmospheric CO₂ (Bradford et al., 2001; Gough et al., 2008; IPCC, 2000; Linder and Karjalainen, 2007; Liu et al., 2002).

Variability in the various Re components have been observed and accredited to various controls, such as temperature and moisture (Gaumont-Guay et al. 2006), and stand physiological characteristics (Bolstad et al., 2004; Vose and Ryan, 2002). However, the interactions of individual component fluxes with each other, their environment and stand physiology are still poorly understood. Several studies have investigated the variability in Re composition within various forest ecosystems (Bolstad et al., 2004; Gaumont-Guay et al., 2006; Lavigne et al., 1997; Law et al., 1999; Tang et al., 2008; Vose and Ryan, 2002), but only two of those were studies of young to mature (0-70-year-old) planted forests in temperate climates (Bolstad et al., 2004 and Vose and Ryan, 2002) and none considered

forests planted on marginal or abandoned former agricultural lands, which have been identified as potential carbon sinks in northern temperate regions (IPCC, 2000).

The eddy covariance method is being widely used by flux tower researchers to estimate R_e (Baldocchi, 2003). However, R_e can also be calculated through scaled-up chamber measurements of various respiratory components (Gaumont-Guay et al., 2006; Lavigne et al., 1997; Law et al., 1999; Tang et al., 2008). R_e estimated using the eddy covariance method is usually lower compared to chamber-based estimates, with differences ranging from 2 to 63%, as shown by various studies in the literature (Gaumont-Guay et al., 2006; Lavigne et al., 1997; Law et al., 1999; Tang et al., 2008). Chamber methods have an advantage over the eddy covariance method, because of their ability to apportionate CO_2 emissions to various ecosystem components, such as soil, foliage, and woody-tissue. This, in turn, can allow researchers to determine the contribution of each component flux to overall ecosystem respiration and improve our understanding of R_e dynamics.

The objectives of this study were: (1) to quantify and compare the contribution of soil (autotrophic and heterotrophic), foliage, and woody tissue respiration to total ecosystem respiration across four forests of different ages; (2) to compare annual and seasonal trends of component fluxes across this age sequence of forests; and (3) to compare total ecosystem respiration derived from

scaled-up chamber measurements with that derived from eddy covariance measurements.

5.3. METHODS

5.3.1. Study Sites

This study was conducted at the Turkey Point Flux Station (TPFS), located on the north-western shore of Lake Erie, in southern Ontario, Canada. TPFS consists of an age sequence of four white pine (*Pinus Strobus* L.) forest stands: 4-, 17-, 32- and 67 years-old at the time of the study in 2006; located within 20 km of each other. All four stands are afforested plantations. The two oldest stands (67- and 32-year-old) were planted to stabilize local sandy soils, while the younger two stands (20- and 7- year-old) were planted on abandoned agricultural lands that were last cultivated 10 years prior to tree planting. Hereafter, we refer to the four sites by their shortened code names: TP39, TP74, TP89, and TP02. The acronyms correspond to “Turkey Point”, followed by stand establishment year, i.e. 1939, 1974, 1989, and 2002, respectively.

All four stands grow on well-drained sandy soils, classified as Brunisolic Gray Brown Luvisols, following the Canadian Soil Classification Scheme (Presant and Acton, 1984), in a cool temperate climate. Based on a 30-year-record from a World Meteorological Organization accredited Environment Canada station, located 10 km north of the sites at Delhi, Ontario, the mean annual air temperature for the area is 7.8 °C and mean annual precipitation is 1010 mm. Normally, the precipitation is distributed evenly throughout the year, with

133 mm falling as snow. At the time of the study, TP39 had a well developed understory of white pine seedlings, black cherry (*Prunus serotina* Ehrh.), white oak (*Quercus alba* L.), poison ivy (*Rhus radicans* L. ssp.), bracken ferns (*Pteridium aquilinum* L.) and blackberry (*Rubus allegheniensis* Porter). TP74 had minimal understory vegetation, patches of moss cover consisting mostly of *Polytrichum* spp., and occasional fungi. TP89 had no understory growth, only a layer of pine needles and occasional fungi. The youngest stand (TP02) had no effective litter layer accumulation. Seasonal herbaceous growth (grasses, weeds, etc.) occurred at TP02 from May to October. Detailed site characteristics are given in Peichl and Arain (2006), but relevant site characteristics are also given in Table 5.1.

5.3.2. Eddy covariance measurements and weather stations

Net ecosystem exchange (NEE) was measured at each site using the eddy covariance method. At TP39, a permanent closed-path system has been operating since 2002, on top of a 28 m walk-up tower. For details regarding the eddy covariance system set-up see Arain and Restrepo-Coupé (2005). A roving open-path eddy covariance system (OPEC) was used to measure NEE at the three younger stands. The OPEC was rotated among the three younger sites on a monthly basis, from 2004 to 2006. Further details on the roving system are given in Restrepo-Coupé (2005). Flux data was quality-controlled using a standard spike-detection protocol (following Papale et al. 2006). Nighttime data was

excluded when. Ecosystem respiration from the eddy covariance method was calculated using mean 5 cm soil temperatures from each site's weather stations and a logistic model (Amiro et al., 2003), on half-hourly timescale. The logistic model used for R_e computation was first parameterized with night-time NEE data (i.e. when $PAR < 10 \mu\text{mol m}^{-2} \text{s}^{-1}$ and half-hourly friction velocity (u^*) was below a site-specific threshold: 0.25, 0.2, 0.15, 0.1 m s^{-1} for the TP39, TP74, TP89 and TP02, respectively, following the Fluxnet-Canada protocols) and associated T_s from weather station measurements taken at the 5 cm soil depth.

Meteorological variables such as radiation, air temperature, humidity, wind speed and direction, etc. were measured using an automatic weather station (Campble Scientific Inc. (CSI), Logan, Utah, USA) at all four sites throughout the year. Additionally, at TP39, precipitation was measured using a heated tipping bucket rain gauge (model 52202; R.M. Young Company, Michigan, USA), mounted above the canopy on the flux tower. Above-canopy air temperature measurements across all four sites were comparable (for a 1:1 linear relationship, $R^2=1.00$ and slope = 1.0, plot not shown). Therefore, mean daily and annual climatic variables presented below are those from the main TPFS site, TP39, since that site had the most continuous record of all the key climatic variables used for data analysis in this study.

At each TPFS site, soil temperature was continuously measured at two locations at 2, 5, 10, 20, 50 and 100 cm depths (using model 107B temperature probes, CSI). Similarly, volumetric soil water content ($\text{cm}^3 \text{cm}^{-3}$) was measured

at two locations at 5, 10, 20, 50 and 100 cm depths using water content reflectometers (CS615; CSI). Meteorological and soil data were recorded at half-hour intervals.

5.3.3. Chamber-based measurements

For this paper a portable chamber system was used. It was the LI-6400 photosynthesis system with various chamber attachments, developed by LI-COR Inc., Nebraska, USA. The LI-6400 uses an infrared gas analyzer to detect changes in CO₂ concentration of sampled air. The LI-6400 has several advantages over some other chamber techniques (Normal et al., 1997): it is commercially available, compact and completely portable. Little auxiliary equipment is needed for its set-up in the field to measure the various components of ecosystem respiration. The system also allows the operator to control some of the environmental parameters, as necessary (e.x. light, CO₂ concentrations and air temperature for foliar gas exchange measurements).

5.3.3.1. Soil respiration

Soil respiration (Rs) was measured on a monthly basis from January 1, 2004 to December 31, 2006, along 50-m transects, using the LI-6400 system that had a LI-COR 6400-09 soil chamber attachment and a LI-COR 6400-013 soil temperature probe attachment (LI-COR, Inc., Lincoln, Nebraska, USA). However, in this study only data from 2006 year is used, since that is the year

when the other two components were measured as well (foliar and woody-tissue). Along each transect, 12 PVC collars (10.16 cm in diameter, 7.5 cm long, inserted about 5 cm deep into the soil) were installed at 4 m intervals, in year 2004, as part of another study. Once installed, collars remained in the ground for the duration of the study. Herbaceous vegetation inside collars was avoided during initial installation. Vegetation that grew-up inside any collar since installation was trimmed back to the soil surface.

At each sampling point, three replicate R_s measurements were recorded. At the same time, soil temperature ($T_{s_LI_COR}$) was also measured, within 20-30 cm of each collar, using a 15 cm temperature probe (LI-COR 6400-013), inserted vertically to its full length. The probe was not used during winter, when the top of the soil was frozen. In modelling analysis below, missing winter $T_{s_LI_COR}$ measurements (3% of total) were supplemented with soil temperature measurements from each site's weather station. Soil temperature from the LI_COR probe and the weather station soil temperature probes (within top 20 cm of soil surface) were comparable within 2% across all four sites ($R^2 = 0.99 - 0.98$, data not shown).

When large snow accumulation covered permanent collars along the transects, R_s measurements were made directly over snow, in the vicinity of permanent collars, using a custom made snow collar.

5.3.3.2. Heterotrophic respiration

Soil heterotrophic respiration, R_h , was measured at all four sites using the trenched plot technique (Hanson et al., 2000). In autumn 2004, trenched plots were dug at all four stands. Three plots ($2 \times 2 \text{ m}^2$ and 1 m deep) were dug at the three older sites, in the vicinity of soil respiration transects, while four ($1 \times 1 \text{ m}^2$ and 50 cm deep) plots were established at TP02. The trenched plots were lined with industrial grade landscape cloth, along their perimeters, to prevent roots from growing back into the trenched plot. The surface of each plot was cleared of any understory vegetation present and covered with a weed-barrier cloth. In autumn of each year, the surface cloth was flipped-over, which caused the litter accumulated on the cloth surface to be deposited onto the soil below, to maintain litterfall accumulation on top of the soil. Three collars (of the same dimensions as the ones used in soil respiration measurements along the transects) were installed in each of the trenched plots at the oldest three stands, and two collars were installed in each plot at TP02.

At the three older stands, one collar from each plot was designated to be litter-free. The litter layer (i.e. LFH soil horizon) was removed from that collar, and any litter that fell during the course of the study was removed from those collars throughout the year. The respiration measurements from these collars in trenched plots without the LFH-horizon (i.e. litter-free and root-free soils) were used to estimate *mineral* soil's heterotrophic respiration at the three older stands.

Measurements of soil respiration in the trenched plots began in June 2005, and lasted until the end of November 2006. Measurements were taken on a

biweekly basis in 2005 and on a monthly basis in 2006, following the same protocol as used for soil respiration measurements along the transects. In this study, data collected only during the 2006 sampling year is used, because this was the year when all three of the major Re components (i.e. soil, foliar and woody tissue respiration) were measured across TPFS.

5.3.3.3. Foliar respiration

Foliar respiration (R_f) measurements were extracted from the light response curves measured at each site, as part of a separate photosynthesis study. LI-6400 was again used, but this time with the 2 x 3 cm² foliar chamber attachment. An artificial light source attachment, 6200-02B LED, and the 6400-01 CO₂ mixer were used to control chamber light and CO₂ conditions, respectively. Light response curves were measured under controlled chamber conditions, i.e. fixed air temperature, which was within 5 °C of ambient temperature, CO₂ concentration between 360 to 380 ppm, and changing chamber light conditions (i.e. stepwise reduction of photosynthetically active radiation (PAR) from saturation at 2000 $\mu\text{mol m}^{-2} \text{s}^{-1}$ to 0 $\mu\text{mol m}^{-2} \text{s}^{-1}$). For R_f estimation, only measurements corresponding to PAR=0 $\mu\text{mol m}^{-2} \text{s}^{-1}$ were used.

Ten to fifteen white pine needles (2-3 whorls) were placed in a single flat layer into the chamber, such that the length of needles inside the chamber was 3 cm. Chamber area was set to 1 cm² in the instrument program that recorded the measurements. Later the measurements were corrected for the so called true half-

surface area (HSA) of the needles in the chamber, which represented an estimate of the surface area of needles exposed to the light source in the chamber. The true HSA was determined using the volume displacement method described by Brand (1987). Corrected respiration measurements were used for Rf model parameterization.

Two trees were sampled at TP39 by accessing their middle canopy from the eddy covariance walk-up tower. At TP74 and TP89, three trees were sampled at mid-canopy, using scaffolding to reach the mid-canopy of the trees. At TP02, the trees were small enough to be reached at mid canopy from the ground, without the aid of towers or scaffolding. Measurements were conducted on 1-year-old needles. One light response curve was measured at each of the sampled trees per sampling campaign. In 2006, these light response curves were measured monthly at each site, from June to August 2006. Additional measurements at TP39 and TP02 were conducted in April, May, September and November of 2007 to capture seasonal variability in foliar fluxes. Interannual variability in Rf was assumed to be small compared to seasonal and inter-site variabilities, based on our previous studies of temporal variability of respiration across these different-age stands.

5.3.3.4. Woody tissue respiration

We used the approach of Xu et al. (2000) to measure woody tissue respiration (R_w) at the three older stands, using the LI-6400 system. In autumn of 2005, four trees of variable diameter were selected around the eddy covariance towers at each stand. Collars (same make and diameter as those used for soil

respiration) were attached vertically at 1.3 m height on the stem of each tree with silicone. Loose bark was removed around the circumference of the collar, as necessary. Woody tissue respiration was sampled on a monthly basis, from April 2006 to November 2006. At the end of the measurement campaign, increment cores were taken from the centre of each collar to determine the sapwood volume under the collars. Measured respiration values were corrected from per surface area to per sapwood volume, before being used in model parameterization.

Sapwood volume below the collar was calculated as the area enclosed by the collar (i.e. πr^2 , where r^2 was the radius of the collar on the stem) multiplied by the width of sapwood below the collar (which was measured from a tree core taken from the centre of the collar, at the end of the experiment).

At the two oldest stands, tree bole temperature (T_b) was measured in several trees using thermocouples that were continuously sampled by the weather station datalogger every half-hour. These thermocouples were inserted into sapwood at 2-5 cm from surface. Missing T_b values and those for TP89 were estimated from air temperature (T_a), separately for each site, using linear regressions developed between T_a and T_b at TP39 and TP74. For model parameterization we used T_b values corresponding to the time of day when R_w was measured.

5.3.4. Data Analysis

We used two different statistical models to simulate component fluxes at TPFS: the Q_{10} model (van't Hoff, 1894; Davidson et al., 2005) and the Gamma

model (see Appendix 5A and 5B for more details). Statistical analysis was performed using the SAS 9.1 software (SAS Inc, USA). Based on Akaike's Information Criterion (AIC) for model selection (Anderson et al., 2000), we showed that for each component flux the best specification (bs) of the Gamma model gave a better fit to observed Ri data compared to the Q₁₀ model (Appendix 5B, Table 5B.2). In addition to temperature, the bs-models included other environmental driving factors that influenced the temporal variability of the individual respiration components (Appendix 5B). Therefore, in this study, reported seasonal and annual Re values were simulated using the best fitted Gamma models (Appendix 5B, Table 5B.1e). However, in order to compare our results with literature reported studies, where the use of the Q₁₀ model prevails, we also report R₁₀ and Q₁₀ values calculated with the best Q₁₀ model for each component (Table 5.2 in text).

Uncertainty in simulated emissions of the component fluxes were estimated as the ratio between ± 2 standard deviations (σ_r) about the predicted value (i.e.

$\sigma_r = 2\sqrt{n\sigma_s^2}$), where n is the sample size (i.e. 365 days of the year) and σ_s^2 is the error mean square from the model output) and the total annual predicted flux (i.e. $(2\sigma_r)/R_i$, where R_i was the annual predicted sum of the component i in the original simulated units prior to upscaling). This ratio was then applied to upscaled monthly sums of the individual foliar and woody-tissue fluxes to obtain an estimate of the error on those values, since the error computed from simulated

values was not directly transferable to upscaled values, as for R_s (i.e. R_s measurements used for model parameterization were already in units of m^2 ground area, unlike R_f and R_w which simulated values had to be upscaled). We also report uncertainty in R_e , which we calculated arithmetically from R_s , R_w , and R_f uncertainties (i.e. as square root of the sum of squared uncertainties of the individual R_e components, for a given time period).

5.3.5. Up-scaling to ecosystem level

Since simulated R_w were in units of per sapwood volume (SWV) and simulated R_f in units of per half-needle-surface area (HSA), we up-scaled them to per ground surface area of the stand, using biometric indices from the individual stands. This way we could compare them with associated R_s values and also use them in calculating R_e (in g/m^2).

5.3.5.1. Upscaling R_f to stand level

Foliar respiration was upscaled using seasonal leaf area indices (LAI) for each site. Seasonal LAI for each site was determined using a combination of measurements from Chen et al. (2006) and our own seasonal measurements. Chen et al. (2006) reported a single LAI value for each site measured in August 2005, using several advanced techniques (Li-2000 and TRAC). However, Vose and Swank (1990) reported that LAI in *Pinus Strobus* L. forests varies

considerably during the year, with peak LAI reported in late July for their site. Therefore, we determined the percent-relative contribution of seasonal LAI values to that of the maximum LAI, which we measured at TPFS during spring, summer, and autumn of 2002, using LI-2000 (LI-COR Inc., Lincoln, NB, USA). We then used these relative percent ratios to determine seasonal LAI values from the single measurement reported by Chen et al. (2006) for each site, assuming Chen et al.'s (2006) measurements to be the more accurate estimates of the maximum seasonal LAI at TPFS, compared to our LI-2000 measurements. Chen et al. (2006) used more advanced and several methods to estimate LAI at TPFS and also corrected their measurements for branch and needle clumping, which we could not do for our LI-2000 measurements due to limited equipment. We also assumed little interannual variability in LAI from years 2002 to 2006 in our calculations. These estimated seasonal LAI values were used to upscale modelled R_f (from g m^{-2} HSA per day) to per ground area (i.e. $\text{g CO}_2 \text{ m}^{-2}$ ground area) for each site.

We also assumed that respiration from one-year-old foliage was a good approximation of the overall mean canopy respiration at our sites. This was based on two reasons. First, Vose and Swank (1990) reported that white pines tend to replace most of their one-year-old needles on annual basis with current growth, even though white pines may retain some of their needles for up to four years. At our sites, we mostly observed 0- to 2-year-old needles. Secondly, previous studies have shown that as the growing season progresses, CO_2 exchange of one-year-old needles will tend to dominate (Maier and Teskey, 1992). This is because one-

year-old foliage will have to upregulate its metabolic activity to sustain the growth of the newly developing needles, until they mature and become self-functional towards the late growing season.

Our Rf measurements were done at mid-canopy. Differences in Rf are expected along the vertical profile of the tree canopy, due to the variable gas exchange dynamics of sun and shade foliage (Givnish, 1988). Accounting for the effects of canopy position on the magnitude of observed Rf is especially pertinent to up-scaling, if Rf measurements are considered on per leaf area basis (Cooper et al., 2006). However, results presented in Turnbull et al. (2003) suggest that mid-canopy measurements for coniferous trees with relatively open canopy structure were similar from those of in the top canopy. Also mature white pines do not have a thick vertical canopy profile, with most branches with needles located several meters above ground, at the top of the stem. Therefore, we assumed mid-canopy measurements to be good representatives of overall canopy Rf.

5.3.5.2. Upscaling R_w to stand level

Woody tissue respiration (simulated on per sapwood volume basis) was up-scaled using mean stem sapwood volume per ground area of each stand. Sapwood volume was determined from a separate destructive sampling study at TPFS sites (Peichl, 2005). Branch sapwood volume was estimated by assuming branches were 100% sapwood and using branch volume per stand as determined by Peichl (2005).

5.4. OBSERVATIONS AND RESULTS

5.4.1. Meteorology during the study period

Year 2006, during which this study was conducted at TPFS, was unusually wet and relatively warm, compared to the 30-year-norm for the area (Figure 5.1 a and b). Mean annual temperature was 1.9°C above the norm, and total annual precipitation was 476 mm above the norm (about 47% higher). Precipitation during normal years should be evenly distributed throughout the year in the region, however, in 2006, peaks in precipitation occurred in winter (February) and later in the year around September (Figure 5.1b). The seasonal course of soil temperature, followed mean daily air temperature (Figure 5.1c). The relatively small seasonal variability in soil moisture at TPFS was reflective of the well-drained nature of the soils at the site (Figure 5.1d). Overall, the soil was relatively dry at TPFS, averaging about $0.12 \text{ cm}^3 \text{ cm}^{-3}$ per year, with a range of 0.06 to $0.20 \text{ cm}^3 \text{ cm}^{-3}$. Between sites, differences in soil temperature were more pronounced than differences between soil moisture, with the youngest stand having some of the highest soil temperatures observed across TPFS. Intersite differences in soil temperature conditions were largely driven by intersite differences in canopy cover and litter-layer presence.

5.4.2. Annual and seasonal trends in component fluxes across TPFS

5.4.2.1. Soil respiration, R_s

Observed mean annual Rs values were 2.2, 1.9, 1.8, and 1.9 $\mu\text{mol CO}_2 \text{ m}^{-2} \text{ s}^{-1}$ for the 67- (TP39), 32- (TP74), 17- (TP89) and 7- (TP02) year-old stands, respectively, with ranges of 0.3-5.9, 0.3-4.5, 0.3-4.7, and 0.3-4.2 $\mu\text{mol CO}_2 \text{ m}^{-2} \text{ s}^{-1}$, respectively (Figure 5.2b-e). Similarly, simulated mean annual Rs values were comparable between the different-age stands: 1.8, 1.6, 1.6, and 1.5 $\text{g C m}^{-2} \text{ day}^{-1}$ for the TP39, TP74, TP89, and TP02 stands, respectively (Figure 5.2a). Mean daily soil respiration was lowest during winter months and peaked in late July to early August (Figures 5.2a and Figure 5.8c).

Soil temperature was the dominant driving factor of temporal variability in Rs across the stands. As soil temperatures increased, Rs increased and vice versa. When Ts reached around 5 °C (Figure 5.1c), Rs began to increase from the winter minimum (Figure 5.2a). Similarly, when Ts went down to about 5 °C, Rs would approach its annual low across all stands (c.f. Figures 5.1c and 5.2a).

Annual and monthly Rs totals varied between the sites. Total annual Rs values were 667 ± 33 , 587 ± 35 , 594 ± 36 , and $533 \pm 32 \text{ g C m}^{-2} \text{ yr}^{-1}$ for the 67- (TP39), 32- (TP74), 17- (TP89) and 7- (TP02) year-old stands, respectively. The highest annual Rs value was observed at the oldest stand, TP39, and was different within estimated error from Rs at the three youngest stands (Figure 5.6). In contrast, annual Rs values between the three youngest stands of various ages were comparable within the margins of uncertainty.

When monthly emissions were considered, the age-related trends observed for annual totals were not necessarily followed (Figure 5.8c). For example, in

March and April, Rs at TP02, the 4-year-old stand, either exceeded or was comparable to that of the older three stands (Figure 5.8c). Overall, intersite differences in Rs were largely driven by intersite differences in stand soil characteristics (i.e. soil nutrient status and presence of LFH horizon), as well as by differences in microclimates between the sites caused by variable canopy and litter-layer covers.

5.4.2.2. Heterotrophic soil respiration, Rsh

The dynamics of seasonal variability in Rs between the four stands were also driven by the variable seasonal composition of Rsh. In general, Rsh consists of several major components: autotrophic soil respiration from roots, Rsa; heterotrophic soil respiration from the mineral soil (Rsh_m); and heterotrophic soil respiration from the litter-layer (Rsh_L).

The overall contributions of the various Rsh components to total Rs differed between the three older stands and the youngest stand (Figure 5.3). To begin with, there was no measurable litter layer accumulated at the youngest site and so the only source of Rsh was from the mineral soil. At the three older stands, Rsh peaked in February. This winter peak in Rsh was most likely driven by litter-layer decomposition activity, as shown by greater seasonal variability of Rsh_L compared to Rsh_m in Figure 5.3. The contribution from Rsh_m across the three older stands appeared more constant, compared to the contribution of the other two Rs components (Figure 5.3). In contrast, Rsh_m contribution to total Rs was

more variable throughout the year at TP02, peaking in July, likely due to enhanced soil organic matter decomposition in mid summer warm temperatures, as discussed below.

The seasonal dynamics of the autotrophic soil respiration, R_{sa} , also varied somewhat between the three oldest TPFS stands and the youngest one. At TP02, unlike at the older three stands, R_{sa} constituted the larger component of R_s throughout the year (about 60%, Figure 5.3d), except from June to August when it decreased to about 40% of R_s . The relative percent-contribution of R_{sa} to R_s at the older three stands was smaller (Figures 5.3a-c), varying between 40 to 50%, compared to the contribution at TP02. However, across TPFS, there appeared to be two peaks in R_{sa} contribution to R_s during the year: one around April and the other in October (Figure 5.3). The two were likely caused by enhanced fine root activity in spring and autumn months (i.e. start and end of growing seasons). The relative percent contribution R_{sa} to R_s varied with age, reflecting the increasing contribution of the R_{sh_L} component (as afforested stands mature, they accumulate litter, which adds to total R_s – i.e. compare the older three stands with TP02) and by decreased root activity of the older inherently less actively growing stands (i.e. compare TP39 with TP89), as discussed further below.

5.4.2.3. Foliar respiration, R_f

Observed annual mean foliar respiration, R_f , values were 1.6, 2.1, 2.5, and 2.9 $\mu\text{mol CO}_2$ (half-surface area of needles) $\text{m}^{-2} \text{s}^{-1}$ at TP39, TP74, TP89, and

TP02, respectively, with the corresponding Rf ranges of 0.2-3.0, 0.9-3.3, 1.0-4.3, and 0.7-5.8 $\mu\text{mol CO}_2$ (half-surface area of needles) $\text{m}^{-2} \text{s}^{-1}$, respectively (Figure 5.4 b-e). Note that measurements at TP74 and TP89 were made only for three months of the year (June through August, n=9), while measurements at TP39 and TP02 spanned over spring and autumn months as well: April through November. Therefore, the observed temperature range is smaller at TP74 and TP89 in Figures 5.4 c and d. Observed Rf rates decreased with stand age, with the highest Rf rates observed at TP02. This trend was in part related to foliar nitrogen content differences between the stands, with the highest amounts measured at TP02 (Table 5.1).

The seasonal course of simulated Rf followed that of soil respiration, rising in the spring, peaking during the summer months and then decreasing again in the autumn (Figure 5.4). However, the peak in monthly Rf occurred one month later, in August, compared to the peak of Rs in July (c.f. Figure 5.8 a and c). Simulated annual mean Rf values were 2.0, 1.4, 3.3, and 0.6 g C m^{-2} ground area for TP39, TP74, TP89, and TP02, respectively (Figure 5.4a). Unlike Rs, mean daily Rf was almost zero up to about April at all four sites, increased from April to August and then decreased again through autumn to a winter low in December. Seasonal variability in Rf was mainly driven by seasonal variability in air temperature. For example, the first spring peak in Rf occurred on March 13, when air temperature reached around 10 °C for the first time in that year (Figures 5.1a, 5.4 and 5.7).

Intersite differences in simulated Rf values, on per ground area basis, were largely driven by LAI differences. Total annual Rf values between TP39 and TP74 were comparable, within the estimated error margins; both were lower than the Rf value of the 17-year-old stand, TP89; and higher than the Rf value of the youngest stand, TP02 (Figure 5.6). The annual Rf values were 729 ± 182 , 529 ± 132 , 1208 ± 290 , and 235 ± 33 g C m⁻² yr⁻¹ for the 67- (TP39), 32- (TP74), 17- (TP89) and 7- (TP02) year-old stands, respectively. The highest annual Rf was recorded at TP89, the site with the highest LAI (Table 5.1). Intersite differences in Rf between the stands were generally maintained throughout the year, when monthly totals were considered, within the estimated uncertainty, which was in contrast to the seasonal age-related patterns of Rs (Figure 5.8 a and c).

5.4.2.4. Woody tissue respiration, *R_w*

Woody tissue respiration, *R_w*, was the smallest of the three major components of *R_e* for all four stands. Observed annual mean *R_w* values were 38.1, 55.4, and 81.1, μmol CO₂ (sapwood volume) m⁻³ s⁻¹ at the 67- (TP39), 32- (TP74), and 17- (TP89) year-old stands, respectively, with the respective *R_w* ranges of 7.4 - 87.0, 7.9-120.9, and 9.8-146.4 μmol of CO₂ (sapwood volume) m⁻³ s⁻¹ (Figure 5.5 b-d). Simulated annual mean *R_w* values were 0.4, 0.5, and 0.8 g C m⁻² ground area for TP39, TP74, and TP89, respectively (Figure 5.5a). Similar to *R_s*, *R_w* was lowest during winter months, increased through spring, peaked in July and decreased thereafter towards winter (Figure 5.5a and Figure 5.8). The

course of temporal variability in R_w followed closely that of air temperature variability. Therefore, similar to R_f , R_w first increased in spring on March 13, when T_{air} reached 10 °C for the first time in 2006 (c.f. Figures 5.1a versus 5.1a and 5.5a). However, the daily magnitude of R_w was much higher at the time versus that of R_f on per ground area basis, suggesting increase in spring woody-tissue activity prior to the start of new foliage development.

Unlike for R_f and R_s , monthly and annual total R_w values followed a distinct linear age-related pattern across the three oldest TPFS stands: R_w decreased with increasing stand age, even when the estimated errors on the sums were considered (Figures 5.6 and 5.8b). Annual total values of R_w were: 131 ± 13 , 197 ± 14 , 277 ± 14 , and $0.7 \pm 0.04 \text{ g C m}^{-2} \text{ yr}^{-1}$ for TP39, TP74, TP89 and TP02, respectively.

5.4.3. Contribution of R_s , R_f , and R_w to R_e

Annual mean ecosystem respiration, R_e , values across all four stands were: 4.2, 3.6, 5.7 and 2.1 g of C m^{-2} , for the 67- (TP39), 32- (TP74), 17- (TP89) and 7- (TP02) year-old stands, respectively (Figure 5.7). Based on up-scaled chamber measurements, annual total R_e values were estimated to be: 1527 ± 137 , 1303 ± 137 , 2079 ± 293 , and $797 \pm 46 \text{ g C m}^{-2} \text{ yr}^{-1}$ at TP39, TP74, TP89, and TP02, respectively (Figure 5.7). Annual totals at the two oldest stands, TP39 and TP74, were comparable, within the margins of error; that of the 17-year-old stand was

the highest of all TPFS stands; while that of the youngest stand was the lowest of all.

The relative percent contribution of the individual Re components to total annual Re was variable across TPFS (Figure 5.9). At the TP02, Rs accounted for 69% of Re, with Rf accounting for the remaining 31%. Rw was minimal, at 0.1%, for that site. This was in contrast to the 17-year-old stand, where Rf accounted for majority of Re (58%), with Rs accounting for an additional 29%, and Rw for 13% of Re. At the two oldest stands, TP39 and TP74, the contributions of Rs to Re were comparable: 44 and 45%, respectively, while the contribution of Rf to Re at TP39 (67-year-old) was higher than that at TP74 (32-year-old): 48 versus 40%, respectively. In contrast, Rw contribution at TP74 was higher compared to TP39: 15 versus 9%, respectively.

Seasonal variability in Re composition across TPFS was also observed and did not always follow the trends in Re composition derived from annual sums. During the winter months, Rs dominated Re, but on some days in winter, Rw was comparable to Rs in its contribution to Re, especially at TP89 (Figures 5.7 and 5.10). While, Rw was not as variable as Rf and Rs throughout the year, accounting for only 10-20% of Re across the older three stands, the largest percent-contribution of Rw to Re was observed in spring in early March, most likely driven by the spring awakening and growth (Maier, 2001; Vose and Ryan, 2002), as mentioned previously. In March, foliage began respiring and by April it began to take over Rw and, later, Rs values (Figure 5.7). Overall, Rf comprised

the largest component of daily R_e values across the three older stands from May to October (Figures 5.7 a-c and 5.10). At TP02, R_f was comparable to R_s in its relative contribution to R_e in August (Figure 5.10), despite R_s being the dominant component of R_e based on annual totals and during most days at this site (Figure 5.7 d).

From August to October, R_e declined, with the rate of decline being faster than the rate of increase in spring (Figure 5.7). This was likely due to the fact that individual component fluxes increased at different rates from spring into summer, but all three components declined after August. Both, R_w and R_s , peaked in July, while R_f peaked in August (Figure 5.8 a-c).

Based on annual totals, the relative contribution of ecosystem autotrophic respiration, R_a , (i.e. sum of R_{sa} , R_f and R_w) and ecosystem heterotrophic respiration, R_h , (i.e. soil R_h) to R_e were comparable for the two oldest stands (Figure 5.11). R_a dominated R_e , accounting for 71-73% of ecosystem CO_2 emissions, while R_h accounted for only 27-29% in both TP39 and TP74. In contrast, the contribution of R_a to R_e was larger at TP89 (85%) and smaller at TP02 (64%) (Figure 5.11). As was reflected by the individual component fluxes, the overall R_a to R_h ratio varied considerably during the year, with R_h dominating in winter and late autumn months, and R_a during spring and summer. The above results show that trends in carbon emissions, derived from annual numbers are not always up-held when smaller temporal periods are considered.

5.4.4. Comparison of Re derived by chamber versus EC methods

On a daily scale, chamber based estimates of Re (Re_{ch}) overestimated eddy covariance based Re estimates (Re_{ec}) from about April to November across all four TPFS stands (Figure 5.12), although estimated Re from the two methods were highly correlated (i.e. for 1:1 relationships $R^2 = 0.94$ to 0.96 , plot not shown). At TP02, upscaled chamber estimates of Re better matched observed Re values (i.e. nighttime NEE values) in July (Figure 5.12d). At the older stands, the goodness of fit of Re estimated from both methods to observed Re values was comparable (but note that Re_{ec} was derived using observed nighttime NEE to begin with).

At all four stands, (Re_{ch}) were higher compared to (Re_{ec}) by: 18% at TP39, 75% at TP74, 24% at TP89 and 39%, at TP02. However, when estimated errors on the Re_{ch} sums are taken into account, the difference between chamber and eddy covariance Re estimates could be much smaller (ex. 6% for TP89 and 8% for TP39) or substantially larger (ex. 93% for TP74).

5.5. DISCUSSION

5.5.1. Annual and seasonal variability in component fluxes

5.5.1.1. Soil respiration, R_s

Observed and simulated R_s values at TPFS and their seasonal trends were within literature-reported values and trends, as discussed in detail in Chapter 4. The trends observed in this study, using a single year of TPFS soil respiration data,

were similar to the results in Chapter 4. Below we also site a few studies to compare our R_s values with those in the literature. Our annual R_s across the stands ranged from 533 ± 32 to 667 ± 33 $\text{g C m}^{-2} \text{ yr}^{-1}$. Tang et al. (2008) and Law et al. (1999) reported annual R_s values of 600 to 742 $\text{g C m}^{-2} \text{ yr}^{-1}$ and 683 $\text{g C m}^{-2} \text{ yr}^{-1}$ in their component-flux studies, respectively. Likewise, Gaumont-Guay et al. (2006) reported a range of R_s , 745 ± 134 to 914 ± 165 in their chamber-based study of R_e in a boreal aspen forest. Finally, in a synthesis study of R_s across northern temperate forests, Hibbard et al. (2005) reported a range of R_s from 438 to 1895 $\text{g C m}^{-2} \text{ yr}^{-1}$ for sites ranging in age from 9 to 300 years old.

Across TPFS stands, differences in R_s were most pronounced between the youngest, 4-year-old stand (TP02) and the oldest, 67-year-old stand (TP39). In spring, R_s increased first at TP02, about one month ahead of the three older stands, because of the relatively open canopy and lack of litter cover at TP02 compared to the other stands (Figure 5.2 a). A similar phenomenon was reported previously by Noormets et al. (2007), but for R_e . In our case, R_e did not respond in the same way as R_s (i.e. be the first to increase in spring for TP02 on per ground area basis), largely because seasonal dynamics in R_e were generally dominated by R_f across TPFS, as discussed below.

The seasonal variability in the contribution of R_{sa} to R_s across our four sites (Figure 5.3) was also comparable to the patterns observed in the literature. For example, Irvine et al. (2008) reported that R_{sa}/R_s increased from March to June (0.18 to 0.50) in a 90-year-old ponderosa pine ecosystem, growing in

Oregon, USA. We also observed an increase in R_{sa} contribution to R_s at the start of the growing season (March to May) and a slight decrease in August, especially at the two older stands (Figure 5.3). Increased fine root activity at the start of the growing season and later in September, as a result of senescence activity, may help explain the trends at TPFS sites.

R_{sh_L} contribution at the three oldest stands was high through winter and spring, at the time when R_{sa} was reduced due to reduced tree root activity (Figure 5.3 a-c). Unlike some coniferous trees that tend to drop needles throughout the year, white pines drop most of their senesced needles during October and November of each year (Vose and Swank, 1990; Peichl and Arain, 2006). This input of fresh labile litter should stimulate heterotrophic respiration at TPFS, driven by enhanced decomposition activity, which could continue under the snow-pack through winter and into early spring months of the following year (McDowell et al., 2000). Alternatively, in the climate experienced by TPFS, enhanced winter R_h could be driven by the high release of stored sugars from freeze-damaged tree roots, which have been shown to enhance microbial populations below snow-pack and thus R_h (Monsoon et al., 2006; Scott-Denton et al., 2006).

The seasonal trends in R_s components (i.e. R_{sa} and R_{sh_m}) at TP02 differed from those of the three older stands (Figure 5.3). At TP02 the spring peak in R_{sa} occurred earlier, around March compared to the older stands because of the lack of litter layer cover, as mentioned previously. However, this effect

may have also been enhanced by the dynamics of herbaceous growth (i.e. grasses and other weeds) at TP02, which was significantly larger compared to ground vegetation of the three older stands (i.e. 423 g m^{-2} at TP02, compared to 51, 54, and 0.31 g m^{-2} at TP39, TP74, and TP89, respectively (Peichl and Arain, 2006)).

There was also a pronounced peak in Rsh_m around July at TP02, which was in contrast to three older stands, where Rsh_m tended to be relatively constant throughout the year (Figure 5.3d). This trend at TP02 could be due in part to the relatively high carbon content of the mineral soil at the site. Mineral soil carbon in the top 55 cm at TP02 was higher compared to TP74 and TP89 and comparable to that of TP39 (Table 5.1). The higher soil C content at TP02 relative to the older two stands was likely the remnant of the more recent agricultural use of the site. Therefore, high soil temperatures at TP02, during peak growing season may have stimulated decomposition of this mineral soil carbon and added to the rise in the relative contribution of Rsh_m to Rs.

The relative percent-contribution of Rsa to Rs at the older three stands was about 10% lower compared to our youngest stand (TP02), a trend which was also in accordance with the literature. For example, in a study of soil respiration across a chronosquence of planted Sitka spruce in central Ireland, Saiz et al. (2006) reported a decrease in relative percent contribution of Rsa to Rs going from 59.3% in their 10-year-old stand to 49.7% for their 47-year-old stand. The decrease was explained by the higher activity of roots at the younger stands (Saiz et al. 2006).

5.5.1.2. Foliar respiration, R_f

Foliar respiration observed at TPFS stands was higher compared to that reported by Law et al. (1999) for their ponderosa pine ecosystem (0.2 to 5.8 versus 0.08 to 0.33 $\mu\text{mol CO}_2$ (leaf half-surface area) $\text{m}^{-2} \text{s}^{-1}$, respectively). However, TPFS measurements were closer to the range and seasonality reported by Cooper et al. (2006) in a mixed conifer forest in Washington, USA (0 to 4.6 $\mu\text{mol CO}_2 \text{m}^{-2} \text{s}^{-1}$), which attained maximum values in June and minimum in December. The differences in R_f values obtained in this study and values reported in the literature may be species related or due to differences in stand age or regional climates experienced by the different sites, as discussed below. In contrast, intersite variability in observed R_f values (on per HSA of needles) among the four TPFS stands were likely driven by intersite variability in foliar nitrogen content, as mentioned previously. Foliar gas exchange has been shown to relate strongly and positively to foliar nitrogen content in past studies (Dang et al., 1997; Vose and Ryan, 2002).

Our simulated annual R_f values, on a per ground area basis, for all but the youngest TPFS stand, were much higher compared to similar studies in the literature. For example, Tang et al. (2008) reported R_f of 69-121 $\text{g C m}^{-2} \text{yr}^{-1}$, while Law et al. (1999) reported 157 $\text{g C m}^{-2} \text{yr}^{-1}$ from their upscaling studies in old-growth forests. Similarly, Gaumont-Guay et al. (2006) reported total estimated R_f in the range of 173 ± 14 to 243 ± 21 $\text{g C m}^{-2} \text{yr}^{-1}$ in their study of component fluxes of an 81-year-old boreal aspen forest. Recall, that the estimated

Rf values across TPFS were 729 ± 182 , 529 ± 132 , 1208 ± 290 , and 235 ± 33 g C m⁻² yr⁻¹ for the 67-, 32-, 17-, and 4-year-old stands, respectively. Intersite variability of upscaled Rf values among the four TPFS stands, and also between TPFS and literature-reported values, was driven by intersite differences in leaf area indices used for upscaling, as discussed further below.

5.5.1.3. *Woody tissue respiration, Rw*

Woody tissue respiration observed at TPFS varied from 7.4 to 146.4 $\mu\text{mol CO}_2$ (sapwood volume), m⁻³ s⁻¹, which was a larger range compared to Rw reported in the literature, but comparable to literature values once upscaled to per ground area basis (131 to 277 g C per m² yr⁻¹, for the oldest three TPFS stands). For example, Tang et al. (2008) reported Rw values of 4 to 40 $\mu\text{mol CO}_2$ (sapwood volume) m⁻³ s⁻¹ in the mixed-wood forest in Michigan, USA, but 130 to 209 g C per m² yr⁻¹. Similarly, Law et al. (1999) reported Rw of 2.5 to 19.5 $\mu\text{mol CO}_2$ (sapwood volume) m⁻³ s⁻¹ in their ponderosa pine forest in Oregon, USA, and 54 g C per m² yr⁻¹. Griffis et al. (2004) reported stem respiration of 155 to 198 g C per m² yr⁻¹ in their 74-year-old boreal aspen forest. The differences between TPFS and literature values of Rw could be due to differences in stand physiology: differences in sapwood volume per ground area between our site and literature values; and also differences in the growth activity of TPFS because of its age versus the old-growth stands studied by Tang et al. (2008) and Law et al. (1999).

Intersite differences in simulated Rw between the four TPFS sites were driven by differences in stand physiology. The very low Rw at TP02 compared to

the other three sites was due to the low sapwood volume of this young seedling site (Table 5.1). The differences among the oldest three stands could be due to differences in their inherent stage of growth and/or in past land-use history of the sites. For example, Maier (2001) has shown that planted loblolly pines that were fertilized with nitrogen had significantly greater stem respiration compared to non-fertilized trees. Unlike, the older two stands, TP89 was under agricultural use prior to planting. Therefore, soils at this site had more soil nutrients compared to the older ones (Khomik, 2004) and may have stimulated growth and thus respiration at TP89. However, we did not analyze the wood tissue for nutrient content to determine if its nutrient content reflected that of soils. Nonetheless, these results highlight the importance of considering regional site characteristics and knowledge of past land-use history of the site when assessing carbon budgets of afforested or planted ecosystems.

5.5.2. Comparison of R_{10} and Q_{10} from TPFS with literature studies

Some of the discrepancies between our observed respiration values and literature-reported values may have also been due to climatic differences (i.e. in the temperature ranges over which the fluxes were measured). Since many studies reported normalized respiration fluxes (i.e. R_{10} values) and accompanying Q_{10} values, we also fit the Q_{10} models to our observed data and computed R_{10} and Q_{10} values in order to compare better our results with those reported in the literature.

In general, Q_{10} values obtained in this study (Table 5.2) were comparable to those reported in the literature. For example, in a study of six different boreal

forests in Canada (ranging in age up to 160 years old), Lavigne et al. (1997) reported Q_{10} values of 2 to 3.3 for R_s , and 1.7 to 2.2 for R_w . The Q_{10} values reported by Tang et al. (2008) for their mixedwood old-growth forest growing in the Great Lakes region of Michigan, USA, ranged from 2.62-2.66 for R_s , 1.89-2.28 for R_f , and 2.23-2.50 for R_w . Finally, Law et al. (1999) reported Q_{10} values of 1.8, 2.1, and 2.2 for R_s , R_f , and R_w , respectively, at their old-growth ponderosa pine forest in Oregon, USA.

Our R_{S10} values (Table 5.2) were also within literature-reported values. For example, Law et al. (1999) reported the R_s normalized to 10 °C of 0.8 – 2.8 $\mu\text{mol of CO}_2 \text{ m}^{-2} \text{ s}^{-1}$. Ryan et al. (1997) reported R_f normalized to 10°C for the boreal forests studied by Lavigne et al. (1997) as 0.21-0.95 $\mu\text{mol CO}_2$ (leaf surface area, m^{-2}) s^{-1} . Ryan et al. (1997) also reported R_w in the range of 18-110 $\mu\text{mol CO}_2 \text{ SWV}^{-1} \text{ m}^{-3} \text{ s}^{-1}$, but this was normalized to 15 °C, while Law et al. (1999) reported R_w of 4-8 $\mu\text{mol CO}_2$ (sapwood volume (SWV)), $\text{m}^{-3} \text{ s}^{-1}$ normalized to 10°C. Thus, our 10°C-normalized R_w values on per sapwood volume were also within literature-reported ones.

5.5.3. Contribution of R_s , R_f , and R_w to R_e at TPFS sites

Total annual R_e values across all four TPFS sites (Figure 5.7) were higher compared to literature-reported values for temperate coniferous forests, especially the value at TP89. For example, in their summary of R_e across a number of plantation forests from various temperate climates, Arain and Restrepo-Coupe

(2005) reported a range of R_e from 481 to 1830 g C per m² yr⁻¹ for forests ranging in age from 15 to 450 years. Law et al. (1999) reported R_e of 894 g C per m² yr⁻¹ from upscaled chamber measurements in their old-growth ponderosa pine forest in Oregon, while Tang et al. (2008) reported a range of 600 to 742 g C per m² yr⁻¹ in their old-growth mixedwood site in Michigan, USA. For comparison, Gaumont-Guay et al. (2006) reported upscaled chamber-based R_e of 1190 g C per m² yr⁻¹ for an 81-year-old aspen stand in Saskatchewan, Canada. In contrast our upscaled chamber-based R_e values were 1527 ± 137 , 1313 ± 137 , 2079 ± 293 , and 769 ± 46 g C m⁻² yr⁻¹ for the 67-, 32-, 17-, and 4-year-old stands.

The main cause of the discrepancy is revealed, when individual R_e components are considered. Our annual R_s estimates, on per ground area basis, were comparable to those reported in the literature, as discussed above. In contrast, our estimated annual R_f values were much higher compared to literature-reported values, especially at TP89, where R_f was so high that it raised the overall annual R_e of the site to a value comparable with annual R_e of an old-growth tropical forests in the Amazon (R_e of 2338 g C m⁻² yr⁻¹) as reported by Grace et al. (1996)).

Part of the discrepancy in upscaled R_f values, and thus R_e values, between this study and those in the literature was due to differences in LAI. TPFS stands have unusually high LAI, especially TP89, compared to a number of Fluxnet sites in Canada (Chen et al., 2006). The high LAI was attributed to high values for needle clumping (Chen et al., 2006), which could be species specific. Maximum

LAI values across the three older TPFS stands varied from 5.9 to 12.8 (Table 5.1), with an estimated annual mean of 3.4 to 7.4 (i.e. mean of estimated monthly LAI values, calculated from the maximum values, as described above). The largest LAI values were for TP89, the stand with the highest Rf estimate (Figure 5.3a). In contrast, LAI of the stands studied by Tang et al (2008) averaged 3.8 to 4.1, while that of the ponderosa pine stand studied by Law et al. (1999) was only 1.5. The high LAI at TP89 may have been due to more favourable soil moisture and nutrient conditions compared to the two older stands, and/or because of the fact that TP89 was in an active growth stage for white pine species. Peak production and growth of white pine species tends to occur around age 15 (Lancaster and Leak, 1978). Indeed, foliar biomass across TPFS, seemed to follow LAI and Rf trends, being highest for TP89, suggesting high productivity (Table 5.1).

In a recent study, Lindroth et al. (2008) have shown that intersite differences in Re across a number of coniferous forests in northern Europe were driven first by differences in LAI and second by differences in stand age. Thus, another cause for the discrepancy between our results and those in the literature on upscaled chamber studies (all of which were conducted on sites older than our own) could be due to differences in stand age. Noormets et al. (2007) studied the effect of age on total ecosystem C fluxes in managed forests (3- to 65-year-old stands) in the Great Lakes region and reported higher Re in younger stands compared to older ones, explaining that the difference was due in part to the inherent greater biological activity of younger stands. High LAI at TPFS could

imply high photosynthetic production (GPP). In a recent review, Litton et al (2007) reported that all carbon fluxes, including R_f , R_w , and R_s , were linearly and positively related to GPP. Thus, the the resulting high R_e at TPFS could be related to the relatively high productivity of these young to mature afforested stands.

Most studies report R_s as the dominant R_e component, based on annual totals. For example, Tang et al. (2008) reported that R_s made up 67-72% and R_f 8-11% of total annual R_e at their sites. Similarly, Law et al. (1999) reported that R_s accounted for 76% of total annual R_e at their ponderosa pine forest, whereas R_f accounted for 18%. In contrast, in our study, based on annual totals, R_f dominated R_e or was comparable to R_s in its percent-contribution to R_e at all but the youngest TPFS stand. Our relative percent contributions better reflected the ranges reported by Lavigne et al. (1997) in his study, where R_s was found to contribute 48 to 71% to R_e and R_f 25 to 43%. The low contribution of R_w to R_e we observed across the three oldest TPFS stands (9-15%) was also comparable to findings in other studies. For example, Acosta et al. (2008) reported that R_w (stems and branches) accounted for 7.6 to 9.2% of R_e during a four-year study of R_w variability in a 22-year-old Norway spruce forest. Law et al. (1999) reported R_w (stem and branches) constituted 6% of R_e at their ponderosa pine site in Oregon. Griffis et al. (2004) reported stem respiration contributed 12% to R_e and Gaumont-Guay et al. (2006) reported 13-14% contribution, in their study of the boreal aspen site mentioned previously. Likewise, Tang et al. (2008) reported that stem respiration made up 13% of R_e in their study. Our stem-only woody tissue

respiration was 89 to 118 g C m⁻² yr⁻¹ for the oldest three stands, which amounts to 6 to 9% of Re.

In terms of the overall contribution of autotrophic and heterotrophic respiration to Re across TPFS, Ra accounted for 64-85% of Re, based on annual totals. The ratio of Ra/Re at the two oldest TPFS stands was comparable at 71-73%, was higher for TP89 (85%), and lower at TP02 (64%). The high ratio at TP89 compared to the other stands was driven by its unusually high LAI values. The ratios of Ra/Re across TPFS stands were on the higher end of literature-reported values. For example, Griffis et al. (2004) reported that Ra constituted 61% of Re determined from up-scaled chamber measurements in boreal aspen forest in Canada. Harmon et al. (2004) reported Ra and Re of 1309 and 1886 g C m⁻² yr⁻¹ in their study of an old-growth forest, which comes out to an Ra/Re ratio of 69%. However, the Ra/Rh ratios across TPFS were quite variable seasonally, and in some months they were closer to literature-reported values. This highlights the usefulness of considering seasonal patterns of Re variability, not just annual, when assessing the carbon budgets and dynamics of various forest ecosystems.

5.5.4. Comparison of Re derived by chamber versus EC methods

Our results agree with literature studies in that chamber-estimated Re (Re_ch) values are higher compared to eddy covariance, estimates (Re_ec). For example, Griffis et al. (2004) reported Re_ch to be higher than Re_ec by 20-37% at the boreal aspen forest in Canada and Gaumont-Guay et al. (2006) reported

Re_{ch} to be higher by 25% at the same aspen site. Similarly, Lavigne et al (1997) reported Re_{ch} to be higher by 20-40% compared to Re_{ec} at the six boreal forest sites in Canada, and Law et al. (1999) reported 50% higher Re_{ch} estimates compared to Re_{ec} in their study. In contrast, Tang et al. (2008) reported only a 2% difference between the two methods, but with Re_{ch} being higher. Our percent differences (18 to 75% on average) were within those reported in the literature, especially if we take into account the estimated errors on our Re_{ch} totals. Then, the differences could be as low as 6% to 8% for some of the sites.

The discrepancy between EC and chamber estimates could be numerous and difficult to account for. For example, the EC method may underestimate emissions during night time due to low turbulence conditions. If the site topography is not flat or if the site is located near large water bodies, lateral air drainage flows may form causing underestimation of fluxes observed by the EC system above the canopy (Aubinet, 2008). For a more detailed account of possible causes of Re_{ec} underestimation see a recent review by Aubinet (2008). Alternatively, it may be possible that what was measured by the chambers was not within the tower's footprint, thus causing discrepancies between the resulting estimated Re values (Lavigne et al., 1997). There could also be a number of errors in chamber methods, related to inadequate estimates of biological indices, such as LAI (i.e. if too few measurements were taken during the year to account for seasonality in LAI) and sapwood volume (i.e. squishing the tree core, when coring the tree to measure sapwood width in a stem sample), used for upscaling.

Lavigne et al. (1997) discusses in more detail some of the challenges in upscaling chamber-based estimates of R_e to those derived with the EC method.

An important consequence stemming from the above finding is the following. Some researchers often estimate the relative percent contribution of R_s to R_e at their sites by using chamber-based estimates of R_s and EC-based estimates for R_e in their calculations and derive conclusions about forest carbon cycling based on such calculations (Davidson et al., 2006). However, we would discourage such practice, until differences between the two methods have been resolved, or unless the groups can show prior close agreement between R_e estimated by both methods for their sites. Otherwise, the relative contribution of R_s to R_e for a given site could be overestimated. For example, R_s contribution to R_e across TPFS stands was calculated to be 44, 45, 29, and 69% at the 67-, 32-, 17-, and 4-year-old stands, respectively, when R_{e_ch} was used. However, if R_{e_ec} was used, then the contribution of R_s would be 52, 78, 35, and 94 % of R_e . Thus, depending on the estimates used, one can reach quite different conclusions regarding the annual C budget of TPFS stands – i.e. R_f dominated in the R_{e_ch} case and R_s dominated in the R_{e_ec} case.

5.6. CONCLUSIONS

Using a portable chamber system, we measured CO_2 emissions from soil (R_s), foliage (R_f), and live woody-tissue (R_w) in four temperate white pine (*Pinus Strobus* L.) ecosystems aged: 67-, 32-, 17-, and 4-year-old, at the time of the

study. These measurements were used to simulate daily, monthly and annual component emissions and summed to estimate Re. Temperature was the dominant environmental factor driving temporal variability of all the individual Re components. Chamber-based estimates of annual Re across the four different stands were: 1527 ± 137 , 1313 ± 137 , 2079 ± 293 , and 769 ± 46 g C m⁻² yr⁻¹ for the 67-, 32-, 17-, and 4-year-old stands, respectively. Rs accounted for 44, 40, 29, and 69% of Re, across the respective stands, while Rf accounted for 48, 40, 58, and 31 % of Re, respectively. Rw respiration was the smallest component of annual Re across TPFS stands, accounting for only 9, 15, 13 and 0.1% of Re, respectively. The composition of Re was variable between the stands when monthly totals were considered, such that the trends in Re composition and dynamics, derived from annual numbers, were not always upheld when monthly values were considered.

The relative percent contribution of each component to Re varied among the stands, with intersite variability attributed to differences in stand physiological characteristics, such as litter layer presence, canopy cover, foliar and soil nutrient status. These differences in stand characteristics were reflective of the past land-use history of the sites and their active growth stage. Unusually high LAI values at TPFS were responsible for differences in Re between TPFS and literature-reported studies, since these LAI values were used to upscale Rf to the stand level. Similarly, intersite differences in LAI were responsible for intersite differences in estimated Re among the four TPFS stands. Our results highlight the importance

of considering site age and knowledge of past land-use history when assessing carbon budgets of afforested or planted ecosystems. Our results also suggest that R_f may be the more dominant and determinant component of R_e budgets and dynamics of young to mature afforested stands, in contrast to the widely reported R_s dominance of R_e reported for old-growth, or naturally-regenerated, or harvest-managed forest ecosystems.

Across all four TPFS stands, annual chamber-based estimates of R_e were higher compared to tower based eddy covariance method estimates, on average by 18, 75, 24 and 39% at the 70-, 35-, 20-, and 7-year old stands, respectively. However, this difference could be as little as 6 to 8% or as high as 93% for some of the sites, if uncertainties in chamber-based R_e estimates are taken into account.

Results from this study fill some of the gaps in the literature on studies of component fluxes of R_e in young to mature (i.e. up to 100 years old), planted forests growing in temperate climate zones. They should be of interest to carbon cycle researchers and those interested in using afforestation or plantation forests as potential sinks for atmospheric CO_2 .

5.7 ACKNOWLEDGEMENTS

Funding for this study was provided by the Natural Sciences and Engineering Research Council (NSERC) of Canada Discovery and Strategic Project Grants and NSERC, the Canadian Foundation for Climate and Atmospheric Sciences (CFCAS), and BIOCAP Canada Foundation funded Fluxnet-Canada Research Network (FCRN). Support from the Canadian Foundation of Innovation (CFI), the Ontario Innovation Trust (OIT), and McMaster University, is also acknowledged. In-kind support from the Ontario Ministry of Natural Resources (OMNR), the Long Point Recreation and

Conservation Authority (LPRCA), the Canadian Forest Service (CFS) and Ontario Power Generation (OPG) is appreciated. We thank Steve Williams, from OMNR, for his assistance in site selection and maintenance of the oldest stands. We thank Frank Bahula and Bruce Whitside, and their families, for providing access to the forests on their properties (TP89 and TP02). We are grateful to Eugenia Aoucheva, Fauzia Arain, Rose Blair, Sven D'Souza, Lara Kujtan, Mahmoud Pejam, Olesia Peshko, Rao Polasam, Talar Sahsuvaroglu, Shuhua Yi, Fengming Yuan, Dali and Jagadeesh Yeluripati for their help in the field. The first author was supported by the Ontario Graduate Student (OGS) in Science and Technology: The David and Grace Prosser Scholarship and OGS Fellowship.

5.8 REFERENCES

- Acosta M, Pavelka M, Pokorný R, Janouš D, Marek MV (2008) Seasonal variation in CO₂ efflux of stems and branches of Norway spruce trees. *Annals of Botany*, 101(3): 469-477.
- Amiro BD, Barr AG, Black TA, Iwashita H, Kljun N, McCaughey JH, Morgenstern K, Murayama S, Nesic Z, Orchansky AL, Saigusa N (2006) Carbon, energy and water fluxes at mature and disturbed forest sites, Saskatchewan, Canada. *Agricultural and Forest Meteorology*, 136: 237-251.
- Anderson DR, Burnham KP, Thompson WL (2000) Null Hypothesis Testing: Problems, Prevalence, and an Alternative. *The Journal of Wildlife Management*, 64, 4: 912-923.
- Arain, MA and Restrepo-Coupe, N (2005) Net ecosystem production in a temperate pine plantation in southeastern Canada. *Agricultural and Forest Meteorology*, 128: 223-241.
- Aubinet (2008) Eddy covariance CO₂ flux measurements in nocturnal conditions: an analysis of the problem. *Ecological Applications*, 18 (6): 1368-1378.
- Baldocchi (2003) Assessing the eddy covariance technique for evaluating carbon dioxide exchange rates of ecosystems: past, present and future. Review. *Global Change Biology*. 9: 479-492.
- Barford CC, Wofsy SC, Goulden ML, Munger JW, Pyle EH, Urbanski SP, Hutrya L, Saleska SR, Fitzjarrald D, Moore K (2001) Factors controlling long- and short-term sequestration of atmospheric CO₂ in a mid-latitude forest. *Science*, 294: 1688-1691.

- Bolstad PV, Davis KJ, Martin J, Cook BD, Wang W (2004) Component and whole-system respiration fluxes in northern deciduous forests. *Tree Physiology*, 24 (5): 493-504.
- Brand (1987) Estimating the surface area of spruce and pine foliage from displaced volume and length. *Canadian Journal of Forest Research*. 17: 1305-1308.
- Chen JM, Govind A, Sonnentag O, Zhang Y, Barr A, Amiro B (2006) Leaf area index measurements at Fluxnet-Canada forest sites. *Agricultural and Forest Meteorology*, 140: 257-268.
- Cooper CE, Thomas SC, Winner WE (2006) Foliar respiration in an old-growth Pseudotsuga-Tsuga forest. *Canadian Journal of Forest Research*, 36: 216-226.
- Dang QL, Margolis HA, Mikailou S, Coyea MR, Collatz GJ, Walthall CL (1997) Profiles of photosynthetically active radiation, nitrogen and photosynthetic capacity in the boreal forest: Implications for scaling from leaf to canopy. *Journal of Geophysical Research*. 102, D24: 28,845 – 28,859.
- Davidson EA, Janssens IA, Luo Y-Q (2005) On the variability of respiration in terrestrial ecosystems: moving beyond Q_{10} . *Global Change Biology*, 11: 1-11.
- Davidson EA, Richardson AD, Savage KE, Hollinger DY (2006) A distinct seasonal pattern of the ratio of soil respiration to total ecosystem respiration in a spruce-dominated forest. *Global Change Biology*, 12: 230-239.
- Elliott and Vose (1994) Photosynthesis, water relations, and growth of planted *Pinus strobus* L. on burned sites in the southern Appalachians. *Tree Physiology*. 14: 439-454.
- Environment Canada - Canadian Climate Normals from http://www.climate.weatheroffice.ec.gc.ca/climate_normals/index_e.html [July 10, 2008]
- Gaumont-Guay D, Black TA, Griffis T, Barr AG, Morgenstern K, Rachhpal SJ, Nestic Z (2006) Influence of temperature and drought on seasonal and interannual variations of soil, bole, and ecosystem respiration in a boreal aspen stand. *Agricultural and Forest Meteorology*, 140: 203-219.

- Givnish TJ (1988) Adaptation to sun and shade: a whole-plant perspective. *Australian Journal of Plant. Physiology*, 15: 63-92.
- Gough CM, Vogel CS, Schimid HP, Curtis PS (2008) Controls on annual forest carbon storage: lessons from the past and predictions for the future. *BioScience*, 58 (7): 609-622.
- Griffis TJ, Black TA, Gaumont-Guay D, Drewitt GB, Nesic Z, Barr AG, Morgenstern K, Kljun N (2004) Seasonal variation and partitioning of ecosystem respiration in a southern boreal aspen forest. *Agricultural and Forest Meteorology*, 125: 207-223.
- Hanson PJ, Edwards NT, Garten CT, Andrews JA (2000) Separating root and soil microbial contributions to soil respiration: A review of methods and observations. *Biogeochemistry*, 48: 115-146.
- Harmon ME, Bible K, Ryan MG, Shaw DC, Chen H, Klopatek J, Li X (2004) Production, respiration, and overall carbon balance in an old-growth Pseudotsuga-tsuga forest ecosystem. *Ecosystems*, 7(5): 498-512.
- Hibbard KA, Law BE, Reichstein M, Sulzman J (2005) An analysis of soil respiration across northern hemisphere temperate ecosystems. *Biogeochemistry*, 73: 29-70.
- Irvine and Law (2002) Contrasting soil respiration in young and old-growth ponderosa pine forests. *Global Change Biology*. 8: 1183-1194.
- Janssens IA, Lankreijer, Matteucci G, Kowalski AS, Buchmann N, Epron D, Pilegaard K, Kutsch W, Longdoz B, Grunwald T, Montagnani L, Dore S, Rebmanns C, Moors j, Grelle A, Rannik U, Morgenstern K, Oltchev S, Clement R, Gudmundsson J, Minerbi S, Berbigier P, Ibrom A, Moncrieff J, Aubinet M, Bernhofer C, Jensen NO, Vesala T, Granier A, Schulze E-D, Valentini R (2001) Productivity overshadows temperature in determining soil and ecosystem respiration across European forests. *Global Change Biology*. 7: 269-278.
- Khomik M (2004) Soil CO₂ efflux from temperate and boreal forests in Ontario, Canada. MSc Thesis. McMaster University, Hamilton, Ontario, Canada.
- Lancaster KF and LeakWB (1978) A silvicultural guide for white pine in the northeast. Forest Service General Technical Report NE-41. Forest Service, US Department of Agriculture.

- Lavigne et al (1997) Comparing nocturnal eddy covariance measurements to estimates of ecosystem respiration made by scaling chamber measurements at six coniferous boreal sites. *Journal of Geophysical Research. Part D. Atmospheres*. 102, 24: 28,977 – 28,987.
- Law BE, Ryan MG, Anthoni PM (1999) Seasonal and annual respiration of a ponderosa pine ecosystem. *Global Change Biology*. 5: 169-182.
- Liaw KL and Frey WH (2007). “Multivariate Explanation of the 1985-1990 and 1995-2000 Destination Choices of Newly Arrived Immigrants in the United States: The Beginning of a New Trend?” *Population, Space and Place*, Vol. 13, pp.377-399. (www.interscience.wiley.com)(DOI: 10.1002/psp.459)
- Linder M and Karjalainen T (2007) Carbon inventory methods and carbon mitigation potentials of forests in Europe: a short review of recent progress. *European Journal of Forest Research*, 126: 149-156.
- Lindroth A, Lagergren F, Aurela M, Bjarnadottir B, Christiensen T, Dellwik E, Grelle A, Ibrom A, Johansson T, Lankreijer H, Launiainen S, Laurila T, Vesala T (2008) Leaf area index is the principal scaling parameter for both gross photosynthesis and ecosystem respiration of Northern deciduous and coniferous forests. *Tellus B*, 60(2): 129-142.
- Litton CM, Raich, JW, Ryan MG (2007) Review: Carbon allocation in forest ecosystems. *Global Change Biology*, 13: 2089-2109.
- Liu J, Peng C, Apps M, Dang Q, Banfield E, Kurz W (2002) Historic carbon budgets of Ontario’s forest ecosystems. *Forest Ecology and Management*, 169: 103-114.
- Maier and Teskey (1992) Interannual and external control of net photosynthesis and stomatal conductance of mature eastern white pine (*Pinus Strobus L.*). *Canadian Journal of Forest Research*. 22: 1387-1394.
- Maier CA (2001) Stem growth and respiration in loblolly pine plantations differing in soil resource availability. *Tree Physiology*, 21: 1183-1193.
- McDowell NG, Marshall JD, Hooker TD, Musselman R (2000) Estimating CO₂ flux from snowpacks at three sites in the Rocky Mountains. *Tree Physiology*, 20, 745-753.

- Monson RK, Lipson DL, Burns SP, Turnipseed AA, Delany AC, Williams MW, Schmidt SK (2006) Winter forest soil respiration controlled by climate and microbial community composition. *Nature*, 439: 711-714.
- Noormets A, Chen J, Crow T (2007) Age-dependent changes in ecosystem carbon fluxes in managed forests in northern Wisconsin, USA. *Ecosystems*, 10: 187-203.
- Norman, J.M., Kucharik, C.J., Gower, S.T., Baldocchi, D.D., Crill, P.M., Rayment, M., Savage, K., Striegl, R.G. December 26, 1997. A comparison of six methods for measuring soil-surface carbon dioxide fluxes. *Journal of Geophysical Research*, 102, D24: 28,771-28-777.
- Otomo A and Liaw K-L (2003) “An Invitation to Multivariate Analysis: An Example About the Effect of Educational Attainment on Migration Propensities in Japan,” *SEDAP Research Paper*, No. 113, SEDAP Research Program, McMaster University, Hamilton, Ontario, L8S 4M4, Canada.
- Peichl M (2005) Biomass and carbon allocation in a chronosequence of white pine (*Pinus Strobus* L.) plantations in southern Ontario, Canada. MSc Thesis, McMaster University, Hamilton, Ontario, Canada.
- Peichl M, Arain MA (2006). Above- and belowground ecosystem biomass and carbon pools in an age-sequence of temperate pine plantation forests. *Agricultural and Forest Meteorology*, 140, 51-63.
- Presant EW and Acton CJ (1984) The soils of the regional municipality of Haldimand-Norfolk, Vol.2. Report No.57 of the Institute of Pedology: Research Branch, Agriculture Canada, Ministry of Agriculture and Food.
- Qi Y, Xu M, Wu J (2002) Temperature sensitivity of soil respiration and its effects on ecosystem carbon budget: nonlinearity begets surprises. *Ecological Modelling*. 154: 141-142.
- Saiz G, Byrne KA, Butterbach-Bahl K, Kiese R, Blujdeas V, Farrell EP (2006) Stand age-related effects on soil respiration in a first rotation Sitka spruce chronosequence in central Ireland. *Global Change Biology*, 12: 1007-1020.
- Scott-Denton LE, Rosenstiel TN, Monson RK (2006) Differential controls by climate and substrate over the heterotrophic and rhizospheric components of soil respiration. *Global Change Biology*, 12: 205-216.

- Turnbull MH, Whitehead D, Tissue DT, Schuster WSF, Brown KJ, Griffin KL (2003) Scaling foliar respiration in two contrasting forest canopies. *Functional Ecology*, 17: 101-114.
- Valentini R, Matteucci G, Dolman AJ, Schulze E-D, Rebmann C, Moors EJ, Granier A, Gross P, Jensen NO, Pilegaard K, Lindroth A, Grelle A, Bernhofer C, Grunwald T, Aubinet M, Ceulemans R, Kowalski AS, Vesala T, Rannik U, Berbigier P, Loustau D, Gudmundsson J, Thorgeirsson H, Ibrom A, Morgenstern K, Clement R, Moncrieff J, Montagnani L, Minerbi S, Jarvis PG (2000) Respiration as the main determinant of carbon balance in European forests. *Nature*. 404: 861-865.
- Van't Hoff JH (1884) Etudes de dynamique chimique. Frederck Muller & Co., Amsterdam.
- Vose and Ryan (2002) Seasonal respiration of foliage, fine roots, and woody tissues in relation to growth, tissue N, and photosynthesis. *Global Change Biology* 8: 182-193.
- Wiseman and Seiler (2004) Soil CO₂ efflux across four age classes of plantation loblolly pine (*Pinus taeda* L.) on the Virginia Piedmont. *Forest Ecology and Management*. 192: 297-311.
- Xu, DeBiase, Qi (2000) A simple technique to measure stem respiration using a horizontally oriented soil chamber. *Canadian Journal of Forest Research*. 30: 1555-1560.

Table 5.1: TPFS site characteristics.

Site Characteristic	TP39	TP74	TP89	TP02
Location	42° 42' 55" N 80° 22' 20" W	42° 42' 34" N 80° 21' 05" W	42° 46' 32" N 80° 28' 28" W	42° 39' 49" N 80° 34' 24" W
Elevation (m)		184	212	
LAI (m ² /m ²) ^a	8.0	5.9	12.8	N/A
Tree height (m) ^b	20.2	11.2	9.1	0.94
DBH (cm) ^b	34.6	15.6	15.8	N/A
Stem volume (m ³ /ha) ^b	376	160	116	0.45
Live branch volume (m ³ /ha)	58	72	101	N/A
Total sapwood volume (m ³ /ha)**	178	170	176	0.45
Foliar biomass (kg/ha) ^b	2855	4601	8727	208
Foliar N (mg/g) ^c	13.9	11.3	13.4	21.4
Foliar CN ^c	38.2	46.2	39.1	34.8
Litter-fall ^{b,c} (kg/ha, Sept-Nov)	1725	1864	3698	N/A
Litter-fall ^{b,d} (kg/ha, total annual)	3990	2980	5190	N/A
Litter thickness (cm)	4.13 ± 1.09	3.63 ± 0.80	4.11 ± 1.27	0
Litter CN ratio	17.4 ± 4.8	24.5 ± 5.6	16.1 ± 7.1	N/A
Mineral soil carbon (top 55 cm) ^b	36.7	30.1	33.9	37.2

^a Taken from Chen et al. (2006), measured in August 2005

^b Mean values, taken from Peichl and Arain (2006); where applicable data are for trees with DBH ≥ 9 cm

^c includes only white pine needles

^d includes needles, leaves, cones

^e measured by Larry Flanagan group (not published)

N/A - measurement unavailable

* for year 2006 of this study

** estimated (i.e. sum of stem and branch sapwood volume, assuming branches are 100% sapwood)

Table 5.2: Calculated R_{10} and Q_{10} values of each component at TPFS sites from the two Q_{10} -models fitted to measured TPFS data. R_{10} for R_s is given in units of $\mu\text{mol of CO}_2 \text{ m}^{-2} \text{ s}^{-1}$, while that for R_f is given in $\mu\text{mol of CO}_2$ (half-surface area of needles, $\text{m}^{-2}) \text{ s}^{-1}$ and R_w is given in $\mu\text{mol of CO}_2$ (sapwood volume, $\text{m}^{-3}) \text{ s}^{-1}$.

Flux	T-only model		Best specification model	
	R_{10}	Q_{10}	R_{10}	Q_{10}
TP39_ R_s	1.3	3.5	0.7	3.9
TP74_ R_s	1.2	3.5	0.6	3.9
TP89_ R_s	1.3	3.9	0.7	4.5
TP02_ R_s	1.0	2.1	0.5	2.4
TP39_ R_f	0.4	3.0	0.3	3.9
TP74_ R_f	0.4	3.0	0.3	3.9
TP89_ R_f	0.4	3.0	0.4	3.9
TP02_ R_f	0.9	2.2	0.8	2.6
TP39_ R_w	15.2	2.5	3.6	2.3
TP74_ R_w	24.2	2.5	8.1	2.3
TP89_ R_w	31.3	2.5	14.5	2.3
TP02_ R_w	---	---	---	---

Figure 5.1: Comparison of climatic and edaphic conditions across TPFS sites during the 2006 study year: a) daily mean air temperature (T_{air}), b) daily mean soil temperature (mean of all sensors in top 20 cm of mineral soil), c) daily mean soil moisture content (mean of all sensors in top 20 cm of mineral soil), and d) daily total precipitation. Also listed in top right corner of each plot are the annual mean or total values, as well as the annual minimum and maximum values.

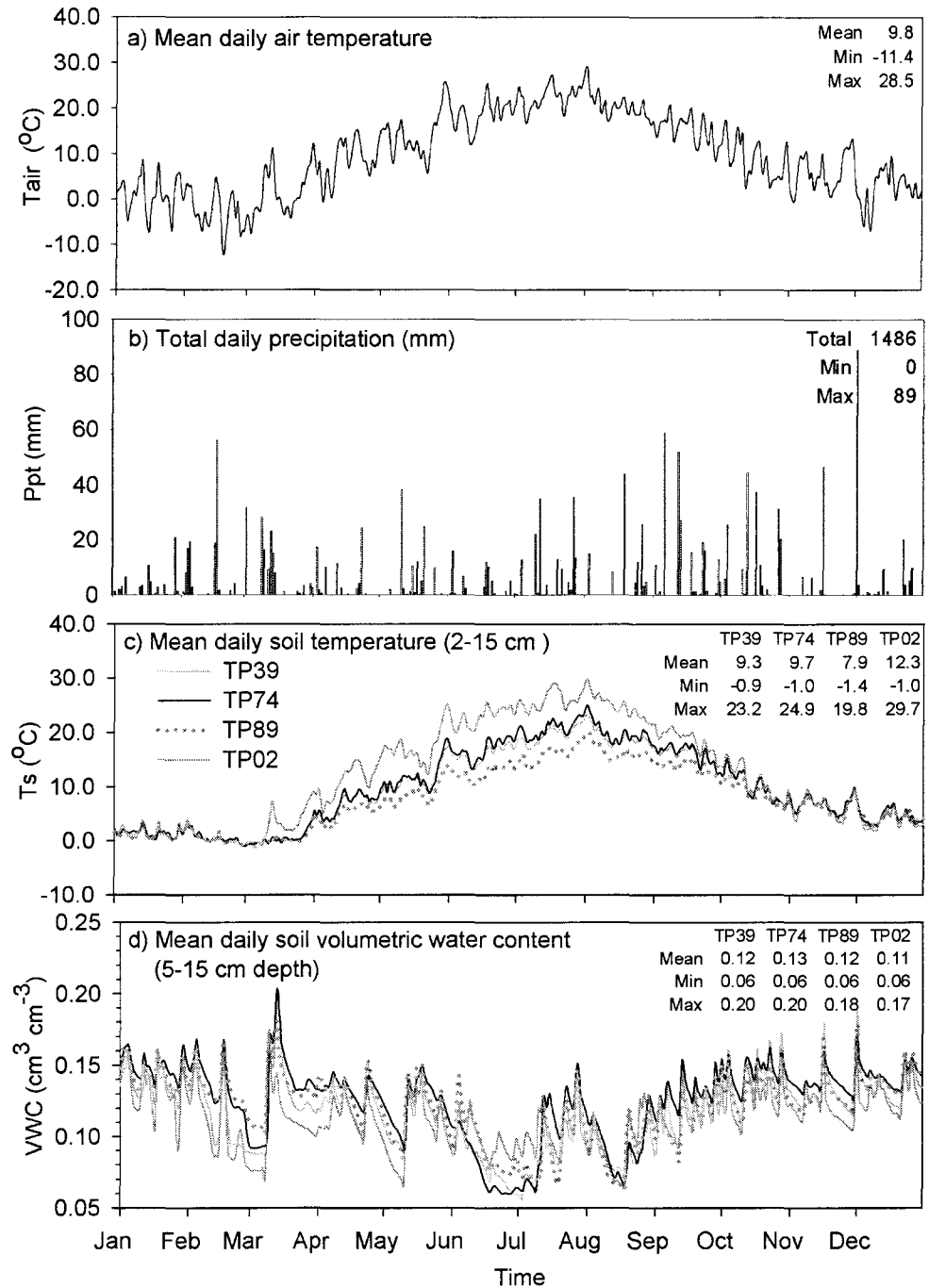


Figure 5.2: Comparison of simulated daily mean soil respiration, R_s , in g C m^{-2} , across TPFS sites during the 2006 study year (a), and relationships between observed R_s (in $\mu\text{mol CO}_2 \text{ m}^{-2} \text{ s}^{-1}$) versus soil temperature (T_s) across TPFS (b-e). Symbols represent measured values, while lines the T_s -only Gamma model. In the upper right corner of plot (a) annual mean, minimum, and maximum simulated R_s values are listed as are total annual emissions with their estimated errors, all in units of g C m^{-2} .

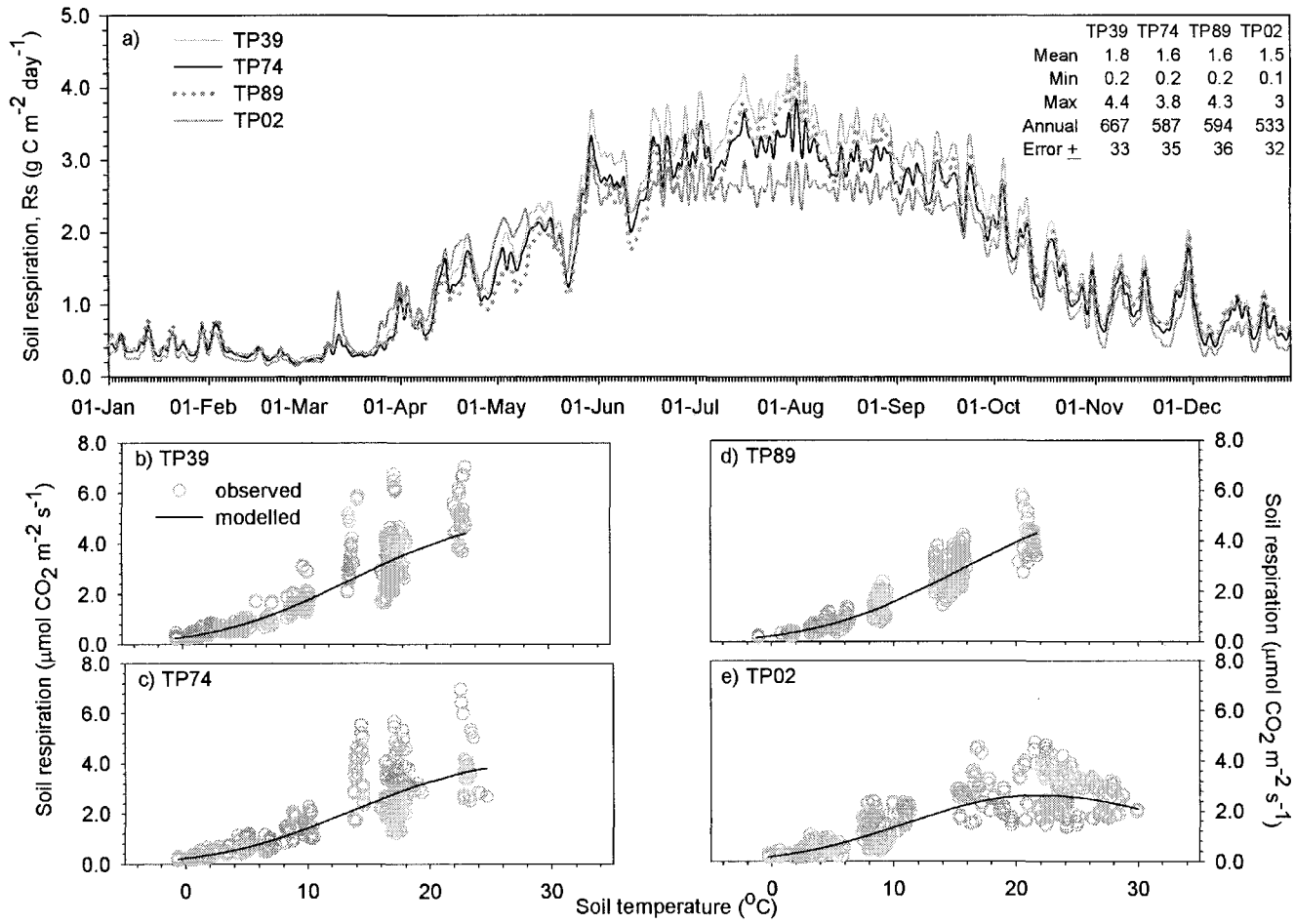


Figure 5.3: Comparison of the relative percent contribution of various components of soil respiration (Rs) across TPFS sites, on monthly basis throughout 2006: a) TP39, b) TP74, c) TP89, and d) TP02. The considered components included: the autotrophic soil respiration component (Rsa), the heterotrophic soil respiration from the mineral soil (Rsh_m), and, where applicable, heterotrophic respiration from the LFH layer (Rsh_L) – as stacked bars. In the upper left corner of the plot, annual totals for each component are listed in $\text{g C m}^{-2} \text{ yr}^{-1}$.

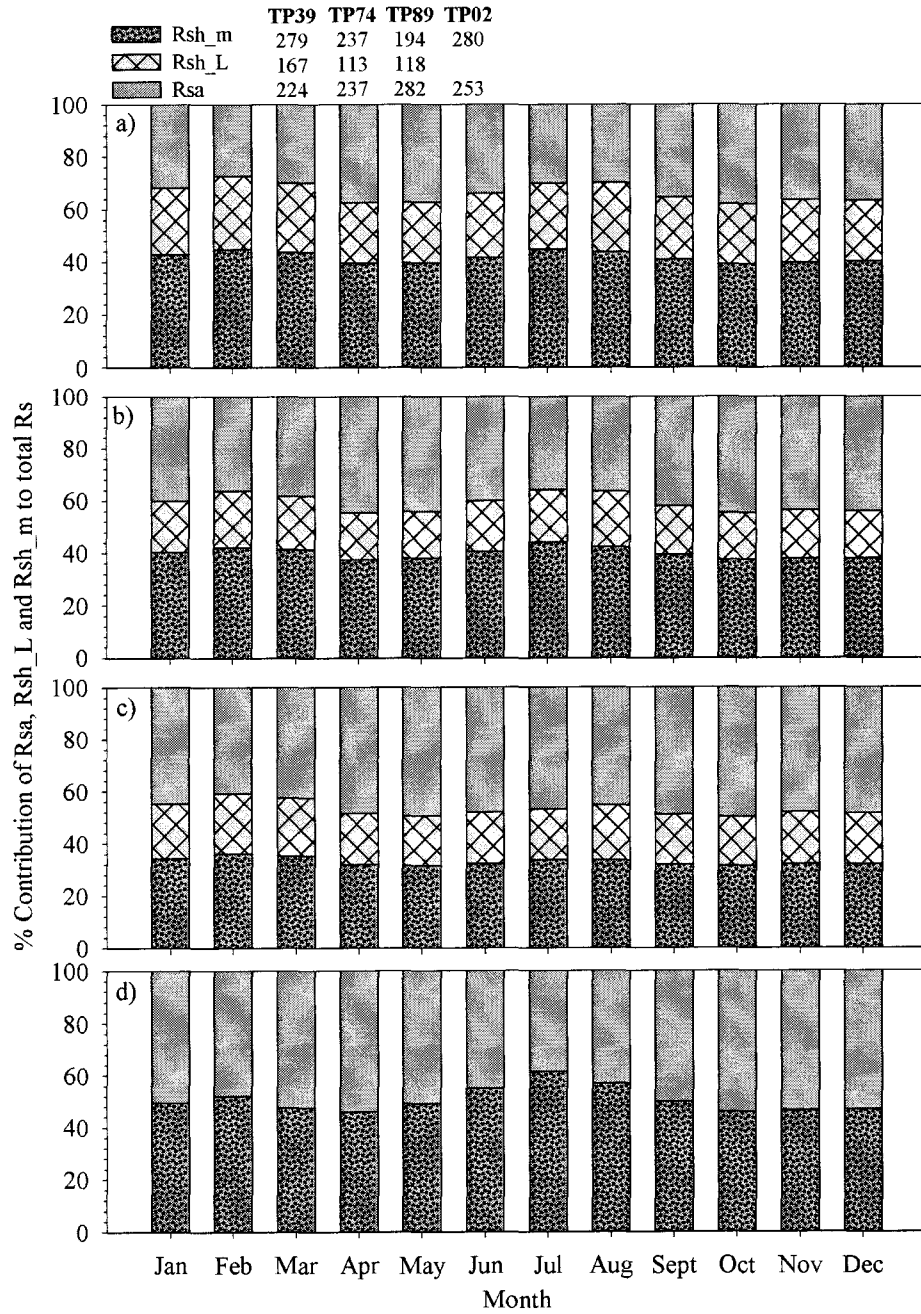


Figure 5.4: Comparison simulated daily mean foliar respiration, R_f , in g C m^{-2} , across TPFS during the 2006 study year (a), and relationships between observed R_f (in $\mu\text{mol CO}_2$ per (half-needle surface area in m^{-2}) s^{-1}) versus air temperature (T_a) across TPFS sites (b-e). Symbols represent measured values, while lines the Ts-only Gamma model. In the upper right corner of plot (a) annual mean, minimum, and maximum simulated R_f values are listed, as are total annual emissions with their estimated errors, all in units of g C m^{-2} .

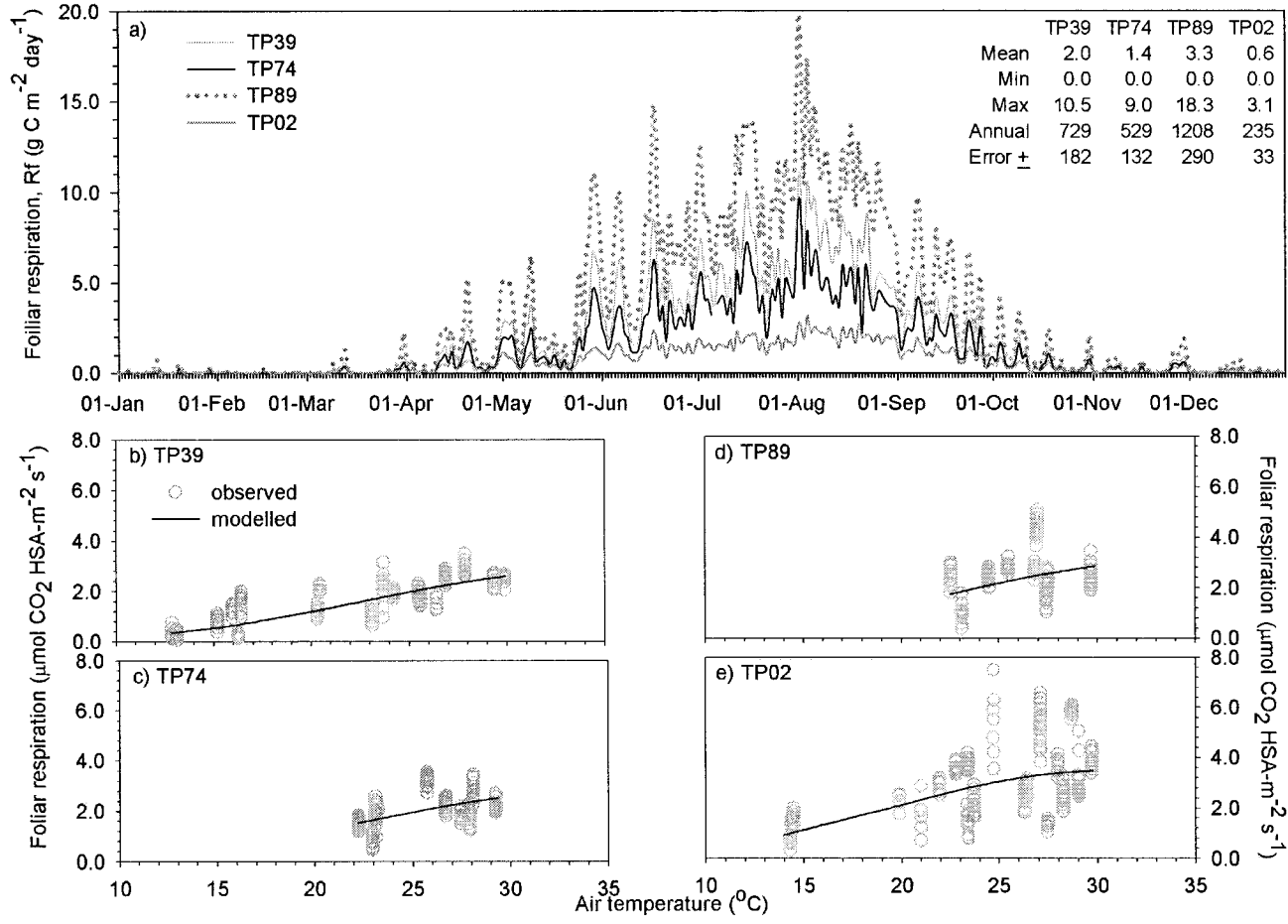


Figure 5.5: Comparison simulated daily mean woody tissue respiration, R_w , in g C m^{-2} , across TPFS sites during the 2006 study year, which included both branch and stem respiration (a), and the relationships between observed R_w (in $\mu\text{mol CO}_2$ per (sapwood volume of stem in m^{-3}) s^{-1}) versus tree bole temperature (T_b) across TPFS sites (b-d). Symbols represent measured values, while lines the T_s -only Gamma model. In the upper right corner of plot (a) annual mean, minimum, and maximum simulated R_w values are listed, as are total annual emissions with their estimated errors, all in units of g C m^{-2} .

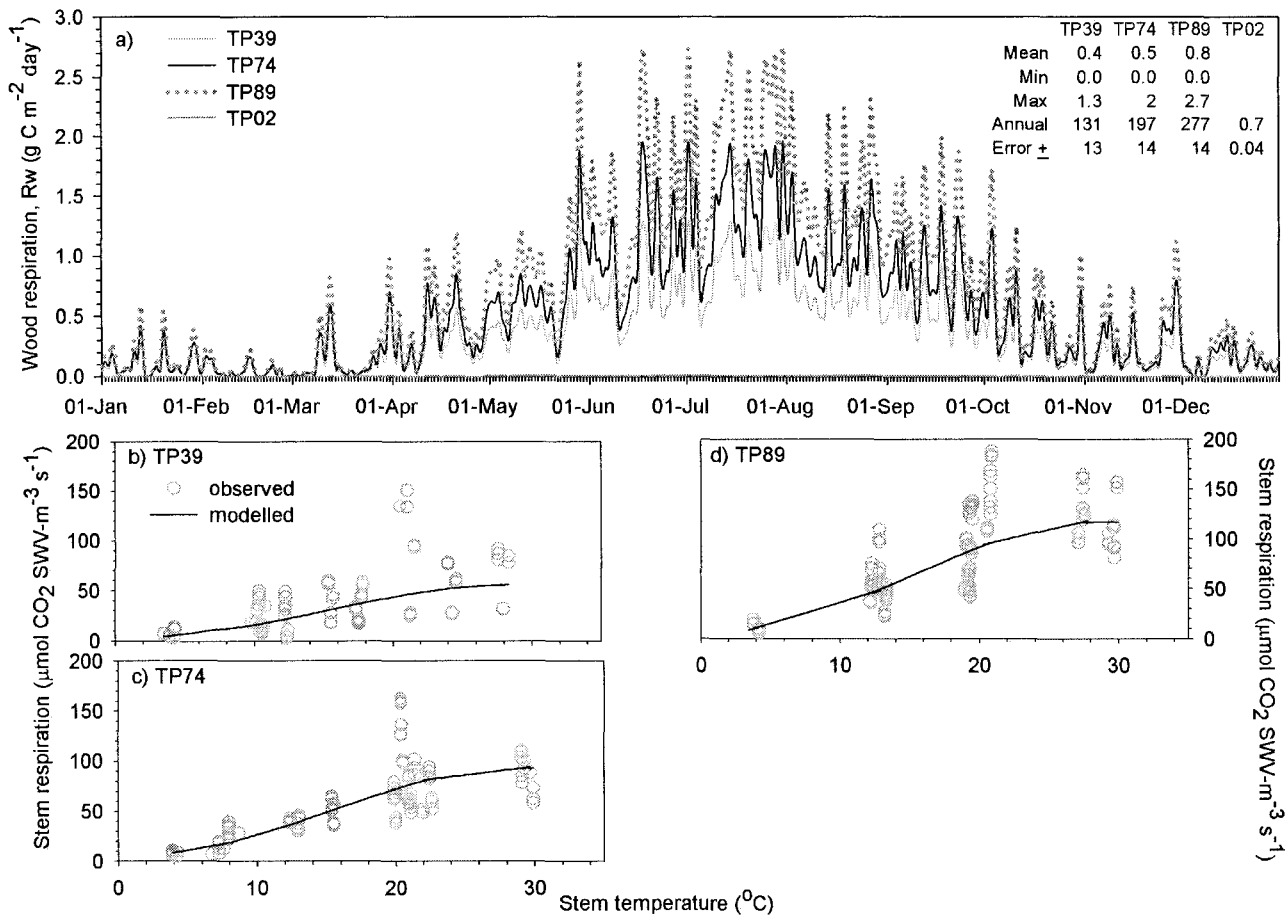


Figure 5.6: Intersite comparison of annual totals of the three major ecosystem respiration components: total soil (Rs), woody tissue (Rw) and foliar (Rf) respiration, in $\text{g C m}^{-2} \text{ yr}^{-1}$. Also included are estimated errors on each total, shown as \pm error bars and numerically.

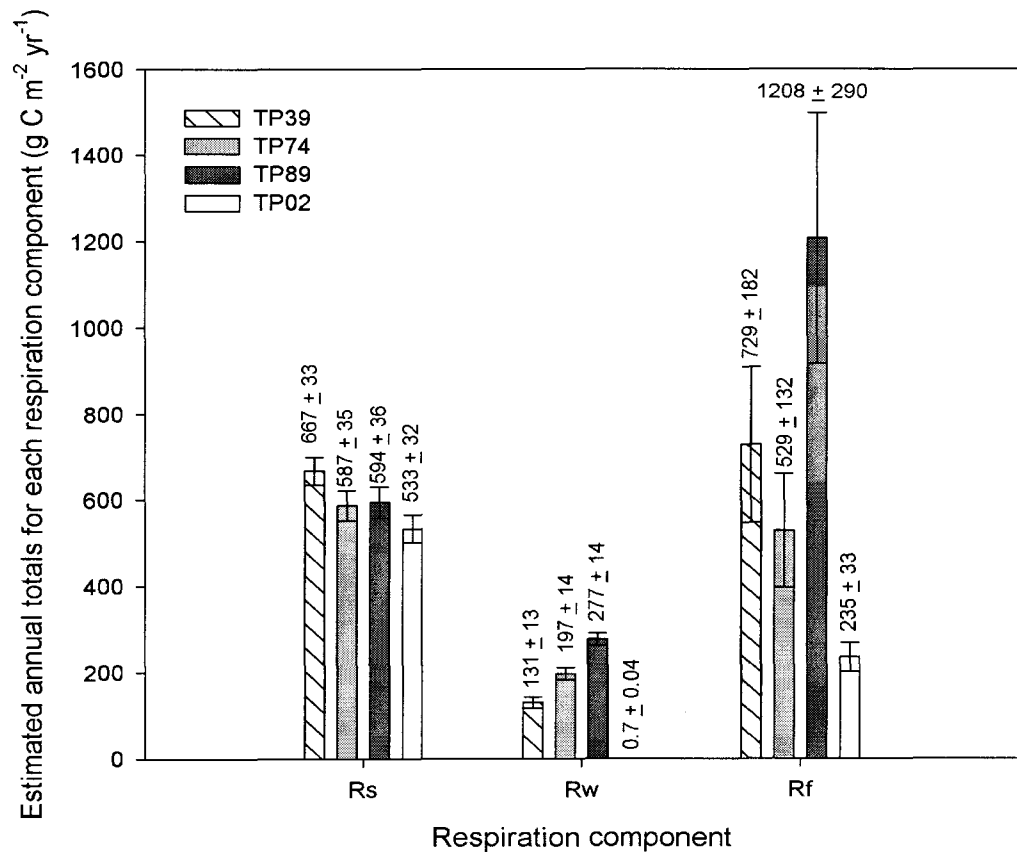


Figure 5.7: Stacked area plots comparing total daily ecosystem respiration (R_e) and its three major components: soil (R_s), woody tissue (R_w) and foliar (R_f) at a) TP39, b) TP74, c) TP89, and d) TP02. The area below each line curve represents mean daily contribution of each component to R_e , with the total sum of all areas comprising R_e . In the upper right corner of each plot, annual mean, minimum, maximum, as well as annual total R_e with its estimated error are also listed. All in units of g C m^{-2} .

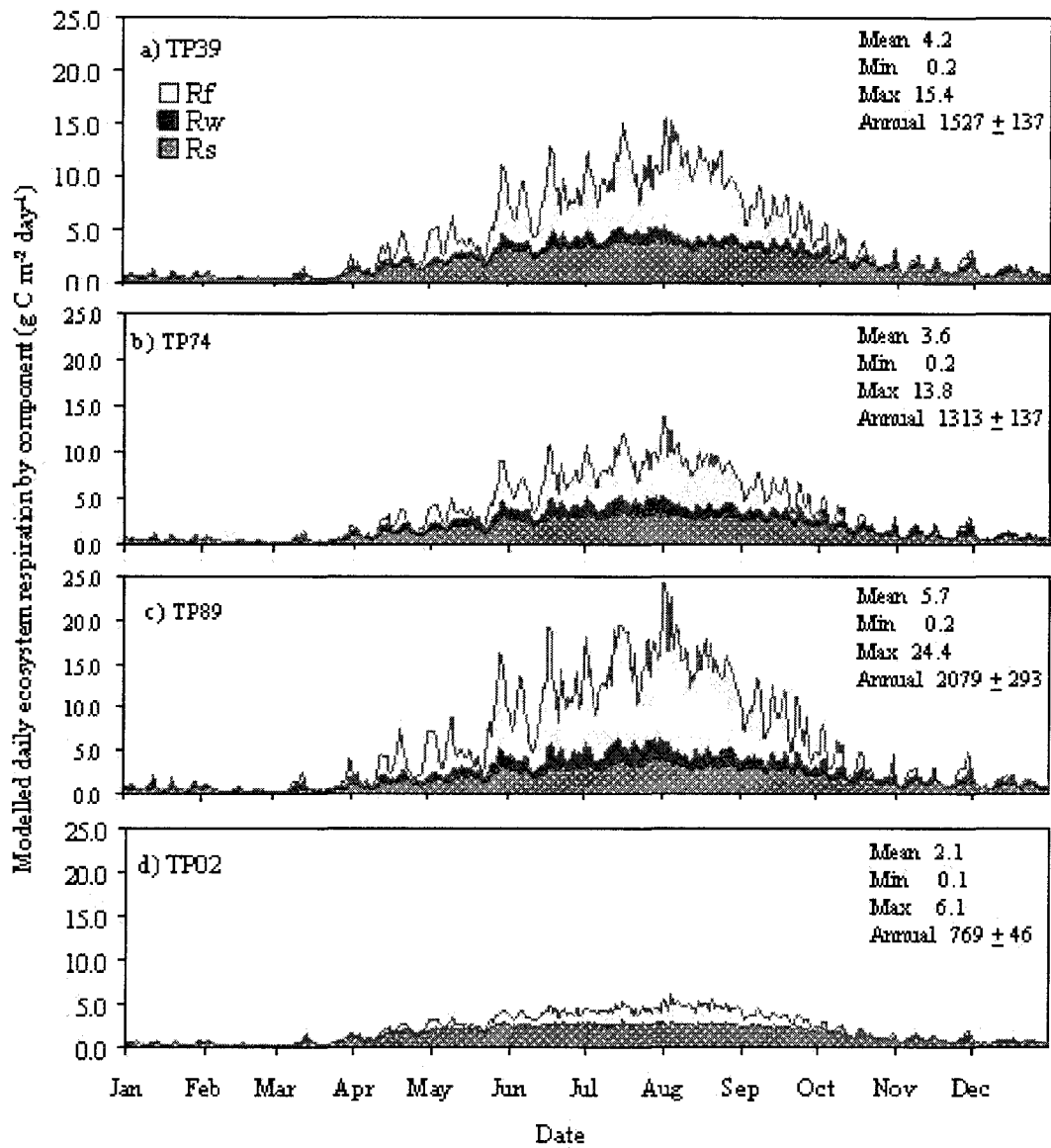


Figure 5.8: Intersite comparison of total monthly carbon emissions from the three major R_e components: a) soil (R_s), b) woody tissue (R_w), and c) foliage (R_f). In d) total monthly ecosystem respiration (R_e) is compared. Error bars represent \pm estimated errors.

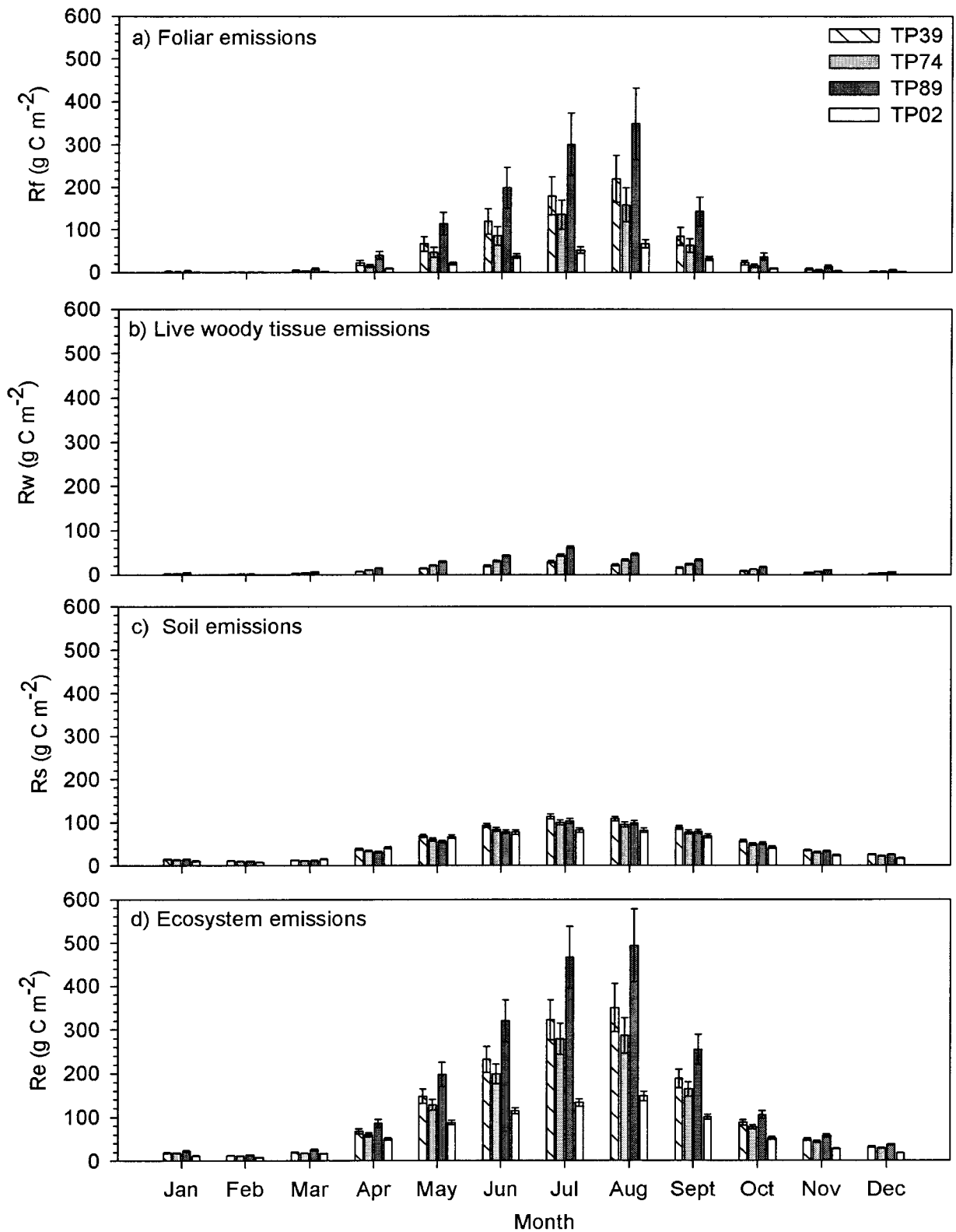
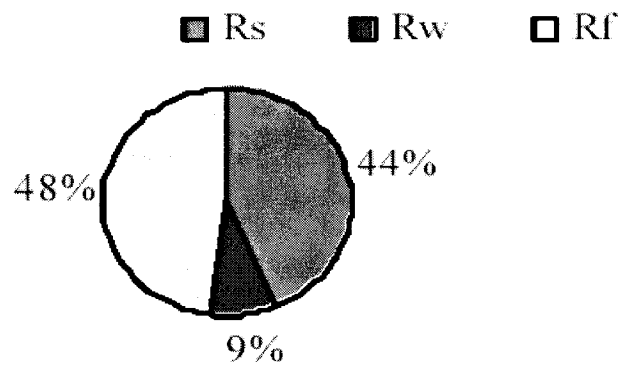
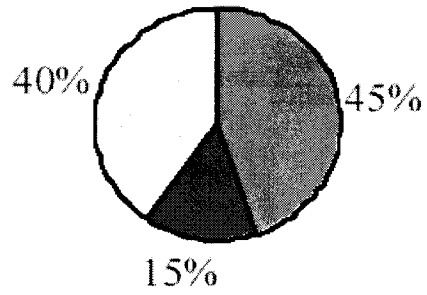


Figure 5.9: Pie graphs comparing breakdown of annual total ecosystem respiration (Re) into soil (Rs), woody tissue (Rw) and foliage (Rf) respiration, as relative percentage of annual total Re at a) TP39, b) TP74, c) TP89, and d) TP02.

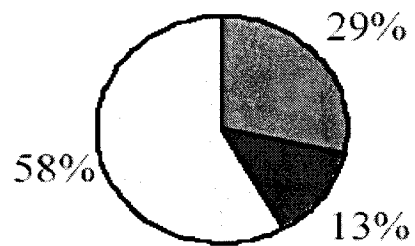
a) TP39



b) TP74



c) TP89



d) TP02

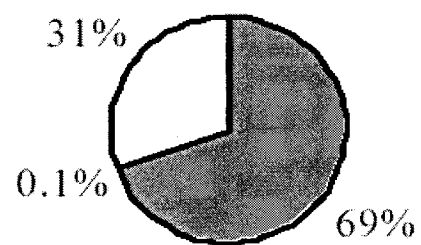


Figure 5.10: Comparison of percentage-relative contribution of monthly soil (Rs), woody tissue (Rw), and foliage (Rf) to total monthly ecosystem respiration at a) TP39, b) TP74, c) TP89, and d) TP02.

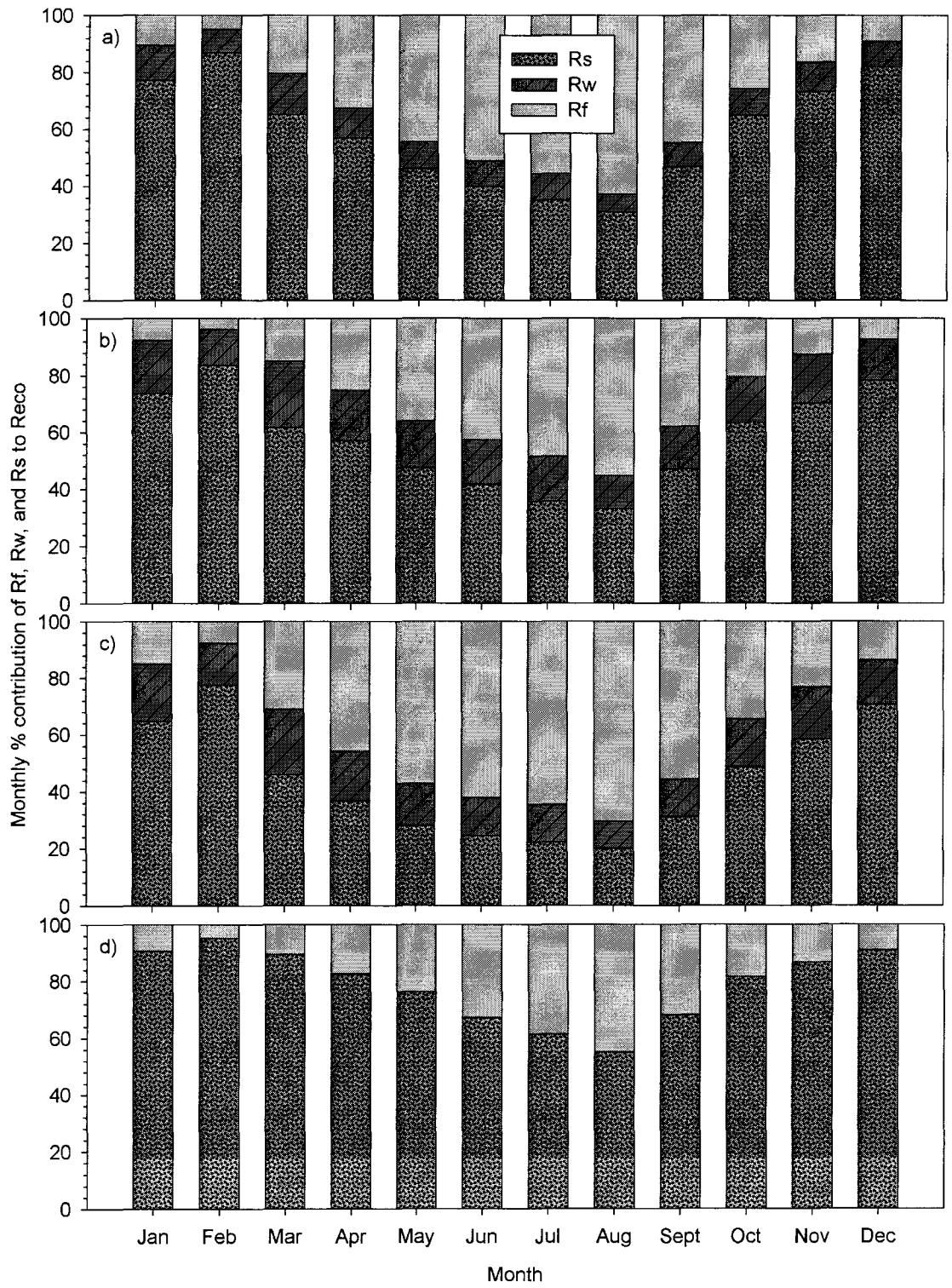
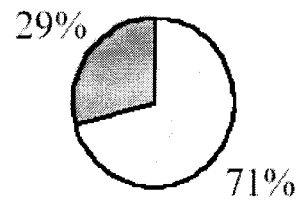


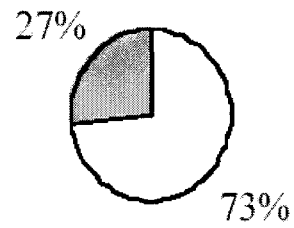
Figure 5.11: Pie graphs comparing breakdown of annual total ecosystem respiration (R_e) into total ecosystem autotrophic (R_a) and total ecosystem heterotrophic (R_h) components, presented as relative percentage of annual total R_e at a) TP39, b) TP74, c) TP89, and d) TP02.

a) TP39

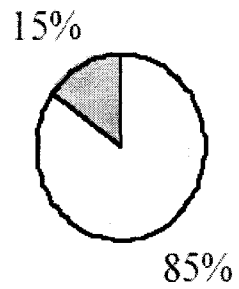
□ Ra ■ Rh



b) TP74



c) TP89



d) TP02

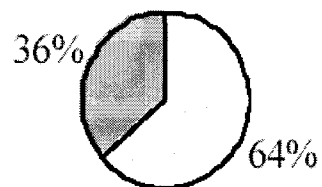
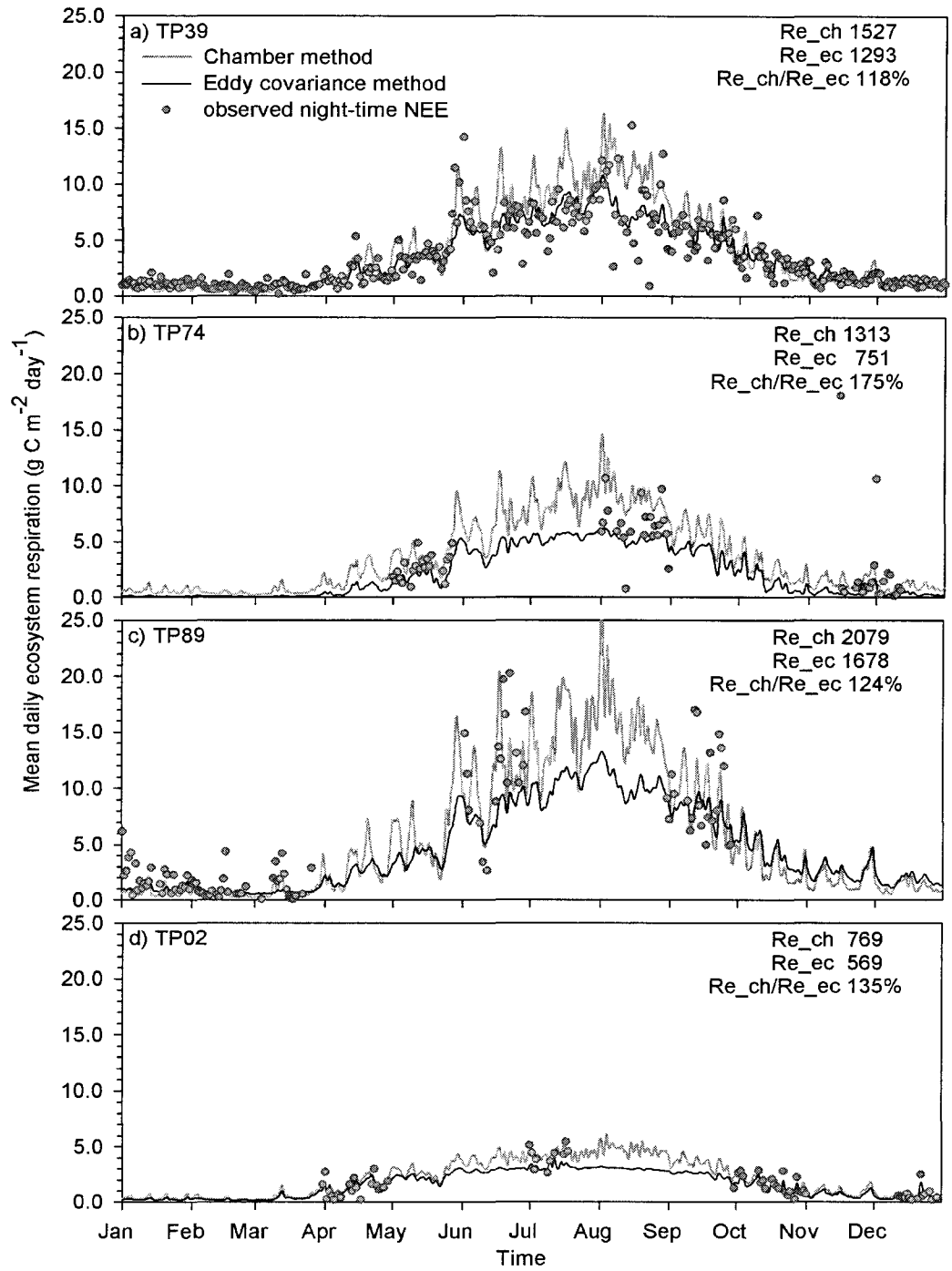


Figure 5.12: Comparison of mean daily ecosystem respiration estimated by the chamber-based method (Re_{ch}) and by the eddy covariance-based method (Re_{ec}), represented by lines. Also shown, as symbols, are daily mean night time net ecosystem observations from available tower measurements across TPFS sites: a) TP39, b) TP74, c) TP89, and d) TP02. In the upper right corner of each plot, annual totals estimated from each method in $g\ C\ m^{-2}\ yr^{-1}$ and their ratios are also given.



APPENDIX 5A: Empirical models used to simulate respiration

We used two different statistical models to simulate component fluxes at TPFS: the Q_{10} model (van't Hoff, 1894; Davidson et al., 2005):

$$R_i = R_{10} Q_{10}^{\frac{(T_i-10)}{10}} \quad 5A.1$$

where R_i is respiration of component i (in $\mu\text{mol of CO}_2 \text{ m}^{-2} \text{ s}^{-1}$); R_{10} is respiration at 10°C ; Q_{10} is a temperature sensitivity factor, which describes increase in R_i for every 10°C increase in temperature (T_i , in $^\circ\text{C}$). Both R_{10} and Q_{10} are unknown coefficients to be estimated;

and the Gamma model (Chapter 3):

$$R_i = T_i^\alpha e^{\beta_0 + \beta_1 T_i} \quad 5A.2$$

where R_i is respiration of component i (in $\mu\text{mol of CO}_2 \text{ m}^{-2} \text{ s}^{-1}$); T_i is $(T + 40^\circ\text{C})$, where T is temperature of component i in $^\circ\text{C}$; α , β_0 and β_1 are unknown coefficients to be estimated.

We linearly transformed the above two models before using multivariate linear regression analysis to evaluate them. The linearized form of the Q_{10} model becomes:

$$\ln R_i = \ln R_{10} + \ln Q_{10} \frac{(T_i - 10)}{10} \quad 5A.3$$

Equation 5A.3 is of linear form, with $\ln Q_{10}$ being the slope of the relationship, and $\ln R_{10}$ the intercept. Similarly, the linearized form of the Gamma model becomes a multivariate linear model:

$$\ln R_i = \alpha \ln T_i + \beta_0 + \beta_1 T_i \quad 5A.4$$

where $\ln(T_i)$ and T_i are treated as two distinct explanatory variables.

APPENDIX 5B: *Environmental and biological controls on TPFS's respiration*

Table 5B.1 lists the models used in simulating respiration of the various ecosystem components. In general two models were used, the Q_{10} model (Equation 5A.3, above) and the Gamma model (Equation 5A.4, above), which related respiration flux to temperature - the dominant driving factor of respiratory variability (Figures 5.2 (b-e), 5.4 (b-d), 5.5 (b-e)). However, we also used the method developed in Chapter 2 and 3 to include additional environmental factors, other than temperature, in Equations 5A.3 and 5A.4, to expand the models. The choice of these additional factors was based on literature studies of individual respiration responses to environmental and physiological drivers (i.e. soil moisture, precipitation, LAI, PAR, etc). These additional factors helped to explain some additional variability in the response and were shown to be statistically significant in improving the overall model fit. The models with additional explanatory factors are referred to as the “best specification” or Best models and are denoted with a subscript “bs” in the tables and text.

Several criteria can be used in model comparison, including coefficient of determination (R^2), residual sums of squares (RSS) and Akaike's Information Criterion (AIC) (Anderson et al., 2000). The statistically better model will have highest R^2 value and lowest RSS and AIC values. The corresponding statistics for the models we fitted to our data are listed in Table 5B.2. For all Re components,

Gamma_bs model was the best model for simulating emissions (Table 5B.2). Therefore, we used results from Gamma_bs to simulate each TPFS Re component. Among the three ecosystem components studied, the highest model R^2 values were obtained for soil respiration, R_s ($R^2 = 0.82 - 0.89$, Table 5B.2), which was comparable to results for woody tissue respiration ($R^2 = 0.69 - 0.82$). The lowest correlation between respiration and temperature was obtained for foliar respiration ($R^2 = 0.52$ to 0.61).

In general, the temperature response of each component flux was statistically different between sites (represented by A_1 - A_4 variables, $p < 0.05$). In addition to temperature, the models for each respiration component had other explanatory factors (Table 5A.1 b and e). The model of soil respiration (R_s) also included soil moisture (θ_s), litter layer thickness (LitterS) and litter layer carbon to nitrogen ratio (CN), mean daily temperature (T_{air}), precipitation occurrence on the day of R_s measurement (PPT_f) and one day prior to measurement (PPT_{f-1}). The model for soil heterotrophic respiration (R_h), fitted to measurements from the trenched plot experiments, included additional variables representing the presence/absence of the litter layer (NoL) and mean daily air temperature (T_{air}). The stem respiration, R_w , model included PPT_f and tree DBH (diameter at breast height). Finally, the model for foliar respiration (R_f) included mean daily vapour pressure deficit (VPD), mean daily photosynthetically active radiation (PAR), PPT_{f-1} , mean daily air temperature.

Table 5B.1: List of models used to simulate daily fluxes of component ecosystem respiration across TPFS sites: Q₁₀ models (a) and (b), and Gamma models (c) and (d).

(a)

Flux	Q ₁₀ –model T-only
Rs	$\text{LnRs} = \text{LnR}_{10} + A_2 * \text{LnR}_{10} + A_4 * \text{LnR}_{10} + \text{LnQ}_{10} * \text{Ts}_{10} + A_3 * \text{LnQ}_{10} * \text{Ts}_{10} + A_4 * \text{LnQ}_{10} * \text{Ts}_{10}$
Rh	$\text{LnRh} = \text{LnR}_{10} + A_1 * \text{LnR}_{10} + \text{NoL} * \text{LnR}_{10} + \text{LnQ}_{10} * \text{Ts}_{10} + A_2 * \text{LnQ}_{10} * \text{Ts}_{10} + A_4 * \text{LnQ}_{10} * \text{Ts}_{10} + \text{NoL} * \text{LnQ}_{10} * \text{Ts}_{10}$
Rw	$\text{LnRw} = \text{LnR}_{10} + A_2 * \text{LnR}_{10} + A_3 * \text{LnR}_{10} + \text{LnQ}_{10} * \text{Tb}_{10}$
Rf	$\text{LnRf} = \text{LnR}_{10} + A_3 * \text{LnR}_{10} + A_4 * \text{LnR}_{10} + \text{LnQ}_{10} * \text{Ta}_{10} + A_4 * \text{LnQ}_{10} * \text{Ta}_{10}$

(b)

Flux	Q ₁₀ –model bs
Rs	$\text{LnRs} = \text{LnR}_{10} + A_2 * \text{LnR}_{10} + A_4 * \text{LnR}_{10} + \text{LnQ}_{10} * \text{Ts}_{10} + A_3 * \text{LnQ}_{10} * \text{Ts}_{10} + A_4 * \text{LnQ}_{10} * \text{Ts}_{10} + B * \theta_s$
Rh	$\text{LnRh} = \text{LnR}_{10} + A_1 * \text{LnR}_{10} + \text{NoL} * \text{LnR}_{10} + \text{LnQ}_{10} * \text{Ts}_{10} + A_2 * \text{LnQ}_{10} * \text{Ts}_{10} + A_4 * \text{LnQ}_{10} * \text{Ts}_{10} + \text{NoL} * \text{LnQ}_{10} * \text{Ts}_{10} + B_1 * \theta_s + B_2 * \text{PPT}_f$
Rw	$\text{LnRw} = \text{LnR}_{10} + A_2 * \text{LnR}_{10} + A_3 * \text{LnR}_{10} + \text{PPT}_f * \text{LnR}_{10} + \text{LnQ}_{10} * \text{Tb}_{10} + B_1 * \text{DBH} + B_2 * \text{Ts} + B_3 * \text{VPD}$
Rf	$\text{LnRf} = \text{LnR}_{10} + A_3 * \text{LnR}_{10} + A_4 * \text{LnR}_{10} + \text{LnQ}_{10} * \text{Ta}_{10} + A_4 * \text{LnQ}_{10} * \text{Ta}_{10} + B_1 * \text{Ts} + B_2 * \text{VPD} + B_3 * \text{PAR} + B_4 * \text{PPT}_f - 1$

(d)

Flux	T-only Gamma model
Rs	$\text{LnRs} = B_0 + B_1 * \text{Ts}_{40} + B_2 * \text{LnTs}_{40} + B_3 * A_2 + B_4 * A_3 + B_5 * A_4 + A_3 * B_1 * \text{Ts}_{40} + A_4 * B_1 * \text{Ts}_{40} + A_4 * B_2 * \text{LNTs}_{40}$
Rh	$\text{LnRh} = B_0 + B_1 * \text{Ts}_{40} + B_2 * \text{LnTs}_{40} + B_3 * A_1 + B_4 * \text{NoL} + \text{NoL} * B_1 * \text{Ts}_{40}$
Rw	$\text{LnRw} = B_0 + B_1 * \text{Tb}_{40} + B_2 * \text{LnTb}_{40} + B_3 * A_2 + B_4 * A_3$
Rf	$\text{LnRf} = B_0 + B_1 * \text{Ta}_{40} + B_2 * \text{LnTa}_{40} + B_3 * A_3 + B_4 * A_4 + A_4 * B_1 * \text{Ta}_{40}$

(e)

Flux	Gamma model bs
Rs	$\text{LnRs} = B_0 + B_1 * \text{Ts}_{40} + B_2 * \text{LnTs}_{40} + B_3 * A_3 + B_4 * \text{Ta} + B_5 * \text{PPT}_f + B_6 * \text{PPT}_{f-1} + B_7 * \text{LitterS} + B_8 * \text{CN}$
Rh	$\text{LnRh} = B_0 + B_1 * \text{Ts}_{40} + B_2 * \text{LnTs}_{40} + A_1 * B_1 * \text{Ts}_{40} + \text{NoL} * B_1 * \text{Ts}_{40} + B_3 * \text{NoL} + B_4 * \text{Ta} + B_5 * \text{PPT}_f$
Rw	$\text{LnRw} = B_0 + B_1 * \text{Tb}_{40} + B_2 * \text{LnTb}_{40} + B_3 * A_2 + B_4 * A_3 + B_5 * \text{PPT}_f + B_6 * \text{DBH07}$
Rf	$\text{LnRf} = B_0 + B_1 * \text{Ta}_{40} + B_2 * \text{LnTa}_{40} + B_3 * A_3 + B_4 * A_4 + A_4 * B_1 * \text{Ta}_{40} + B_5 * \text{VPD} + B_6 * \text{PAR} + B_7 * \text{PPT}_f - 1$

where $T_{i10} = (T_i - 10) / 10$, T_i in °C;
 A_2, A_3, A_4 are dummy variables representing sites TP74, TP89, TP02, respectively.
 PPT_f and PPT_{f-1} – dummy variables representing precipitation occurrence on the day of R_i measurement and one day prior to R_i measurement, respectively.
 NoL – dummy variable representing litter presence/absence (if $\text{NoL}=1$ whenever the litter layer was absent)
 $R_{10}, Q_{10}, B, D, T, V$ are model parameters
 Ta – air temperature (above canopy)
 Tb – tree bole temperature (2-5 cm, °C)
 Ts – soil temperature (2-20 cm, °C)
 θ_s – soil moisture (2-20 cm, $\text{cm}^3 \text{cm}^{-3}$)
 VPD – vapour pressure deficit
 B_1 - B_7, R_{10} and Q_{10} – model parameters to be estimated

Table 5B.2: Comparison of model statistics for all the models used in simulating component respiration across TPFS sites. Annual totals estimated by each model for each respiration component is also given by site.

		Estimated flux (g C m ⁻² yr ⁻¹)							
	Model	R ²	RSS	k	AIC	TP39	TP74	TP89	TP02
Rs, n=2031	Q₁₀	0.82	290	6	-1704	680	652	525	552
	Q₁₀_bs	0.84	270	7	-1767	698	683	533	559
	Gamma	0.89	189	9	-2074	679	600	529	559
	Gamma_bs	0.89	178	9	-2131	667	587	594	533
Rsh, n=833	Q₁₀	0.75	124	6	-678	437	362	289	279
	Q₁₀_bs	0.76	118	9	-688	475	393	313	298
	Gamma	0.77	117	6	-699	417	357	287	280
	Gamma_bs	0.77	115	8	-702	446	350	312	280
Rw, n=336	Q₁₀	0.69	90	4	-184	125	193	261	---
	Q₁₀_bs	0.79	59	8	-237	133	188	268	---
	Gamma	0.76	69	5	-221	127	204	268	---
	Gamma_bs	0.82	50	7	-263	131	197	277	---
Rf, n=719	Q₁₀	0.52	136	5	-510	1114	801	1899	385
	Q₁₀_bs	0.59	116	8	-554	762	555	1294	280
	Gamma	0.55	128	6	-527	1033	736	1711	333
	Gamma_bs	0.61	111	9	-565	729	529	1208	235

Abbreviations used: R² – coefficient of determination; RSS – residual sum of squares; k – number of model parameters; AIC – Akaike's Information Criterion; Rs – total soil respiration; Rsh – heterotrophic soil respiration; Rw – woody tissue respiration; Rf – foliar respiration; n – number of observations.

CHAPTER 6

CONCLUDING REMARKS

6.1 Scientific contribution of the study

This dissertation filled some gaps in the literature on studies of ecosystem respiration (R_e), and its component fluxes, in planted young-to-mature (7 to 70-year-old) forests, growing in the temperate climate zone of eastern North America, where afforestation and plantations are most likely to occur in the future.

Key interesting findings that add to our knowledge of C cycling in forested ecosystems are as follows:

- a) foliar respiration (R_f) may be the more dominant and determinant component of R_e in young to mature afforested stands, especially when they reach their peak productivity/growth stage (Chapter 5);
- b) considering site age and past land-use history of the site is important when assessing the carbon budgets of afforested or planted ecosystems (Chapters 4 and 5);
- c) soil moisture availability may have a larger effect on the heterotrophic rather than on the rhizospheric component of soil respiration at TPFs and similar sites (Chapters 4 and 5);
- d) in the case of soil respiration (R_s), the Q_{10} exponential relationship between R_s and T_s may be limited to the so called “ecologically optimum T_s range” for fine root growth (Chapter 2);
- e) the functional form of the Q_{10} model is inadequate for simulating the annual R_s - T_s relationship across a wide range of T_s experienced by some forests, even after model modifications that allow, R_{10} and Q_{10} , model parameters to vary temporally (Chapter 2);
- f) accounting for *seasonal* variability in model parameters, when simulating the annual R_s - T_s response, is most important, followed by *stand age (decadal)* variability; of the three factors,

interannual variability was the least important explanatory factor of Rs-Ts variability (Chapter 2).

As part of this study, a temporally flexible Q_{10} model (Chapter 2) and an alternative empirical model, the Gamma model (Chapter 3), were developed to simulate the various respiration components. A novel approach to data analysis, using the models, was presented and should be of a general interest to anyone analyzing empirical data collected in complex environments, where variability in the data is explained by several factors with overlapping explanatory powers (Chapters 2-3).

6.2 Summary of results

Carbon dioxide gas (CO_2) emissions from soil (Rs), foliage (Rf), and live woody tissue (Rw) were measured using a portable chamber system across four different-aged planted white pine (*Pinus Strobus* L.) forests, called the Turkey Point Flux Station (TPFS). These measurements were used to characterize each of the three component fluxes and to estimate annual and monthly ecosystem respiration (Re) across TPFS (Chapters 2-5). Furthermore, the relative contribution of each component to total ecosystem respiration, across TPFS stands was quantified and compared on monthly and annual time scales (Chapter 5).

Chamber-based estimates of annual Re across the four different stands were: 1527 ± 137 , 1313 ± 137 , 2079 ± 293 , and 769 ± 46 g C m⁻² yr⁻¹ for the 70-,

35-, 20-, and 7-year old stands, respectively (Chapter 5). Across the age-sequence, estimated R_e at the 20-year-old stand was the highest, being higher than that of the two older stands (70- and 35-year-old). The relative percent contribution of each component flux to R_e also varied among the stands and temporally, with the variability driven by environmental and physiological factors. R_f dominated R_e (48, 40, 58, and 31% of R_e for the 70-, 35-, 20-, and 7-year-old stands, respectively), particularly during the growing season and at the three older stands. However, R_s was the second largest component of R_e across the four TPFS sites (44, 40, 29, and 69% of R_e , respectively), dominating R_e during the dormant winter months and at the youngest TPFS stand. LAI difference between stands were largely responsible for intersite variability in R_e among TPFS stands and also between TPFS and other literature-reported studies (Chapter 5).

Temperature was the dominant explanatory factor responsible for temporal variability in all of the R_e components. However, other environmental and physiological factors, such as precipitation, vapour pressure deficit, photosynthetically active radiation, the thickness of the soil LFH horizon, and soil carbon to nitrogen ratio, provided additional explanations for some of the observed variability in respiration measurements (Chapter 4 and 5).

Total ecosystem respiration derived from scaled-up chamber measurements, R_{e_ch} , was compared with that derived from eddy covariance tower measurements, R_{e_ec} , (Chapter 5). Across all four stands, annual chamber-based estimates of R_e were higher compared to the estimates from the tower-

based eddy covariance method, by 18, 75, 24 and 39% at the 70-, 35-, 20-, and 7-year-old stands, respectively. However, within estimated uncertainty on Re_{ch} values, the difference between Re_{ch} and Re_{ec} may be as little as 6% or as high as 93%.

Since R_s is often considered as the dominant component of Re , R_s variability was studied in more detail compared to the other Re components (Chapter 4). In particular, intersite and interannual variability in R_s was investigated during this study, using three years of R_s measurements across the four different-age TPFS stands (Chapter 4). Over the three study years, annual totals of R_s ranged from 539 ± 31 to 600 ± 31 ; 558 ± 31 to 662 ± 31 ; 587 ± 31 to 665 ± 31 ; 645 ± 31 to 732 ± 31 $g\ C\ m^{-2}\ yr^{-1}$, for the 7-, 20-, 35-, and 70-year-old stands, respectively. Annual total soil CO_2 emissions were higher, within the margins of error, between the oldest TPFS stand and the two youngest ones, during all three study years. In contrast, emissions between the younger three stands were comparable, except during the warmest study year. Soil CO_2 emissions tended to be higher for years with higher air temperatures. Intersite differences in soil CO_2 emissions were driven mostly by stand physiology, while interannual and seasonal differences were driven by temporal variabilities in regional climate, as well as each site's microclimate.

6.3 Suggestions for future work

There were a number of findings in this study that raised further questions or interesting points to consider pursuing in future research at the Turkey Point Flux Station or in similar studies. For example, results in this dissertation suggested the possibility that photosynthesis dominated R_s variability in summer months across TPFS sites, as opposed to soil temperature variability (Chapter 2). Since newly photosynthesized carbon can be relocated to roots and respired back out into the atmosphere in as little as 4 days (Carbone et al., 2007; Moyano et al., 2008), our methodology for R_s measurement (i.e. on a biweekly to monthly scale) was inadequate for directly capturing any such phenomenon. However, automated soil chambers have been recently installed at TP39 (i.e. in summer 2008). The high frequency data from those measurements should be suitable for investigating any photosynthesis- R_s relationship at TPFS, using an approach similar the one presented in Liu et al. (2006), where variability in photosynthetically active radiation was used as a surrogate for summer-time photosynthetic variability and related to the summer-time soil respiration variability.

The possibility of Q_{10} being a constant within the “optimal T_s range” for a particular tree species or region should be investigated in further detail, to know if the current practice of using constant Q_{10} values in models of terrestrial carbon cycling (ex.: Arain et al., 2002) can be maintained. Thus, studies that incorporate year-round surface soil respiration measurements with minirhizotron techniques (Johnson et al., 2001) that monitor intact root growth dynamics would be very

valuable in that regard. It would be even more valuable, if such studies are conducted at a number of forest ecosystems, monocultures and those with mixed-species composition, and in various climate regions to determine if the optimal T_s range is species- or climate-region-specific.

Interestingly, some researchers have shown that photosynthesis is also sensitive to a T_s threshold, somewhere between 5 and 10 °C, at which the trees emerge from dormancy in spring (Schwarz et al., 1997; Strand et al., 1997). This could be happening when roots start to elongate at similar T_s . Spring increase in gross ecosystem productivity (GEP) has been previously associated with an increase in annual growth of fine roots (Cote et al., 1998; Hendrick and Pregitzer, 1996). Across the TPFS age-sequence sites, spring-time GEP increase and autumn-time GEP decrease occurs in the 4 to 14 °C T_s range (Arain and Restrepo-Coupe, 2005). Therefore, GEP could be confounding the effect of T_s on the R_s - T_s relationship in the $4 \leq T_s \leq 14$ °C T_s -range at TPFS sites, which corresponds to the so called “ecologically optimum T_s range” for fine root growth identified for TPFS in this study. If techniques for monitoring leaf phenology (Richardson et al., 2007) are also added to the above proposed minirhizotron and R_s - T_s measurements at a particular site, then a couple of questions could be addressed that will help advance our understanding of forest carbon cycling and dynamics: a) How does spring time foliar growth/expansion and autumn senescence effect/confine the temperature-sensitivity of soil respiration processes during these transition seasons?; and b) Are the start of fine root growth and the start of

foliar expansion independent of each other in forest ecosystems? – Something still debated in the literature (Cisneros-Dozal et al., 2006).

Results presented in this study also suggest that foliar respiration tended to dominate ecosystem respiration in the three oldest (17- to 67- year-old, at the time of measurements) TPFS stands, which was in contrast to the more widely reported dominance of R_s on R_e (Bolstad et al., 2004; Law et al., 1999; Gaumont-Guay et al., 2006; Tang et al., 2008; Zha et al., 2007). The unusually high R_f in this study, especially for the 17-year-old stand, may be due to the young age of the stands and their inherent high productivity. Recent studies have suggested a strong positive link between CO_2 emissions in forests and their primary productivity, whereby increased productivity leads to increased respiration (Hibbard et al., 2005; Litton et al 2007). Furthermore, there is increasing evidence that across different forest biomes, productivity tends to increase with forest age up to an age of about 120 years (Pregitzer and Euskirchen, 2004; Noormets et al., 2007; Gough et al., 2008), with peak production occurring around the age of 11-30 years in temperate forests (Pregitzer and Euskirchen, 2004). The apparent importance of primary productivity in determining the dynamics and budget of ecosystem respiration in young to mature planted forests requires further study and confirmation at TPFS and in similar planted chronosequences across varying climates. This highlights the value of continuing measurements at TPFS and establishing more forest chronosequence study sites world wide.

Results from this study also highlight the need to consider past land use history of a site, in addition to stand age, when assessing its carbon budgets. Currently, there are more forest chronosequence studies of post-harvest sites (Humphreys et al., 2006; Kolari et al., 2004; Kowalski et al., 2004; Law et al., 2003; Tedeschi et al., 2002) than of sites planted on abandoned marginal or former agricultural lands (Saiz et al., 2006 and this study). Therefore, there is a need for more studies similar to the ones at TPFS, which focus on carbon fluxes of forest stands planted on abandoned marginal or former agricultural lands, to understand better the sink potentials of different afforestation schemes.

Results from this study also suggest that differences in methods for estimating R_e (i.e. chamber versus eddy covariance) should be resolved if researchers are to continue to mix estimates, derived from the two methods, to draw conclusions about the annual C budgets and dynamics of different forested ecosystems (ex.: Davidson et al., 2006). In particular, at TPFS, the possibility that the eddy covariance approach underestimates R_e at TP74 should be investigated, given that the difference between R_{e_ec} and R_{e_ch} at this site could be anywhere from 57 to 93%, compared to only 6 to 43% for the other three stands.

Finally, from our modelling exercise, we feel strongly that the Gamma model can be applied to *ecosystem* respiration simulations and should be tested in the future for its suitability and applicability in gap-filling eddy covariance flux data at TPFS and other sites.

6.4 REFERENCES

- Arain MA, Black TA, Barr AG, Jarvis PG, Massheder JM, Verseghy DL, Nesic Z (2002) Effects of seasonal and interannual climate variability on net ecosystem productivity of boreal deciduous and conifer forests. *Canadian Journal of Forest Research*, 32: 878-891.
- Arain, MA and Restrepo-Coupe, N (2005) Net ecosystem production in a temperate pine plantation in southeastern Canada. *Agricultural and Forest Meteorology*, 128: 223-241.
- Bolstad PV, Davis KJ, Martin J, Cook BD, Wang W (2004) Component and whole-system respiration fluxes in northern deciduous forests. *Tree Physiology*, 24 (5): 493-504.
- Carbone MS, Czimczik CI, McDuffee KE, Trumbore SE (2007) Allocation and residence time of photosynthetic products in a boreal forest using low-level ^{14}C pulse-chase labeling technique. *Global Change Biology*, 14: 466-477.
- Cisneros-Dozal LM, Trumbore S, Hanson PJ (2006) Partitioning sources of soil-respired CO_2 and their seasonal variation using a unique radiocarbon tracer. *Global Change Biology*, 12: 194-204.
- Cote B, Hendershot WH, Fyles JW et al. (1998) The phenology of fine root growth in a maple-dominated ecosystem: Relationships with some soil properties. *Plant Soil*, 201, 1: 59-69.
- Davidson EA, Richardson AD, Savage KE, Hollinger DY (2006) A distinct seasonal pattern of the ratio of soil respiration to total ecosystem respiration in a spruce-dominated forest. *Global Change Biology*, 12: 230-239.
- Gough CM, Vogel CS, Schimid HP, Curtis PS (2008) Controls on annual forest carbon storage: lessons from the past and predictions for the future. *BioScience*, 58 (7): 609-622.
- Hendrick R, Pregitzer K (1996) Temporal and depth related patterns of fine root dynamics in northern hardwood forests. *Journal of Ecology*, 84: 167-176.
- Hibbard KA, Law BE, Reichstein M, Sulzman J (2005) An analysis of soil respiration across northern hemisphere temperate ecosystems. *Biogeochemistry*, 73: 29-70.
- Humphreys ER, Black TA, Morgenstern K, Cai T, Drewitt GB, Nesic Z, Trofymow JA (2006) Carbon dioxide fluxes in coastal Douglas-fir stands

- at different stages of development after clearcut harvest. *Agricultural and Forest Meteorology*, 140: 6-22.
- Johnson MG, Tingey DT, Phillips DL, Storm MJ (2001) Advancing fine root research with minirhizotrons. *Environmental and Experimental Botany*, 45: 263-289.
- Kolari P, Pumpanen J, Rannik Ü, Ilvesniemi H, Hari P and Berninger F (2004) Carbon balance of different aged Scots pine forests in Southern Finland. *Global Change Biology*, 10: 1106-1119.
- Kowalski AS, Loustau D, Berbigier P, Manca G, Tedeschi V, Borhetti M, Valentini R, Kolari P, Mencuccini M, Moncrieff J, Grace J (2004) *Global Change Biology*, 10: 1707-1723.
- Law BE, Ryan MG, Anthoni PM (1999) Seasonal and annual respiration of a ponderosa pine ecosystem. *Global Change Biology*, 5, 169-182.
- Law BE, Sun O, Campbell J, Van Tuyl S, Thorton PE (2003) Changes in carbon storage and fluxes in a chronosequence of ponderosa pine. *Global Change Biology*, 9: 510-524.
- Litton CM, Raich, JW, Ryan MG (2007) Review: Carbon allocation in forest ecosystems. *Global Change Biology*, 13: 2089-2109.
- Liu Q, Edwards NT, Post WM, Gu L, Ledford J, Lenhart S (2006) Temperature-independent diel variation in soil respiration observed from a temperate deciduous forest. *Global Change Biology*, 12: 1-10.
- Moyano FE, Kutsch WL, Rebmann C (2008) Soil respiration fluxes in relation to photosynthetic activity in broad-leaf and needle-leaf forest stands. *Agricultural and Forest Meteorology*, 148: 135-143.
- Noormets A, Chen J, Crow T (2007) Age-dependent changes in ecosystem carbon fluxes in managed forests in northern Wisconsin, USA. *Ecosystems*, 10: 187-203.
- Pregitzer KS and Euskirchen ES (2004) Carbon cycling and storage in world forests: biome patterns to forest age. *Global Change Biology*, 10: 2052-2077.
- Pregitzer KS and Euskirchen ES (2004) Carbon cycling and storage in world forests: biome patterns to forest age. *Global Change Biology*, 10: 2052-2077.

- Richardson AD, Jenkins JP, Braswell BH, Hollinger DY, Ollinger SV, Smith M-L (2007) Use of digital webcam images to track spring green-up in a deciduous broadleaf forest. *Oecologia*, 152: 323-334.
- Saiz G, Byrne KA, Butterbach-Bahl K, Kiese R, Blujdeas V, Farrell EP (2006) Stand age-related effects on soil respiration in a first rotation Sitka spruce chronosequence in central Ireland. *Global Change Biology*, 12: 1007-1020.
- Schwarz PA, Fanhey TJ, Dawson TE (1997) Seasonal air and soil temperature effects on photosynthesis in red spruce (*Picea rubens*) saplings. *Tree Physiology*, 17: 187-194.
- Strand M, Lundmark T, Söderbergh I, Mellander P-E (2002) Impacts of seasonal air and soil temperatures on photosynthesis in Scots pine trees. *Tree Physiology*, 22: 849-847.
- Tang J, Bolstad PV, Desai AR, Martin JG, Cook BD, Davis KJ, Carey EV (2008) Ecosystem respiration and its components in an old-growth forest in the Great Lakes region of the United States. *Agricultural and Forest Meteorology*, 148: 171-185.
- Tedeschi V, Rey A, Manca G, Valentini R, Jarvis P, Borghetti M (2006) Soil respiration in a Mediterranean oak forest at different developmental stages after coppicing. *Global Change Biology*, 12: 110-121.
- Zha TS, Xing ZS, Wang KY, Kellomaki S, Barr AG (2007) Total and component fluxes of a Scots pine ecosystem from chamber measurements and eddy covariance. *Annals of Botany*, 99: 345-353.

The End